Near Real Time Monitoring of Land Cover Using Satellite Imagery

Madeleine Philp

A thesis submitted in fulfilment of the requirements for the degree of Doctor of Philosophy

Aberystwyth University

Supervisors: Dr Pete Bunting, Dr Andy Hardy &

Dr Richard Jensen

Acknowledgements

Thank you first and foremost to my supervisors Dr. Pete Bunting, Dr. Andy Hardy and Dr. Richard Jensen for their guidance and support over the last three years. Thanks also to the whole Earth Observation and Ecosystem Dynamics Research Group for their assistance and encouragement. I am also grateful to Aberystwyth University and the Department of Geography and Earth Sciences for facilitating this project and my study for the last seven years.

Thanks also to all partners involved in the project at the Welsh Government and Geosmart Decisions, in particular Alex Harris, Claire Horton, Crona Hodges and Doug Scott, for your feedback, advice and support throughout. I am also grateful to those at the Knowledge Economy and Skill Scholarship office; Penny Dowdney, Linda Cook, Anwen Roberts and Helena Norris for their support accessing project and personal development opportunities and funding.

My family and friends deserve huge thanks for their continued support, encouragement and time. My parents and husband have been monumental in helping me through everything so far. I can never be grateful enough to them for all their love, care and support.

Abstract

Accurate identification of historic and current land cover changes is vital for monitoring and managing the environment. Earth Observation satellite archives provide cost-effective and consistently measured time series of data at a scale appropriate for land managers. Current time series change detection approaches require a data density not present in historic archives and can be computational complex, limiting application to large-scale areas. In light of these challenges, the 'map-to-image' approach was developed, requiring only a base map and a satellite image to identity change features (i.e. map-to-image change detection).

The aim of the study was to assess and develop the 'map-to-image' change detection technique as a component of a multi-class land cover monitoring system for Wales. The approach assumes that within a base map class area the pixel values (e.g. reflectance or backscatter) of the satellite image are homogeneous, therefore any land cover change features will exhibit different responses. Three methods to categorise these changes were developed using; histogram distributions, probabilities from repeated random forest classifiers, and outlier analysis. The approaches were applied to a time series of Landsat (5, 7, and 8) and Sentinel 2 data covering Wales, UK acquired between 1990 and 2017. They were initially tested and compared on coniferous forest change, performing well when identifying clear-felling and producing accuracies of 89.4-94.1%. When applied to a full land cover map change detection accuracies of 69.2 %-89.1% were produced. Outlier and histogram distribution-based approaches outperformed repeated random forest classifier probabilities in most cases.

The method performed well when detecting large-scale changes for spectrally homogeneous classes. However, in cases where change vectors were spectrally

similar limitations in accuracy were identified. The change map use case, and likely land cover change drivers and types, must be considered when selecting a change detection approach. The 'map-to-image' approach should be used when a computationally efficient, robust algorithm is needed to analyse large-scale high magnitude changes in a time series of data where the time period between capture dates varies greatly or data volume is low.

Table of Contents

List of Figures

List of Tables

Glossary

Atmospheric Correction The process of removing the effects of the atmosphere on reflectance values from the Earth's surface acquired by satellite mounted sensors. (Lillesand et al. 2015).

Atmospheric Noise Meaningless information caused by variation in reflectance due to the composition of the atmosphere. (Lillesand et al. 2015).

Bayes Logic Bayes therom or Bayes logic includes information from a prior event in the probability of an event occurring (Joyce 2019).

Binary Map A map consisting of two land cover classes. Typically this is one class of interest and a broad class of everything else..

Change Detection The process of identifying where the surface of the Earth has changed in a given period of time. Typically this is a change in land cover between remote sensing images acquired on two separate dates. .

Change Vector Analysis A process which describes the change of an feature between two dates in time as a vector in n-dimensional space. A vector can have a magnitude (size or scale of change) and a direction (type of change)

component. A threshold is applied to this vector to identify changed areas (Malila 1980).

Cloud Cover A constraint of optical remote sensing data. Cloud cover refers to the proportion of the reflectance of the radiation from the sun that has been intercepted by cloud, meaning the Earth's surface can not be observed. The longer wavelength of radar data can 'see through' the cloud. (Lillesand et al. 2015).

Clustering The process of dividing a population of data points into groups so that each point is more similar to the group or cluster it belongs to than the rest of the population..

Confusion Matrix A table which describes the performance of a classifier against a reference dataset. The reference data should represent reality or the ground-truth. It displays the percentage of points which were classified correctly and where the classification error, or confusion was. (Lillesand et al. 2015, Congalton 2008).

Earth Observation The gathering of information about the nature of the Earth's surface using remote sensing technologies. Earth observation monitors the status of the Earth's surface and systems..

Extremely Randomised Trees A decision tree ensemble machine learning classifier. It is very similar to the popular random forests classifier. Extremely randomised trees has an extra layer of randomness in the sampling of training data. The training data are sampled with replacement, this has been show to reduce overfitting. (Geurts et al. 2006).

False Colour Composite A remote sensing image where the reflectance information displayed in red, green and blue colours was not collected from red, green and blue sections of the electromagnetic spectrum.

False Positives When a object or pixel is identified as a change feature by the change detection process but is not actually changed on the ground. It is most often used in a land cover classification context.

Fuzzy Logic A mathematical concept which allows for certainty of set or class ownership. It is an alternative to boolean logic that deals with ambiguity in a dataset (Zadeh 1988).

Fuzzy-Rough Nearest Neighbour A supervised machine learning classifier which assigns a data point a class based on the fuzzy-rough logic uppper and lower approximations of the classes of K nearest neighbours (Jensen & Cornelis 2011).

Fuzzy-Rough Set Applies fuzzy logic to the upper and lower approximations of rough sets. Allows for ownership to the 'core' and 'outer' class observations (Dubois & Prade 1990).

Geometric Registration Is the process of assigning an image coordinates based on the area it covers on the ground (Lillesand et al. 2015).

Image Classification Image classification is the process of categorising all of the pixels in a remotely sensed image into a set of labels, themes or classes. Typically these are land cover themes. (Lillesand et al. 2015).

Image Objects Image objects or segments are groups of spatially connecting pixels with similar values which have been segmented..

Improved Change Vector Analysis A change vector analysis approach which improves change threshold selection. Instead it uses a flexible double-window search to determine the change threshold. It also includes more information on the cosine of change vector (Chen et al. 2003).

Jeffries Matusita Distance A commonly used separability criterion for determining the separability of land cover class remote sensing data (Kavzoglu & Mather 2000, Padma & Sanjeevi 2014).

K Means A clustering algorithm which is designed to sort observations into K clusters. K is a user defined parameter which reflects the dimensionality of the dataset. Each observation is assigned to the nearest cluster in n-dimensional space (Macqueen 1967).

K Means ++ An algorithm to optimise the number of seeds for a clustering algorithm. It is a development of a K Means classifier which assigns a class based on the closest k cluster centres (Arthur & Vassilvitskii 2007).

K Nearest Neighbour An algorithm which assumes that data points which are close to each other in space display similar characteristics, that similar things are next to each other. Therefore, by examining a characteristics of a number of neighbours information can be learnt about a point in question. (Fix & Hodges 1989).

Land Cover A description of the physical material covering the earth's surface. It indicates the physical land type such as forest or open water (Lillesand et al. 2015).

Land Cover Classification A type of image classification. The image pixels are categorised into classes which relate to land covers, for example forest or water (Lillesand et al. 2015).

Land Use A description of how people are using the land. For example grass might be used as a golf course or a football field (Lillesand et al. 2015).

Landsat A series of Earth-observing satellite missions jointly managed by NASA and the U.S. Geological Survey. The programme has been running for over 20 years and both Landsat 7 and Landsat 8 are currently in orbit and collecting data.

Machine Learning A system or algorithm which is able to automatically learn or improve without explicit programming. Machine learning classification and regression of image data are commonly used in remote sensing applications.

Mahalobis Distance A measure of the difference between a point and a given distribution of data. It is a multi-dimensional generalisation of number of standard deviations a point is from the mean of dataset (McLachlan 1989).

Map-to-Image The process of combining ancillary produced thematic land cover map data with remote sensing image data for change detection.

Minimum mapping unit The minimum area on the ground that an single type land cover needs to cover before it is included in a map product. Minimum mapping units reduce the effects of noise in a classification product.

Mixed Pixels Occur when the pixel value represents information from several different land cover surfaces within the pixel spatial area on the ground surface (Lillesand et al. 2015).

Moderate Resolution Imaging Spectroradiometer A satellite mounted remote image sensor built by Santa Barabra. It was first launched into orbit in 1999 and has a long archive of earth observation image data.

Modified change vector analysis Reduces the impact of the threshold selection on change vector analysis by outputting continuous change data (Nackaerts et al. 2005).

Neural Networks A type of classifier which endeavour to recognise and categorise relationships in data based on a process that is similar to the network of neurons that form a human brain (Atkinson & Tatnall 1997).

Normalised Difference Vegetation Index Quantifies the photosynthetic activity of vegetation by measuring the difference between the near infra-red and red light (Lillesand et al. 2015) .

Optical Data In remote sensing optical data makes use reflectance information in the the visible, near infra-red and short wave infra-red range of the electromagnetic spectrum (Lillesand et al. 2015).

Orthorectification The process of correcting for the effects of terrain and/or sensor angle in remote sensing imagery. The end result is an image which has a constant scale and features in georefenced 'correct' positions (Lillesand et al. 2015).

Overfitting Occurs when a machine learning model fits too closely to one sample of data, typically training data. Therefore, it may fail to accurately handle other data.

Parametric Assumes a normal distribution in the dataset.

Pixel Value A pixel is a tiny square of colour. A digital image is composed of a grid of pixels. The data value associated with each pixel is called the pixel value. The pixel value could represent any type of data, for example radar or optical reflectance (Lillesand et al. 2015).

Post Classification Comparison A change detection process which identifies change features based on land cover classifications. Any pixels or objects assigned to a different land cover class at two different points are considered to be land cover change (Swain 1976).

Principal Component Analysis A process by which the dimensionality of a dataset is reduced. It is the process of transforming a large dataset with many variables into a smaller dataset with reduced variables without losing information of interest from the larger dataset (Jolliffe & Cadmia 2016).

Python A high-level computing language which is commonly used in data science processing.

Radar Data A type of remote sensing data. Radar scans the surface of the Earth with microwave electromagnetic radiation. The radar sensor transmits microwave pulses and receives backscatter from the Earth's surface (Lillesand et al. 2015).

Radiometric Correction The process of removing the effects of noise and the atmosphere on reflectance values from the Earth's surface acquired by satellite mounted sensors (Lillesand et al. 2015).

Random Forests A machine learning algorithm. It is a ensemble method, a large

number of rough decisions trees are constructed from training data. Class is assigned based on the most common result from these decision trees (Tin Kam Ho 1998).

Reflectance The proportion of electromagnetic radiation which strikes a surface that is reflected of it. It is a fraction of the incident electromagnetic radiation (Lillesand et al. 2015).

Remote Sensing The process of acquiring information about an object without coming into direct contact with the object (Lillesand et al. 2015).

Rough Set An approximation of of a set or class. It defines a pair of sets, a upper and lower approximation of the original set. A rough set is a set of observations or data points which lie between the upper and lower approximations of a crisp or conventional set (Pawlak 1982).

Segmentation The process of grouping or partitioning an image into segments of pixels with similar values. The image objects produced is to represent the data of the image in a manner that is easier to analyse..

Sentinel The Sentinel programme is a series of satellites in the Copernicus Programme launched by the European Space Agency. Sentinel-2 acquires optical imagery from two twin satellites.

Shapiro-Wilks Test A statistical test for if a value comes from a normally distributed dataset (Shapiro & Wilk 1965).

Simple Image Differencing The process of identifying land cover change by differencing the pixel values of one corrected Earth Observation Image from another acquired at a different time.

Spatial Resolution The size of the smallest object that can be detected by the sensor and displayed in the image. It is typically reported as a ground area or linear dimension on the ground represented by a single pixel (Lillesand et al. 2015).

Spectral Separability The separability of different land covers based on the spectral signature produced. Land cover with similar spectral signatures have a lower separability.

Spectral Signature The variation in reflectance from an object across different electromagnetic wavelengths. Typically it is displayed in a plot and used in land cover classification (Lillesand et al. 2015).

Spectral Unmixing The process of separating the signatures within a mixed pixel to constituent spectra, called endmembers (Shi & Wang 2014).

Support Vector Machines A machine learning algorithm that constructs a hyperplane in n-dimensional space around a class (Boser et al. 1992).

Tasseled Cap A transformation of the spectral information into indicators. Indicators can provide information on vegetation greenness and phenological stages (Kauth & Thomas 1976).

Temporal Resolution The time between data acquisitions. Typically in remote sensing this is expressed as the number of days it takes a satellite to return to the same location (Lillesand et al. 2015).

Thematic Data The extraction of pixel or object information into themes, typically land cover classes.

Time Series A sequence of data points or images which were acquired in

successive order through time at regular or irregular intervals.

Training Data A subset of dataset which is used to construct a machine learning algorithm so it can make predictions on a wider dataset.

Vegetation Index A spectral transformation of at least two bands of electromagnetic reflectance data to enhance the detection or measurement some feature of vegetation.

Acronyms

BFAST Breaks for Additive Season and Trend.

CDZ Core Disease Zone.

CORINE Coordination of Information on the Environment.

CVA Change Vector Analysis.

CVAPS Change Vector Analysis in Posterior Probability Space.

DI Disturbance Index.

EO Earth Observation.

ERT Extremely Randomised Trees.

FCC False Colour Composite.

FRNN Fuzzy-Rough Nearest Neighbour.

ICVA Improved Change Vector Analysis.

JM Jeffries Matusita Distance.

KNN K Nearest Neighbour.

LCC Land Cover Change.

LCM Land Cover Map.

MCVA Modified change vector analysis.

MODIS Moderate Resolution Imaging Spectroradiometer.

NDVI Normalised Difference Vegetation Index.

NFI National Forest Inventory.

NIR Near Infrared.

OD Outlier Detection.

PCA Principal Component Analysis.

PCC Post Classification Comparison.

PV Pixel Value.

PyOD Python Outlier Detection.

QQ Quantile Quantile.

REDD++ Reducing emissions from deforestation and forest degradation.

RF Random Forests.

ROI Region of Interest.

RRF Repeated Random Forests.

RS Remote Sensing.

SAVI Soil Adjusted Vegetation Index.

SID Simple Image Differencing.

STL Seasonal Trend Loss.

SVM Support Vector Machines.

SWIR Short-wave Infrared.

TC Tasseled Cap.

UK United Kingdom.

VI Vegetation Index.

XGBOD Extreme Gradient Boosting Outlier Detection.

Chapter 1

Introduction

1.1 Land Cover Change and Earth Observation

The landscape and surface of the Earth is dynamic and constantly changing due to anthropogenic (human) or natural activities, for example, agricultural expansion, storms, wildfires, socio-economic factors (e.g. migration) or urban growth (Borak et al. 2000, Al-doski et al. 2013). The impacts, drivers, and long-term effects of these processes must be understood. The dynamic nature of the Earth results in Land Cover Change (LCC). LCC is defined as the transformation of the land or replacement of one land-cover type on the Earth's surface (Meyer & Turner 1992). The Land Cover is the state of the land surface (e.g forest or cropland), this is distinct from the Land Use, which refers to how humans use the land surface (e.g. agriculture) (Lillesand et al. 2015). However, changes in land cover are often the result of or result in, a change of land use. The two processes (land cover

and land-use change) are interdependent and closely related. For example, socio-economic pressures have led to widespread deforestation of the Amazon basin for agriculture where the land cover has changed from forest to bare soil and the land use has become agriculture (Smith et al. 1999, de Espindola et al. 2012, Marquardt et al. 2019). This interconnected nature makes unpicking the true, often combined causes of land cover change a complex task.

LCC is typically the result of individual or multiple related processes operating at a range of scales both spatially and temporally (Foody 2002). These drivers of change were described by Lambin & Ehrlich 1997 as falling into three categories; biophysical, economic, or political. At a global scale, changes are cumulatively transforming land cover at an accelerating pace (Houghton 1994, Hongquan et al. 2011, Cole et al. 2018). This pace is particularly evident in the tropics, where the biophysical changes brought on by anthropogenic climate change are expanding deserts and economic driven change has led to rainforest deforestation for agriculture or palm oil plantations. (Houghton 1994, Lillesand et al. 2015). These changes are occurring at all spatial scales, from global to regional, and the relationship between global changes and regional changes must be understood. A variety of LCC data at all scales is needed to facilitate management practices and policymakers to address the drivers and effects of LCC (Duveiller et al. 2020).

Within the UK the landscape is dynamic and LCC is largely driven by human activity rather than natural phenomena (Thomson et al. 2007, Cole et al. 2018). From the 1940s onwards, urban areas have expanded to cover more of the landscape due to increasing population sizes. Agricultural land has been farmed more intensively, driven by increasing food demands. This has impacted the land

cover of the agricultural areas and those nearby, with a reduction in scrubby vegetation and forest land cover. Since the UK joined the EU in 1973, political pressures reduced intensive farming practices and financial initiatives have led to a diversification of agricultural land cover. Semi-natural woodland has been used for leisure and tourism, leading to changes in land cover due to paths and car parks. The biophysical drivers of land cover in the UK are primarily flooding and vegetation disease, for example, Ash dieback (*Hymenoscyphus fraxineus*). Wales is a dynamic region (Lucas et al. 2011), with drivers of change very similar to those affecting the rest of the UK. Urban expansion due to population increases has occurred over recent decades, particularly in southeast Wales and agricultural practices have a large effect on the landscape. Commercial timber plantations result in dynamic changes in forest cover as harvesting and replanting occur. Similarly, Wales is impacted by flooding and in recent years significant land cover change has occurred due to the biophysical driver of larch disease (*Phytophthora ramorum* Chadfield & Pautasso 2012). Timely and accurate extent and change information on these phenomena are important for national and regional management and planning practices.

Information on the types and drivers of change, at spatial scales from global to regional, is vital for a variety of effective monitoring, management, and policy development and implementation practices (*Change detection techniques* 2009, Lillesand et al. 2015). For example monitoring of forest change alone can relate to deforestation (Kerr & Ostrovsky 2003), flooding (Apollonio et al. 2016, Sterling et al. 2012, Wissmar et al. 2004, Yoon et al. 2003), carbon stock (Bagan & Yamagata 2014, Fuchs et al. 2016, Sohl et al. 2012, Zhao et al. 2009, 2010, 2013) and natural disaster (Bourgeau-Chavez et al. 2002, Epting et al. 2005,

Lupo et al. 2001, Wulder et al. 2009) responses and policy. It is equally important that these data are of a high Temporal Resolution, accurate, and can be produced in a timely manner (Jong et al. 2017, Mekasha et al. 2014). The spatio-temporal patterns of land-use change can be documented using satellite imagery and Earth Observation (EO) practices. EO satellites provide cost-effective, consistently measured, relatively high spatial and temporal resolution data acquired at a scale appropriate to a range of management and policy applications, such as those previously identified (Hester et al. 2010, Masek et al. 2015, Tewkesbury et al. 2015). EO data allows researchers to study the causes and results of land cover and land-use change in relation to natural and anthropogenic effects (Cardille & Foley 2003). Therefore, land cover and land use Change Detection has been an important area of research in Remote Sensing (RS) and EO analysis since the 1970s (Lo & Shipman 1990).

RS describes the science of obtaining information about an object, area, phenomenon, etc. without coming into direct contact with the object (Lillesand et al. 2015). Typically, this means recording the electromagnetic spectral properties of the surface of an object. RS information collected from satellite platforms provides a vast amount of data on the nature of the Earth's surface (Lillesand et al. 2015). RS satellite imagery, or EO data, is a powerful tool for determining the reasons for and consequences of land use and land cover changes (Cardille & Foley 2003, Lillesand et al. 2015). The increasing volume of satellite data available since the 1990s represents an archive of data of changes in the Earth's surface. Furthermore, the digital format of the majority of this data makes it easy to analyse over larger areas than field studies, with computer image processing. Therefore, RS and EO are useful tools for land cover change

detection, monitoring, and management. The process of detecting and analysing land-cover change is commonly referred to as 'change detection' (Singh 1989*b*, Coppin & Bauer 1996). Change detection has been defined as 'the process of identifying differences in the state of an object or phenomenon by observing it in different times' (Singh 1989*b*).

RS techniques and EO data have been used to study the types of land cover changes outlined. Researchers have studied many types of natural and anthropogenic changes at regional, national and global scales. For example, the crop rotation of agriculture (Macleod & Congalton 1998), urban expansion (Luo et al. 2018) deforestation assessments (Smith et al. 1999, Kerr & Ostrovsky 2003, de Espindola et al. 2012, Marquardt et al. 2019), and land degradation detection (Metternicht et al. 2010, Yiran et al. 2012, Dubovyk 2017) A focus of RS research has been delineating LCC on local and global scales by combining multi-temporal data from different RS sources (e.g. satellite and aerial photography).

Prior to satellite RS data, surveys to assess land cover change were field-based, expensive, and uncommon. Additionally, these surveys used methods of recording and thematic classes, which are not directly comparable, making LCC difficult to characterise. RS techniques and EO data can be combined with this type of ancillary data to provide change information. This involves combining mapped data with a manual interpretation of recent EO data such as aerial photographs or satellite imagery. Adding RS data represents a significant increase in efficiency over field-based change detection approaches, which are often expensive and have a significant date lag between a change occurring on the ground and being detected. The mapped data could take the form of an existing RS dataset, for example combining Coordination of Information on the Environment (CORINE)

Land Cover Classification map data with delineated change from satellite and aerial photography (Thomson et al. 2007, Cole et al. 2018).

Change detection studies commonly combine two or more RS datasets acquired at different dates to detect change. Change is detected by direct comparison of the spectral data using a change detection algorithm or the differencing of classified data where the spectral responses have been grouped or classified representing different land covers. These images need to be free of noise, phenological differences (e.g. trees are a different colour due to deciduous nature not due to change), and illumination angle differences (e.g. shadows) for change detection processes to work effectively (Du et al. 2002, Song et al. 2001, Wang & Xu 2010). These restrictions could result in the time step between imagery being several years, causing a low temporal resolution of change detection or the acquisition date being different in parts of a study area, 'blurring' the temporal resolution, and possibly leading to inconsistencies across the study region (Lindquist et al. 2008, Lück & van Niekerk 2016).

However, recent increases in data volume (reduced revisit periods) and availability (more free and open data) has led to the development of approaches, which use the dense Time Series and large numbers of images to track trends and model breaks in a signal to identify land cover changes. These approaches are potentially powerful early warning systems of land cover change or degradation (Verbesselt et al. 2010). These dense time series approaches use an increased data volume to reduce the effect of noise and allow change identification at a higher (sub-annual) temporal resolution. Dense time-series methods produce a signal from the values of each pixel at each time step. Change features are located by documenting differences between this signal and a reference signal or

model of expected values (Bontemps et al. 2012, 2008, DeVries et al. 2015, Eckert et al. 2015, Schmidt et al. 2015, Verbesselt et al. 2012, Zhu & Woodcock 2012). These metrics can be used to generate a land cover classification for each time step (Zhu & Woodcock 2014). Studies using these approaches focus on present monitoring or recent history. The fragmented nature of most RS archives means it is unlikely that there is a sufficient volume of historical data to identify past change using these approaches. Additionally, the high computation expense of generating time series models typically limits the study area to less than $1000km^2$, although some dense time series approaches are viable over a larger area. However, larger study areas are needed to detect global changes for example producing baseline and subsequent forest cover change for initiatives like Reducing emissions from deforestation and forest degradation (REDD++) (Bontemps et al. 2008, Zhu & Woodcock 2012, Cai & Liu 2015, Hermosilla et al. 2015, Schultz et al. 2016, Hamunyela et al. 2016, Tang et al. 2019).

Going forwards in time it is likely that these approaches will become increasingly important in modeling and monitoring land cover change and signals. However, it is unlikely there is an adequate volume of historical data to establish past signals and model historical changes to inform current management (Ju & Roy 2008). Additionally, generating a time series model is computationally expensive and could be difficult at a continental or global scale. In light of these challenges a different approach, better able to exploit the plethora of historic EO data to generate accurate land cover and land cover change data products is needed. This approach must (i) not have data volume requirements, (ii) able to handle noise inherent in RS data, and (iii) computationally efficient to be able to automatically produce high temporal resolution land cover change data over large areas through

history.

The 'Map-to-Image' change detection approach, applied by Thomas et al. 2018 to map mangrove forest extent, has the potential to fit these characteristics. Similar to previous change detection work, which combines ancillary and RS data, the 'map-to-image' change detection approach combines a base map and EO satellite image data to detect change features (i.e. map-to-image change detection). However, unlike these studies, the EO satellite image data are not manually interpreted, instead, the spectral reflectance in the EO data are analysed to locate likely change features. The satellite image data are subset based on their spatial location within different mapped classes or regions, for example in Thomas et al. 2018's study, all the data mapped as mangrove regions were extracted. In this subset, the distribution of the extracted mangrove values is expected to be normal or Parametric, with any deviations being the result of land cover changes between the mapped data and image acquisition date. This 'parametric distribution map-to-image change detection' approach assumes that the majority of the values within a single class are close to the median, as the land cover response is homogeneous, and that any values from change features are far from the median towards the tails of a distribution. A threshold for change features can be identified by iteratively removing the tails of a distribution (moving from tails towards the median) until the distribution is most normal based on the skew and kurtosis statistics of the extracted data's frequency histogram. The image data value at the iteration where the combined lowest skew and kurtosis is reached is selected as the change threshold and applied to threshold the image data into change/no change features. Thomas et al. 2018 found the approach produced change detection accuracies in excess of

80%, with confidence intervals at 99% likelihood, demonstrating that the method can successfully detect changes in mangrove extent.

1.2 Rationale

The 'parametric distribution map-to-image change detection' approach has the potential to meet all three of the criteria identified as gaps in current RS change detection approaches. It is automatic, computationally efficient, and has no data volume requirements, it is theoretically equally applicable to a base map and a single image as a base map and time series of image data. If applied on a per-class basis, this approach could form part of a historic LCC detection and monitoring system. The change detection output is a set of change and stable features, these can be used to provide training regions for a Machine Learning classifier to identify the updated land cover class of change features and produce a new map. The updated classification could then form the map input into the next iteration (time step) in a monitoring system (Figure 1.1).

However, research is needed to test the approach:

1. When applied to a time series of historic and current EO image data. In particular, how the length and data volume of the time series may impact accuracy.

2. In a temperate region and on land covers which are both dynamic and stable.

3. To remove the assumption that change class is homogeneous and has a parametric distribution, by testing different analysis approaches for change identification.

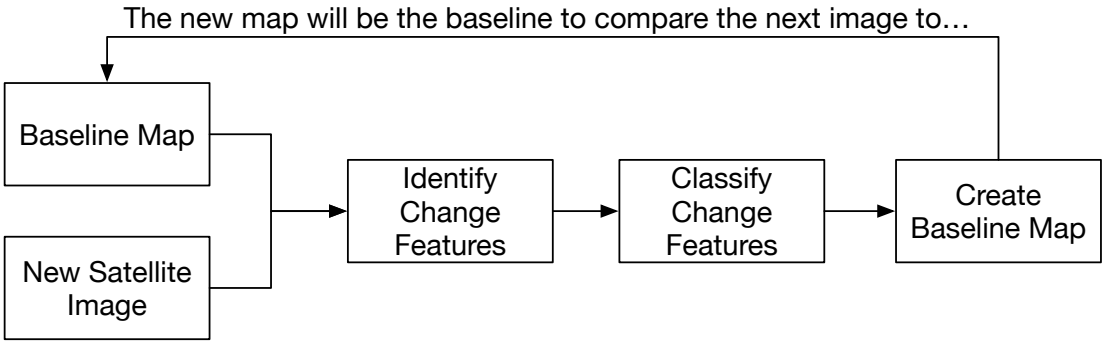

Figure 1.1: Processing chain for map-to-image monitoring system

This approach could be adapted and applied to non-parametric land cover classes to detect change in dynamic and stable land cover from a fragmented time series with high accuracy. It represents a possible solution for generating an automatically updating 'living map' of land cover classification. This system is capable of outputting a series of maps and change date of land cover changes and extents from both historical and current image data. Therefore, it is important the potential of the method and each of the research areas identified above are properly addressed and tested.

Wales, UK was selected as a study site to research the proposed monitoring approach and test different analysis approaches to identify change. Wales was selected for three reasons:

1. Welsh land cover is controlled by natural and anthropogenic drivers of change. There are several dynamic classes (e.g. conifer forest plantations) and some more stable land covers (e.g. agriculture extent and bracken). This allows different types of change to be studied in a relatively small area.

2. The Welsh EO image data archive covers a near 27 year period but is

fragmented. As Cloud Cover in Wales is persistent, and historical imagery has not always been stored, the length of time between images and the volume of imagery within a given period is highly variable. This allows for study of how change detection and map accuracy is impacted by different data volumes and time steps.

3. The Landsat archive for Wales has already been downloaded and atmospherically corrected, reducing the pre-processing required to test changes to the approach

1.3 Aims and Objectives

The aim was to assess the 'map-to-image' change detection technique as a component of a monitoring system for Wales, that utilises and generates a time series of accurate multi-class land cover classification maps and change detection statistics. To address this aim, different approaches for identifying likely change features, which do not assume class distribution (unlike the 'parametric distribution map-to-image change detection' approach) were developed. Analysis and description of the approach limitations, assumptions, and inaccuracies was also undertaken.

To achieve this aim the following objectives were laid out:

1. Determine if the 'parametric distribution map-to-image' change detection approach (Thomas et al. 2018) can accurately detect land cover change in another forest type in a temperate region (currently only tested on tropical mangroves).

2. Ascertain if the approach can be applied to a fragmented time-series of imagery to accurately map land cover and classify change as part of a monitoring system.

3. Develop a new way of identifying change features which removes the assumption that change class has a parametric (normal) distribution, without a significant loss in accuracy.

4. Determine if this approach can accurately detect multiple types of land cover change at one time-step on a full land cover classification. Could this approach be used to generate an automatically updating 'living map'?

1.4 Thesis Structure

This thesis is divided into 9 chapters. The first introduces land cover change detection EO data and the RS context and importance of the research. The aim being to produce land cover and change maps for Wales as part of an automated monitoring system. A literature review of the characteristics of a good monitoring system and the strengths and weaknesses and potential developments of current RS change detection approaches are presented in Chapter 2. This chapter expands on the rationale presented in the introduction for selecting the 'parametric distribution map-to-image' change detection approach for development. It also provides a wider context of RS change detection approaches, practices, and accuracy assessments.

Wales, UK was selected as the study site due to the varied landscape of change and challenging, fragmented EO data. Information on the primary land covers,

key drivers of change, and the topographic and climatic features of Wales, UK are presented in Chapter 3. The challenges and volumes of the time series of EO data covering Wales is described in the next chapter. Chapter 4 also details the fragmented nature of the 27-year time-series of EO data was used to address the study objectives and the approaches used to pre-process this data before it was used to test the objectives.

The next three chapters, Chapters 5 through 7, address the objectives outlined in the previous section. The applicability of the 'parametric distribution map-to-image' change detection approach to non-mangrove classes is tested on coniferous forests in Wales, UK. The time series of imagery from 1990 until 2017, described in Chapter 4, was used to classify coniferous change features, from a single 1990 base map, as part of an automated monitoring system. The methods and results from this are presented in Chapter 5. Chapter 6 focuses on objective 3, removing the data distribution assumption from analysis so it can be applied to a greater variety of classes. A brief review of different statistical and classification approaches which could be used to identify likely change features is presented. This is followed by repeat analysis of these approaches on the same data as before to determine if there is a significant difference in accuracy. Objective 4 is addressed in Chapter 7, where the approaches developed in Chapter 6 were applied to a full land cover classification to determine if multiple land cover changes can be detected in a single map product and time-step.

In Chapter 8 the applicability and limitations of the approach are discussed. This chapter returns to the characteristics of a good monitoring system and the potential of other RS techniques outlined in Chapter 2, to describe where this work sits in the plethora of RS change detection techniques. Method limitations

and potential future developments and research which could address difficulties encountered during the study are presented here. Finally, Chapter 9 concludes the thesis by returning to the aims and objectives presented in the previous section and presenting the key findings of the study as answers to the questions presented. The accuracy, limitations, and applicability of the approaches developed as part of the study are summarised.

Chapter 2

Land Cover Change Detection Literature Review

2.1 Introduction

Monitoring of land cover change is vitally important for understanding and managing the impacts of environmental changes and anthropogenic activities (Kerr & Ostrovsky 2003, Gillanders et al. 2008, Van Lier et al. 2011). These changes can only be quantified by comparing data collected at different times (Singh 1989*a*, *Change detection techniques* 2009). Automating the collection and comparison process increases data volume and land cover monitoring potential. EO satellites can provide cost-effective data acquired at a high temporal resolution (daily – annual depending on the system and cloud cover) and at a meaningful scale for studying land cover dynamics (Hester et al. 2010, Hansen & Loveland 2012, Tewkesbury et al. 2015). There is no universal approach for using

EO data to detect land cover change, due to the large variety of data sources, types (radar, Optical Data etc.) and change detection applications.

2.1.1 Literature Review Aim

As the project is focused on monitoring land cover change, change detection techniques will be reviewed based on their ability to be integrated into an automatic monitoring system. This system must be: i) able to handle data from a variety of sources, ii) able to handle seasonal differences to increase temporal resolution, iii) able to generate useful change metrics from both historical and current data, iv) efficient so as not to require a large amount of time (compute or operator) to identify change in each image v) accurately represent change features on the ground without significant false positives (change identified when not present) or false negatives (change not identified when present).

2.1.2 Literature Search Method

As no specific EO database exists, the review was performed using the Web of Science database. Web of Science was selected as it is connected to numerous smaller databases, including conference proceedings, for peer-reviewed literature. The final search parameters (e.g., Land Cover AND Change Detection AND Map*) were developed using analytics, targeting the research fields: EO, RS, physical geography, and the environment. To ensure any examples given were current and up-to-date, the search for change detection approach examples were limited to articles published since the year 2000. Review articles and papers documenting any original approaches still in use published before 2000 were also used to provide

a broad overview of the field. Supplementary searches were conducted where the topic area was not covered by change detection articles (e.g. statistics on EO data availability).

2.2 Approaches for Land Cover Change Detection

Although no universal change detection approach exists typically change features are identified using one of five approaches; i) Manual; changes are identified by visual interpretation of the data. ii) Classified approaches; changes in classified land cover areas in thematic (similar spectral signatures grouped within classes) images building a matrix of land cover change. iii) Pixel Value (PV) approaches; significant changes in PV from the same location. iv) Satellite image time series methods; a PV signal is derived from a dense time series to identify changes. v) Biophysical parameter approaches; transform the EO data into a representation of a biophysical measure, comparing these measurements from different time periods.

2.2.1 Manual Approaches

Manual approaches are unique from other change detection techniques as they do not require a computing system for analysis beyond visualisation, instead change features are located using visual interpretation techniques. An operator digitises features they interpret to be a stable land cover or evidence of change, sometimes with the assistance of air photo interpretation manuals. Manual digitisation of

change areas typically produces change detection accuracies of over 80% (Fensham & Fairfax 2003, Benfield et al. 2005). However, this is dependent on the ability of the operator to recognise and delineate change features. For example, despite delineating 90% of the burnt area after forest fires in Canada (1992 & 1996) and Russia (1997) Bourgeau-Chavez et al. (2002) only identified 60% of individual burn events, suggesting that only large-scale features were identified.

However, Benfield et al. (2005) used intimate knowledge of local land cover characteristics in Panama to distinguish mangroves from other forest types, which may have been confused if reliant on spectral differences, with an overall accuracy of 83%. Thomas et al. (2017) documented global changes in mangrove extent between 1996 and 2010 based on contextual identification of change signatures, such as straight edges forming aquaculture ponds. Additionally, manual techniques may be the only viable approach when studying change over long time periods using traditional OS maps and newer imagery.

In some situations, manual techniques may be the only viable change detection approach. However, the high number of operator hours and lack of reproducibility means that manual approaches are not well suited for automatic or high temporal monitoring of change over large areas.

2.2.2 Classification Approaches

Identifying changes by comparing classified land cover types, Post Classification Comparison (PCC) change detection is an intuitive and common method of identifying land cover change (Swain 1976). PCC is typically used to monitor landscape change dynamics from and to classes or a class of interest (Table 2.1),

particularly deforestation and urbanisation (Renó et al. 2011, Griffiths et al. 2012, Son et al. 2015, Souza-Filho et al. 2015). Image Classification is a significant area of RS research and ample subject for a dedicated literature review. (Phiri & Morgenroth 2017, Gavade & Rajpurohit 2019). However, the majority of classification approaches use a set of labelled training data and measure the similarity of the unlabelled pixels to each of the training classes. The similarity or thresholds to split the data are determined by the classification algorithm. Common classification algorithms including; Support Vector Machines (SVM) (Boser et al. 1992) or a type of Random Forests (RF) classifier (Breiman 2001). The inclusion of thematic land cover data produces land cover dynamics data (from-to change matrix) and classifications which can provide more information about the nature of change occurring (Coppin et al. 2004). For example, Baumann et al. (2012) documented forest and agriculture dynamics in eastern Europe (1985-2010) useful for historical documentation and future land management practices.

PCC assumes that each land cover classification accurately represents the land cover of the site both geometrically (shape, size, edge, and position of the classified land cover) and thematically (classification of the land cover class; Coppin et al. 2004, van Oort 2005, *Change detection techniques* 2009). A significant source of error in PCC is that it is assumed that the classes are well defined with little confusion, so any change between classification maps is the result of true change on the ground, not differences in the classifier at each time step. Errors can be created by differences in the classifier and imagery used at each time step. As differences between classifications are used to identify land cover changes, any inaccuracies in the initial classifications are compounded in

Table 2.1: Example studies using classification change detection techniques. Information about and a reference for each of the studies is given in the table. The location, length of time change was detected over, method variations and accuracy statistics (these statistics are not comparable)

*BAY = Bayesian, PCC = post classification comparison, PCC+ = Post Classification Comparison hybrid, MRF = Markov Random Fields Model.

Region	Period of Change	Classification Accuracy (%)	Change Detection Accuracy (%)	Change Detection Method*	Data Mining (Y/N)	No of Images	Study Area	Reference
Quebec, Canada	2013-2014	93	78	BAY	N	11	39,600 km^2	Cardille & Fortin (2016)
West Russia	1985-2010	95	93	PCC	N	12	-	Baumann et al. (2012)
North Central USA	1980-2000	85	-	PCC+	N	-	417,385 km^2	Bergen et al. (2005)
Bochum, Germany	1986-2011	82	-	PCC	N	4	145 km^2	Henits et al. (2016)
Paraguay	1990-2001	91	90	MRF	N	2	6,761 km^2	Liu et al. (2008)
Itacaiúnas River watershed, Amazon	1984-2013	96	-	PCC	N	20	-	Souza-Filho et al. (2015)
Rondonia, Amazon	1984-2000	-	-	PCC+	Y	6	-	Frohn & Hao (2006)
Lower Amazon Floodplain	1970-2008	86	80	PCC+	N	16	600 km	Renó et al. (2011)
Carpathian Mts	1987-2000	93	-	PCC	N	2	185 km^2	Kozak et al. (2007)
Nile Delta	2001-2010	96	-	PCC	N	9	-	Aide et al. (2013)
Rondônia, Amazon	1984-2002	-	-	PCC	N	19	900 km^2	De Barros Ferraz et al. (2005)
Chihuahua, Mexico	1999-2006	88	77	PCC	N	2	8,405 km^2	Aguirre-gutiérrez et al. (2012)
Klias Peninsula, Malaysia	1985-2013	92	97	PCC	N	3	-	Kamlun et al. (2016)
Beijing, China	2000-2005	-	88	CVAPS	N	2	24 km^2	Chen et al. (2011)
Italy	1996-1997	-	-	BAY	N	2	-	Castellana et al. (2004)
Xingi-Iriri watershed, Amazon	1997-2004	-	94	PCC+	Y	2	150,000 km^2	Silva et al. (2008)
USA	1999-2004	93	90	PCC	N	2	-	Zhou et al. (2008)
Andes	1987-2001	-	78	PCC	Y	2	2,141 km^2	Kintz et al. (2006)
Italy	1996-1997	-	97	BAY+	N	2	-	Castellana et al. (2007)
Guangzhou, China	1998-2003	89	-	PCC	N	4	21,388 km^2	Fan (2008)
Atlanta, USA	2000-2010	90	-	PCC	N	6	-	Liu & Yang (2015)
Chihuahua,Mexico	1999-2006	86	-	PCC	N	2	8,405 km^2	Aguirre-gutiérrez et al. (2012)
Shanghai, China	1979-2009	-	75	PCC	N	4	7,038 km^2	Yin et al. (2011)
Megacities	1975-2010	74-93	-	PCC+	N	114	-	Taubenböck et al. (2012)
Greater Dhaka, Bangladesh	1975-2003	85-90		PCC	N	-	-	Dewan & Yamaguchi (2009)
Northwestern Coast, Egypt	1987-2001	91	-	PCC	N	2	3,750 km^2	Shalab & Ryutaro (2007)
Minnesota, USA	1986-2002	90	80-90	PCC+	N	8	7,700 km^2	Yuan et al. (2005)
Tema, Ghana	1990-2010	-	-	PCC	N	3	366 km^2	Mariwah et al. (2017)
Central USA	1977-2008	77-96	81	MRF	N	4	7,038 km^2	Liu & Cai (2012)
North Carolina, USA	2002-2005	89	-	PCC+	Y	2	71 km^2	Hester et al. (2010)
Candarli Bay, Turkey	1990-2005	-	-	PCC	N	2	105 km^2	Kesgin & Nurlu (2009)

the change product. False positives (objects classified differently when no change has occurred) and false negatives (objects classified the same when change has occurred) can be caused by this propagation of error (Singh 1989*a*). The product accuracy, typically over 82% (Bergen et al. 2005, Kozak et al. 2007, Silva et al. 2008, Fan 2008, Hester et al. 2010, Renó et al. 2011, Baumann et al. 2012, Souza-Filho et al. 2015, Liu & Yang 2015, Cardille & Fortin 2016), is restricted by quality of the original classifications. Accuracy reporting should not focus on the accuracy of these classifications, but on the change, features identified. Although the classification accuracy is an important indicator of change feature accuracy it is not the same or comparable with identifying the accuracy of the change features directly.

Generating accurate land cover classifications requires operator hours. This requirement restricts the feasible temporal resolution of the analysis. Studies using PCC do not often perform analysis at a sub-annual or annual resolution (Table 2.1; Bergen et al. 2005, Kozak et al. 2007, Silva et al. 2008, Kesgin & Nurlu 2009, Fan 2008, Hester et al. 2010, Renó et al. 2011, Chen et al. 2011, Baumann et al. 2012, Souza-Filho et al. 2015, Liu & Yang 2015, Cardille & Fortin 2016, Mariwah et al. 2017). The large number of operator hours and possible propagation of error through a time series are important limitations in the application of PCC as part of an automated monitoring system.

Much PCC research focuses on reducing the propagation of error, the majority of which manifests as 'slivers' of false change at the edges of land cover features. 'Slivers' are the result of pixels containing more than one land cover (mixed pixels) or geometric misalignment (Serra et al. 2003). Multi-date segmentation reduces the appearance of 'slivers' (Desclée et al. 2006, Duveiller et al. 2008). Propagation

of error can also be reduced by introducing fuzzy logic to quantify class uncertainty as a change feature where in both maps the class ownership is uncertain is likely to be a false positive and can be removed (Hester et al. 2010).

Another approach to reducing error propagation is the use of multiple classifiers with uncorrelated error to record change indicated in both images (Kittler et al. 1996, Bruzzone et al. 2004). Temporal correlation approaches, like Markov Random Field Model or Bayes Logic, uses the temporal order of thematic classes to assign a probability to detected change (Castellana et al. 2004, Liu & Zhou 2004, Benedek et al. 2015, Cardille & Fortin 2016). For example, applying Bayes logic could result in changes from forest cover to urban being given greater weight than a change from urban to forest. When Bruzzone et al. (2004) compared PCC and Bayesian techniques a 3-4% increase in overall accuracy was recorded when applying an Bayesian approach (Table 2.1).

Probability is also used to improve accuracy in Change Vector Analysis (CVA) in Posterior Probability Space, an approach that compares classifications using the probability of each pixel belonging to each land cover class. Change Vector Analysis in Posterior Probability Space (CVAPS) requires the determination of a supervised or unsupervised threshold of change in the posterior probability space to identify likely change features (Chen et al. 2011). Chen et al. (2011) tested CVAPS on two Landsat images from April 2000 and July 2005 of Shunyi District, Beijing. CVAPS produced change data with an overall accuracy of 88-89%.

Many studies of PCC detection accuracy compare pixel or object-based analysis (Zhou et al. 2008, Hussain et al. 2013, Lv et al. 2017). However, those which compare different classification-based approaches indicate that these additions (e.g. bayes logic) improve change detection accuracy (Bruzzone et al. 2004,

Hester et al. 2010, Chen et al. 2011). However, statistical tests of the significance of the improvement (e.g., McNemar's test) are not often performed. It is unlikely that improvements reported at 1-3% are significant. Therefore, in most cases, PCC is sufficient, especially as more complex approaches require some combination of increased training data or parameterisation, which can be undesirable in an automated monitoring system.

The number and complexity of classes that can be accurately identified are limited by their spectral separability, especially in multispectral imagery (Sesnie et al. 2010, Fernandes et al. 2012). Therefore, changes in areas of individual vegetation species, types of buildings, or defoliation due to disease cannot be easily or likely accurately identified. Although homogeneity can help increase separability, for example in commercial forest stands where age and species of large blocks of forest are the same, the problem is often more complex. Continuing the previous example, healthy conifer species may have a similar spectral signature to unhealthy broadleaf trees (Xiao & McPherson 2005). Therefore, it is often the case that defoliation, disease, changes to species-area, and type of urban growth cannot be easily identified using PCC methods in the majority of scenarios.

Independent analysis of Thematic Data provides several possible advantages over PV data comparison when used in a monitoring system: (i) analysis is independent of uncertainty introduced by errors in Atmospheric Correction (Coppin et al. 2004); (ii) different sources of data (e.g., optical and radar) acquired during different seasons can be introduced into the analysis, increasing potential temporal resolution (Serra et al. 2003). If consideration is given to ensure the classes have a 1:1 correspondence with each other, mixing datasets,

sensors and seasonality can add valuable complexity and improve understanding of land cover dynamics. However, the majority of studies acquire all data from the same source and season. This is likely due to the number of operator hours required to ensure correspondence (Serra et al. 2003) and generate classifications. If PCC could be conducted without the high operator hour requirements of current approaches it has many useful characteristics (e.g., reduced radiometric requirements, ability to combine multiple sources and seasons) and outputs (e.g., from-to matrix, land cover classifications) for and automatic land cover monitoring system.

2.2.3 Pixel Value Approaches

Another method of identifying land cover changes is by comparing the PV in images acquired at different times. The PV could be Reflectance or radar backscatter. Identification using PV assumes that the signature from an unchanged land cover is constant through time (Du et al. 2002, Wang & Xu 2010). Therefore, a significant transformation in an object's data, identified using a threshold, is likely due to land cover change occurring between the two image acquisition dates. PV are typically used to detect changes within a region or land cover type of interest (e.g. defoliation or disease spread in vegetation; Thomas et al. 2007, Dennison et al. 2009, Babst et al. 2010). This represents a potential advantage over classification-based approaches. However, unpicking true changes from seasonal or other conditional variation can be difficult and without thematic information, the nature of change is hard to determine.

By detecting change/no change features only, PV change detection accuracy

Table 2.2: Example studies using changes in pixel numbers between dates to characterise change features. Provides information on accuracy, type of data input, the approeach used. Accuracies are not directly comparable.

* SID = Image differencing, CVA = Change Vector Analysis, PCA = Principal Component Analysis, ICVA = Improved Change Vector Analysis, MCVA = Modified Change Vector Analysis, CVA+ = Other Variation of Change Vector Analysis.

+ P = Pixel, O = Object.

O = Optical, I = Indices, T = Transformed Data, R = Radar.

Region	Period of Change	Change Detection Accuracy (%)	Change Detection Method*	Object+	Data Type #	No of Images	Study Area	Reference
Fennoscandia, Sweden	1986 & 1994	-	SID	P	O	4	-	Babst et al. (2010)
Interior Alaska	1999 – 2001	-	SID	P	I	2	-	Epting et al. (2005)
Beijing Region, China	2000 – 2008	78	ICVA	P	O	4	55,775 km^2	Chunyang et al. (2013)
Lower Pearl River Valley, USA	Apr – Aug 05	78	SID	P	I	2	-	Wang & Xu (2010)
Lower Pearl River Valley, USA	Apr – Aug 05	86	PCA	P	I	2	-	Wang & Xu (2010)
Lower Pearl River Valley, USA	Apr – Aug 05	80	CVA	P	I	2	-	Wang & Xu (2010)
Basilicata, Italy	1984 – 2010	91	SID	P	I	2	-	Mancino et al. (2014)
El Rawashda forest, Sudan	2003 – 2006	84	PCA	P	O	2	78,000 km^2	Nori et al. (2009)
El Rawashda forest, Sudan	2003 – 2006	71	CVA	P	O	2	78,000 km^2	Nori et al. (2009)
Italy	1995 – 1996	96	CVA	P	O	4	-	Bovolo et al. (2012)
New England Tablelands, Australia	2007 – 2009	96	PCA	P	O	6	34,200 km^2	Sinha & Kumar (2013)
New England and Savannah River Basin, USA	2001 – 2002	90	SID+	P	O	68	370 km^2	Xin et al. (2013)
Lake Garda, Italy	Apr – May 94	96	SID+	P	O	2	185 km^2	Bruzzone & Serpico (1997)
Himalayas, India	2010 – 2011	70	CVA	P	O	2	-	Singh & Talwar (2014)
Himalayas, India	2010 – 2011	86	ICVA	P	O	2	-	Singh & Talwar (2014)
Himalayas, India	2010 – 2011	82	MCVA	P	O	2	-	Singh & Talwar (2014)
Mississippi, USA	1972 – 2002	82	MCVA	O	I	8	4,939 km^2	Wilkinson et al. (2008)
Mississippi, USA	1972 – 2002	77	MCVA	P	I	8	4,939 km^2	Wilkinson et al. (2008)
Mississippi, USA	1972 – 2002	73	MCVA	O	T	8	4,939 km^2	Wilkinson et al. (2008)
Mississippi, USA	1972 – 2002	72	SID	P	I	8	4,939 km^2	Wilkinson et al. (2008)
Mississippi, USA	1972 – 2002	71	SID	P	T	8	4,939 km^2	Wilkinson et al. (2008)
Mississippi, USA	1972 – 2002	70	SID	O	T	8	4,939 km^2	Wilkinson et al. (2008)
Mississippi, USA	1972 – 2002	65	MCVA	P	T	8	4,939 km^2	Wilkinson et al. (2008)
Mississippi, USA	1972 – 2002	63	SID	O	I	8	4,939 km^2	Wilkinson et al. (2008)
Mississippi, USA	1984 – 1999	-	MCVA	P	T	3	421 km^2	Nackaerts et al. (2005)
Beijing, China	2010 – 2014	86	CVA+	P	O	2	-	Chen & Chen (2016)
Beijing, China	2012 – 2013	88	CVA+	P	O	2	-	Chen & Chen (2016)
Pearl River Delta, China	2013 – 2017	98	CVA	P	O	2	144 km^2	Xu et al. (2018)
Yushu County, China	2015 – 2017	87	PCA	P	R	2	-	Li et al. (2018)
North Rhine- Westphalia, Germany	2009 – 2010	95	CVA+	P	O	2	8.25x4.25 km^2	Thonfeld et al. (2016)
Beijing Region, China	2004 – 2007	90	CVA	P	T	2	-	He et al. (2011)

assessments are based on determining if change features identified are true change or the result of noise. The assessments also determine if all change features on the ground have been identified. As all change types have different alterations in PV response, the accuracy figures from different change detection studies are not typically comparable. PV research focuses on reducing noise relative to change and determining the best threshold of difference in PV between images for identifying change features. There are two main areas of research for improvement: i) manipulating pixel values to exaggerate the differences the land covers of interest and ii) developing new approaches to better identify the threshold at which the differences between the pixel values of the two images most accurately indicates change.

Data transformation can be used to reduce false positives by reducing differences due to different sensors (Nackaerts et al. 2005, He et al. 2011). However it is often used to exaggerate the differences between healthy and unhealthy vegetation. For example, the Tasseled Cap (TC) transformation (Kauth & Thomas 1976) increase information by rotating the data axes to better represent the differences in vegetation greenness, brightness or wetness, which are related to productivity (Healey et al. 2006, 2005, Masek et al. 2008, Zhu et al. 2012). A Disturbance Index (DI), calculated using a linear, scaled transformation of the three TC transformations, has more recently been developed to locate large area forest disturbance. However, Vegetation Index (VI) are more commonly used to maximise vegetation signal (Table 2.2). Short-wave Infrared (SWIR) and red bands best represent vegetation disruption. Combining these bands in a simple or normalised ratio (e.g., Normalised Difference Vegetation Index (NDVI) or Soil Adjusted Vegetation Index (SAVI)) is an established method of representing

vegetation productivity (Table 2.2; Myneni et al. 1995). The difference in accuracy between change detected using VI and transformations is small, Wilkinson et al. (2008) recorded a less than 2% disparity in his comparisons on Landsat images covering a 4,939 square kilometers area of east-central Mississippi. Additionally, VIs are simple to calculate and are available in analysis-ready products (e.g. Moderate Resolution Imaging Spectroradiometer (MODIS) and NDVI), both desirable qualities for a monitoring system (Epting et al. 2005, Wilkinson et al. 2008, Wang & Xu 2010, Mancino et al. 2014).

There are numerous approaches for identifying land cover change using digital values. The least complicated approach is Simple Image Differencing (SID). SID applies a user-generated threshold to an image populated with a calculation of the ratio or differences in values between two time steps. The threshold can be generated manually or automatically using the difference or ratio image's parametric histogram. The accuracy of SID is dependent on the success of noise reduction pre-processing techniques (e.g. radiometric correction) and the selection of the threshold at which change is identified (e.g. deforestation is easier to detect than defoliation because the difference in Spectral Signature is much greater). The optimal parameters for change detection can vary between image acquisitions, which is undesirable in an automated monitoring system as product accuracy could not be assured. This might require the removal or reprocessing of low accuracy time steps, decreasing potential temporal resolution and system efficiency.

The majority of the studies in Table 2.2 use some variation of CVA (Malila 1980). Generally, CVA approaches identify change as a function of an object's spectral reflectance within the feature space and the vector which connects these features.

The angle and length of the vector are described as direction and magnitude. A threshold is applied to the direction and magnitude metrics to identify change features. CVA research alters the input data (e.g., TC transformation (Rene & Barbara 2008), RCVA (Thonfeld et al. 2016), expanding to n-dimensions (Warner 2005) or the threshold location process (e.g., training samples (Allen & Kupfer 2000), double-window flexible pace search (Chen et al. 2003, Sharma et al. 2013), pixel kernel window (Varshney et al. 2012), spectral angle mapper (Osmar et al. 2011, Zhuang et al. 2016, Salih et al. 2017) and cross correlogram (Chunyang et al. 2013). The many variations of CVA are ample subject for a separate review (e.g. Singh et al. 2014). Therefore, only the most commonly applied approaches are discussed here (Table 2.2). Change detection comparison studies have found that Improved Change Vector Analysis (ICVA) (Hoffmann 1975) or Modified change vector analysis (MCVA) (Nackaerts et al. 2005) can increase change detection accuracies by 10% (Wilkinson et al. 2008, Singh & Talwar 2014). In particular, MCVA has produced statistically significant increases in accuracy over CVA when detecting forest change.

Principal Component Analysis (PCA) can also be used to transform the image data into a series of interrelated variables which retain as much variation as possible from the original imagery. When PCA is applied to the combined images; areas with high correlation are assumed to be unchanged and areas with low correlation represents the changed areas (Deng et al. 2008). PCA often produces accuracies of over 80% (Deng et al. 2008, Wang & Xu 2010, Sinha & Kumar 2013, Li et al. 2018). PCA approaches are relatively simple to implement and are included in many industry-standard software packages, making them particularly useful for quickly identifying the effects of natural disasters (Li et al. 2018).

These approaches all assume that any significant changes in the PV are the result of land cover change (Du et al. 2002, Wang & Xu 2010). Therefore, accuracy is limited by other possible causes of change, which can include: i) changes in sensor calibration ii) noise and iii) any seasonal changes a land cover may exhibit. False Positives created by seasonal changes limit the temporal resolution of this range of techniques to annual in locations where the vegetation exhibits a strong seasonal signal, representing a limitation to a monitoring system using these techniques beyond equatorial regions. Additionally, the effects of sensor and Atmospheric Noise makes it difficult to analyse to data from different sensors, potentially limiting temporal resolution.

2.2.4 Satellite Image Time Series Approaches

Time-series approaches make use of increases in EO data and computer processing power to produce a near-continuous signal of spectral data for a given land cover through time. Deviations in pixel response, independent of those produced by seasonal variation, indicate land cover change. The image acquisition dates provide high temporal resolution change data, allowing improved interpretation of the temporal variability of change features and potentially the consistency of the change events. The ability to identify and track change events at a sub-annual resolution is perfect for a monitoring system.

Currently dense time-series research focuses on identifying changes in vegetation including; tracking infestation or disease (Eklundh et al. 2009, Hird et al. 2016, Schroeder et al. 2017), deforestation (Bontemps et al. 2008, 2012, Huang & Friedl 2014, DeVries et al. 2015, Dutrieux et al. 2015, Verbesselt et al. 2010) and burn

events (Huang & Friedl 2014, Eckert et al. 2015, Schroeder et al. 2017). The literature identifies two broad approaches for identifying land cover change using a dense time series: i) analysis of fit to a reference signal and ii) breaks or trends in the time series. Both approaches report accuracies between 75% and 95% (Table 2.3). This is a range of reported figures only and as different data and changes are detected the figures are not comparable. Similar to PV approaches accuracy is characterised as a reflection of if a change has occurred on the ground however, in a trend-based time series approach there is an added dimension. The trends reported should be observable on the ground and the magnitude of change should be similar, a large-scale change such as a fire event in a forest should have a greater magnitude of change than an infestation where trees in the forest are diseased but still standing. The accuracy of change magnitude is not typically characterised by studies as it is complex to quantify.

A reference signal is the signal produced by an unaltered land cover (e.g. a sinusoidal curve with no annual variation in the sine and cosine from temperate vegetation; Azzali & Menenti 2000, Huang & Friedl 2014). It can be synthesised, observed, or an earlier subset of the same time series (Azzali & Menenti 2000, Huang & Friedl 2014). Different reference signals can also be generated for different types of land cover change (Huang & Friedl 2014), providing some information of the change process occurring, a useful feature of a monitoring system.

The distance or fit between the measured and referenced signal is used to identify likely change features. Mahalobis Distance, linear regression and the shape of actual and reference cross-correlogram (Bontemps et al. 2008, Wang et al. 2009, Huang & Friedl 2014) have been used to identify change features with comparable

Table 2.3: Examples of the accuracy, inclusion of seasonal variability, period and type of change studied using time series change detection techniques.

* Trend = changes in a seasonal trend, DiMet = distance metrics; distance from reference data set, Fit = level of fit with reference signal, Break = algorithm for identifying breaks in an established pattern.

+ O = Optical, I = indices, T = Transformed data.

Region	Period of Change	Seasonal (Y/N)	Change Detection Method*	Change Detection Accuracy (%)	Data Type +	No./Frequency of Images	Study Area	Reference
Southeastern Norway	2004 - 2005	Y	Trend	82	I	16 day	-	Eklundh et al. (2009)
Abisko, Sweden	2000 – 2013	Y	Trend	74	I	8 day	-	Olsson et al. (2016)
Mongolia	2001 – 2011	Y	DiMet		O	16 day	1200 km^2	Eckert et al. (2015)
Savannah River Basin, USA	2001 – 2003	Y	Fit	95	O	64	60 km^2	Zhu et al. (2012)
Rodonia, razil	2001 – 2004	N	DiMet	95	O	daily	500,000 km^2	Bontemps et al. (2008)
Kafa Biosphere Reserve, Ethiopia	1999 – 2012	Y	Break	73	O	monthly	165 km^2	DeVries et al. (2015)
Santa Cruz, Bolivia	2000 – 2014	Y	Break	87	O	-	40x50 km	Dutrieux et al. (2015)
Rondonia, Brazil	1984 – 2014	Y	Break	95	O	-	10,000 km^2	Hamunyela et al. (2016)
Santa Cruz, Bolivia	1984 – 2014	Y	Break	85	O	-	10,000 km^2	Hamunyela et al. (2016)
Queensland, Australia	1999 – 2011	Y	Break	94	O	97	-	Schmidt et al. (2015)
Dianchi Lake basin, China	1998 – 2000	Y	DiMet	90	O	-	306 km^2	Wang et al. (2017)
Southern Africa	1981 – 1991	Y	Trend	-	I	108	-	Azzali & Menenti (2000)
Spain	1989 – 2002	Y	Trend	-	I	10 day	-	Martínez & Gilabert (2009)
Yinan River Forest, China	2001 – 2009	Y	Trend	-	I	16 day	-	Kong et al. (2015)
Marovoay Watershed, Africa	2000 – 2007	Y	Trend	-	I	16 day	32.8 km^2	Jacquin et al. (2010)
Arctic	2000 – 2001	Y	Trend	-	O	-	-	Eastman et al. (2009)
southeastern Ohio, USA	2000 – 2012	Y	DiMet	-	I	16 day	800 km^2	Cai & Liu (2015)
southeastern Ohio, USA	2000 – 2012	Y	DiMet	-	I	16 day	800 km^2	Cai & Liu (2015)
Pacific Northwest, USA	1985 – 2007	Y	Trend	-	T	-	-	Kennedy et al. (2010)
Curragh mine, Australia	1989 – 2014	Y	Trend	85	T	56	123 km^2	Yang et al. (2018)
Saskatchewan, Canada	1984 – 2012	N	Break	92	O	28	651,900km^2	Hermosilla et al. (2015)
Australia	2000 – 2008	Y	Break	-	O	-	-	Verbesselt et al. (2013)
Palangka Raya, Kalimantan Province	2000 – 2012	Y	Break	-	O	277	-	Darmawan & Sofan (2012)
Paragominas, Brazil	2010 – 2013	Y	Break	85	O	83	550 km^2	Schultz et al. (2016)
Kafa, Ethiopia	2010 – 2013	Y	Break	75	O	108	530 km^2	Schultz et al. (2016)
Trabui, Vietnam	2010 – 2013	Y	Break	89	O	114	510 km^2	Schultz et al. (2016)
Vietnamese border, Cambodia	2000 – 2012	Y	Break	-	O	-	-	Grogan et al. (2016)
Rondônia, Brazil	2013 – 2015	Y	Break	93	O	-	185 km^2	Tang et al. (2019)
Pará, Columbia	2013 – 2015	Y	Break	93	O	-	185 km^2	Tang et al. (2019)
Australia	2000 – 2008	Y	Break	-	O	184	-	Verbesselt et al. (2010)
China	1999 – 2004	Y	Break	87	O	194	185 km^2	Zhu et al. (2016)

accuracy of >95%. Zhu et al. (2012) developed the Continuous Monitoring of Forest Disturbance Algorithm (CMFDA) which uses a magnitude approach to generate predicted reference values, allowing for the removal of inter-annual change effects. CMFDA is applied to the time series using a multi-image approach, where the differences between the predicted and observed data must be greater than a threshold in three subsequent images to be identified as change. CMFDA is an accurate detector of forest disturbance with a spatial and temporal accuracy of >94%.

Analysis of the data signal removes the need for the generation of complex reference data. These dense time series approaches can be broadly split into; i) spectral-frequency approaches and ii) statistical approaches. Spectral-frequency approaches identify the dominant variations or trends within a time series (e.g multi-resolution analysis-wavelet transform; Martínez & Gilabert 2009 and empirical mode decomposition; Kong et al. 2015). Statistical approaches attempt to identify changes in land cover dynamics (e.g. gradual trends and sudden shifts) during the time series. Statistical analysis techniques have been found to be marginally more accurate (Abbes et al. 2018) and are of greater use when analysing and monitoring land cover change. Statistical approaches include; Seasonal Trend Loss (STL); Jacquin et al. 2010, seasonal trend analysis (Eastman et al. 2009), sub-annual change detection (Cai & Liu 2015), and Breaks for Additive Season and Trend (BFAST); Dutrieux et al. 2015, DeVries et al. 2015, Dutrieux et al. 2015, Hamunyela et al. 2016, Verbesselt et al. 2010).

Comparing the accuracy of different dense time series approaches is complex and comprehensive studies are lacking (Abbes et al. 2018). However, where overall accuracy data are reported, figures range between 80 and 95%. For example,

studies using the BFAST algorithm, which has been largely applied to the tropics, report accuracies of around 85-94% (DeVries et al. 2015, Dutrieux et al. 2015, Hamunyela et al. 2016). It has been suggested that BFAST could be easily integrated into early warning systems to identify and monitor the spread of continuous changes (Verbesselt et al. 2010). Additionally, the metrics produced by BFAST can be used to generate a full land cover classification for each time step (Zhu & Woodcock 2014, Olofsson et al. 2014, Zhu et al. 2016, Hamunyela et al. 2016)

A major advantage of dense time-series change detection is the increased temporal resolution. As noise is ephemeral and land cover change is persistent, the impact of atmospheric and sensor noise on the accuracy of change detection is reduced. Dense time series approaches account for several of the limitations of digital value approaches and make use of the seasonal variation data. Using only bi-temporal imagery does not allow for the characterisation of temporary fluctuation and persistent change. Dense time series approaches facilitate the study of complex trajectories of land cover change. Land cover changes like insect infestation, disease, or illegal felling can be tracked in near-real time, enabling mitigation and management practices, perfect for a monitoring system.

A significant volume of data are needed to build up an established land cover signal either to produce a reference signal or to measure changes. The data for each pixel or object must be temporally dense enough to produce a meaningful time series. The effects of the volume or gaps in this data on change detection accuracy have not been widely studied. However, it seems unlikely that a meaningful identification of a trend or break point can take place where data volume is limited to a few or no observations in a year (Zhu & Woodcock 2012). In locations where present

or historic data are limited or cloud cover is high lower data volumes may reduce the applicability or accuracy of time series approaches. Cloud cover tends not to restrict studies where composite annual images are required but can represent an issue for some parts of the world (e.g., Northern Europe, Coastal Regions of Central Africa) when studying seasonal variability (Lindquist et al. 2008).

Time-series approaches are computationally expensive. The expense of generating and fitting time series models typically limits the study area to a single Landsat or MODIS scene (Table 2.3). However, monitoring studies and management practices (e.g. REDD++) routinely use baseline data at a national or regional level, limiting the applicability of dense time-series approaches to a monitoring system.

2.2.5 Biophysical Approaches

An alternative method of detecting change features is to transform the remotely sensed signal to a value that directly represents a biophysical parameter and measure the change between these values through time. There are numerous biophysical parameters that could be detected, but vegetation structure and soil moisture changes are commonly measured (Table 2.4). The accuracy of these studies can relate to the ability of any approaches to characterise true changes on the ground and also the ability of the RS signal to accurately reflect the biophysical parameter it is representing.

Radar Data RS has the capability to directly observe soil moisture on a global scale (Njoku & Entekhabi 1996). Radar data are also unaffected by cloud cover and solar illumination, meaning soil moisture data can be collected at a high temporal resolution anywhere in the world (Njoku & Entekhabi 1996). Global soil moisture

Table 2.4: Examples of the accuracy, change detection method, data and type of change studied using biophysical change detection techniques. The accuracy of different studies is not directly comparable.
IMG = image, FD = field data, DS = dataset.
* Comp = Comparison, Trend = Trend analysis.
+ O = Optical, I = indices, R = Radar.
ˆ VHR = very high resolution, FD = field data, REF = reference data, IMG = satellite image, DS = Ancillary dataset

Region	Period of Change	Reference Dataˆ	Change Detection Method*	Change Detection Accuracy (%)	Data Type +	No of Images	Study Area	Reference
Global	2000 - 2012	VHR REF	Comp	99	O	-	Global	Hansen et al. (2013)
Finland	2007	FD	-	-	O	8	-	Hadi et al. (2016)
Sundarbans Forest, Tropics	2000 - 2010	REF	Trend		O	-	-	Ishtiaque et al. (2016)
Landsat path-47, row-27 scene, Mongolia	2000 - 2005	REF	Trend	95	O	2	-	Sexton et al. (2015)
Burkina Faso, Africa	2012	VHR FD	-	-	O	2	100 km^2	Karlson et al. (2015)
USA	2007 - 2008	VHR	-	-	O	-	9.834 million km^2	Hansen et al. (2011)
West of Kahoma, Zambia	2000	VHR FD	-	-	O	11	-	Hansen et al. (2002)
Kasai-Occidental province, DRC	2000 - 2010	VHR REF	Comp		O	8881	2.345 million km^2	Potapov et al. (2012)
Southeast, China	2004	IMG	-	-	O	-	2,988 km^2	Bai et al. (2012)
Bangladesh	2000 - 2014	VHR REF	Comp		O	-	147,570 km^2	Potapov et al. (2017)
Tibetan Plateau, China	2002 - 2012	DS FD	-	-	R	-	-	Zeng et al. (2015)
Poyang Lake, China	2007 - 2008	IMG	Comp	93	R	-	4,000 km^2	Dronova et al. (2015)
Loess Plateau, China	2003 - 2007	DS FD	-	-	R	-	640,000 km^2	Feng et al. (2017)
Kruger National Park, South Africa	2015 - 2016	IMG FD	-	-	R	69	50 km^2	Urban et al. (2018)
Kruger National Park, South Africa	2015 - 2016	IMG FD	-	-	O	44	50 km^2	Urban et al. (2018)

data sets such as the National Aeronautics and Space Administration soil moisture product (NASA 2019), the Land Parameter Retrieval Model soil moisture product (VUA-NASA 2019), and the Japan Aerospace Exploration Agency soil moisture product (Japan Aerospace Exploration Agency 2019) are available at accuracies comparable to ground measurements (Zeng et al. 2015, Kim et al. 2015, Sun et al. 2016, Wu et al. 2016, Ullah et al. 2018). However, differences in the soil moisture algorithms mean care must be taken to ensure the algorithm used produces the most accurate results for the study site (Kim et al. 2015).

Additionally, the accuracy of soil moisture estimation is limited to areas with bare soil or low vegetation cover (Njoku & Entekhabi 1996, Dronova et al. 2015). This restrains many soil moisture change studies to sites of known land cover (e.g. global wetlands monitoring system; Jones et al. 2009). The other common

use of soil moisture data are to study the effects of a known land cover change on soil moisture dynamics. For example, studying the effects of; revegetation; (Feng et al. 2017), management schemes (An et al. 2017, Ye et al. 2019) or natural phenomenon (Urban et al. 2018, Sazib et al. 2018). The soil moisture data are used to provide data for further analysis (e.g. for modeling of land surface evaporation; Miralles et al. 2011, surface runoff prediction; Brocca et al. 2010 or modeling drought likelihood Sazib et al. 2018) rather than directly detecting likely land cover change features (e.g. ESA Climate Change Initiative; Hollmann et al. 2013). This could bolster the effectiveness and usefulness of a monitoring system for land managers.

However, vegetation structure metrics are used to both identify and study changes in vegetation cover, such as deforestation (Hansen et al. 2013, Potapov et al. 2012, 2017, Ishtiaque et al. 2016, Sexton et al. 2015) or defoliation (Ishtiaque et al. 2016). There are numerous biophysical parameters commonly used to monitor changes within areas of mapped forest (e.g. changes in above-ground biomass and carbon sequestration) and their detection is ample subject for a separate review (Lutz & Washington-Allen 2008). Therefore, only the canopy cover metrics, often used to indicate changes in the extent of forest cover, are discussed here.

One approach to generate canopy cover metrics is using Spectral Unmixing techniques to determine the percentage of vegetation cover in a pixel. Spectral unmixing uses endmembers, examples of pure spectral signals, to produce an estimate of the canopy cover within a pixel. The endmembers are sourced from the field (field spectroscopy), a library, or a signature within the image (Somers et al. 2011, Bai et al. 2012). These signatures need to be of high quality to ensure that the linear or non-linear unmixing process produces accurate results.

This process is time-consuming and the accuracy is limited by changes to the spectral signature caused by seasonality and noise. Therefore, most studies using spectral unmixing to produce vegetation cover percentages do so for only one-time step and do not apply change detection techniques

An approach more commonly used in change detection studies (Table 2.4) is to extrapolate a smaller dataset where the biophysical parameter of interest is known over a larger area represented by EO data. The reference dataset could be sampled in the field or RS data (e.g. operators identifying examples of 25%, 50%, 75%, and 100% canopy cover in high-resolution imagery). Regression (e.g. reduced major axis or regression trees; Cohen et al. 2003) or classifiers are used to correlate the two datasets. Hansen et al. (2013) used visual interpretation of very high-resolution imagery, global MODIS percent tree cover data, and a bagged classification model to identify forest extent change on a global scale at 30m resolution between 2000 and 2012. Results were disaggregated by reference percent tree cover stratum (e.g. >50% crown cover to 0% crown cover) and by year producing trends, metrics, and maps of change areas and forest cover (identified using trends in canopy cover percentage).

The addition of biophysical datasets to EO data can provide unique change data (e.g. Canopy cover can produce change data outside of forest stand areas and is better for this type of forest cover; Potapov et al. 2017). However, these approaches often require increased operator hours and the creation of a reference dataset (e.g. a library of spectra or field data; Hansen et al. 2014). These expenses often limit the change products to annual resolutions. Additionally, although possible, the process of automating biophysical data generation is more complex and potentially subject to the propagation of error (Sexton et al. 2015).

2.2.6 Hybrid Approach

Biophysical data are sometimes used in conjunction with land cover classifications and change datasets to study the effects of change, but the land cover change detection is performed using one of the previously described approaches. Different data sources (e.g. classified map and satellite image) can be combined to produce land cover change metrics.

The 'map-to-image' approach combines two different data sources; a thematic map and a satellite image to identify change features (Thomas et al. 2018). The approach uses a land cover classification as a 'baseline' to detect change from. It assumes that the signal from any unchanged land cover regions should be homogenous in nature. Therefore any deviance from this is likely the result of land cover change. Distribution statistics can be used to apply a threshold and separate likely change objects from the class whole. These regions can be reclassified automatically generating a new land cover classification. However, this subjects it to the same limitations as PN and classification approaches as it is unable to look at the time series as a whole identify trends events, or any changes within the land cover class.

2.3 Discussion

Change detection approaches should be selected based on the type of change being studied, data availably, quality, and the desired change products. The ideal land cover monitoring system would provide data on continuous (within land cover changes) and discontinuous (change to land cover) changes and information on

the drivers of the recorded changes.

2.3.1 Change Detection Accuracy Assessments

In all the change detection projects presented, three major steps were undertaken: (1) image preprocessing (e.g. Radiometric Correction, Orthorectification etc.) to ensure data compatibility; (2) selection of suitable change detection technique for analysis; and (3) accuracy assessment. However, sometimes the accuracy assessment is more of an afterthought than a focus of the study, indeed some of the studies presented do not produce a specific change detection accuracy figure (Congalton 1991). It is a key part of any monitoring system that the changes detected are a meaningful representation of change on the ground for users (e.g. land managers and policymakers). The accuracy of classification of RS imagery into thematic classes (e.g. classes of land cover) is commonly assessed using an error or Confusion Matrix (Congalton 1991). This is an array of numbers that represents the proportion of samples correctly assigned to the class they are on the ground. The ground data may be generated by field surveys or comparison with higher resolution imagery. An error matrix illustrates the accuracy of each class, demonstrating errors of commission (inclusion in a class) and omission (exclusion from a class). An overall assessment of accuracy is illustrated by the percentage of correctly classified samples. Although other approaches include the total and expected class area in the accuracy (e.g. a low accuracy class which covers a small area of the map will have less effect than a large area that is poorly classified), the error or confusion matrix remains the most common way of illustrating RS product accuracies (Pontius & Millones 2011).

There are two different matrices commonly reported in accuracy assessments of change detection studies: (i) single date error matrices and (ii) binary change/no change error matrices (van Oort 2007). Where RS data has been assigned a class (e.g. a series of land cover classifications) a full error matrix is commonly reported. In this case, the overall accuracy means the number of objects assigned to the correct class, this does not assess the accuracy of the change detection directly, but instead as a proxy of the single date classifications. If the objective is to detect change with no land cover class information then a change/no change matrix is often reported, where the overall accuracy is the percentage of change/no change objects correctly classified. The change/no change matrix and other derived statistics are very commonly used in change detection publications and are useful for assessing the accuracy of characterising a particular transition. Change/no change matrices directly assess the accuracy of the change class.

Accuracy percentages from single date error matrices and binary change/no change matrices are not comparable. The change/no change matrix characterises if a change has occurred on the ground, whereas the single date error matrices supply change information as a function of the accuracy of a series of classifications. Additionally, change detection accuracies can not be used to compare the accuracy of methods between different studies, because they are affected by many things beyond the method. Change detection accuracy is also affected by: (i) Geometric Registration between the imagery, (ii) calibration, normalisation or atmospheric correction of images, (iii) ground truth data quality and availability, (iv) any transformation or classification scheme used, (v) the scale of the change being detected, (vi) the analyst skill/experience and familiarity with the study site. These would likely have a greater or as great

effect on accuracy as the change detection approach used. Therefore, only studies where the same land cover change is detected using the same RS data and analysts is comparable, these studies are not common.

A common limitation of change detection accuracy assessments is characterising any omission, that is where change has occurred on the ground but has not been detected by the change detection approach. As change is rarer than no change, the no-change area is typically a larger area to sample and the chances of sampling a change feature within it are very small. Producers accuracy or the presences of false positives within the change class are much easier to identify. This just relies on confirming if the change features are changed on the ground. Due to this difficulty in characterising users accuracy or omission in a meaningful way, change detection approaches which do not identify all change, will appear more accurate statistically than those that over identify change features. This can be counteracted with targeted sampling in known change areas, but this requires knowledge of where change has occurred at a site, as such characterising omission remains a limitation in change detection studies (Foody 2009).

The meaning of change detection accuracies and the nature of typical errors of commission and omission needs to be properly communicated to map users. Additionally, end-users and map use cases should be considered alongside accuracy assessment. For example, commission error is preferable to omission in a monitoring system which is being used to 'flag' potential locations of changes for field surveys or targeted management, as needing to visually verify change is preferable to missing change features. However, if calculating the total area of changed land cover or the areas of from/to change classes, this commission error would be undesirable. These are both common outputs and requirements of

monitoring systems for practitioners and should be considered in change detection method selection.

2.3.2 Comparison of Change Detection Approaches and Outputs

Much of the research described within each change detection approach introduces additional parameters, transformations, or hybrid data to improve accuracy. However, due to the relatively small number of studies comparing very different change detection approaches in the same landscape and change case, it is impossible to determine if these methods improve accuracy and if that improvement is statistically significant. It seems unlikely that these new approaches always produce accuracy figures which represent a statistically significant increase in overall accuracy or fall within the range of accuracy figures generated using other approaches. Therefore, discussion of their potential to form a monitoring system will largely take place in types (manual, classification, PN, time-series, and biophysical approaches), as within these groups their advantages and limitations to a monitoring system are broadly the same (Table 2.5).

Manual change detection approaches produce highly accurate results but lack reproducibility and the high number of operator hours make them impractical for long-term, high temporal resolution, or large area change detection monitoring (Table 2.5). Although research has increased robustness, PV approaches remain more sensitive to noise from illumination, atmospheric and seasonal variation (Song et al. 2001, Du et al. 2002, Wang & Xu 2010) than other approaches (Table 2.5). This limits the data volume, potential data sources, and temporal

Table 2.5: Characterisation of the different approaches as part of a monitoring system. The input requirements, typical uses, and monitoring system characteristics for different types of change detection approaches are presented
*Con = Continuous Change; change without change in the land cover, Dis = Discontinuous Change; the land cover has changed
+Preprocessing = Only takes time to prepare algorithm, low = very few hours required, high = a high number of operator hours and knowledge required.
- Noise which present in the dataset before significant false positives (low/medium/high).
Y = Yes and N = No when used anywhere in the table

Approach	Data	Con/Dis*	Operator hours +	Level of Noise -	Sub-Annual Res (Y/N)	Multiple Sensors (Y/N)	Max applicable area
Manual	Any form of site image	Dis	High	High	N	Y	Local
Classification	Multispectral image/composite	Dis	High	Mid	N	Y	Country/Region
Digital Number	Multispectral or radar image	Con Dis	Pre	Low	N	N	Country/Region
Time Series	Series of spectral data	Con Dis	Pre	Mid/High	Y	Y	Local
Biophysical	Multi/Hyperspectral, LiDAR, Field	Con Dis	High	Mid	N	Y	Country/Region

resolution of a monitoring system using these approaches. Finally, a substantial volume of operator hours and knowledge is needed to produce change data from classified maps, reducing the temporal resolution of classification approaches (Table 2.5). The time step for these three approaches could be several years, resulting in a low temporal resolution monitoring system or 'blurring' of each time step due to image compositing (Lindquist et al. 2008, Lück & van Niekerk 2016). Most change detection studies do not give detail on the requirements of end users of change detection data. For example, in use cases that require from/to change information (e.g measuring changing landscape dynamics) to characterise the landscape, the increased operator hours required for PCC approaches are useful. However, approaches which utilise the existing wealth of historic classifications to produce comparable statistics could reduce the requirements for operator hours in classification generation (e.g. manual verification from classifications). If only change objects are required then, PV approaches reduce time and meet requirements. End user requirements must be

considered in change detection method selection.

Satellite imagery time series approaches represent a viable option for near real-time monitoring of land cover change (Table 2.5). These approaches are the most practical method for making use of all the data in a dense and/or long time series of imagery, requiring a limited number of operator hours per analysis. Current and future increases in data volume mean these methods will likely be more important in the near future. Dense time series approaches have been shown to identify many types of vegetation cover change (Bontemps et al. 2008, 2012, Verbesselt et al. 2012, Zhu et al. 2012, Eckert et al. 2015, Schmidt et al. 2015) and produce land cover maps at each time step (Zhu & Woodcock 2014). They are potentially powerful monitoring and early warning systems of land cover change (Verbesselt et al. 2010). However, studies using dense time series approaches are typically limited to a single or a few Landsat or MODIS scenes in area, due to the high compute power needed to generate and fit a time series model. Increases in compute power or algorithm efficiency will be needed to apply these approaches at a higher Spatial Resolution at a global or regional scale.

The temporal resolution of biophysical data are typically sub-annual due to the expense of collecting field data or generating a dataset. However, unique monitoring data and information about the effects and process of change can be provided using these approaches (An et al. 2017, Ye et al. 2019). For example, Global Forest Watch (Hansen et al. 2013), launched in 2014, provides forest canopy extent statistics to researchers, charities, and governments to assist deforestation, fire, and illegal felling management practices.

The ideal monitoring system has the capacity to identify land cover change areas and also provide information on the change process and any effects on the

environment with minimal delay. For example, land cover, reflectance, trend and break data could be monitored using a dense time series approach and organised and stored in events (e.g. clusters of objects which exhibited similar changes for the same time period). Biophysical data could be manually generated or collected and incorporated into the monitoring system at reasonable time intervals (e.g. annually or seasonally). This data should influence the dense time series system, so the system can increase accuracy. Consideration and research would need to be given to the best way system (e.g. data cube; Hermosilla et al. 2015, 2018) to store, handle differing spatial resolutions, query, and report (e.g. the nominal date of a mixed map) on the data.

Research and monitoring systems such as those described will likely be integral to land cover change monitoring practices and research in the years to come. However, historical land cover change data are also important for informing management practice and determining the magnitude of change events. The Landsat archive contains a wealth of past change data, which may not be best analysed with dense time-series approaches. In most locations, the data volume may be too small to form a meaningful signal or trend at a reasonable temporal resolution.

2.4 Conclusions

In conclusion, there is no single change detection approach, which is a good fit for all end users and use cases. Future monitoring systems are likely to make use of the increased data availability and processing power to illustrate trends and patterns of change to 'flag' likely change objects based on trajectories of image data. However, in landscape change studies where from-to information is important classifications

of RS data are required. Additionally, data density may not always be high enough to apply these dense time-series approaches.

Therefore, a gap has been identified in RS change detection approaches for monitoring systems. Although, the wealth of current and future data will allow for dense time-series approaches to characterise trends and changes an approach is needed which is better able to make use of the wealth of historic data and is computationally efficient to apply to large areas. This approach must be robust to the effects of noise and different sensors, allowing the use of all data present in a fragmented historic time series including the ability to make use of non-cloud pixels in a scene with partial cloud cover, to maximise change information. Thereby, able to provide sub-annual resolution change data where the imagery is available and not requiring interpolation or failing to identify change data where there is a sustained period of no new data. The 'parametric distribution map-to-image' approach fits a number of these characteristics, requiring only a base map and a satellite image to detect change features and a lower number of operator hours than PV approaches or PCC. However, current research is limited and further work is needed to study performance in different locations and with different types of land cover. Potential statistics for the identification of changed regions should also be tested in addition to researching an approach that can be used to generate change data for a full land cover classification through time.

Chapter 3

Study Site

3.1 Introduction

Wales, United Kingdom (UK) was selected as a study site to research the performance of the 'parametric map-to-image change detection' approach in a new region and develop new approaches to identify change features. Wales is a 20,779 km^2 (2,077,900 ha) nation (Figure 3.1) with a high diversity of landscapes (Blackstock et al. 2007, Lucas et al. 2011). It is predominantly rural and managed for various agricultural and forestry practices. The majority of the urban centers are in the southeast (Figure 3.1). Wales is topographically variable, with more than 20 distinct mountainous areas (e.g., the Berwyn Mountains, Cambrian Mountains, Brecon Beacons, Black Mountains; Lucas et al. 2011). The majority of lowland areas are on the coast, to the east of the nation, and in valleys within upland areas. The welsh landscape experiences both natural and anthropogenic drivers of change typically representative of changes

that occur at a national level in the UK.

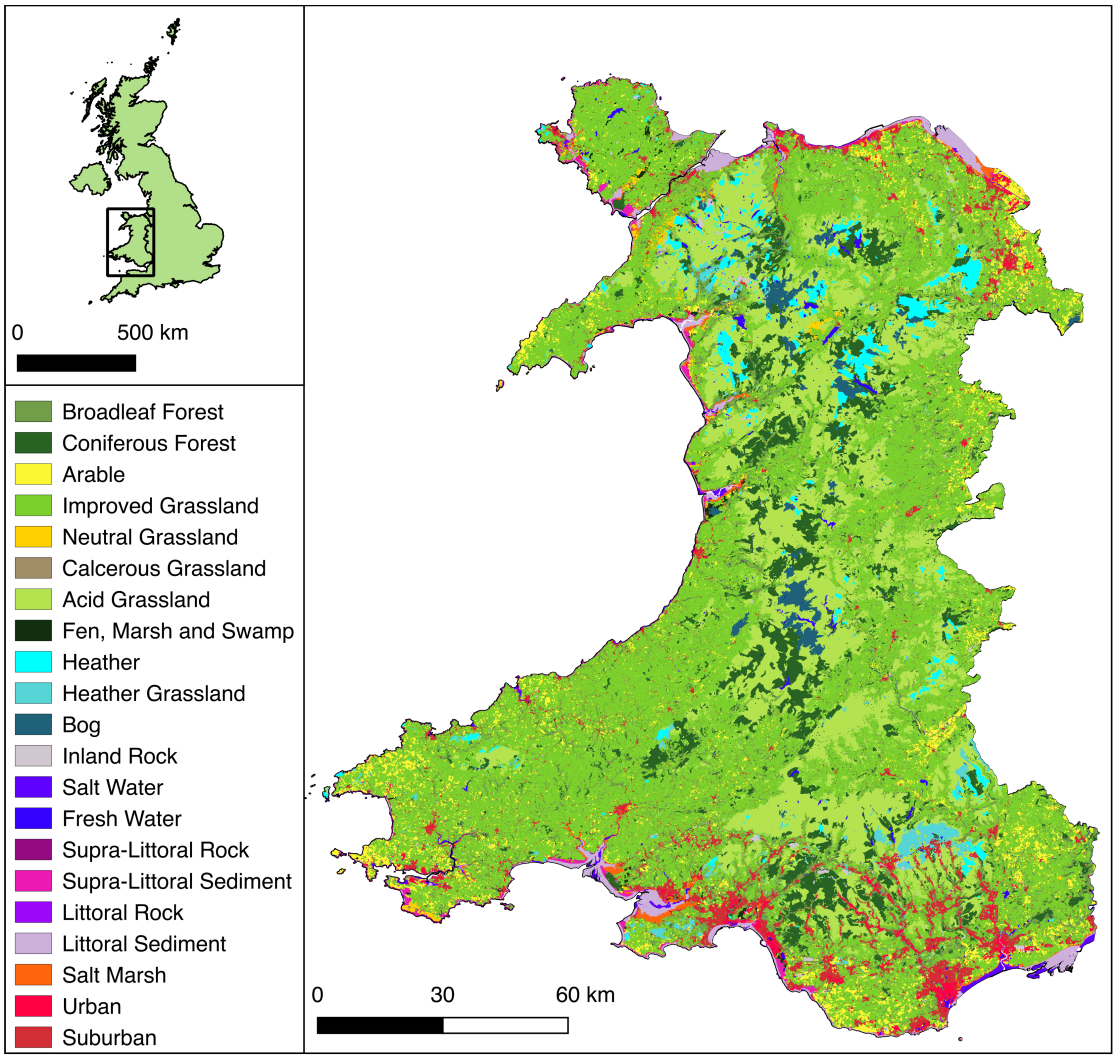

Figure 3.1: Location of Wales in Great Britain. Spatial distribution of land cover from subset of UK Land cover map 2015 (Rowland et al. 2017).

Wales was selected for the study because;

- Persistent cloud cover poses a significant challenge for EO-based monitoring (Met Office 2016).
- The historic data volume is relatively small (Wulder et al. 2009).

- The Welsh landscape is varied (e.g. topographically) and the vegetation species (e.g. spruce and pine; Hyde 1977) are representative of other boreal regions (Brandt et al. 2013, Swedish Wood 2019).
- Management practices create dynamic land covers.

3.2 Climate and Topography

Around three-quarters of the Welsh border is coastline meaning it is highly sensitive to changes in circulation systems in the North Atlantic (Sibley et al. 2015). The climate of Wales is maritime, often wet, windy, and mild (Parry et al. 1996, Lucas et al. 2011). Wales experiences an average of 183 rain days a year (Met Office 2016). The clearer part of the year is from April 27 until October 4, totalling 5.3 months, with an average temperature of around 19.1°C in July (Parry et al. 1996, Lucas et al. 2011). In the clearer months, the sky is clear, mostly clear, or partly cloudy 56% of the time, and overcast or mostly cloudy 44% of the time (Met Office 2016, Diebel et al. 2019). In the cloudier months, the sky is overcast or mostly cloudy 70% of the time (Diebel et al. 2019) and the average temperatures are around 6.5° C in January (Lucas et al. 2011). However, the weather varies with topography and distance from the coasts (Lucas et al. 2011). Average precipitation in the coastal regions and eastern lowlands is between 600-1100 mm, however, the mountainous regions receive $>$ 3000 mm (Parry et al. 1996, Lucas et al. 2011).

The Welsh topography also leads to increased precipitation and cloud cover through the 'orographic effect'. This occurs when air is forced upwards and cools

due to increased elevation. The adiabatic cooling could lower the air to its dew point causing the condensation of water vapour, forming a cloud, and eventually precipitation. As the elevation or topography varies cloud cover is formed. (Roe 2005, Houze 2012) Although generally upland the Welsh topography consists of three mountainous areas: the Brecon Beacons, the Cambrian Mountains, and Snowdonia. The largest mountains are located in the northwest. Radar and rain gauges have indicated the influence of topography in Wales on precipitation and cloud cover due to the orographic effect. Precipitation in mountainous areas is around 700mm/year higher in mountainous areas compared to lowland areas (Hill et al. 1981, Dore et al. 2006, Mayes 2014, MET Office 2015).

The climate and topography of Wales both lead to persistent cloud cover, which represents a challenge for EO monitoring as it creates fragmented optical satellite data and limits the number of observations per year.

3.3 The Welsh Landscape and Drivers of Change

3.3.1 Vegetation Cover

3.3.1.1 Forestry

Forestry is a significant sector in the Welsh economy and large areas of Welsh forests are plantations. Welsh forestry has been managed by multiple organisations (Forestry Commission and Natural Resources Wales and several

private individuals and companies) and strategies since 1990. As such, comparable forest cover and species, data can be difficult to obtain, especially for pre-2000. Between 1998 and 2017 there was an increase of approximately $70km^2$ (7,000 ha), from $3000km^2$ (300 thousand ha) to $3070km^2$ (307 thousand ha) in overall woodland cover across Wales (Forestry Commission 2002, 2017*a*). Coniferous forest covers approximately $1510km^2$ (151 thousand ha) and is located in mid and north Wales (Figure 3.2). Broadleaved stands are more fragmented across Wales covering approximately $1560km^2$ (156 thousand ha; Figure 3.2; Forestry Commission 2017*a*).

Welsh coniferous forest cover is dynamic due to forestry operations and disease. The majority of coniferous forestry are plantations of Sitka Spruce *(Picea sitchensis)* and European Larch *(Larix decidua)* in predominantly upland areas. A sizeable proportion of Welsh coniferous forests are managed plantations therefore, stands are regularly clear-felled and restocked (Welsh Assembly Government 2009). Changes in coniferous forest areas are largely driven by plantation practices and the economic requirements for wood and timber products. Conifer trees in Wales are typically clear-felled at 40-60 years old (Figure 3.3; Mason et al. 1999, Welsh Assembly Government 2009, Forestry Commission 2017*a*). Between 2001 and 2017 there was a decrease in the total coniferous woodland area of $170km^2$ (17 thousand ha) (Forestry Commission 2002, 2017*a*) The *Phytophthora ramorum (P. ramorum)* pathogen spread into Wales is a biological driver, which led to a significant increase in the felling operations of Welsh Larch, to reduce the spread (Drake & Jones 2017, Natural Resources Wales 2017*a*, Wright 2017, Xu et al. 2009). *P. ramorum* was first identified in 2011 (Natural Resources Wales 2017*b*) with 9 thousand ha of extra

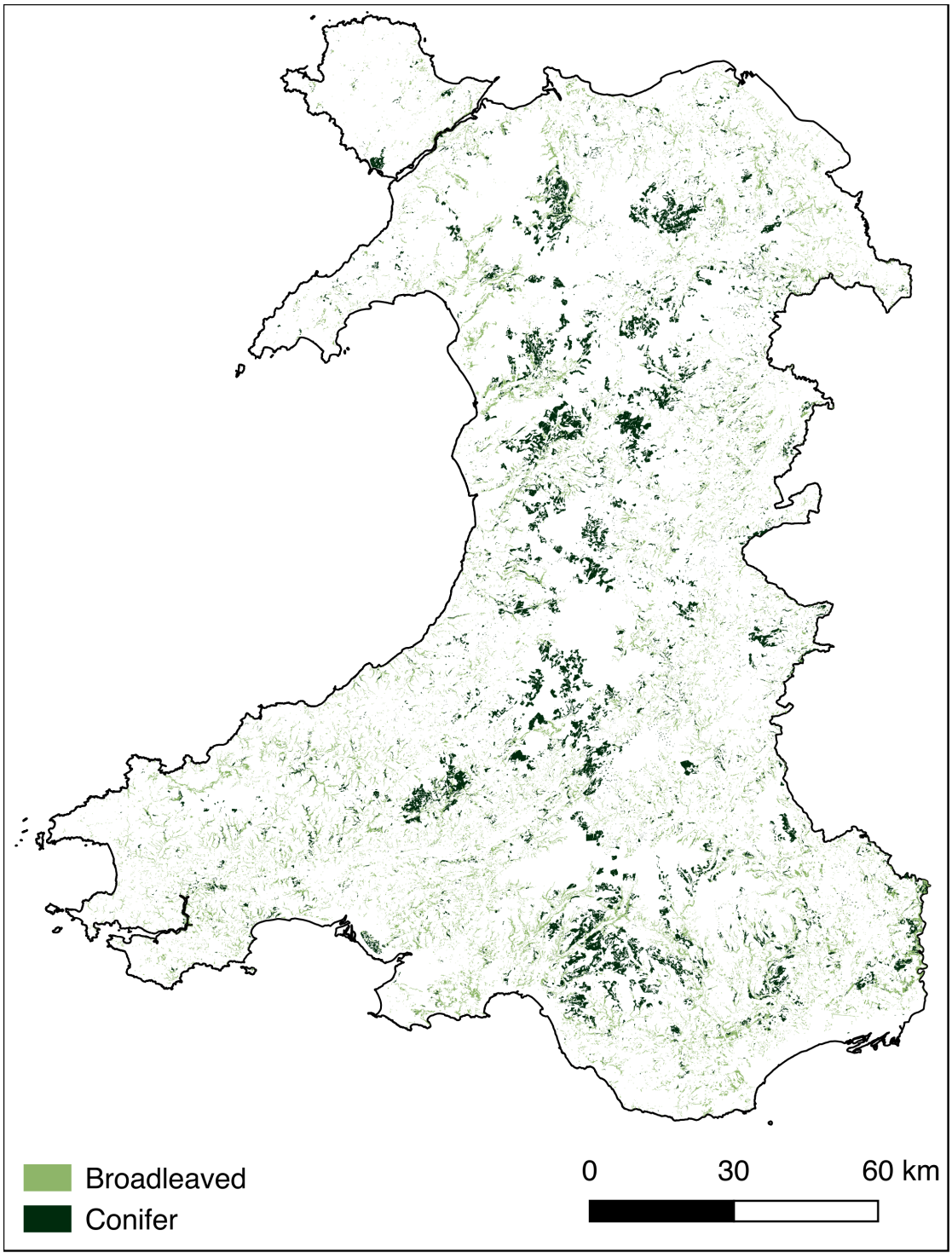

Figure 3.2: Forest cover in Wales from National Forest Inventory 2017 (Forestry Commission 2017*b*)

felling occurring after 2013 (Forestry Commission 2015, Natural Resources Wales 2017*a*). As of August 2017, approximately 33% of pre-infection Larch forest had been felled across Wales with the majority (3,125 ha) destroyed in the South Wales core disease zone (Wright 2017).

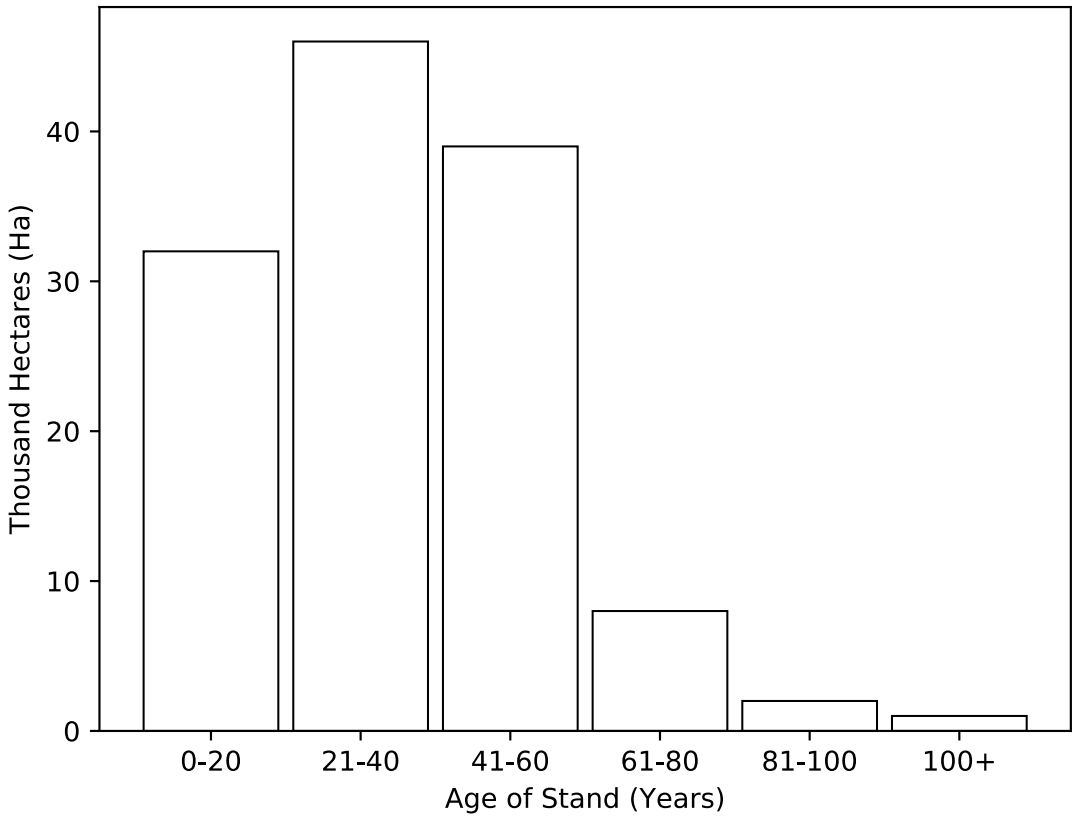

Figure 3.3: Area of conifer stands in each age group (Forestry Commission 2017*a*)
.

Welsh broadleaved and mixed forests are typically found in the lowlands (Lucas et al. 2011). Broadleaved forests are generally not plantation forests or subject to widespread disease (Forestry Commission 2002, Welsh Assembly Government 2009, Forestry Commission 2015, 2017*a*). As such there are fewer drivers of change on this land cover and it is a more stable feature of the landscape.

Broadleaved stands are not routinely felled at a particular age (Figure 3.4; Forestry Commission 2017*a*), making the land cover more stable than coniferous forest. A greater proportion of broadleaved stands are smaller than 2 ha (Forestry Commission 2002), suggesting they form features such as hedgerows and trees in urban spaces (Welsh Assembly Government 2009). Between 2001 and 2017 broadleaved forest area in Wales has increased by 19.5 thousand ha (Forestry Commission 2002, 2017*a*).

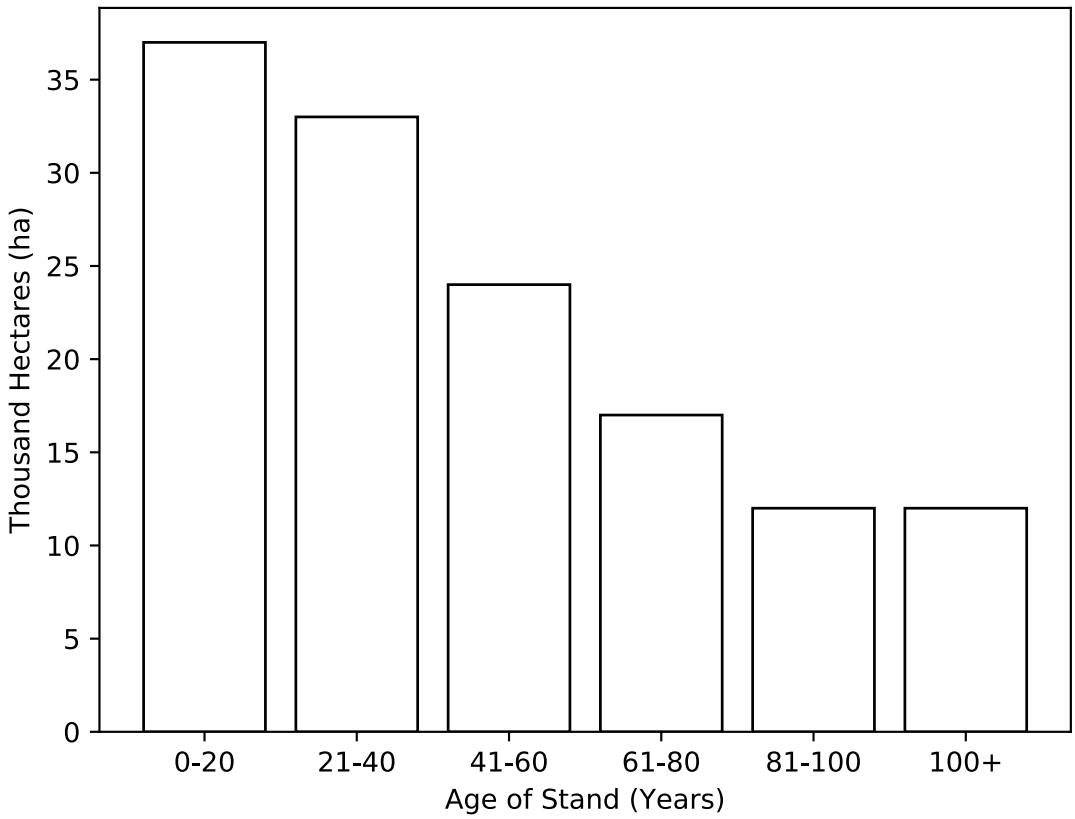

Figure 3.4: Area of broadleaved stands in each age group (Forestry Commission 2017*a*)

.

3.3.1.2 Upland Vegetation

Welsh uplands consist of heather moorland, bogs, scrub, and grassland much of which is used for low-intensity agricultural practices (e.g. sheep grazing) (Job & Taylor 1978). The vegetation is predominately scrub-like. The grasslands are dominated by dominated by *Molinia caerulea* (purple moor grass), *Nardus stricta* (Mat grass), *Agrostis* (Bent) and *Festuca* (Sheep's fescue) plant species (Lucas et al. 2011). Management practices maintain the current land cover and preventing any potential overgrazing (RSPB et al. 2017). Inspection in Google Earth Pro shows the land cover in these areas does not and would not be expected to change significantly in twenty years and there are no large-scale drivers of land cover change acting on the upland environment.

3.3.2 Anthropogenic Land Use

3.3.2.1 Agriculture

Agriculture is a significant proportion of Welsh land cover (Welsh Government 2017). Geospatial data of agricultural land cover change is not routinely collected in Wales. The agriculture area data which is available is collected from a random sample of farmers by the UK Department for Food and Agriculture (DEFRA) and the Welsh Government annually (June Agricultural Survey). Increased food requirements and political incentives have led to an increase in agricultural areas in Wales. Government data estimates the total agricultural area in Wales to have grown between 1998 and 2017 by 139,353 ha, from 1,438,481 to 1,577,834. As previously mentioned, some low-intensity agricultural

practices (e.g. sheep farming) occur in the unforested upland areas. However, agriculture dominates the lowland areas of Wales (e.g. grazing and arable crops; Lucas et al. 2011). Grasslands are often improved through fertilisation for sheep and cattle grazing, leaving fragmented areas of natural habitats in the lowlands (e.g. natural grassland, marsh, and mires; Lucas et al. 2011).

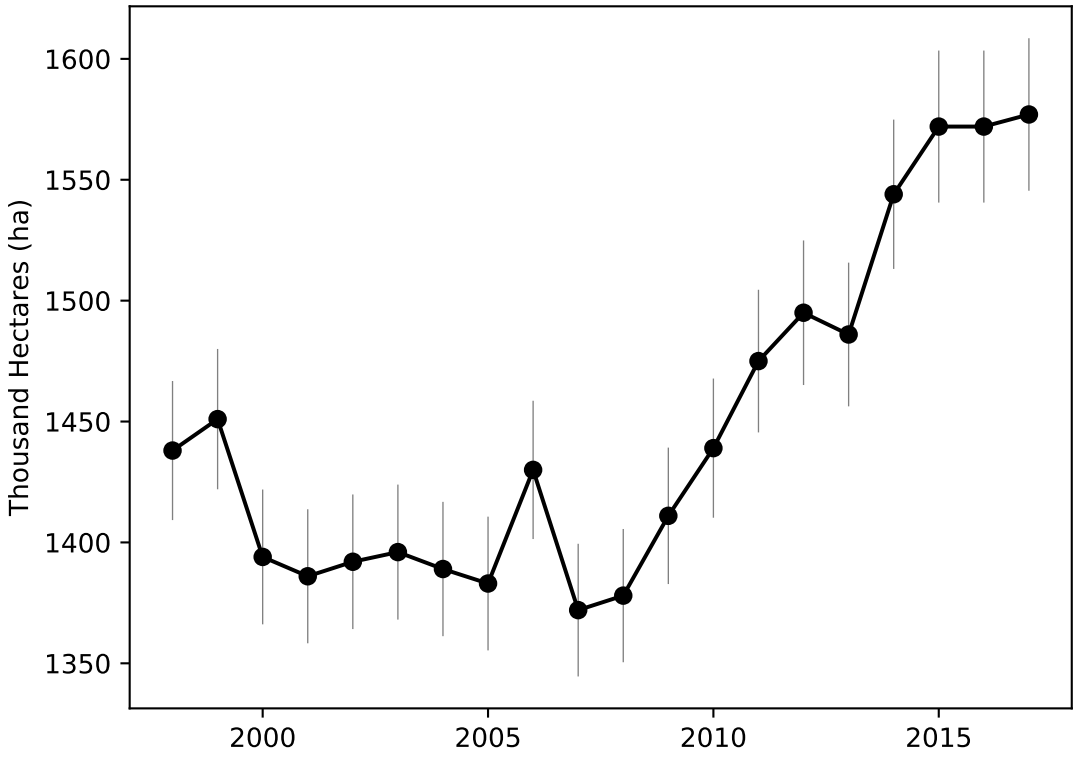

Figure 3.5: Changes in recorded area of agricultural practices between 1989 and 2017 (Welsh Government 2017). Error bars illustrate ±2%.

.

3.3.3 Urban Cover

The largest urban centres in Wales are located in the southeast. There are smaller significant urban centres in the north. Mid-Wales and the coastal areas are largely

rural (Figure 3.6). Increases in population have driven an increase in urban areas across Wales. The urban land cover class increases in area in Wales in the UK land cover maps (LCM; Centre for Ecology and Hydrology 1995, Fuller et al. 2002, Morton et al. 2011, Rowland et al. 2017). A significant increase is recorded between 2007 and 2015 (Figure 3.7). Area change was not quantified as the maps were made using different processes and any change area figure would likely contain false positives. The UK LCM and inspection in Google Earth Pro suggest an increase in the area of pre-existing urban centres between 1990 and 2017.

3.4 Summary

In summary, changes in Wales are largely driven by anthropogenic factors in particular economic changes and population growth. Anthropogenic pressures have led to increases in the area of agricultural and urban landscapes. The coniferous forest class is particularly dynamic due to the routine felling and replanting of trees. Additionally, a significant biological driver of change, larch disease, has led to widespread increases in felling. The climate and topography in Wales present significant challenges for EO monitoring; the climate leads to persistent cloud cover and reduces data volume and the varied topography complicates atmospheric correction and creates shadows, which may be confused for change features.

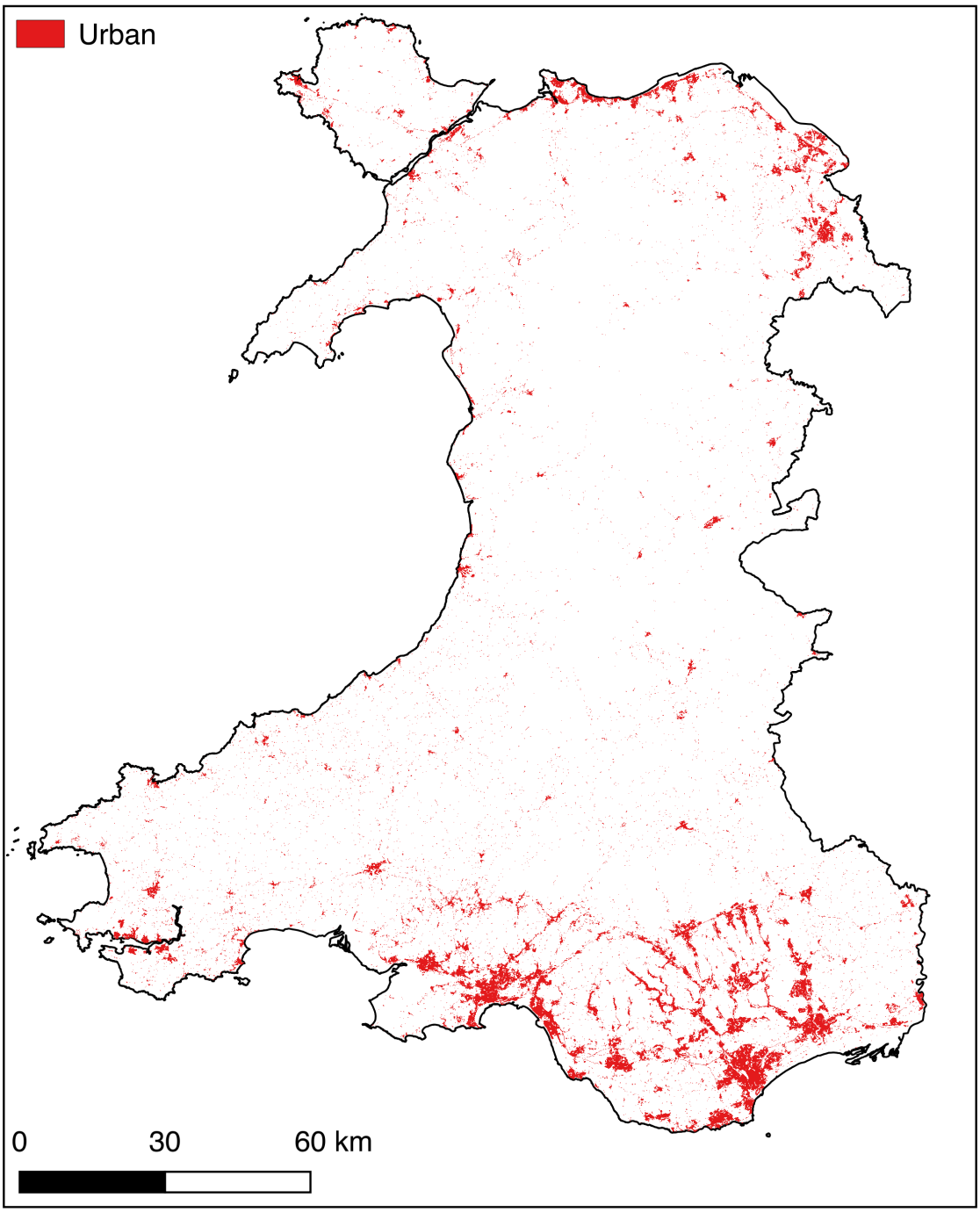

Figure 3.6: Location of Urban land cover in Wales (Morton et al. 2011).

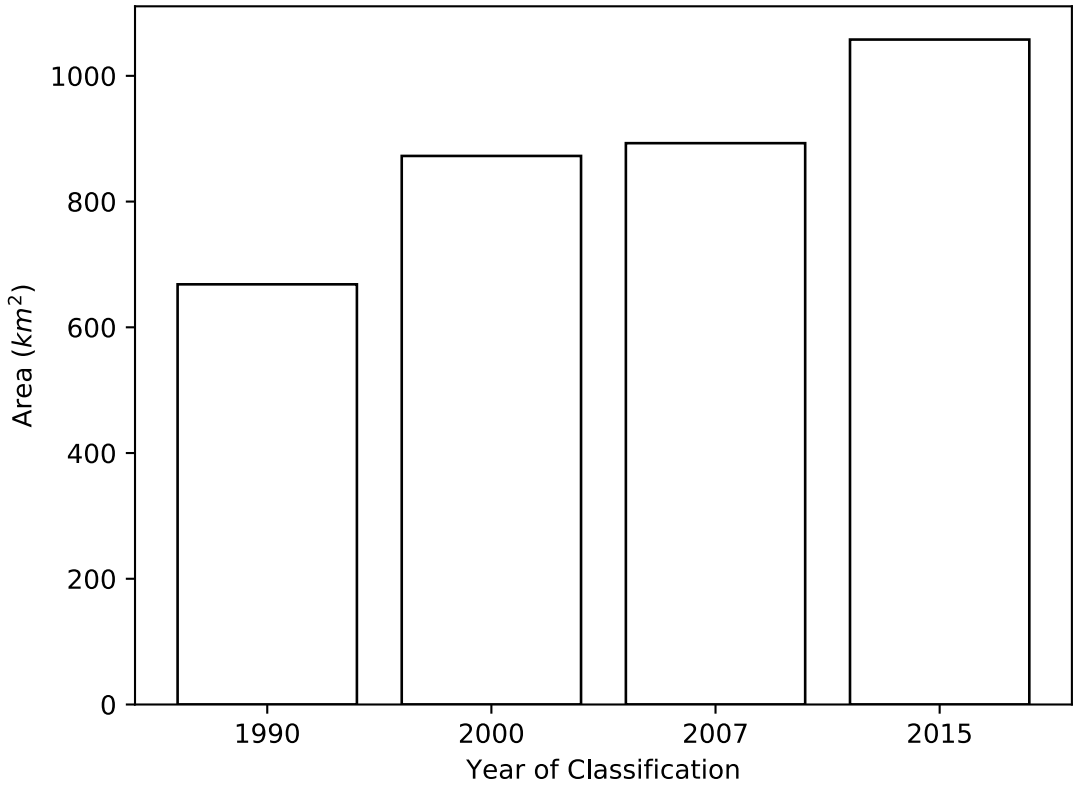

Figure 3.7: Area covered by urban and suburban classes in Wales in the UK land cover map 1990, 2000, 2007 and 2015 (Centre for Ecology and Hydrology 1995, Fuller et al. 2002, Morton et al. 2011, Rowland et al. 2017).

Chapter 4

Data Sources and Preprocessing

4.1 Introduction

Wales was selected as a study site due to the availability of the Landsat archive for Wales, an analysis-ready data set of data from 1990 to 2017. This reduced the pre-processing requirements of the study. The time series of EO image data used to detect LCC and develop the 'parametric map-to-image change detection approach' are described in this chapter. The atmospheric correction and data volume are presented in addition to image segmentation. Change analysis was conducted at an object level (clusters of similar pixels) on a mixed dataset of Landsat and Sentinel 2 data.

4.2 Time Series Data Set

4.2.1 Data Source and Preprocessing

The Landsat archive (TM, ETM+, and OLI; Paths 219-220 and Rows 23-34) for Wales and Sentinel 2 MSI (Tiles: 30UVE, 30UVD, 30UVC, 30UWC, 30UWD, 30UUC, 30UUD, and 30UUE) optical data was utilised for the period between 1989 and 2017. The archive is atmospherically and topographically corrected (6S algorithm) (Shepherd & Dymond 2003) and cloud masked (Fmask; Zhu & Woodcock (2012)) using the ARCSI software version 3.1.6 (Bunting et al. 2018).

The Sentinel-2 image data were downloaded from Google Earth Engine and pre-processed as part of this study. For compatibility with the Landsat imagery, the Sentinel-2 imagery was to 30m pixel resolution. Image bands were subset to blue (0.45-0.52μm), green (0.52-0.60μm), red (0.63-0.69μm), near-infrared (0.77-0.90μm), and the two short wave infrared bands (1.55-1.75μm and 2.09-2.35μm). The imagery was also atmospherically and topographically corrected using the (6S algorithm; Shepherd & Dymond (2003)) and cloud masked (Fmask; Zhu & Woodcock 2012) using the ARCSI software version 3.1.6 (Bunting et al. 2018). Both Landsat and Sentinel 2 images with less than 500 km^2 (approx. 750 x 750 pixel area) of the continuous terrestrial area were removed. Data were also reviewed to remove imagery where the cloud masking contained significant errors of omission. Imagery captured between November and March often contained large amounts of cloud cover and topographic shadowing from low illuminations angles and was removed from the analysis.

4.2.2 Data Set

The final time series of image data contained 178 images acquired between 1990 and 2017. Each pixel in the study area was viewed at least once during this period. On average each pixel was acquired 48 times with a maximum of 79 images (Figure 4.1). No images met the selection criteria in 1993, 2003, and 2012. Data volume reduced between 2012 and 2015, at the end of Landsat TM's life span and after the 2003 failure of the Landsat ETM+ scan-line corrector (SLC). The Landsat ETM+ SLC failure caused an estimated loss of 22% of each scene (Scaramuzza et al. 2004), which resulted in many of the scenes containing insufficient terrestrial data to be included in the data set. Data volume increases significantly after the launch of Landsat 8, Sentinel 2A and Sentinel 2B (2013, 2015 and 2016; Figure 4.2).

4.2.3 Software

Unless otherwise stated analysis was undertaken using the Remote Sensing and GIS software library (RSGISLib; Bunting et al. 2014) and the KEA file format (Bunting & Gillingham 2013) using the Python scripting language as outlined by Clewley et al. (2014). The scikit-learn library (Pedregosa et al. 2011) was used for all machine learning algorithms.

4.2.4 Segmentation

Image analysis, classification, and interpretation can be aided by the use of segmentation techniques (Shepherd et al. 2019). All change detection in the

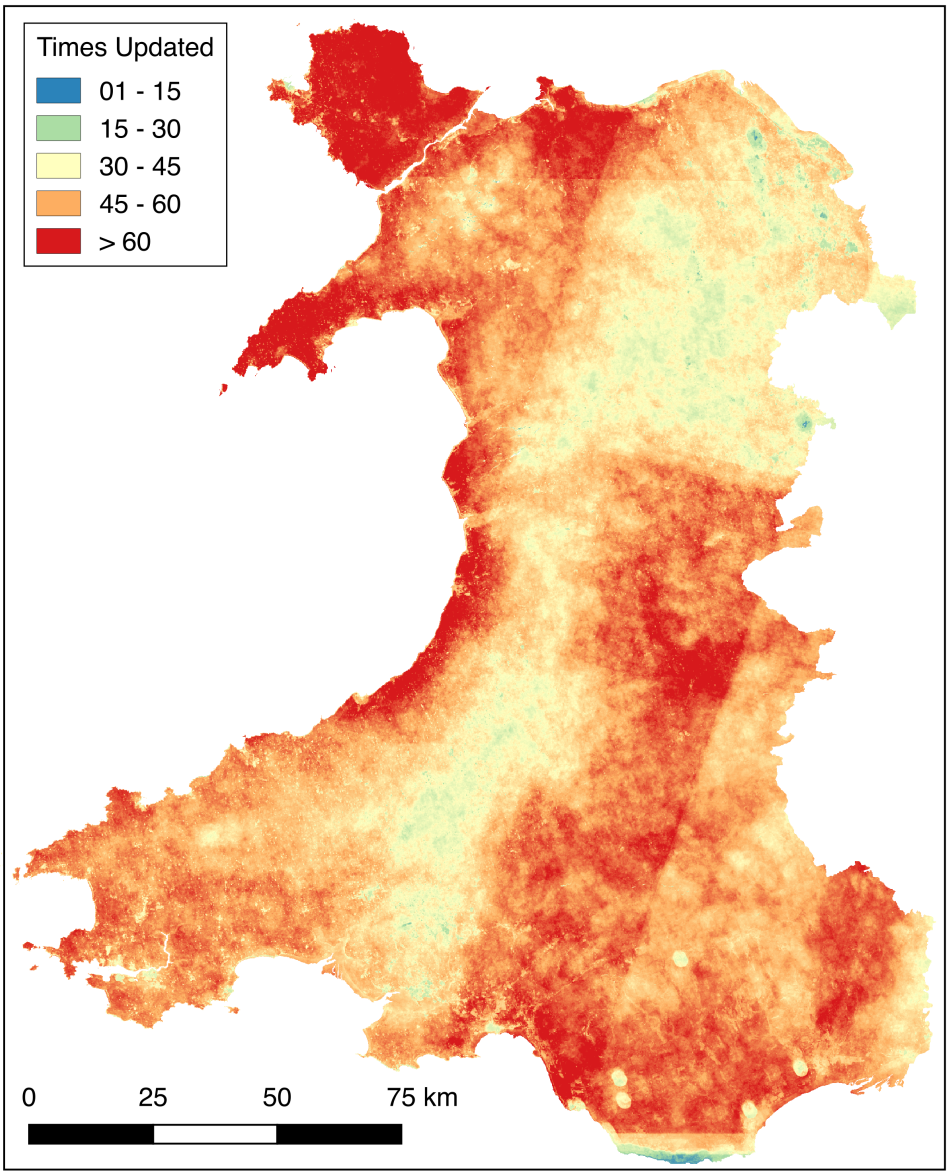

Figure 4.1: Number of times each pixel was viewed and not covered by cloud in the time series.

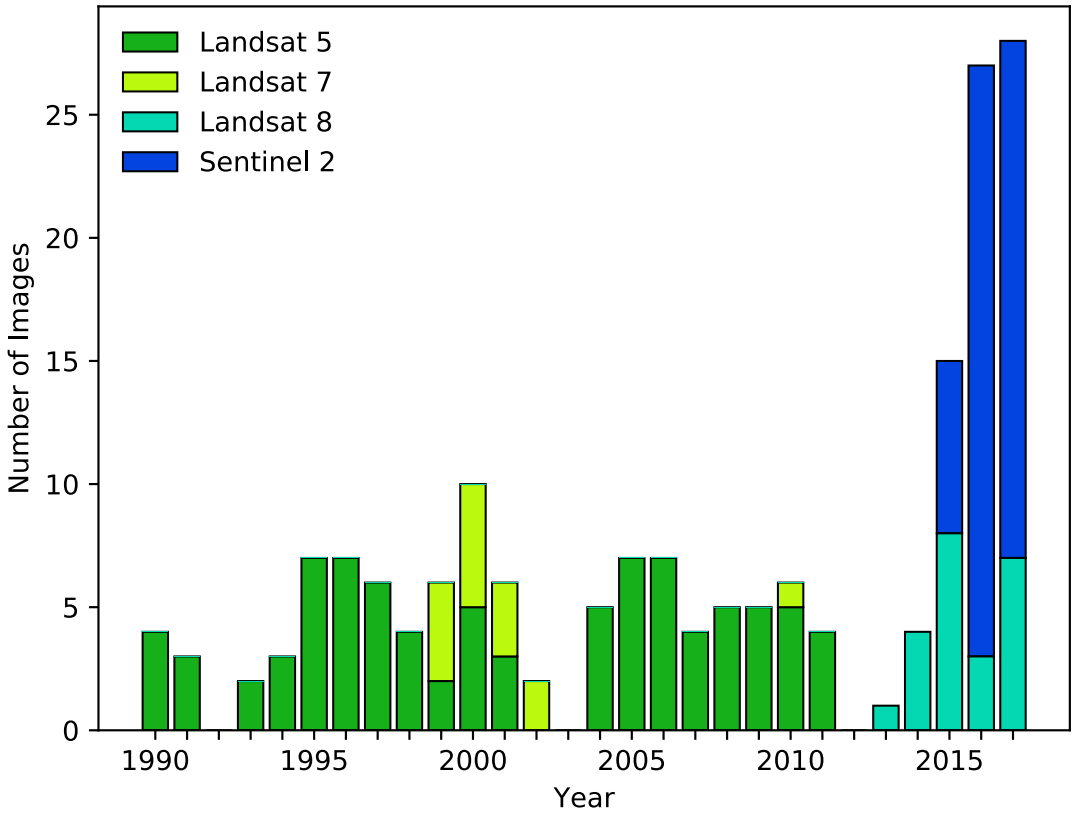

Figure 4.2: Data source and the number of images per year in the time series dataset.

study was performed on Image Objects (groups of pixels containing similar values). Pre-processed images underwent segmentation before change detection analysis. To maintain the regions from the baseline map, a union between the clump edges and the map region boundaries was also performed. Separate segments were produced for each image, to ensure that changes were reflected in the image objects (e.g. felling of part of a forested area resulted in a separate object).

Object-based analysis was deemed to be more appropriate than pixel-based analysis for identifying change features. Utilising objects reduces the effects of noise in the calculation of statistics from the map regions and the change detection. Pixel analysis in change detection is susceptible to producing false positives of change, due to class variability and noise. This is termed the 'salt and pepper' effect and is widely discussed in classification and change detection literature (e.g. Chen et al. 2012, Hussain et al. 2013, Radke et al. 2005, Tewkesbury et al. 2015).

There are a large number of approaches for segmenting remotely-sensed imagery (Fu & Mui 1981, Pal & Pal 1993, Chang et al. 2001, Dey et al. 2010). Segmentation approaches can be broadly split into top-down or bottom-up approaches. Top-down approaches progressively break up an image into smaller regions, whereas bottom-up methods start with an individual pixel and grow a region until a criterion is met. eCognition contains a popular bottom-up approach, multi-resolution segmentation. In the multi-resolution segmentation algorithm, each pixel is considered to be a single object and merged with the nearest most similar object based on a homogeneity criterion. This process continues until the user-defined homogeneity criterion threshold is reached.

eCognition is commonly used with RS data and could be considered to be the 'gold' standard of segmentation techniques and is often part of comparison studies. However, eCognition is a licensed software package and a license was not available so free and open software options were explored instead.

There are numerous methods for grouping similar pixels to form objects for example, region growing, histogram shift thresholding, clustering, and numeral networks (Tilton 1998, Soille 2008, Tasdemir 2011, Zhao et al. 2011, Ghamisi 2011). The Felzenswalb algorithm, which produces a segmentation of multi-band images using spanning tree-based clustering, was also considered as it is popular in image processing (Felzenszwalb & Huttenlocher 2004). Felzenszwalb segments objects based on Euclidean distances in colour space, however, the number and size of segments are not directly controlled. Therefore, segment size can vary greatly depending on contrast (Felzenszwalb & Huttenlocher 2004).

The Sheppard segmentation approach was selected as it is scalable to a large area or data stack, is designed for a 30m per pixel resolution RS imagery, and has parameters that can be consistently used across a range of data sources and types. Additionally, it has been applied on a large scale and to a time series dataset (Shepherd et al. 2019). The algorithm uses a K Means clustering approach, generating seeds where pixels are associated with a cluster centre. The approach has two parameters the number of seeds (K) and the minimum object size. Clumps are iteratively eliminated, joining the most similar nearby cluster (defined with euclidean distance), if they are below the minimum pixel size. When optimal parameters are selected the algorithm is comparable to other segmentation techniques such as eCognition (Shepherd et al. 2019).

The minimum object size is a Minimum mapping unit, objects which are smaller

than this parameter will be merged with their most spectrally similar neighbour. The ability to set the minimum mapping unit is useful in change detection as it allows small change features to be identified. Change features are typically small, therefore, this value needs to be large enough that objects are not merged with neighbours. The K controls the number of cluster centres, if the number is too small features that are close in the feature space will be merged and the image will be under-segmented. If it is too large then the image will be over-segmented.

Assessing the accuracy of a Segmentation approach is highly complicated and the subject of many reviews. In the absence of a series of best-edge datasets to validate the segmentation algorithm against, visual inspection was used to assess the parameters. There are no specific rules when setting parameters for the Sheppard segmentation approach. Therefore as suggested in Shepherd et al. 2019, the parameter selection was determined based on visual inspection of the number, size, and spectral variability of segmented produced using different parameters. For vegetation studies, a value of 60 seeds has been consistently used across a range of studies (Dymond et al. 2012, Lucas et al. 2014). To compare segmentation parameters, a sensitivity analysis of different cluster numbers and minimum object sizes was performed on a subset of the data (Table 4.1). The results were visually inspected to determine the parameters used in the study (Figures 4.3 and 4.4). As change features are often small, the minimum number of pixels in each object is needed to capture this variation without introducing noise. For the image segmentation, the number of clusters was set to 80 and the minimum number of pixels 50 (Figures 4.3 and 4.4).

The main limitation of object-based analysis are 'sliver' objects produced by inconsistent edges in segmentation (Chen et al. 2012, McDermid et al. 2008,

Table 4.1: Segmentation parameters tested in sensitivity analysis

Number of Clusters	Min Object Size
125	10
90	25
80	50
70	75
60	100
50	125
40	150
20	200

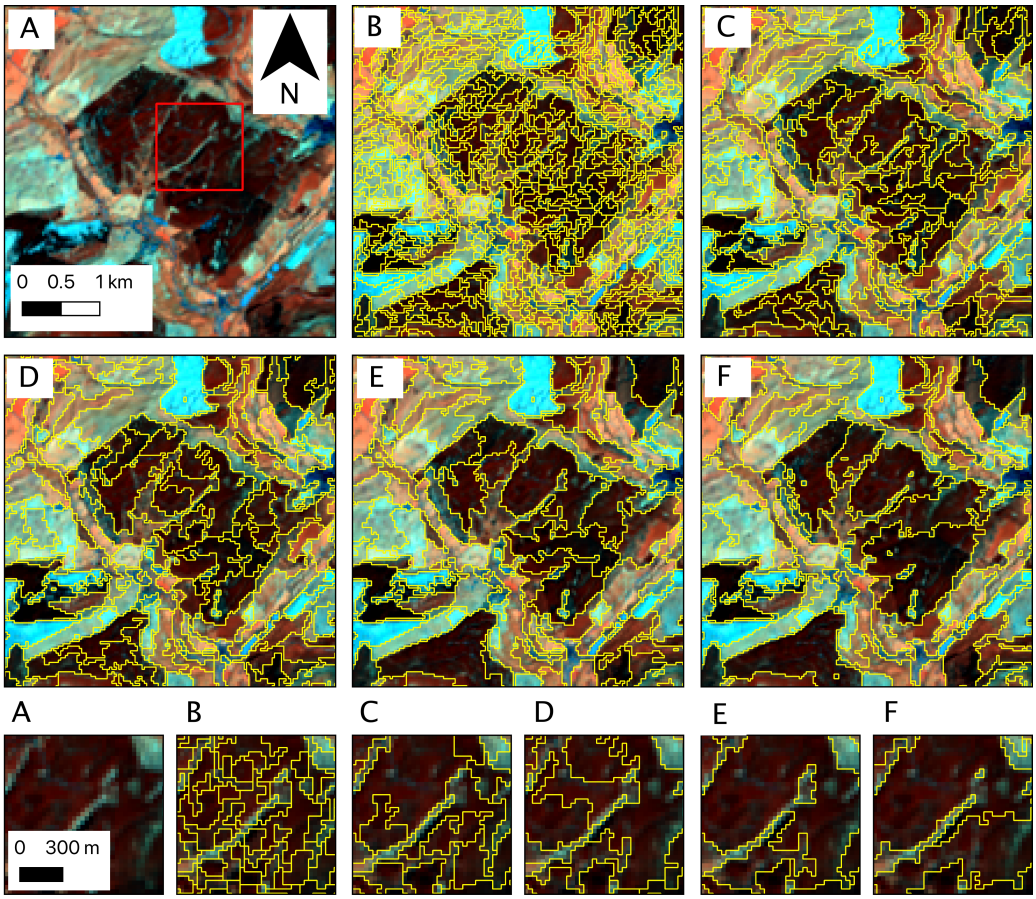

Figure 4.3: Comparison of different segmentation parameters. A = Landsat 5 image with NIR, SWIR1 and Red band combination, B = 125 clusters and min pixel size of 10, C = 80 clusters and min pixel size of 50, D = 60 clusters and min pixel size of 100, E = 40 clusters and mim pixel size of 150, F = 20 clusters and min pixel size of 200.

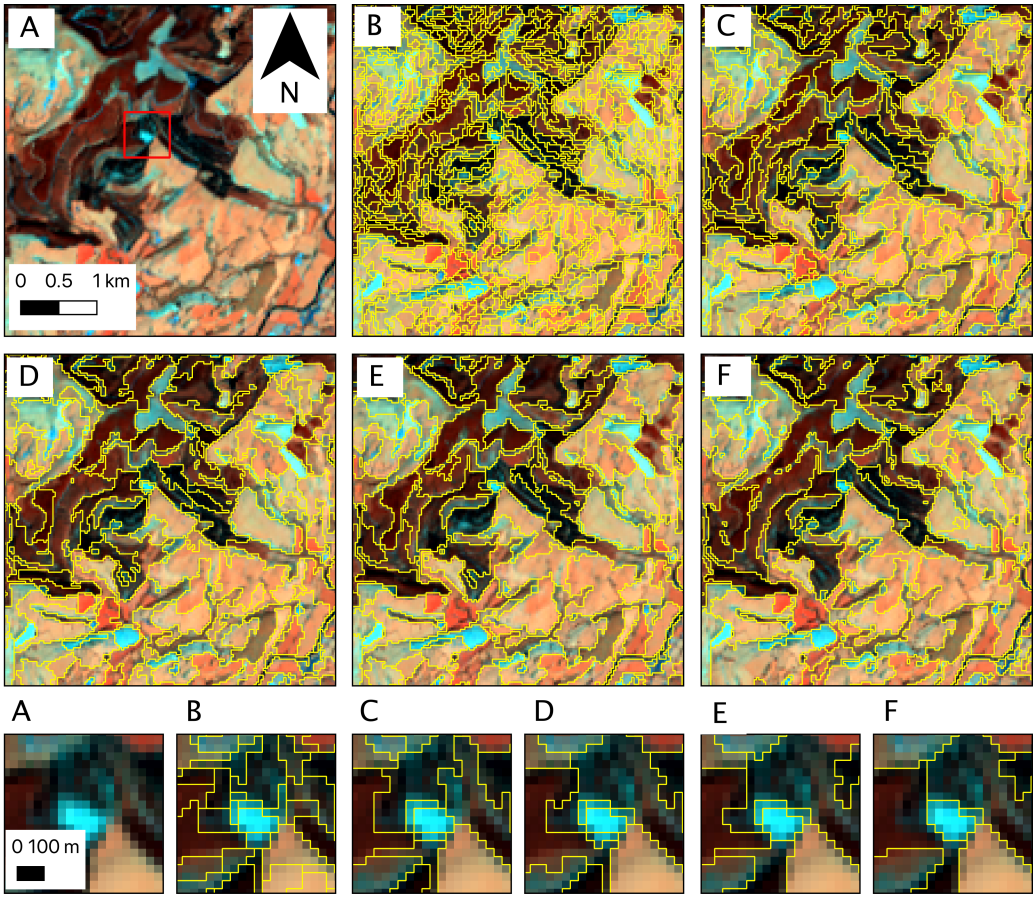

Figure 4.4: Comparison of different segmentation parameters. A = Landsat 5 image with NIR, SWIR1 and Red band combination, B = 125 clusters and min pixel size of 10, C = 80 clusters and min pixel size of 50, D = 60 clusters and min pixel size of 100, E = 40 clusters and mim pixel size of 150, F = 20 clusters and min pixel size of 200.

Tewkesbury et al. 2015). These objects can result in false positives of change and impact overall change detection product accuracy. Small objects and 'slivers' were produced after the image segmentation by the union with the map region edges. The effects can be minimised by removing smaller change objects (e.g. Boldt et al. 2012). However, this represents a systematic reduction in the scale of change analysis and information loss. Therefore the effects of noise must be weighed against the loss of information when using this approach. To reduce the effects of 'slivers' a minimum mapping unit for change features of 9 pixels (8,100 km^2 or approximately 1ha) was introduced after visual inspection of true and false change.

Chapter 5

Parametric Map-to-Image Change Detection in a Temperate Coniferous Forest as part of a Time Series

5.1 Introduction

A change detection approach is needed which is efficient, robust to noise, and able to handle dense and/or sparse long time series of data. The 'parametric distribution map-to-image change detection approach' meets many of these criteria. However, the approach remains untested beyond temperate regions and on forest types other than mangroves. Furthermore, it has not been applied as part of an automated monitoring system. Therefore, the accuracy and nature of

change detected by the approach as part of a monitoring system in a temperate region must be ascertained. Additionally, results from this study can form a baseline for comparison with any subsequent method developments.

Land cover change in a single class (binary map) was analysed in Wales between 1990 and 2017, using the dataset described in Chapter 4. Coniferous forest was selected as the change class as it is spectrally homogeneous, with a parametric distribution. Spectrally homogenous meaning that it does not vary very much in colour, darkness, or productivity; there is not a large variation in the spectral signature of different coniferous forest cover pixels compared to other land cover classes such as urban. Forestry is a significant economic sector in Wales resulting in sizeable managed coniferous forest plantations and stands that are regularly clear-felled and restocked (Welsh Assembly Government 2009). These felling practices mean that land cover change will have occurred in the study period and that there are high magnitude change features that should be detected by the method within the data set. A proportion of Welsh coniferous forest is Larch which is deciduous and subject to disease after 2011. The seasonal abscission of larch and potential infection during the time series can provide further information on the type of changes that are identified using this approach.

Coniferous forest gain and loss between 1990 and 2017 was mapped using a automated monitoring version of the 'parametric distribution map-to-image approach'. Coniferous forest cover was selected for analysis because it is homogeneous, dynamic, and clear-felling creates very definite events on which to test a change detection method.

5.2 Methods

5.2.1 Parametric Distribution Map-to-Image Approach

The approach assumes that within a single class, defined by the input thematic map, the PV response (e.g. reflectance or backscatter) is homogeneous and that any subsequent change will manifest itself as a change in PV value response. In this case, we have assumed that homogeneous features should produce a normally distributed histogram. Therefore, any change can be identified by a shift away from this normal distribution, quantified by a change in the skewness and kurtosis of a features histogram (Thomas et al. 2018). A histogram is generated where the bin size is determined by Freedman-Diaconis rule (Freedman & Diaconis 1981). Iterative thresholds are placed on the histogram to identify outlier change pixels, by producing an optimal distribution close to normal using the skew and kurtosis (Figure 5.1). Applied on a per-class basis, this produces a set of change and stable features, where the stable features can be used to provide training regions for a classifier (e.g. RF) to be trained and classify the identified change features to allocate to a class. The updated classification then forms the map input into the next iteration (time step) in a monitoring system (Figure 5.2). In doing so, not only are change pixels identified and mapped but an updated land cover map is produced, together with subsequent change-to thematic information. Therefore, any change features must exhibit new spectral responses which are beyond the range of values produced in a normal distribution of the class.

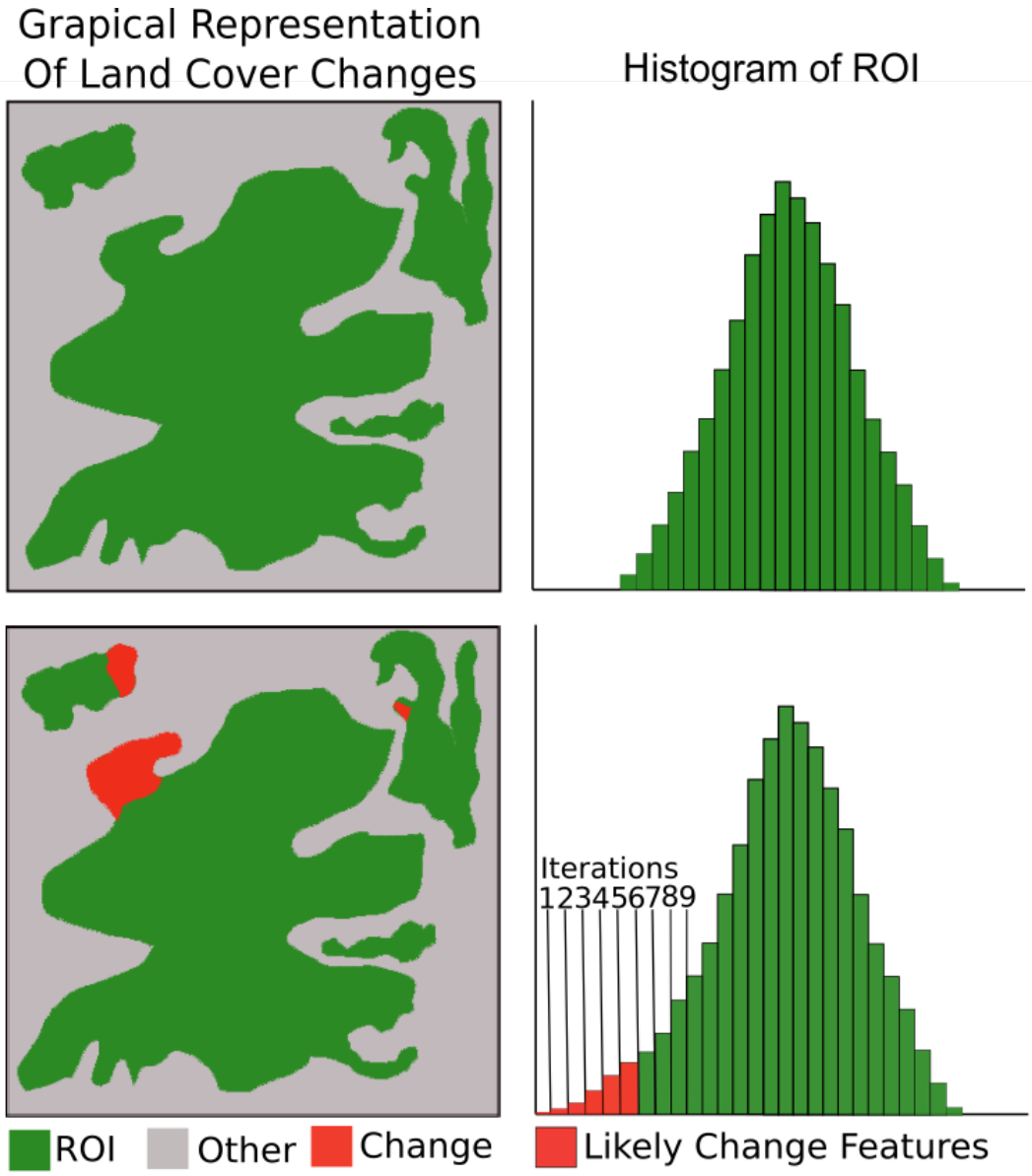

Figure 5.1: Graphical representation of the differences in the region of interest (ROI) histogram when change features are introduced. Top is a parametric histogram produced before the change and the bottom indicates the effect of change features. The bottom histogram also illustrates the iterative thresholding used to identify when a parametric distribution is reached and likely change features have been identified.

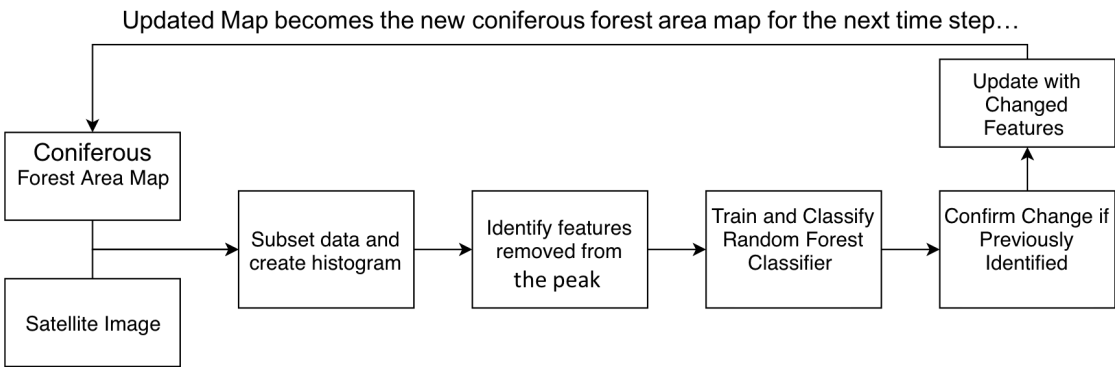

Figure 5.2: Processing chain for each time step that forms the basis of the approach. Inputs are shown on the left, likely change features are identified in the centre and the output is a updated coniferous forest cover map.

5.2.2 1989 Base Classification

A composite of 13 Landsat TM images from Summer (April-September) 1989 were used to generate a single Landsat scene from which a baseline forest/non-forest map was classified. 88% of the composite's terrestrial area was from images acquired on July 4th 1989. The remaining 12% was selected based on proximity to this date and image noise. Training Data was identified manually, informed by the 1km resolution Land Cover Map of Great Britain 1990 (LCM1990; Centre for Ecology and Hydrology 1995). SVM and Extremely Randomised Trees (ERT) (Geurts et al. 2006) classifiers were compared, ERT being proven to handle noisy data (Gislason et al. 2006, Rodriguez-Galiano et al. 2012) and SVM established as good binary classifier (Huang et al. 2002). ERT is a version of an RF classifier which samples training data without replacement, meaning trees will not be grown from the same sample twice. Alternatively, RF samples with replacement, meaning that the same training sample can be used multiple times in classifier training. The classifiers were compared using the same

training data with parameters optimised using a grid search, and an accuracy assessment of 10,000 stratified random points (5,000 in the Forest class and 5,000 in the other class). The ERT classification significantly outperformed SVM (Table 5.1). A z-score test indicated that there was a significant difference in the accuracy scores for the two classification approaches (z-score = 25.4, p <0.05; Congalton 2008). To reduce the effects of noise and classification error a minimum mapping unit of 9 pixels (0.81 ha) was imposed due to the minimum number of pixels in each segmented object. In the final baseline classification, the optimal number of estimators and the max features parameters were determined to be 50 and 2 respectively using a grid search. The other class contains marginally more error than the forest class (Table 5.2).

Table 5.1: Comparison of different machine learning classification approaches for 1989 base classification generation. The accuracy of random forests and support vector machine classifiers on 1989 composite classification is presented.

Classifier	Overall Accuracy (%)	Kappa
Support Vector Machines	80.7	0.62
Extra Random Forests	98.8	0.98

5.2.3 Change Analysis

The green, red, Near Infrared (NIR), SWIR and NDVI are known to relate to forest productivity (Myneni et al. 1995). A sensitivity analysis was performed to

Table 5.2: 1989 Base Classification Confusion Matrix percentages. Would expect 50% in forest and urban due to stratified sampling.

	Other	Forest	Users (%)
Other	50	0.5	99
Forest	0.5	49	99
Producers(%))	99	99	99

determine the band(s) or index best able to identify change features from each time step's image data. The volume of true change features identified using each band and NDVI was tested using 18,000 points across a 20-image subset with 300 stratified random points over 3 classes: stable forest, stable other, and forest loss (the change features). SWIR and NDVI identified the most true change features with the least false positives of change (Figure 5.3). This version of the map-to-image approach assumes a parametric distribution, therefore, the distribution of the NDVI and SWIR data for coniferous forests were tested using a histogram, Quantile Quantile (QQ) plots and the Shapiro-Wilks Test (Keskin 2006, Mendes & Pala 2003, Razali & Wah 2011, Shapiro & Wilk 1965). Reflectance data were extracted from 4,000 random points within forested area. The P-Values returned (NDVI: 0.93, SWIR1: 0.95) both indicate that the data are parametrically distributed. The QQ plots suggest that the data, especially NDVI, measurements are tailed (Figure 5.4), but not sufficiently to discount the use of a parametric distribution. Therefore, change features were identified using SWIR1 (upper quartile) and NDVI (lower quartile) measurements.

As the input classification is a binary forest and non-forest map a specific case needs to be considered. The non-forest ('Other') class contains a variety of land covers and therefore does not have a specific spectral signature, making it non-parametric. An optimised RF classifier was used to identify forest directly from the 'Other' class. The maximum number of features and the number of estimator parameters were optimised using a grid search. Training data for the classifier was randomly sampled from the regions known to be forest (i.e., following the application of the map-to-image approach to the forest class). The 'Other' training data were randomly sampled from across the whole image, to capture the in-class variability.

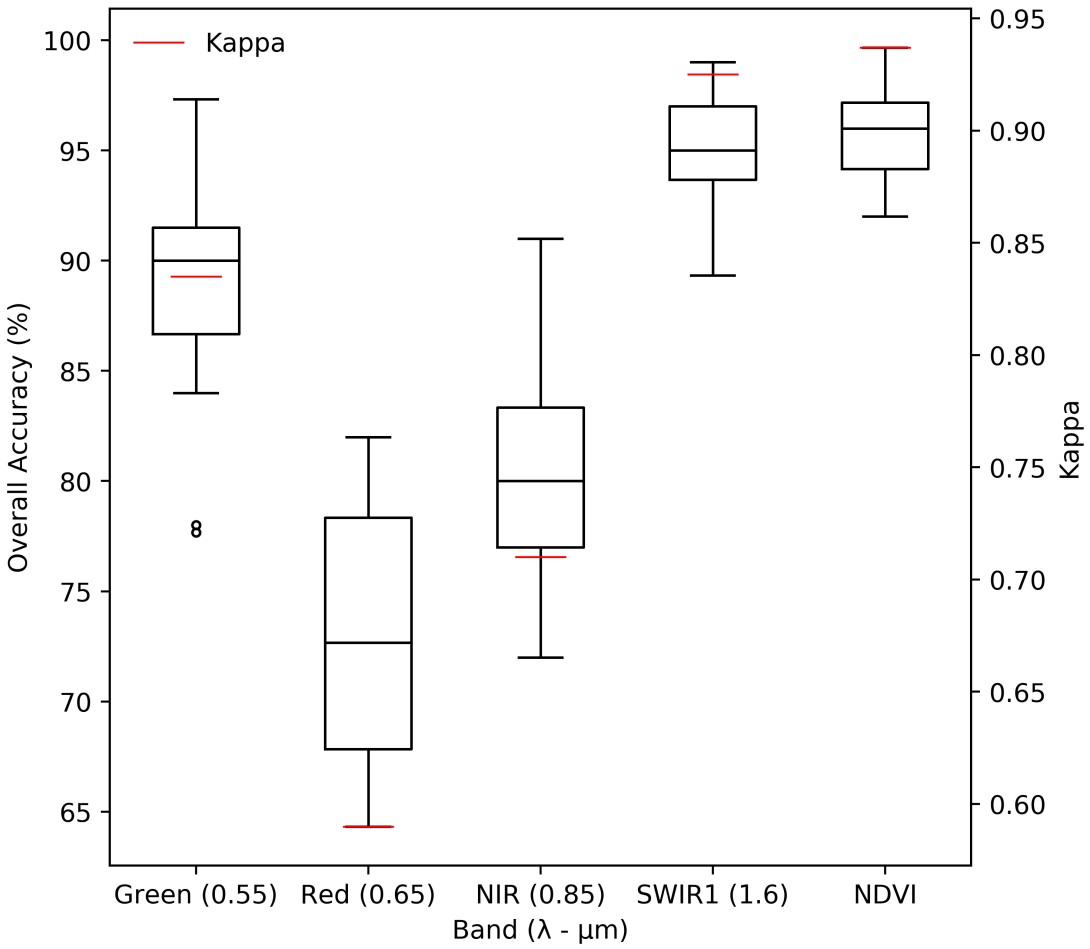

Figure 5.3: Sensitivity of different bands and index to forest cover loss. The mean and range of the 20 accuracy assessments for each band are shown. Mean kappa is shown in red.

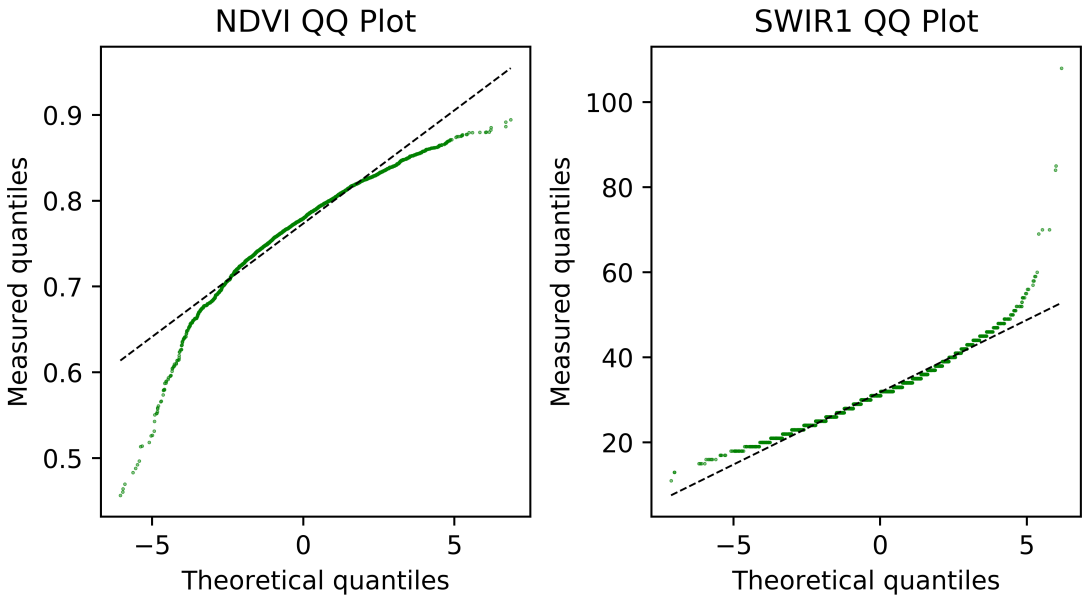

Figure 5.4: Quantile-quantile (QQ) plots for coniferous forest NDVI and SWIR1 bands.

The number of training samples per class was balanced at 20% of the total number of forest objects. If the forest region was > 1000 objects (> 200 training objects, occurred in 32 images) the volume was deemed insufficient to perform a regrowth classification. For these scenes, only forest loss was mapped.

The significant variation in signatures in the 'Other' class, could cause confusion with the forest regrowth class. Given the 27 year period of the analysis and typical 40+ year rotation of forest in Wales it is unlikely that a region of the forest was planted and harvested within the 27 year period. Therefore, regrowth classification was constrained to areas that were defined as a forest at the start (1989 baseline classification) and end (National Forest Inventory 2017; Forestry Commission 2017*b*) of the time series.

To reduce misclassification due to noise (e.g. geometric errors, image striping,

unmasked cloud) only persistent change features were committed to the classification. A sensitivity analysis was performed to identify the number of consecutive images change features needed to be identified in before being classified as true change in the map. The accuracy of change being committed after one, two, and three consecutive images was tested on a 20-image random subset. 80,000 points were tested in total, 1,000 stratified random points (4,000 per image) over four classes: stable forest, stable other, forest loss (negative change), and forest gain (positive change). Two consecutive identifications of forest cover change provided the most accurate result and was used in the time series analysis (Table 5.3).

Table 5.3: Sensitivity analysis for number of images recorded as a change features before change was committed.

Number of Consecutive Images	Overall Accuracy (%)
1	89.2
2	94.1
3	91.7

5.2.4 Accuracy Assessment

Accuracy assessments were performed on 20% of all output classifications (35 images). To ensure that the accuracy assessment was carried out over the range of the study period, 1 image in every 5 images was selected randomly. In total 70,000 points were tested. Within each image, 2,000 stratified random points were generated within the subset of the study area which was updated by that image for four classes (500 points per class): stable forest, stable other, forest loss, and forest gain. As the 'stable other' category covered such a large area the 500 random points were selected from within a 200m buffer of 'stable forest'

areas to ensure that sufficient points are placed within an area where change and error within the forest classification are likely to occur (Congalton 2008).

5.3 Results

5.3.1 Coniferous Forest Extent Change Across Wales (1990-2017)

178 classifications of Welsh coniferous forest extent were generated over the period 1990-2017. Figure 5.5 gives an illustrative example of forest cover changes for a location in South Wales throughout the time series. Coniferous forest cover in Wales was dynamic with a mean annual loss of 2,343 ha and a gain of 963 ha (Figure 5.6). Therefore, the algorithm documented an average loss in forest area of 1,380 ha per year (Figure 5.6). 117,600 ha are recorded as forested in the final classification from 2016.

5.3.2 *P. Ramorum* Felling Identification and Comparison

P. ramorum infection of Larch in 2013 had a significant impact on Welsh felling practices. Change was not identified when trees were infected with *P. ramorum* only when subsequent felling occurred. Infection is largely concentrated in the 2015 core disease zone (Core Disease Zone (CDZ)) and 2017 expansion in South Wales (Figure 5.7).As of August 2017, 3,125 ha of larch has been felled in the CDZ (Wright 2017) where the map-to-image approach has identified 3,621.7 ha

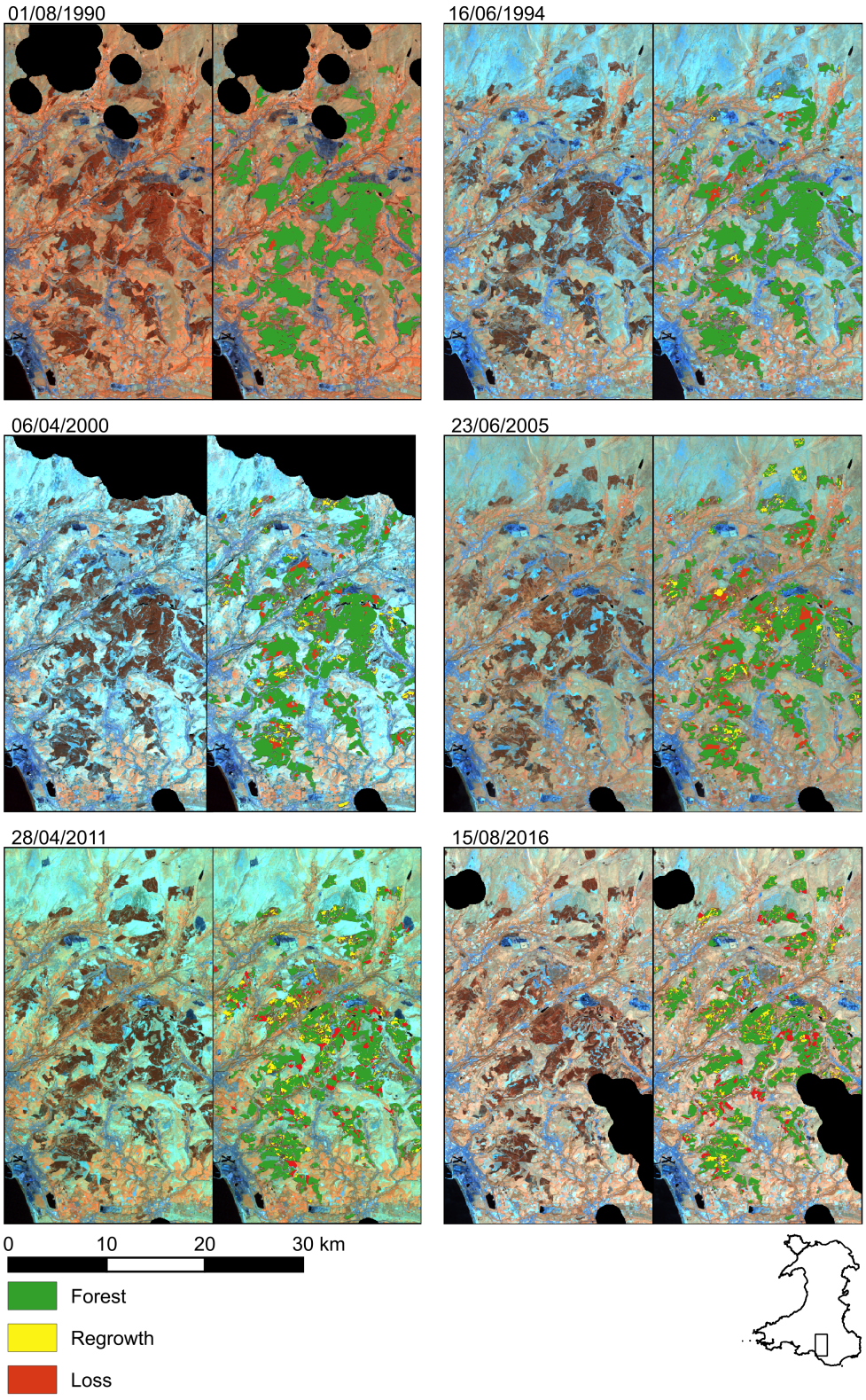

Figure 5.5: Classified forest, loss and regrowth classes from the histogram approach for a dynamic area in South Wales alongside the corresponding NIR, SWIR1, SWIR2 composite for six example dates in the time series.

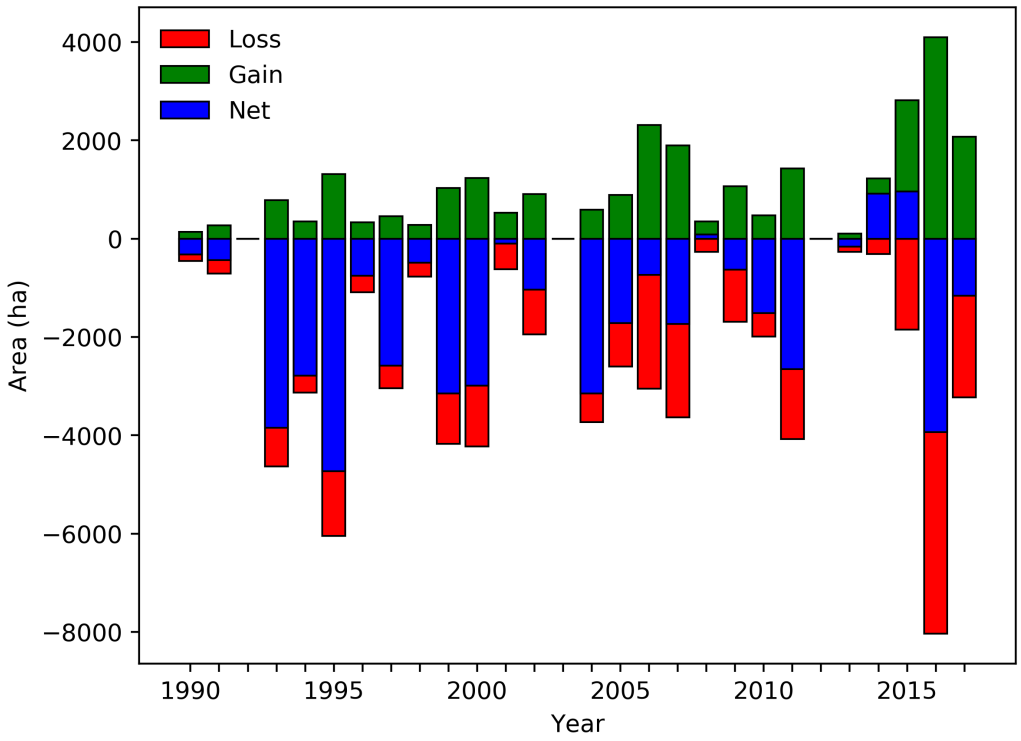

Figure 5.6: Area of loss, gain and net forest cover change identified using the histogram based approach per year.

of conifer loss. The 503.3 ha difference is likely due to the map-to-image figure including normal felling practices in addition to *P. ramorum*.

The majority of infections in the 2015 CDZ occurred between 2013 and 2015. However, reduced data volumes between 2012 and 2014 and the time series not including reflectance data for the entire CDZ in 2015 resulted in the majority of felling in the 2015 CDZ being identified in 2016. The felling in the 2017 expansion occurred during an increase in available imagery. Although the 2015 data likely contains some felling which occurred in the three years previously, the increase in coniferous loss area in 2016 likely relates to the increase of *P. ramorum*.

The spread of *P. ramorum* in the UK National Forest Inventory (NFI) and high-resolution optical data (Google Earth) was compared with the output classifications in a 12 km^2 area at Bwlch Nant Yr Arian (near Aberystwyth) between 2013 and 2016 (Figure 5.8). Spatially, the felling areas are similar to the reported infections and felling record (Figure 5.8). Temporally, the majority of the felling was identified within the same year (Figure 5.8) as reporting. The solid black and red boxes in Figure 14 indicate locations where the NFI and map-to-image felling dates differ by several years. The black box shows an area that appears to have been felled in 2011, before the *P. ramorum* was identified at Bwlch Nant Yr Arian and was not presented as forest within the baseline classification. The red box indicates a location, which appears to have been felled in 2015 but was not identified as felling within the NFI. This illustrates that the map-to-image approach can accurately identify felled areas and with the correct spatial and temporal pattern.

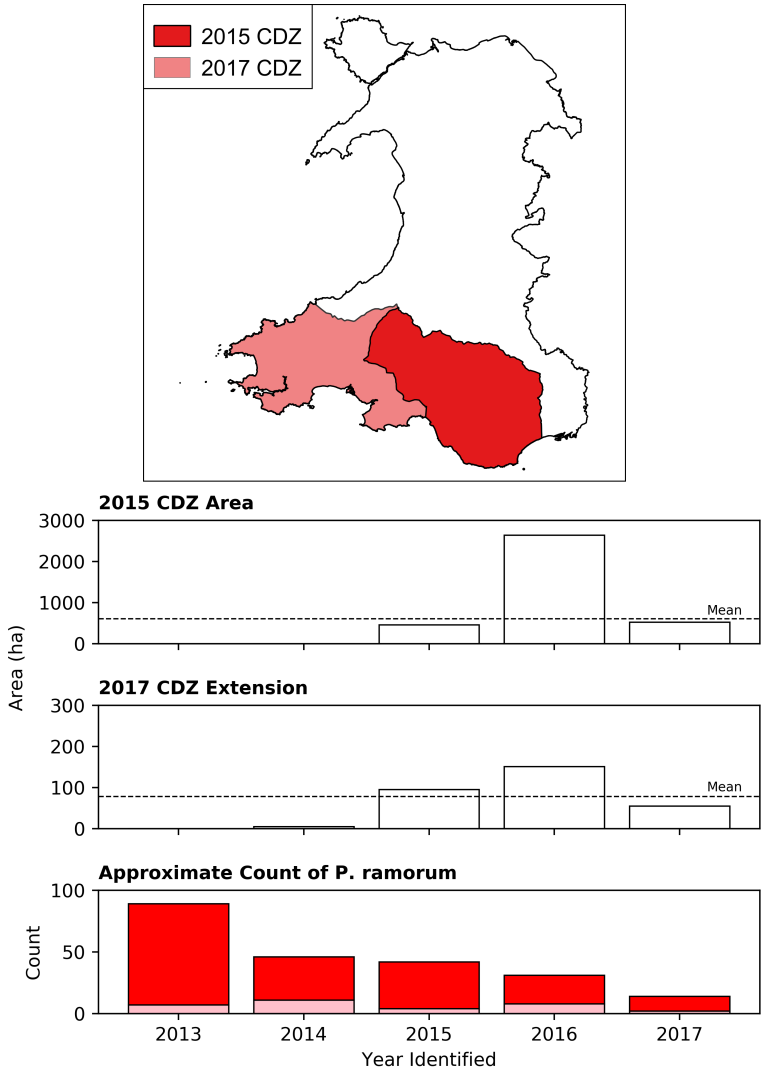

Figure 5.7: Forest loss in the 2015 core disease zone and the 2017 core disease zone (CDZ) expansion area (while the CDZ includes the 2015 area analysis was carried out on the expansion area separately). Approximate forest object count of P. ramorum infection derived from Wright (2017). The mean shown is the mean coniferous forest loss for each area over the 10 years previous to the initial infection (2000-2009).

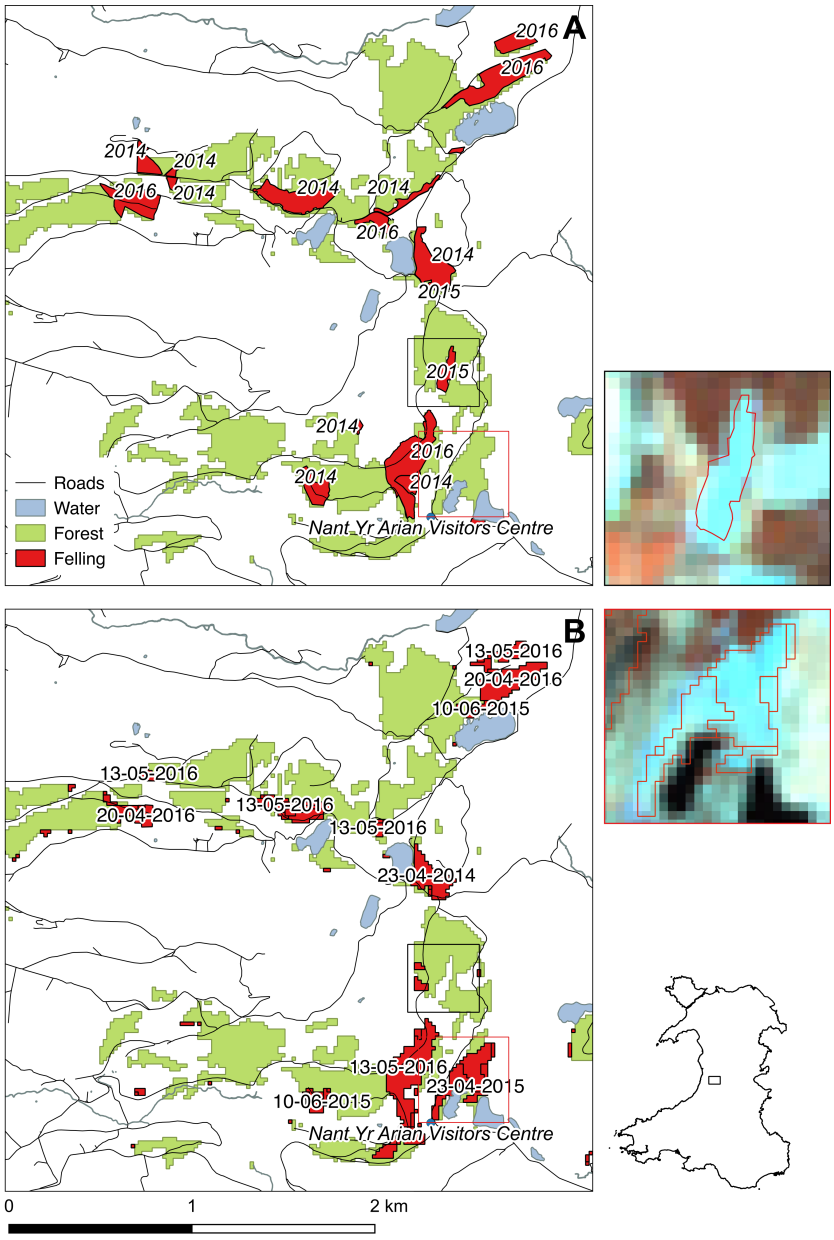

Figure 5.8: Felling activities at Bwlch Nant Yr Arian near Aberystwyth after *P. ramorum* was identified in 2013. A) NFI forest felling records from 2014 to 2015. B) map-to-image outputs of felling from 2014 – 2017. Black inset shows Red, NIR, SWIR1 composite from 2011 and region recorded as felled in 2015 NFI, Red inset shows Red, NIR, SWIR1 composite from 2015 and region not recorded as felled in the NFI.

5.3.3 Accuracy

Overall accuracy, calculated by summing the values from the 35 image confusion matrices, was 93.6% (±0.031 at a 99% confidence interval) with a kappa of 0.915. The mean overall agreement was 0.956 (Figure 5.9). The overall accuracy, quantity (total area of each land cover in the classification) and allocation (locations classified as each class) disagreement ranges increase with time. However, there is no significant loss of accuracy through the time series. The quantity disagreement is consistently lower when compared to the allocation disagreement suggesting that the overall area assigned to each class is correct and there is broadly equal miss-classification between the two classes. The user's and producer's accuracies of the forest 'gain' and 'loss' classes suggest that this is due to a slight under-identification of change features. Although accuracy is not as high as the forest loss change identification, the regrowth reclassification was largely over 80% accurate.

Table 5.4: Full confusion matrix for the histogram map-to-image land cover classification accuracy assessment percentages. Would expect 25% of points in each class due to stratified sampling

	Stable Forest	Stable Other	Forest Loss	Forest Gain	Users (%)
Stable Forest	23	0	2	0	93
Stable Other	0	24	1	1 0	94
Forest Loss	1	0	24	1	94
Forest Gain	0	0	2	22	93
Producers (%)	96	99	84	84	94

As coniferous forest is typically felled at 40-60 years old and is replanted, the class of a pixel should change once (due to felling) but may change twice (felling and regrowth to mature forest) during the study period (27 years). Pixels which change class more than twice are likely to be false positives. Nearly half (47%) of

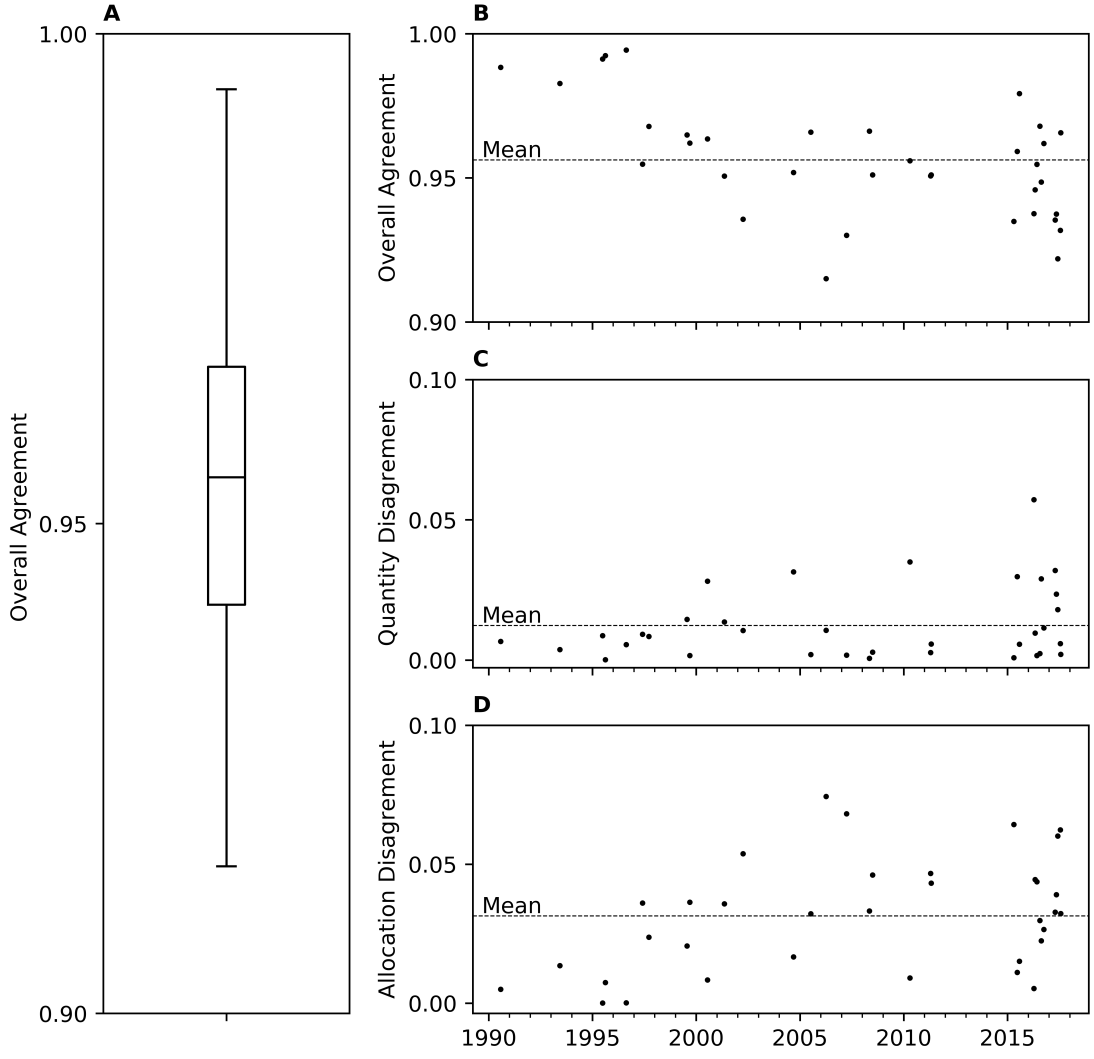

Figure 5.9: Accuracy metrics from across the time series. A) boxplot showing differences between the 35 images overall agreement. B) Overall agreement across the time series. C) Quantity disagreement across the time series. D) Allocation disagreement across the time series

forested locations (areas identified as forest at any point in the time series) changed class between 1990 and 2017 (5.10). 76.4% of changed pixels were altered once and 19.4% twice, the remaining 4.2% are likely false positives. Typically these are Mixed Pixels or registration errors located on the edge of objects (Figure 5.10).

5.4 Discussion

5.4.1 Comparison with existing datasets

The European land cover map (Land Cover Map (LCM)) series, using the coordination of information on the environment (CORINE) land cover classification, provides land cover data from across the study period (Land Monitoring Service 2021). LCM products have been produced for 1990, 2000, 2007, 2015, and 2017. However, as each map product is produced using different classification techniques and data resolutions, the products are not directly comparable for mapping land cover change and should not be used in PCC change detection analysis. Although the centre for ecology and hydrology has produced a change dataset using comparable approaches for the period 1990 to 2015, this only measures change in a woodland class rather than coniferous forest. The different coniferous forest areas for different dates are given in Table 5.5. There is a difference in the areas of around $300km^2$ but it is not possible to determine if the differences are due to error compared with ground change from the 'parametric distribution map-to-image approach' or differences in mapping technique, or coarser spatial resolution (all the LCM before 2017 were produced

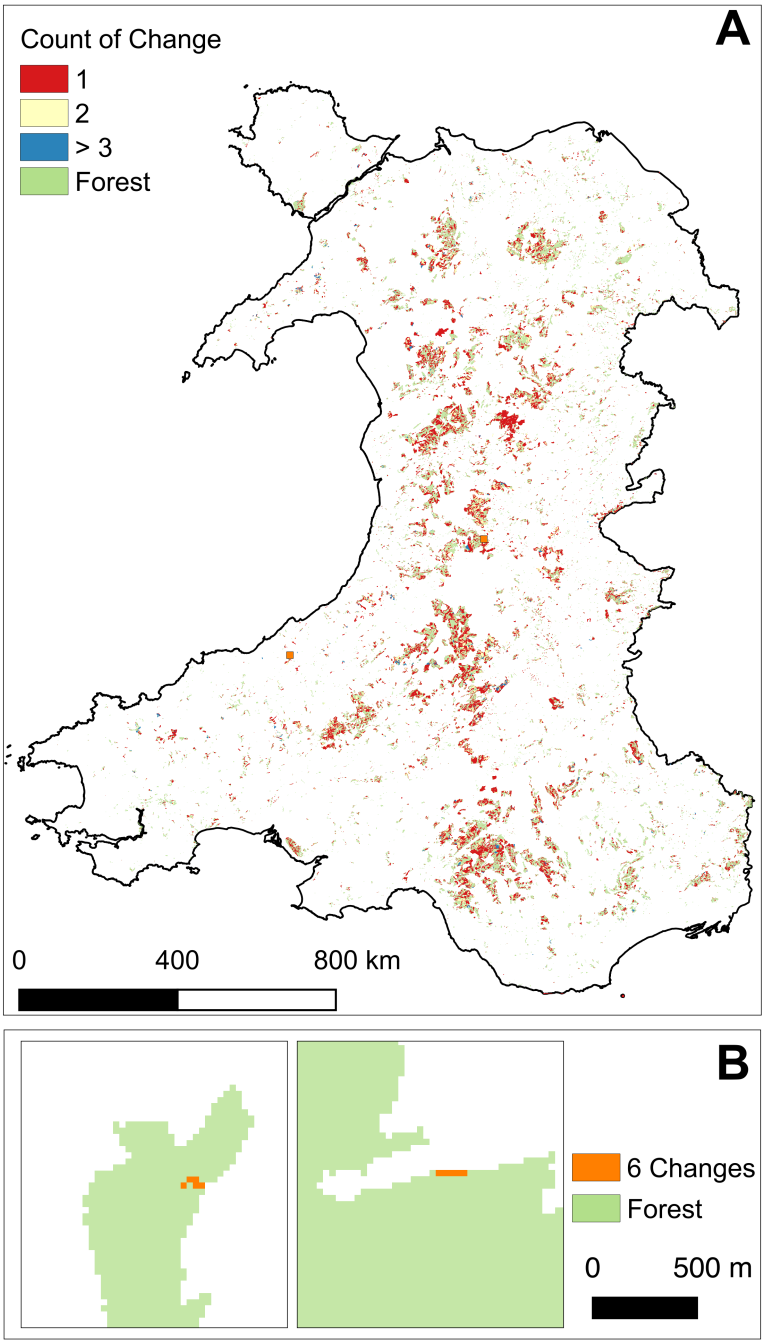

Figure 5.10: Number of times a pixel changed land cover throughout the time series. A) Number of times the pixel changed during the time series, where 1 = Only forest loss or regrowth, 2 = Forest loss then regrowth or forest regrowth then loss, 3 = A higher number of class changes than expected. B) Represents a change of land cover class on six occasions over the study period.

at a 1km per pixel resolution). The differences may be due to mixed pixels, where part of the $1km^2$ area is conifer, leading to different areas.

Table 5.5: Coniferous forest area produced by the European land cover map series and the parametric distribution map-to-image approach. As the land cover map is a nominal date the output product from the end of the same year was used in area calculations. The differences in area between the land cover maps should not be used to infer change areas, as the maps were produced using different approaches and are not directly comparable. The mapping scale was also different for the land cover maps produced before 2017.

Classification Type	1990	2000	2007	2015	2017
CORINE Land Cover Map Series	76 km^2	$1274km^2$	$1378km^2$	$1443km^2$	$1488km^2$
Map-to-Image approach	$1209km^2$	$1038km^2$	$1033km^2$	$1075km^2$	$1085km^2$

Although sporadic forest surveys and inventories have been conducted across Great Britain since 1924, the NFI, which started in 2009, is a rolling programme monitoring woodland and trees within Great Britain, providing data on the size, distribution and composition, and area of forests through time (Forest Research 2021). This was proceeded by the National Inventory of Woodlands and Trees, which produced a spatial dataset of tree cover at a forest type level in 2001. This is the earliest publicly available data set of coniferous forest cover in Wales, mapped at a comparable spatial resolution. Using these datasets coniferous forest area loss between 2001 and 2017 was measured at approximately 170 km^2. The approach presented here recorded 166 km^2 of loss over the same period. The 2016 NFI documents $1030km^2$ of coniferous forest with the mapped outputs from the same time estimating $1087km^2$. This difference may be due to the slight under classification of forest regrowth indicated by forest gain accuracy statistics. Additionally, the NFI includes a 'Young Trees' class which may not yet be considered coniferous forest cover in the approach and has a larger minimum mapping unit of 0.5 hectares.

5.4.2 Applicability to other Locations, Land Cover Classes and Data Sources

Changes in coniferous forest extent were accurately identified in the map products. To be classified as a change feature, the type of change needed to be of a large magnitude, such as felling events that exhibited a change in spectral response beyond the range of the parametric distribution. As change features were located as deviation from the peak of a parametric histogram the magnitude and consistency of any changes in spectral response are not considered. Smaller magnitude changes due to seasonal variation or infection and disease were not identified however, this does not represent and change in land cover. The approach assumes that the spectral response of a class is homogenous and the area of change within the class is small relative to the class extent. Assumptions that were true to reality here. The method outlined in this study would be directly applicable to regions of similar biome, with the same species, topography, and cloud cover such as; Northern Europe, Scandinavia, Siberia, North America, and New Zealand (Beland et al. 2017, Brandt et al. 2013, Swedish Wood 2019).

A key strength of the approach is that EO datasets are not directly compared. Therefore, different data sources can be used to increase the temporal resolution. The present example includes two sources of optical satellite imagery, but equally the approach could incorporate information from radar systems (e.g. Thomas et al. 2018). Deviations in textural rather than spectral response could also be included. The incorporation and study of radar data should be considered for futures studies where appropriate.

Based on visual comparison with the Welsh tree species subcompartment database, there does not appear to be any difference in the accuracy of felling identification in evergreen and deciduous species. This comparison was limited to a visual inspection as the database has a nominal date of 2018, after the end of the study period and the polygon boundaries do not always correspond well with ground cover (NRW 2021). The approach only appears to identify high magnitude changes, such as felling, therefore defoliation is not significant enough of any change to be identified. Where the assumptions hold, this methodology can be applied to other classes and data modalities such as mapping mangroves change using ALOS PALSAR data (Thomas et al. 2018) and rotating agriculture associated with savanna woodlands in Tanzania (Mabaso et al. 2016). The parametric distribution assumption may hold for other land covers (e.g. water) but is not universal (e.g. urban and grassland). Further research is required before it could be accurately applied to a full land cover classification.

5.4.3 Impacts of Assumptions and Limitations on Coniferous Forest Change Detection

There are three assumptions in the developed approach; (i) the class has a parametric distribution (ii) the area of change is small and (iii) change features are spectrally different from other land covers. These assumptions were true to reality in this example. The most significant errors were due to mixed pixels displaying characteristics of coniferous forest and other land covers.

Using a parametric distribution to identify likely change features resulted in a slight under-identification of coniferous forest cover loss. It fails to identify the

few change features which may fall within the normal distribution. In this case these were typically vegetated but not coniferous forest, removing the parametric assumption could help combat this.

All EO approaches change is identified by image acquisition date not by when it occurred on the ground. When data availability is limited (due to cloud cover, on-demand Landsat collections, and other issues related to image acquisition), the difference between when forest extent change occurred on the ground and when an image of the change is captured could be a number of years. This results in 'spikes' of comparatively high change figures after periods of lower data volumes (e.g. 1994 and 2016).

5.5 Conclusion

Change in coniferous forest cover can be accurately identified by detecting a deviation in feature spectral statistics away from a normal distribution. The approach was applied to coniferous forest cover change in Wales, UK between 1990 and 2017, using Landsat and Sentinel 2 imagery. The forest cover products had an overall accuracy 0.915 with a close agreement with Great Britain forest inventories. Accurate forest cover maps can be automatically produced at a sub-annual temporal resolution without the need for a dense time series of image data and with reduced dependence on radiometric normalisation.

This study has determined that the 'parametric distribution map-to-image' change detection approach (Thomas et al. 2018) can accurately detect land cover change in another forest type in a temperate region. Furthermore, the approach has been

applied to a fragmented time series of imagery to accurately map coniferous forest cover change. The next step is further research to ascertain if the parametric assumption can be removed and determine if this approach represents a tractable solution for generating a 'living map' of land cover data that is scalable to a large geographical area and time span.

Chapter 6

Removing Parametric Assumption For Coniferous Forest Change Detection

6.1 Introduction

The previous chapter illustrated that the 'parametric distribution map-to-image approach' can be applied to detect large magnitude changes in coniferous forest cover in temperate regions as part of an automated monitoring system. However, to apply this approach to more classes research is needed to determine if similar results can be produced from statistical analysis for change features which does not assume data distribution. The approach of combining map regions to subset image data assumes that (i) the area of change within a land cover class is small and (ii) that change features are spectrally distinct. Identifying a change threshold using

the skew and kurtosis of a parametric histogram introduces the assumption of a normal distribution. However, not all land cover classes follow this assumption, as they are typically made up of several surfaces with discrete spectral signatures (e.g. urban). Therefore, the approach must be developed before it could be applied to a full land cover map. An alternative approach for identifying likely change objects is required. Using the change and accuracy statistics from the previous chapter as a baseline for the current state of the approach, alternative methods for identifying change features were studied. Any alternative approaches need to be automatic, unsupervised, applicable to different sensors, and ideally make use of all appropriate data, as more information can be gained by using multiple inputs rather than a single band or index. Additionally, these approaches need to produce results of comparable or improved accuracy to those in the previous chapter. Consideration must also be given to any implications or limitations of these new approaches.

As new versions of analysis for identifying change features are introduced in this chapter for readability and brevity, the developed change detection approaches will be referred to based on the statistic used to identify change features. Therefore, the'parametric distribution map-to-image approach' will be referred to as the histogram approach in this chapter.

6.1.1 Data Clustering and Outlier Detection

Within the data subset from the map region, any potential change features are likely to be spectrally different from the unchanged regions. Outliers are data points that are considerably dissimilar to the remainder of the dataset.

Identifying outliers (e.g. financial fraud detection) is a significant area of statistical research (Bansal et al. 2016, Zimek & Filzmoser 2018, Niu et al. 2011, Chauhan & Shukla 2015, Wang et al. 2019) which could be used to identify likely change features. The spectral data from the new image, the data of which would be used to identity outliers, is multi-dimensional with an unknown distribution. Of the numerous outlier detection approaches, depth-based outlier detection algorithms may be appropriate to use to identify change features as they are typically used on multi-dimensional datasets of an unknown distribution (Johnson et al. 1998, Ramaswamy et al. 2000, Mandhare & Idate 2017).

Depth-based approaches could be used to find the outliers or likely change features in the image data (Figure 6.1). Clustering algorithms (e.g. KNN) are used to calculate distances to other points in the dataset. Assuming the data are homogenous in each dimension, outliers will be the points at the greatest distance from the cluster centre. These distance-based algorithms are widely used due to their effectiveness and simplicity (Huang et al. 2017). These algorithms can also identify outliers independent of detailed knowledge, typically this is with a hard threshold (e.g. percentage of data most likely to be outliers; Ramaswamy et al. 2000, Mandhare & Idate 2017). An algorithm of this type could be used, with a hard threshold, to identify potential change objects from each class region using all available spectral information (Figure 6.1).

6.1.2 Probability of Class Ownership

Change features could be located by identifying objects which have a low probability of belonging to their previous class based on new image data.

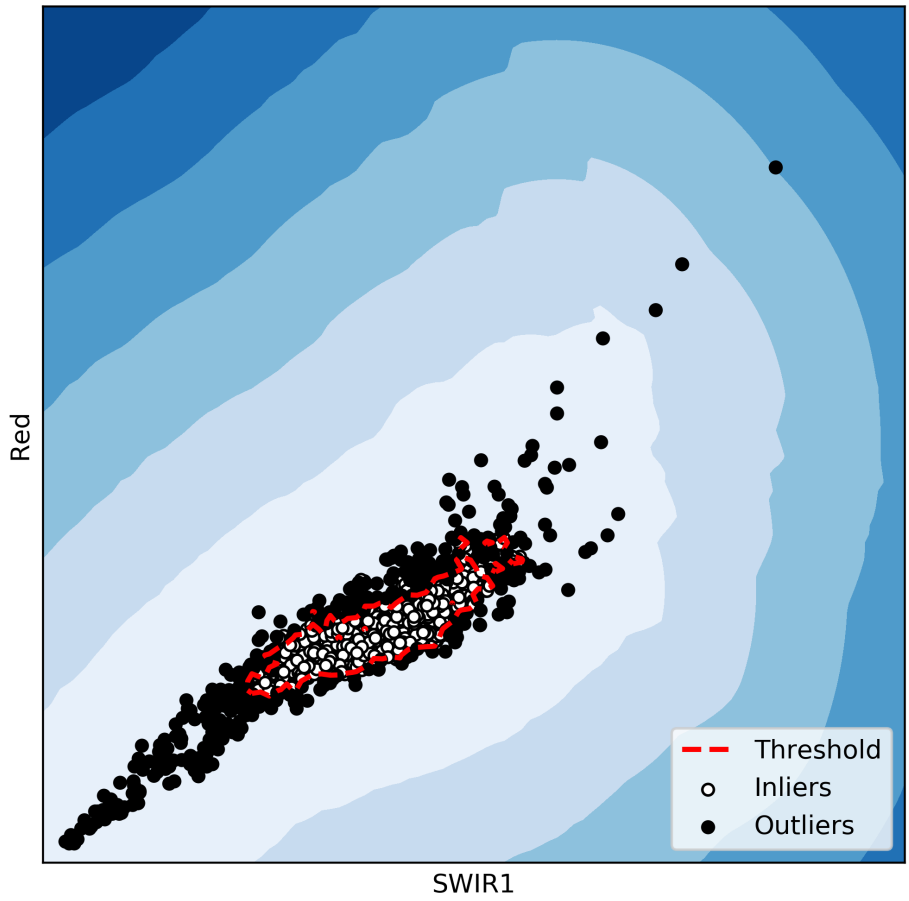

Figure 6.1: Graphical representation of outlier detection for identifying potential change objects. The centre of the cluster (inliers) being most certain to belong to the previously mapped class and teh edges (outliers) being potential change features.

Fuzzy-rough logic is used in classification problems to generate quantitive descriptors of class membership, events are ranked into classes by degrees of approximations (similarity to known/observable group parameters).

Fuzzy-rough classifications define a boundary for each class, inside which certainty is quantified using fuzzy relations and upper and lower approximations. Fuzzy Logic allows 'degrees of truth' or 'degrees of membership' as opposed to boolean logic, 'true' or 'false' only (Zadeh 1988). Rough Set theory is an approach to quantifying uncertain knowledge using upper and lower approximations to define groups. If completely indistinguishable from the members of a class an element belongs to the lower approximation, if there is an intersection in only some attributes the element is part of the upper approximation (Figure 6.2). Put another way, a fuzzy set means that the elements are not determined (Figure 6.3), they change by the observer and a rough set means the boundary of the set and some elements are not determined and they change by the observer. A rough set could be thought of as a rough edge to a set of elements whereas fuzzy logic is the inclusion of each element in a set by degrees.

A Fuzzy-Rough Set is a generalised rough-set, calculated by fuzzyfying (calculating degrees of membership) the upper and lower approximations (Dubois & Prade 1990, Radzikowska & Kerre 2002, Yao 1997, Cock et al. 2004, Jensen & Shen 2009, De Cock et al. 2007). Fuzzy-rough sets result in a 'core' of observations determined to be more certain to belong to a class, which is surrounded by other observations which show some similar characteristics. The certainty of each object in remaining within the previous class could be used to identify likely change features, as the spectral differences in change objects would result in reduced certainty values for

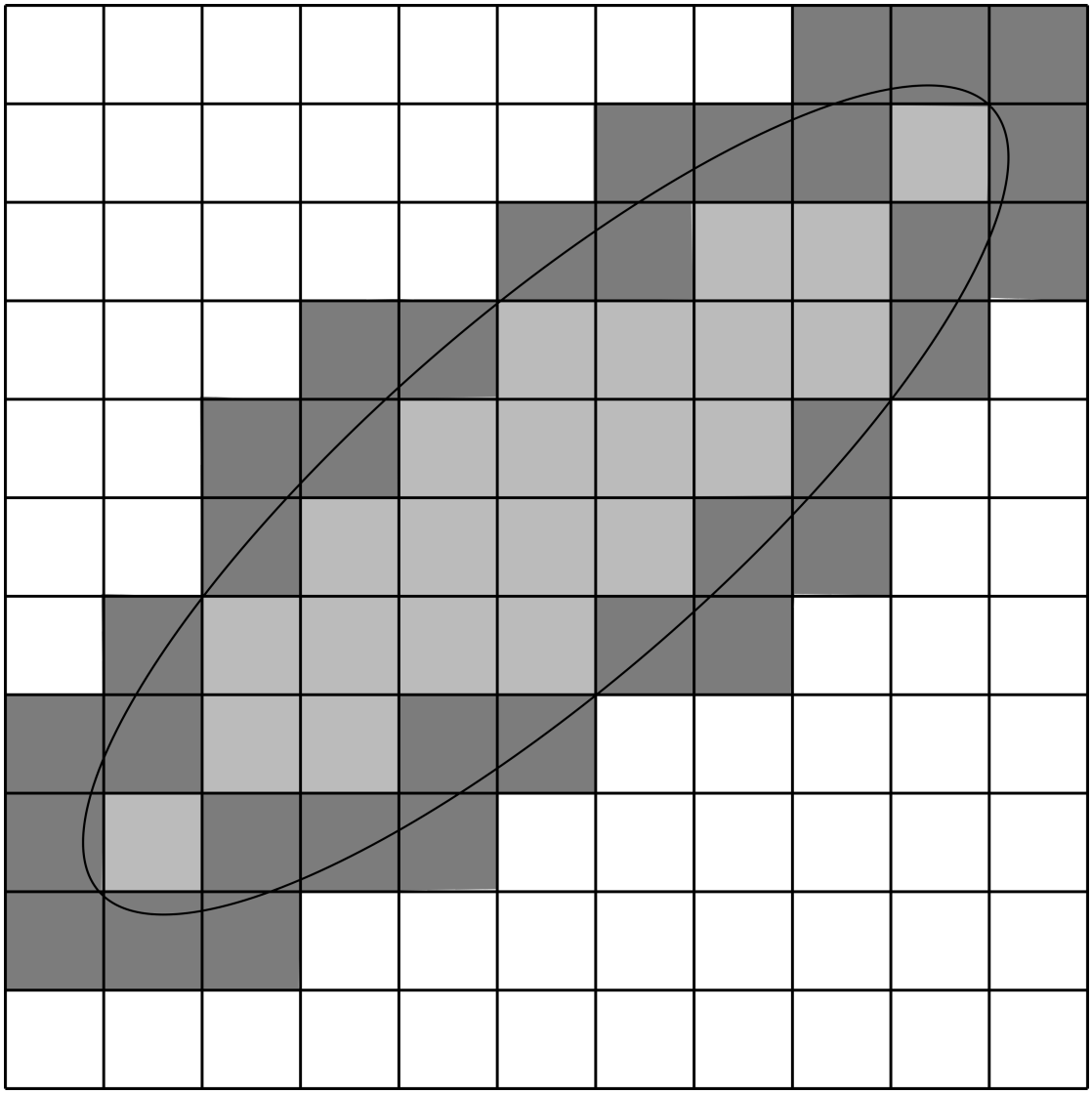

Figure 6.2: Graphical representation of a rough set. The circle is the boundary of a class or concept. The light shading represents the lower approximation, where objects are equivalent if they are included in the class. The dark shading represents the upper approximation, where objects only intersect with the class.

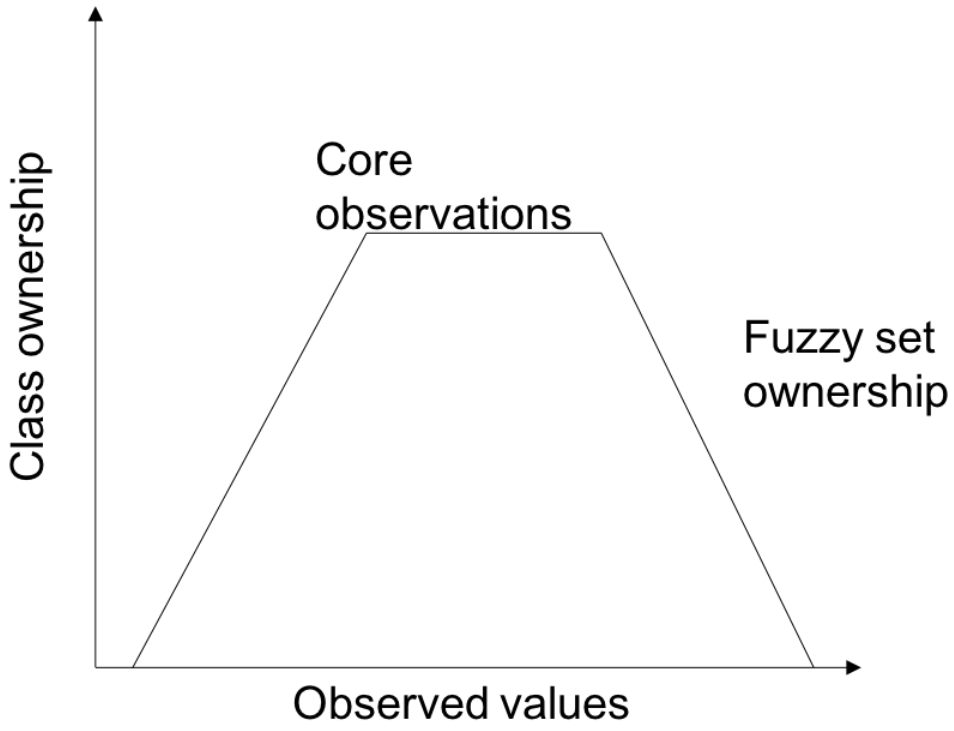

Figure 6.3: Graphical representation of fuzzy logic. The x axis represents different observable characteristics of a set, the y axis represents the ownership in the class, the plotted line represents the changes in ownership at different characteristics. In the centre there is a core of observations with maximum ownership.

belonging to the previously mapped class.

Zhao & Hryniewicki (2018) have demonstrated how machine learning classifiers can be used to determine outliers in a dataset. They used a semi-supervised ensemble algorithm, Extreme Gradient Boosting Outlier Detection (Extreme Gradient Boosting Outlier Detection (XGBOD)), to accurately detect outliers in practical datasets such as mammography and cardio images, speech and satellite data (Zhao & Hryniewicki 2018). XGBOD uses multiple unsupervised machine learning algorithms to extract information from the dataset, which is fed into a supervised classifier. Building on this work, machine learning probability metrics could be used to identify likely change features. Working on the assumption that change is spectrally distinct, change features should exhibit a low probability of class ownership in their previously mapped class. The probability metrics generated from an unsupervised machine learning technique could be fed into an improved supervised classifier to identify likely change features from the image data.

In summary, change features could be directly classified onto the image or probability of class ownership used to separate change features.

6.2 New Likely Change Feature Identification Methods

Three different approaches for identifying likely change features, which do not assume the distribution of the land cover class were identified. For brevity and ease of understanding these alternative approaches will be referred to by the statistical

process used to identify change. The previous approach, which used a histogram and parametric distribution, will be called histogram change detection. These approaches all combine map and image data to identify change features:

1. Using outlier statistics to identify likely change features based on the assumption that change features are rare and statically different from their previous mapped class. This approach will be called outlier change detection

2. Fuzzy-rough logic to calculate class ownership. Change features should exhibit lower ownership to their previous mapped class this can be used to identify likely change features. This approach will be called fuzzy-rough logic change detection

3. Repeated sampling and performing random forest classification of training data to assign a probability of class ownership. Assuming that change features are spectrally distinct they will have a low probability of belonging to the class in which they were previously mapped. This approach will be called repeated RF classifier change detection.

The accuracy of these approaches for detecting change features automatically in a time series was assessed by applying the approaches to the same time series of satellite imagery used in the previous chapter. The same binary classification of coniferous forest and other classification for 1989 was also used as a starting map to identify changes in coniferous forest extent. The process of combining the map and image data and reclassifying likely change features using an optimised RF classifier remains unchanged from the previous chapter, therefore the methodology is not repeated here. However, the histogram statistics for change detection were

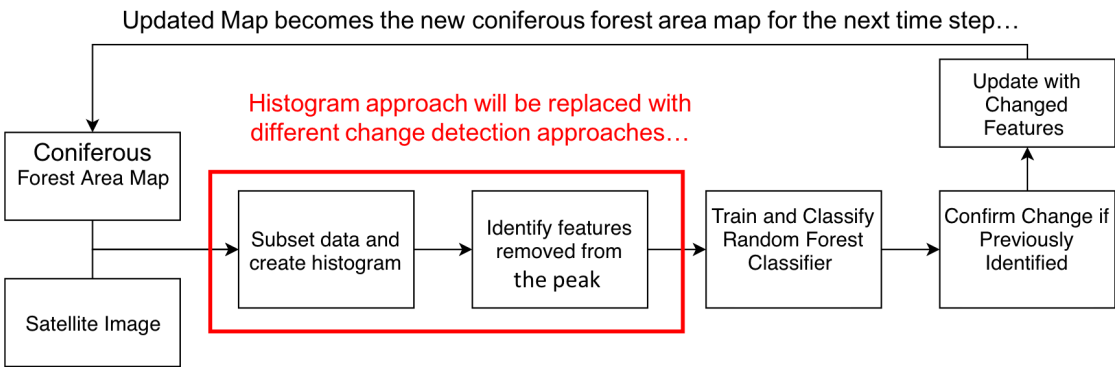

Figure 6.4: Processing chain applied to each time step in the time series in the previous chapter. The section of the processing chain identifying likely change features using a histogram distribution is in the red box. This section will be replaced by the three new approaches being tested. The rest of the processing chain combining map and image data and classifying likely change features will remain unchanged in each approach.

replaced with the three new statistical approaches (Figure 6.4), the changes to the processing chain and parameters selected for each of the three approaches are detailed in the following sections.

6.2.1 Outlier Change Detection Algorithm

An outlier detection algorithm was used to detect likely change features from the spectral data from the coniferous forest area. The outlying data with the largest euclidean distance from an unsupervised K Nearest Neighbour (KNN) cluster centre was identified as likely change features (Figure 6.5). The majority of the features are assumed to be unchanged. Therefore, they should form a cluster, the objects furthest from these clusters are the most likely to have changed land cover. Ramaswamy et al. (2000)'s KNN proximity-based algorithm in the Python Outlier Detection (PyOD) module was used to identify these outliers. The

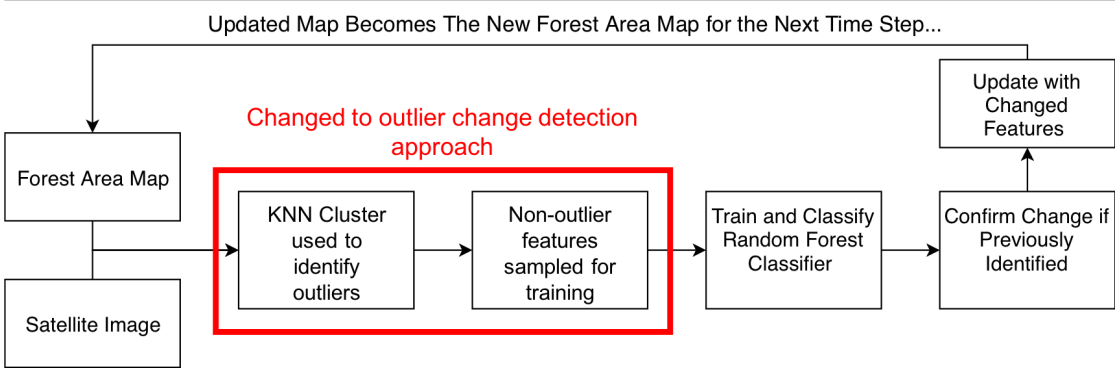

Figure 6.5: Outlier change detection processing at each time step in the time series. The red box illustrates the steps which were changed from the previous chapter. Clustering is now used to identify change features. Samples on the edges of clusters are more likely to be change features. The core of the cluster is sampled for training data to reclassify the outliers. The rest of the processing chain combining map and image data and classifying likely change features is unchanged from the approach in the last chapter.

outlier detection algorithm returns a binary outlier or non-outlier result based on a percentage threshold (i.e. the 10% of data furthest from a KNN cluster centre). The percentage threshold parameter was determined using a sensitivity analysis.

6.2.1.1 Outlier Threshold Sensitivity Analysis

The outliers in Ramaswamy et al. (2000)'s algorithm are identified using user-defined percentage of the whole dataset (i.e. 10% of this dataset are likely to be outliers so identify the 10% of the data points furthest away from KNN cluster centres in the euclidean distance and n-dimensions). The user-defined percentage parameter has a large impact on the data identified as outliers. In this case, a small percentage would result in an under-identification of change features and too large a percentage could introduce many false positives of change.

Therefore, to identify a percentage threshold that related well with likely change features in coniferous forests a sensitivity analysis of different percentages of the map regions as outliers was performed on a subset of 20 images. Thresholds of between 10 and 50% of the mapped regions were tested in 10% increments and an accuracy assessment was performed. One thousand five hundred sample points were stratified across three classes (five hundred points per class); stable forest, stable other, and loss. The accuracy fell from the base classification accuracy of 98% especially at 10 and 50% thresholds. The 20% threshold produced the highest accuracy coniferous forest loss change detection on the 20 image subset (Table 6.1). Therefore a 20% outlier threshold was used to analyse the whole time series dataset.

Table 6.1: Percentage of change features which where correctly identified (neither a false positive or negative) using different Outlier Thresholds on 20 image subset

Threshold (%)	Accuracy (%)
10	95.98
20	97.98
30	97.8
40	96.85
50	94.15

6.2.2 Fuzzy Rough Logic Change Detection

Fuzzy-rough logic statistics were used instead of the data distribution to identify likely changes in coniferous forest cover in Wales (Figure 6.6). A Fuzzy-Rough Nearest Neighbour (FRNN) algorithm was selected because KNN is widely used in image processing and has proven that nearest neighbours can be used to identify meaningful clusters of similar spectral data in satellite imagery. In the FRNN algorithm data are assigned a similarity score to the sample's KNN in a training

data set. If the K nearest neighbours are more different, it indicates the sample is on the edge of the training cluster and more likely to be a change feature. The number of K was set at 5. This was determined using sensitivity analysis of K between 2 and 10 on a 10 image subset and clean training data generated using a histogram threshold of the coniferous forest and other classes. Table 6.2 illustrates the results of an accuracy assessment of 2000 points (200 points per image) on the stable forest and forest loss areas (100 points per class). Similarity metrics, based on the differences between each sample and its 5 nearest neighbours were used to help separate true features and noise. A threshold of 0.5 was applied to the similarity metric, as this would mean at least one of the samples nearest neighbours was not from the coniferous forest class. This threshold was selected based on the similarity metrics produced by objects correctly classified change features using the histogram change detection approach in the previous chapter.

Table 6.2: ercentage of change features which where correctly identified (neither a false positive or negative) using different Fuzzy Rough Nearest Neighbour K Values on 10 image subset

K Nearest Neighbours	Accuracy (%)
2	92.3
3	93.7
4	95.6
5	96.8
6	94.1
7	94.3
8	92.4
9	91.2
10	93.4

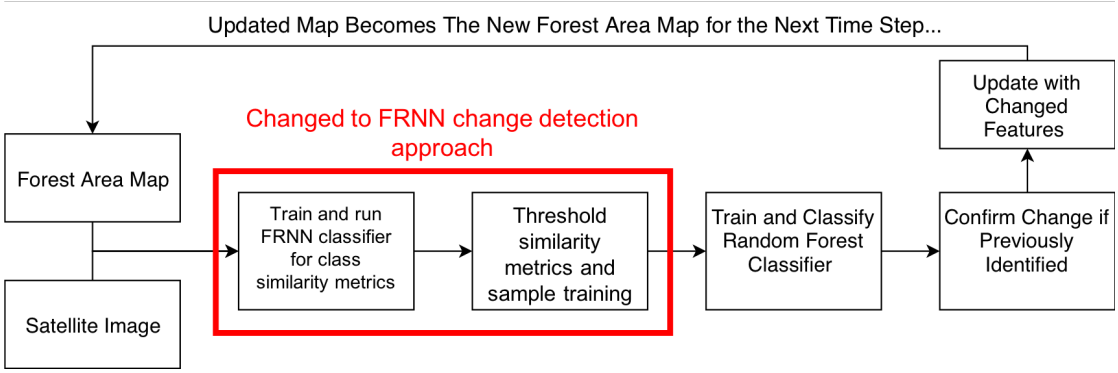

Figure 6.6: Fuzzy-rough logic change detection processing at each time step in the time series. The red box illustrates the steps which were changed from the previous chapter. Fuzzy rough nearest neighbour similarity metrics based on a sample's closeness to the core of the distribution are used to identify likely change features. Samples on the edge of the dataset are more likely to be change features, these are sampled by applying a threshold the similarity metric. The samples which are not likely to have changed are sampled for training data to reclassify the outliers. The rest of the processing chain combining map and image data and classifying likely change features is unchanged from the approach in the last chapter.

6.2.3 Repeated RF classifier change detection

Class ownership probabilities from a machine learning classifier were used to identify likely change features, based on the assumption that change features would exhibit a smaller ownership probability in their mapped class than the unchanged data (Figure 6.7). As the quality of training data can not be assured because the map regions contain errors and some change features any machine learning classifier used needs to be resistant to noise in training data. The ERT classifier was selected due to RF's 'natural' tendency to reduce the effects of noise in training (Breiman 2001) and Overfitting. The RF algorithm grows hundreds or thousands of classification trees from individual random subsets of the training data, which are combined to produce a final classification. As the noise is a small part of the whole training data set it is less likely to be part of the random subsets. Additionally, the ensemble voting reduces the impact of any selected noise on the final classification. RF type classifiers are resilient to up to 10% noise in training and as much as 30% can be accounted for (Agjee et al. 2018).

An unsupervised K Means ++ classification was performed on the 'Other' class to ensure that the full variety of spectral responses in the class was represented in the training data. A sensitivity analysis determined the parameters in Table 6.3 were best able to reliably capture variability in the 'Other' class.

Twenty percent of the forest objects and an equal number of objects from the 'Other' class were sampled to train the RF classifiers. The bagging performed by RF classifiers can result in the same sample being selected to grow multiple trees. It is possible for the change features (noise) to be repeatedly selected to generate

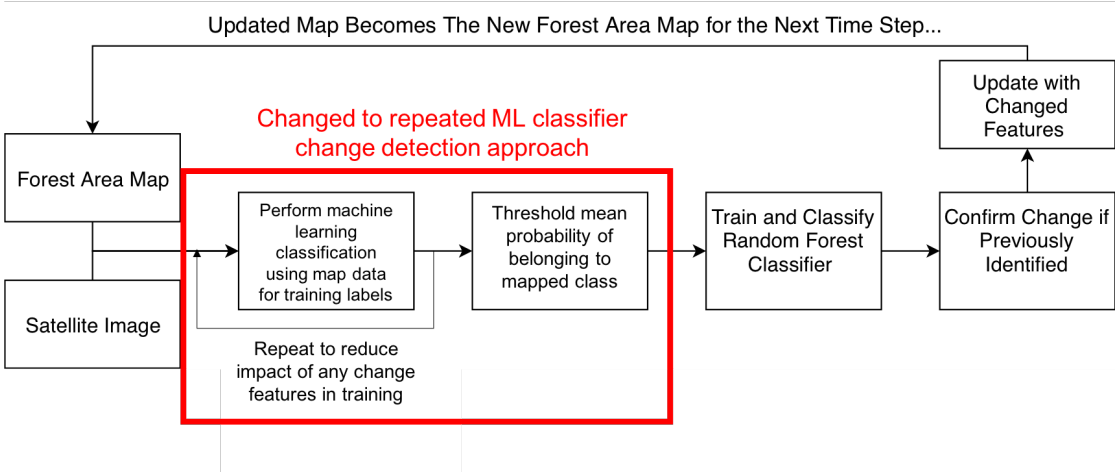

Figure 6.7: Repeated RF classifier change detection processing at each time step in the time series. The red box illustrates the steps which were changed from the previous chapter. Training data are sampled from the map regions and fed into an optimised machine learning classifier. If a sample is no longer displaying the characteristics of its mapped class the probability of belonging to this class will be low. To reduce the impact of any changed features on the training data multiple ML classifiers are trained and the probability of class ownership is averaged. The samples with a low probability of ownership in their mapped class are likely change features. These features are classified using a further random forest classifier as in the previous chapter. The rest of the processing chain combining map and image data are also unchanged from the approach in the last chapter

Table 6.3: K Means Parameters selected by sensitivity analysis of different parameters for sampling the range of values in the 'Other' class.

Parameter	**Value**
Batch Size	100
Maximum Iterations	400
Maximum with no Improvement	10
Number of Clusters	4
Number of Intialisations	3

the random forest, or that the majority of the forest features in the training dataset are examples of change. To ensure this did not occur the training data was split 50 times and used to train 50 RF classifiers optimised using a grid search. The probability of class ownership for each class was stored and a mean probability was calculated for each object. the 50 classifier limit was determined based on the point at which the changes in the mean probability of class ownership for each object remained similar despite further and further classifiers trained(Figure 6.8).

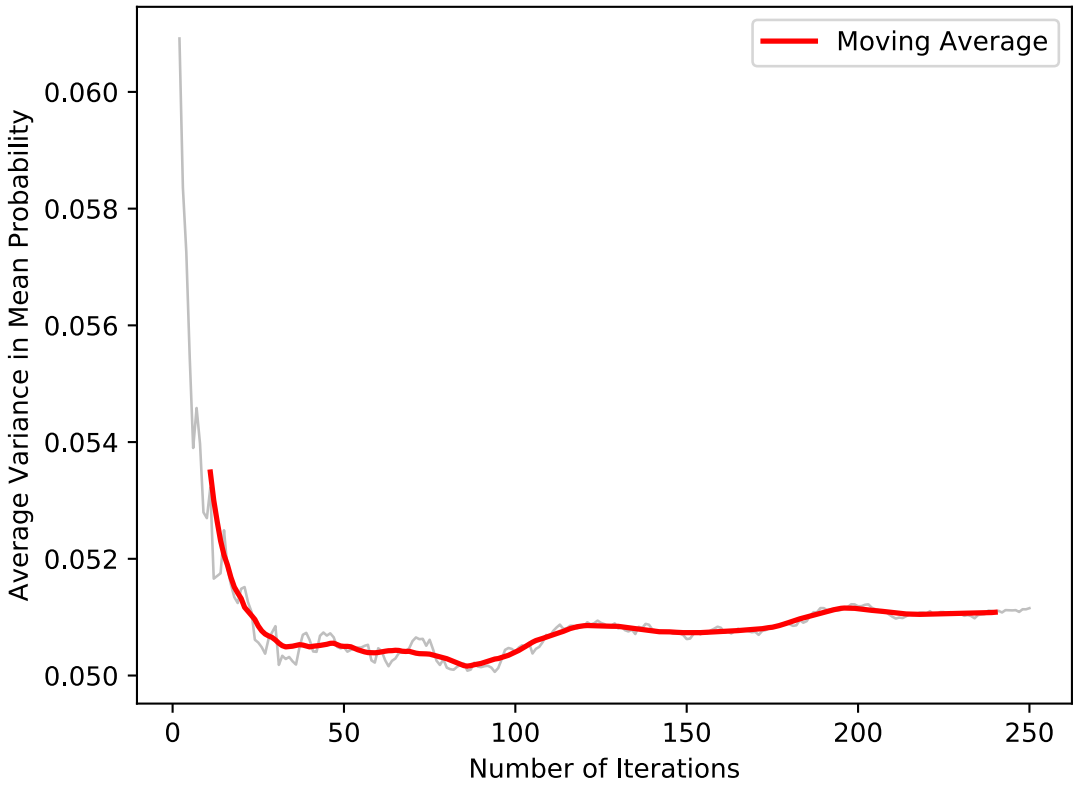

Figure 6.8: Differences in mean probability by the number of iterations of extra random trees classifiers generated. The average variance in the mean probability of class ownership is on the y axis and the number of classifiers trained is on the x-axis. After around 50 classifiers the reduction in average variance is reduced and does not decrease further suggesting there is little point in performing further classifications.

A threshold was then applied to the mean probability values to determine the likely change features based on the probability of previous class ownership. Following the assumption that change is a small part of the whole, the majority of the data should exhibit a similar probability of class ownership. Values lower than this are more likely to be change features. Accuracy of a threshold at $\mu - 2SD$ and the highest frequency histogram 'bin' was compared on a subset of 10 images. Using the value of the highest frequency 'bin' as a threshold produced training data which led to higher accuracy figures (Table 6.4) therefore, this was used in the analysis.

Table 6.4: Accuracy of different thresholds on probability scores for selecting likely change features from whole class area on subset of imagery.

Threshold	**Accuracy(%)**
$\mu - 2SD$	93.4
Highest Frequency	95.3

The objects with a high probability of belonging to the coniferous forest or other class were then used to train a final optomised extra random trees classifier to reclassify the likely change objects and update the previous map. The new classification was used to define training data and identify likely change features at the next time step (Figure 6.7).

6.2.4 Accuracy Assessment

An accuracy assessment was performed on the same 20% of all output classifications (35 images) as in the previous chapter, to allow for comparison. A total of 70,000 points were tested. Within each image 2,000 stratified random points were generated within the area updated with new image data across the

same four classes as in the previous chapter (500 points per class); stable forest, stable other, forest loss, and forest gain. The 'stable other' category was sampled in a 200m buffer of the 'stable forest' areas to ensure sufficient points were placed in the area where errors in the change detection were likely to have occurred (Congalton 2008).

This method of accuracy assessments provides statistics on the accuracy of large-scale land cover change detection in addition to the accuracy of the Binary Map products produced. The stable and gain/loss classes of each class can provide information on any over or under classification of change and the overall confusion matrix provides information on map product accuracy.

The accuracy assessment is limited by the availability of reference data for the study period. The ground truth for the points was tested against Google Earth imagery and the time series dataset. Ideally there reference data would be based upon a higher resolution dataset than the map products were generated from or field samples but this data was not available for the study period. Ideally, change features recorded at the end of the time series would be verified in the field, but this was not possible due to resource constraints. However, if this study was to be repeated ground reference data collection would be recommended. As the changes are large-scale land cover changes such as felling these should be identifiable from the imagery alone.

It is important to note that the accuracy assessment can not characterise the percentage of all change objects which have been identified. It is simple to characterise false positives or commission error as this can be sampled within the change features (the forest gain and forest loss classes) but any omission is much more difficult to identify. As a small part of the whole stable class, it is unlikely

that omission error will be randomly sampled, even after biassing sampling towards likely omission areas. By its nature omission is difficult to identify as its location is unknown. Without a dataset of all change features to compare data to omission will be unrepresented in any sampling and the final accuracy. The change detection accuracies are likely lower than those calculated due to omission features.

6.3 Results

6.3.1 Fuzzy Rough Logic Change Detection

The fuzzy rough logic change detection vastly over-identified forest loss throughout the time series. The coniferous forest extent produced by fuzzy rough logic change detection was 42% lower than the histogram generated extent on average (as no ground truth data are available for the whole study period and the histogram approach was accurate it is used for comparison here). It is highly unlikely the ground truth figures vary as wildly from those produced using histograms as the fuzzy rough logic change detection data suggests. A full accuracy assessment was not performed on the fuzzy rough logic change detection products because the change detection was incorrect in the majority of cases (Figures 6.10 and 6.11).

This over-identification of forest loss was due to the definition of training data in the coniferous forest and other classes. It stems from a lack of definition in the other class. The similarity metric used to reduce error and identify possible change features from the coniferous forest data removes samples where at least one

neighbour was not classified as coniferous forest in the base map. In cases where classes exhibit defined clusters, this would result in the removal of the data on the edge of the cluster, most likely to belong to change features (i.e. the removal of the data on the edge of the coniferous forest cluster or any outliers of the cluster). However, as the majority of the other class is also vegetation, it overlaps with the coniferous forest cluster in the feature space (Figure 6.9). Additionally, the 20% of other data sampled as training may contain little or no examples of bare ground.

In this situation, large amounts of coniferous forest data are identified as potential change features, causing the training data for the coniferous forest class to become unrepresentative. This results in unchanged areas of coniferous forest appearing closer to the vegetation in the other class than the coniferous forest training and subsequently being identified and classified as a change feature (Figure 6.9). Without clean, well-defined training data the threshold identified did not accurately reflect forest change (Figures 6.10 and 6.11), consequently, analysis using fuzzy rough logic change detection was terminated. Potentially, training data quality could be improved by introducing expert rules or an unsupervised clustering of the other class to ensure variety (see repeated RF change detection), but these approaches are not explored here.

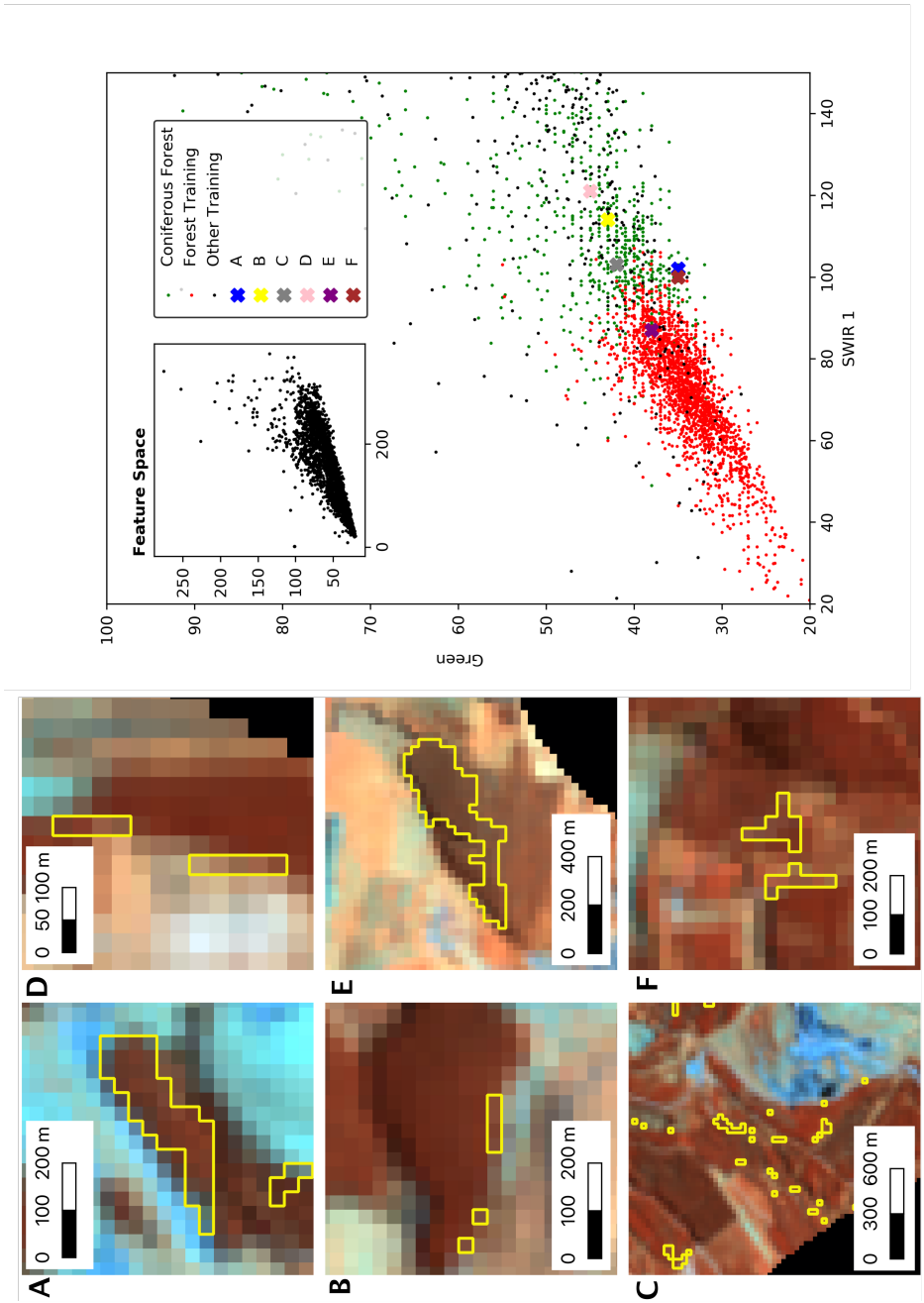

Figure 6.9: Six examples of coniferous forest areas identified as forest loss by FRNN in 2015 and their location in a SWIR1 and Green feature space. The images are a FCC of NIR, SWIR1 and SWIR2. The range of the coniferous forest training data, all Coniferous Forest data and the Other training data are shown in a subset of the feature space. The distribution of the full feature space is illustrated by the insert.

6.3.2 Outlier Change Detection

Coniferous forest extent change in Wales was mapped between 1990 and 2017 in 146 binary classification products. The mean annual loss was 17.35 km^2 and the mean annual gain was 15.12km^2. Therefore, the algorithm documented an average loss in forest area of 2.15km^2 per year.

Overall accuracy, calculated by summing the values from the 35 image confusion matrices, was 91.6% (±0.6 at a 99% confidence interval) with a kappa of 0.888 (Table 6.5). The mean overall agreement was 0.99 (Figure 6.12) and the Z-Score 61.69, significant to a P-Value of $< .00001$. There is a slight increase in the range of the quantity and allocation disagreement values with time. However, there is no significant fall in accuracy through the time series. The commission error in the forest gain class suggests an over-classification of regrowth combined with a slight under-identification of loss features was the primary source of error.

Table 6.5: Full confusion matrix for outlier change detection coniferous forest extent change accuracy assessment percentages. Forest in the table refers to coniferous forest only. Would expect 25% of points in each class due to stratified sampling

	Forest	Forest loss	Other	Forest Gain	Users (%)
Forest	23	0	2	5	76
Forest Loss	1	23	0	0	95
Other	0	0	25	0	99
Forest Gain	0	0	0	21	99
Producers (%)	95	100	91	80	91

The majority of the change area should change once or twice during the study period. Areas which exhibit a greater number of changes are likely to be false positives. The over classification of regrowth and subsequent re-identification

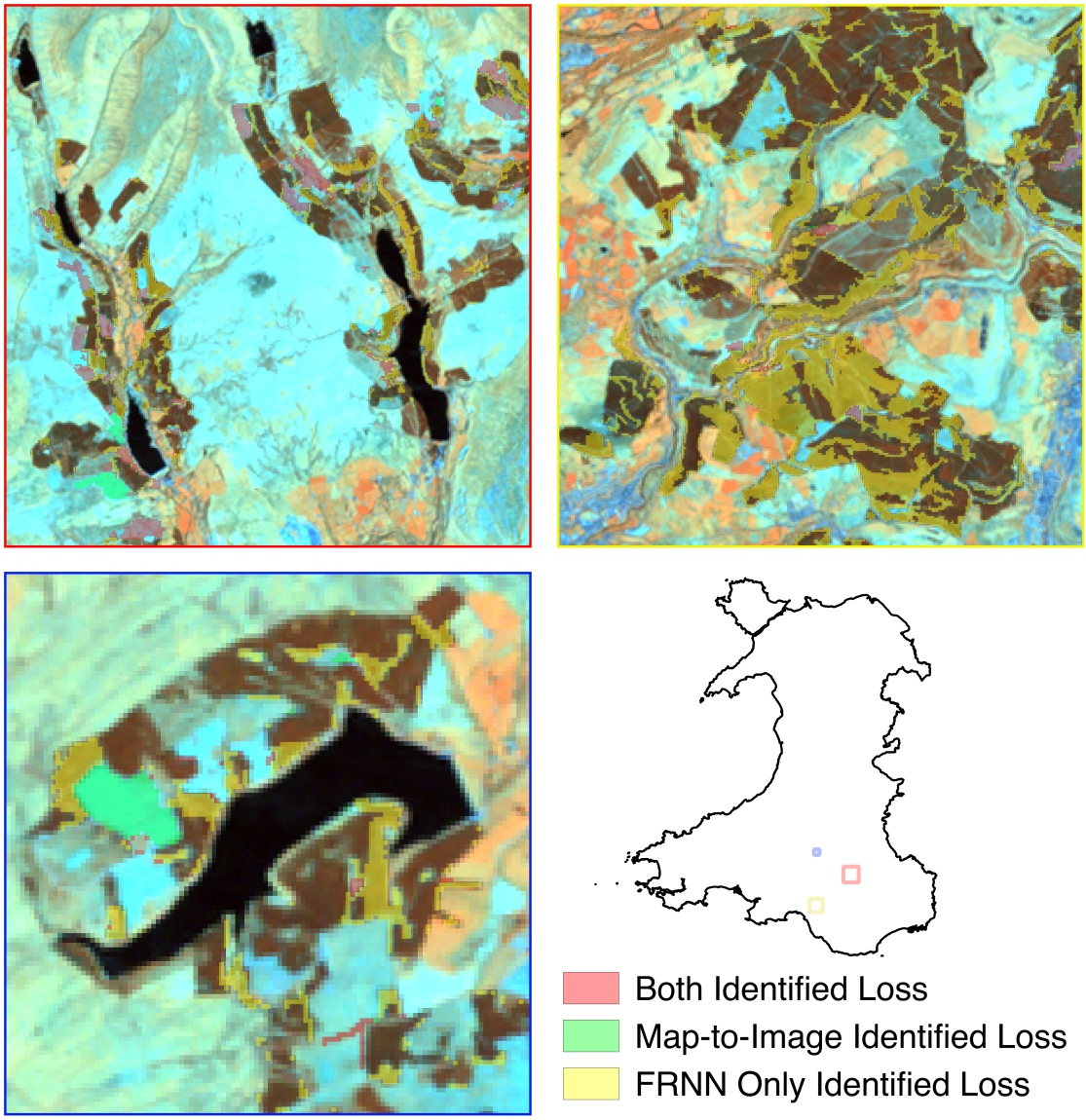

Figure 6.10: Differences in forest loss regions between histogram (map-to-image) change detection loss and fuzzy-rough logic(FRNN) change detection loss, similarity metrics threshold for three forested areas in mid and south Wales in 2015. Imagery is a FCC of red = NIR, Green = SWIR1 and Blue = SWIR2.

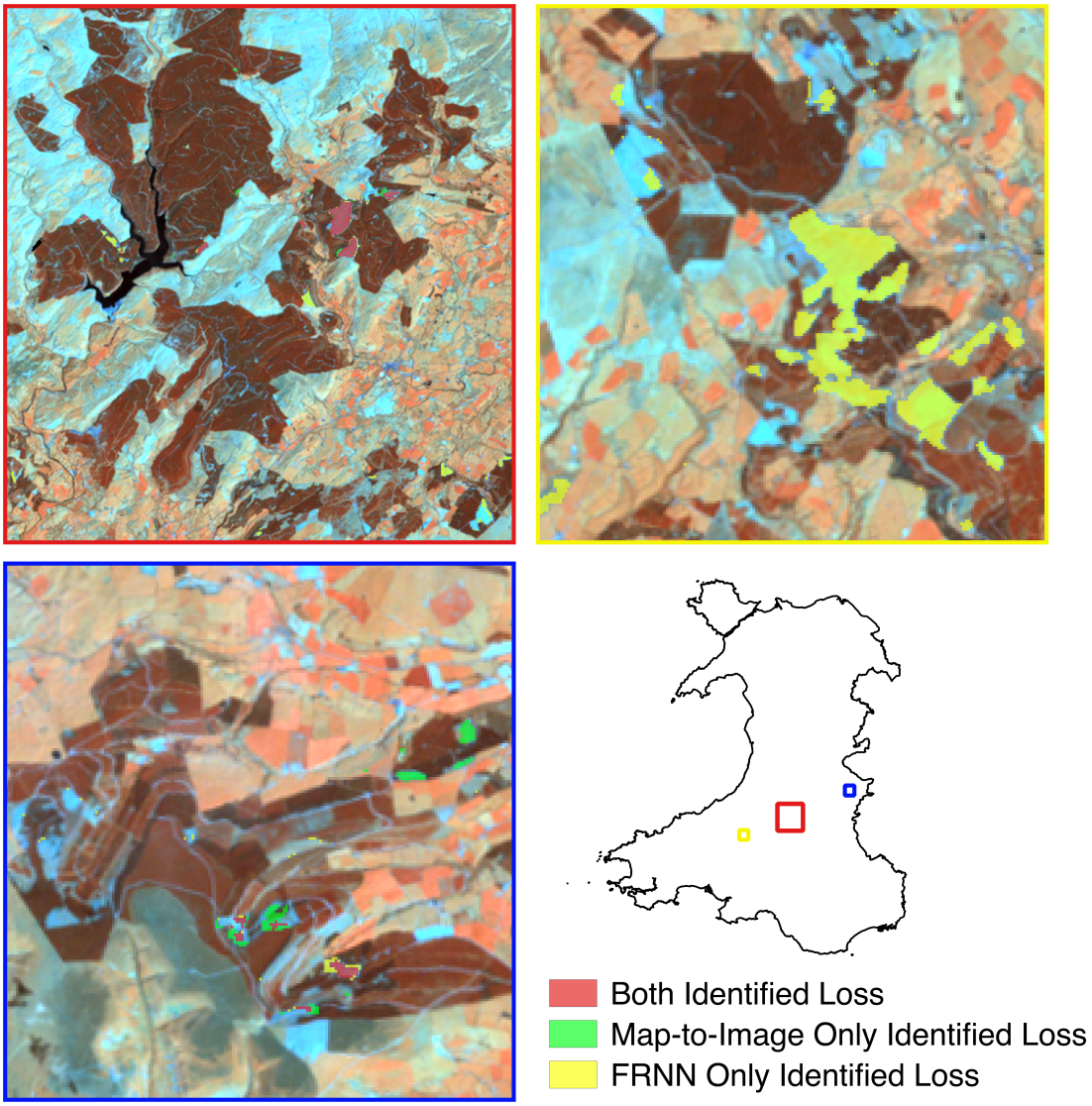

Figure 6.11: Differences in forest loss regions between histogram (map-to-image) change detection loss and fuzzy-rough logic(FRNN) change detection loss, similarity metrics threshold for three forested areas in mid and south Wales in 2016. Imagery is a FCC of red = NIR, Green = SWIR1 and Blue = SWIR2.

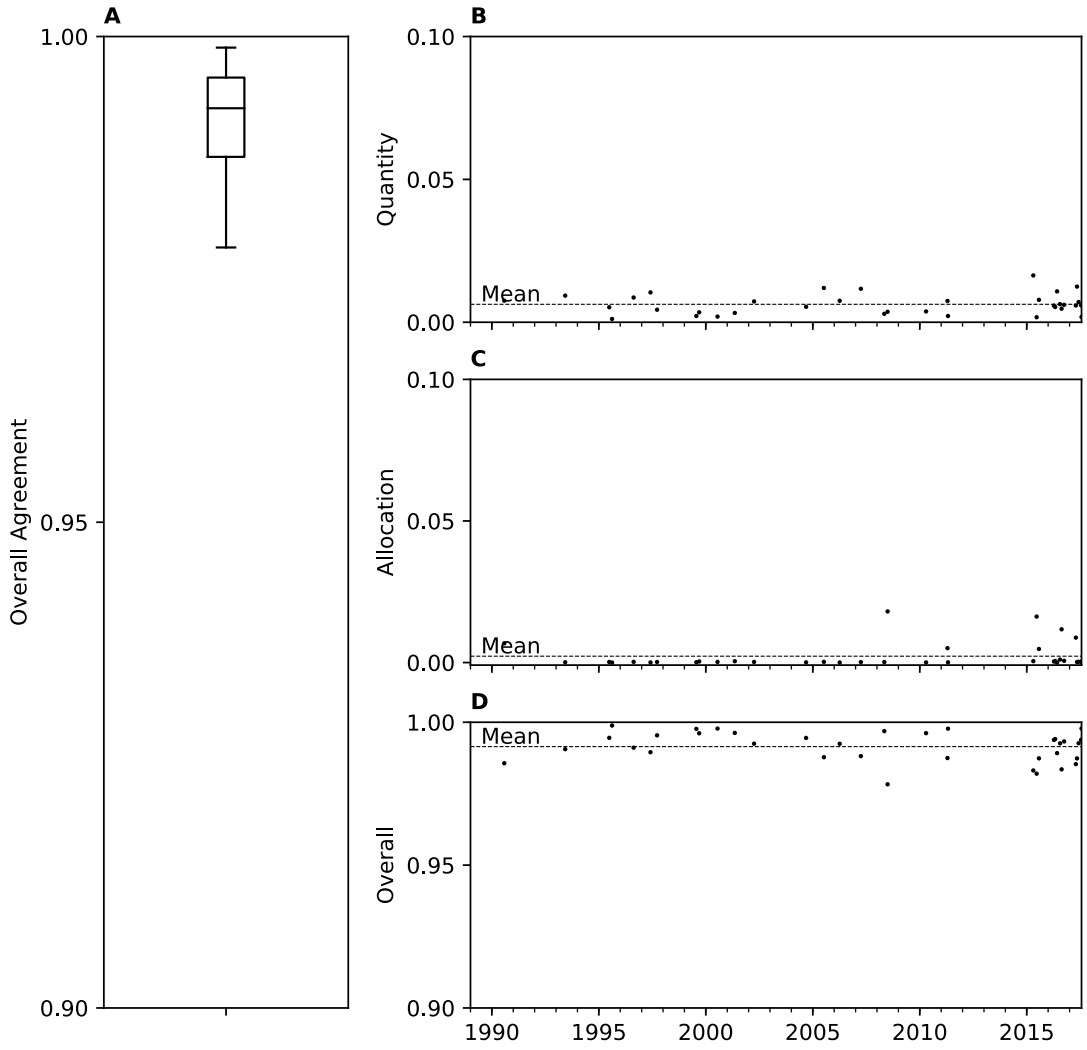

Figure 6.12: Area based accuracy metrics from outlier change detection. A) boxplot showing the range of the overall agreement. B) Quantity disagrement. C) Allocation disagrement. D) Overall agreement through the time series.

caused some false positives of change. 41.7% of change pixels were altered once and 32% twice. The remaining 25% are likely false positives on at least one occasion, due to non-forest areas being classified as regrowth and subsequently re-identified as forest loss.

6.3.3 Repeated Random Forest Classification Change Detection

The mean overall accuracy was 89.4% with an overall agreement of 0.973 (± 0.0023 at the 99% confidence interval) and a kappa of 0.878. All but one of the individual image accuracies were over 80%. Although there is no statistically significant trend the range in the overall agreement and quantity error increases through the time series (Figure 6.13). The consistently lower allocation disagreement suggests that the locations classified are correct but the quantity or area of class is in error. The range of user's accuracies and the high producer's accuracies for the 'forest loss' class suggest a slight over-classification of change features. The regrowth classifications were similar to the histogram approach (Chapter 4), however as that version used a random forest classifier this is to be expected.

Table 6.6: Full confusion matrix for repeated RF change detection coniferous forest extent change accuracy assessment. Forest in the table refers to coniferous forest only.

	Forest	Forest loss	Other	Forest Gain	Users (%)
Forest	24	4	1	0	82
Forest Loss	3	17	1	0	84
Other	0	0	25	0	99
Forest Gain	0	0	2	23	93
Producers (%)	89	80	89	99	89

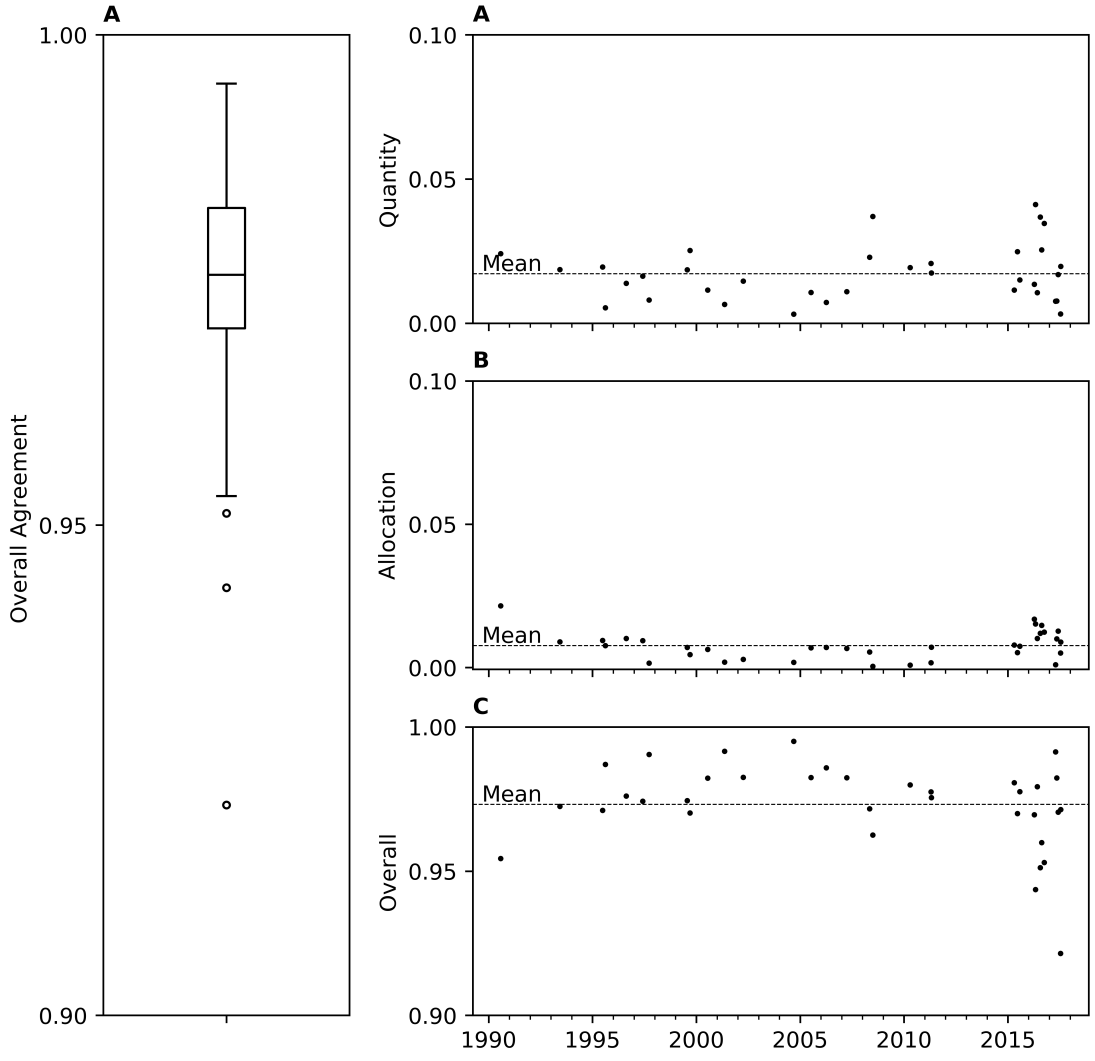

Figure 6.13: Area based accuracy metrics from repeated RF classifier change detection. A) boxplot showing the range of the overall agreement. B) Quantity disagrement. C) Allocation disagrement. D) Overall agreement through the time series.

Most objects change between 1 and 3 times during the time series but a proportion of the data exhibits possible false positives of change. Mixed pixels and those on the edges of objects are handled differently by the segmentation at different points and therefore can be classified differently changing classes 11-20 times during the time series. These false positives are removed from the analysis by manually setting the class for one-pixel objects which change classes more than three times. There is also an increase in the false positives of change due to no longer using a hard threshold. Some borderline objects change class due to the nature of the training data in each image or the spectral response of most of the forests present in the images. This also highlights a difficulty in determining the true class of these objects for accuracy assessment.

6.4 Discussion and Comparison Change Detection Approaches

Of the methods tested only the Histogram, Outlier detection and repeated RF classifiers change detection approaches produced a meaningful result, therefore only these approaches will be discussed here. The objective of this chapter is to assess if the new approaches which do not assume class distribution can be used to automatically identify change features in a time series with similar accuracies as the histogram approach in the previous chapter. Therefore, comparison and discussion will be focused on determining if this was achieved.

Accuracy statistics indicate changes in coniferous cover were accurately mapped using mean probabilities from repeated RF classifiers, KNN outlier detection,

and the parametric distribution of a histogram (Table 6.7). The overall accuracy figures do not significantly differ using any of the three approaches, however, repeated RF did consistently produce lower accuracies than outlier change detection or the histogram change detection approaches. Although the overall accuracy of the histogram approach was not improved upon, the different approaches successfully identified change features without assuming data distribution and without a significant difference in overall accuracy.

Table 6.7: Differences in key accuracy statistics between the Histogram, Repeated RF and Outlier approaches for detecting change features.

Accuracy Metric	Histogram	Outlier	Random Forest
Overall Accuracy (%)	93.6	91.6	89.4
Kappa	0.915	0.888	0.878
Mean Agreement	0.957	0.98	0.967
Mean Allocation Disagreement	0.001	0.005	0.008
Mean Quantity Disagreement	0.012	0.015	0.025
Z Score	791.78	62.06	60.78
Z Score P Value	$<$ .00001	$<$ .00001	$<$ .00001

Despite the overall accuracies being similar, there were some consistent differences in the change features identified using each method. The repeated RF change detection products contained the smallest total coniferous forest extent, the outlier change detection estimating the largest forest areas, and the histogram approach between the other two. The 2016 NFI documents $1030km^2$ of coniferous forest with the Histogram approach estimating $1087km^2$. In the final classification of 2016, forest area estimated by outlier change detection and Repeated RF classifiers was $1142km^2$ and $993km^2$respectively ($<$10% difference from the histogram approach). These patterns can also be seen in the classified coniferous forest areas in Figures 6.14, 6.15 and 6.16. Additionally, all change detection approaches had difficulty assigning a class to mixed pixels. The mix of

spectral signatures universally resulted in these pixels being classified differently at different times, creating false positives of change.

The area of change identified each year followed a broadly similar pattern for each approach, all exhibited an increase in the volume of change recorded after the launch of Sentinel 2 (Figure 6.17). Where the same features were identified they were recorded as change objects in the same images (Figures 6.14, 6.15 and 6.16). Although there is some variation in the total area, all the approaches indicate an overall loss of coniferous forest area, in line with available NFI and Forestry Commission statistics. The NFI documents approximately 170 km^2 of coniferous forest loss between 2001 and 2017. The histogram change detection approach recorded 166 km^2, the outlier change detection approach recorded 159 km^2, and the repeated RF classifiers documented 198 km^2 of coniferous forest loss.

The drivers for these land cover changes were discussed in the previous chapter, in recent years larch disease infection has lead to large areas being felled. Before this changes in coniferous forest area were typically due to commercial felling. The outlier change detection and histogram change detection approaches are closer in total area and coniferous forest loss and gain areas. However, these approaches are more similar as they both select data to be removed from the map area as likely change features as opposed to identifying the features least likely to have changed from the whole dataset.

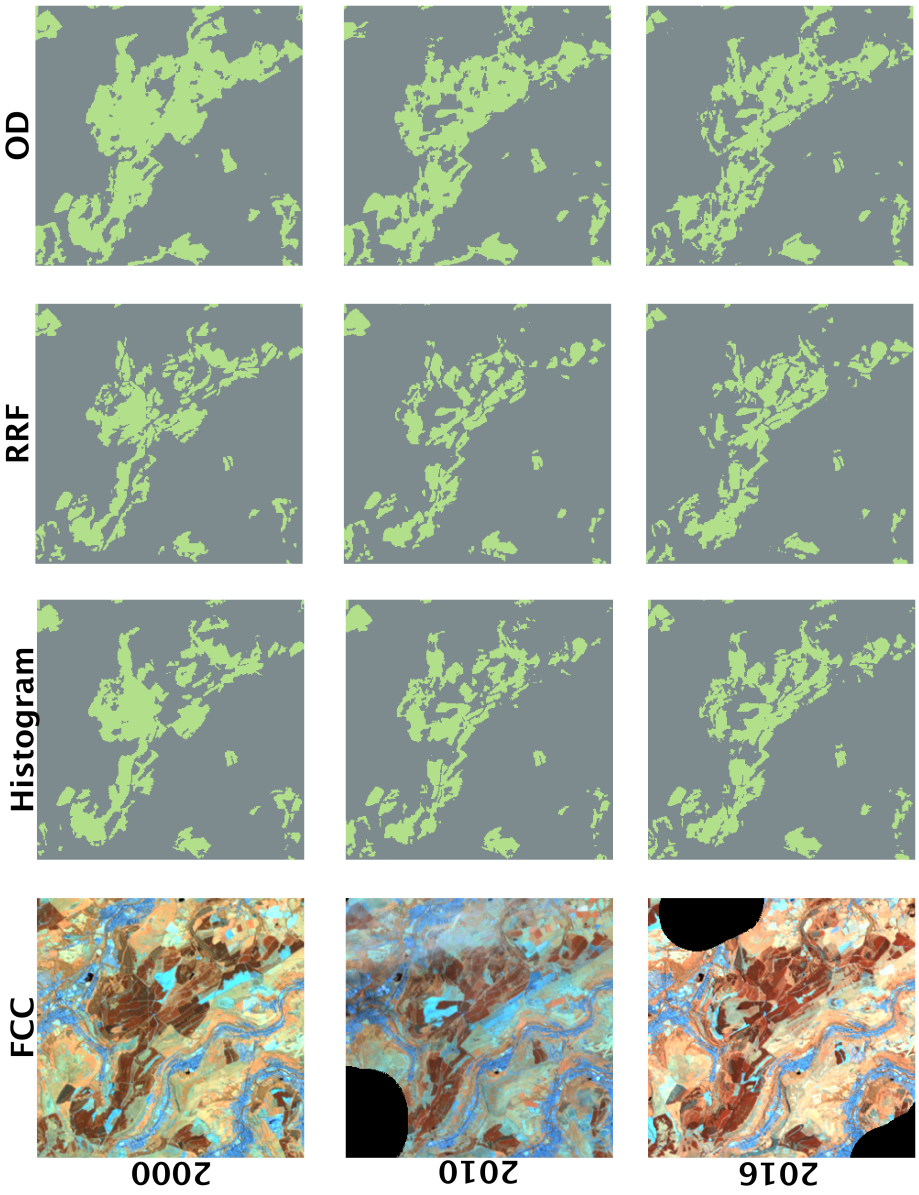

Figure 6.14: Example differences in the Histogram, repeated RF (RRF) and outlier change detection (OD) coniferous forest extent map products for a location in South Wales in April 2000, 2005 and 2015. The images are FCC where red = NIR, green = SWIR1 and Blue = SWIR2.

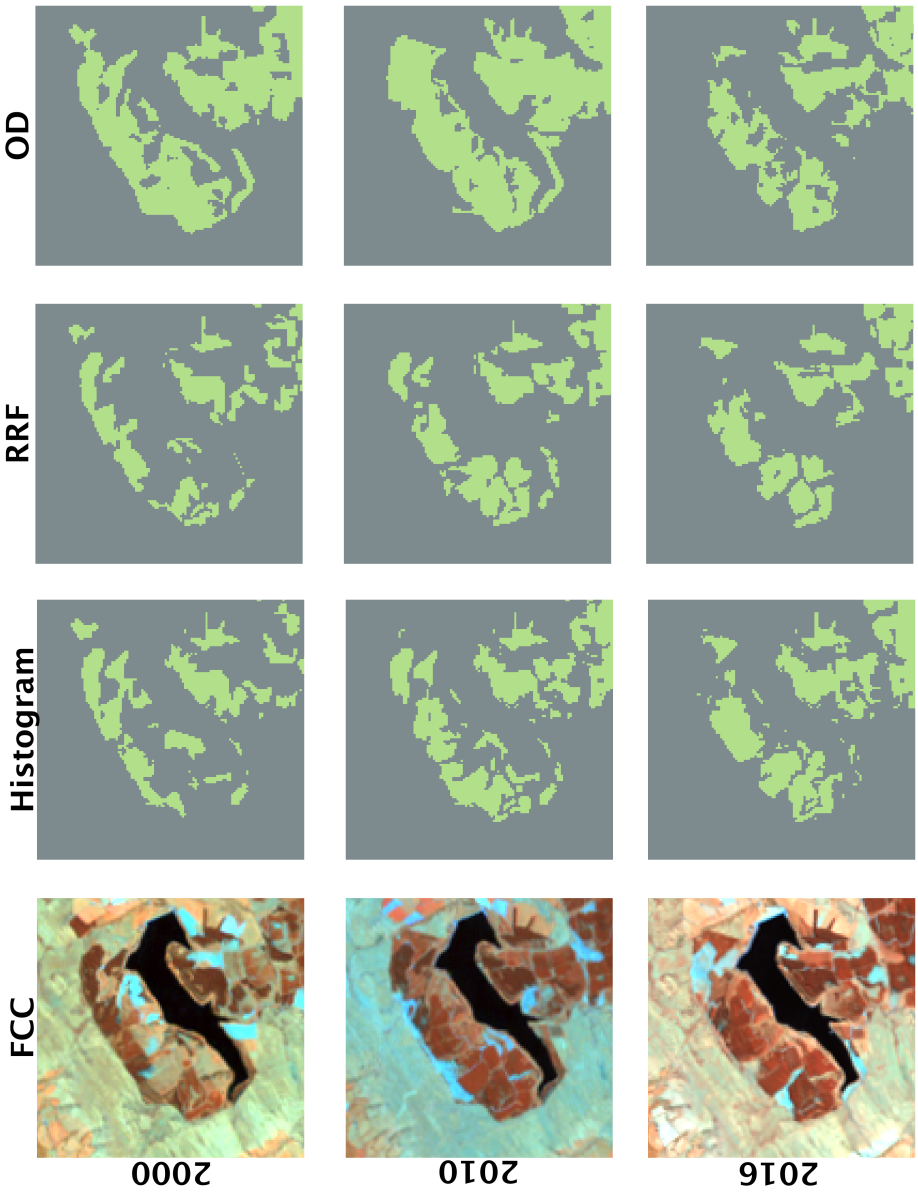

Figure 6.15: Example differences in the Histogram, repeated RF (RRF) and outlier change detection (OD) coniferous forest extent map products for a location in South Wales in July 2000, 2005 and 2015. The images are FCC where red = NIR, green = SWIR1 and Blue = SWIR2.

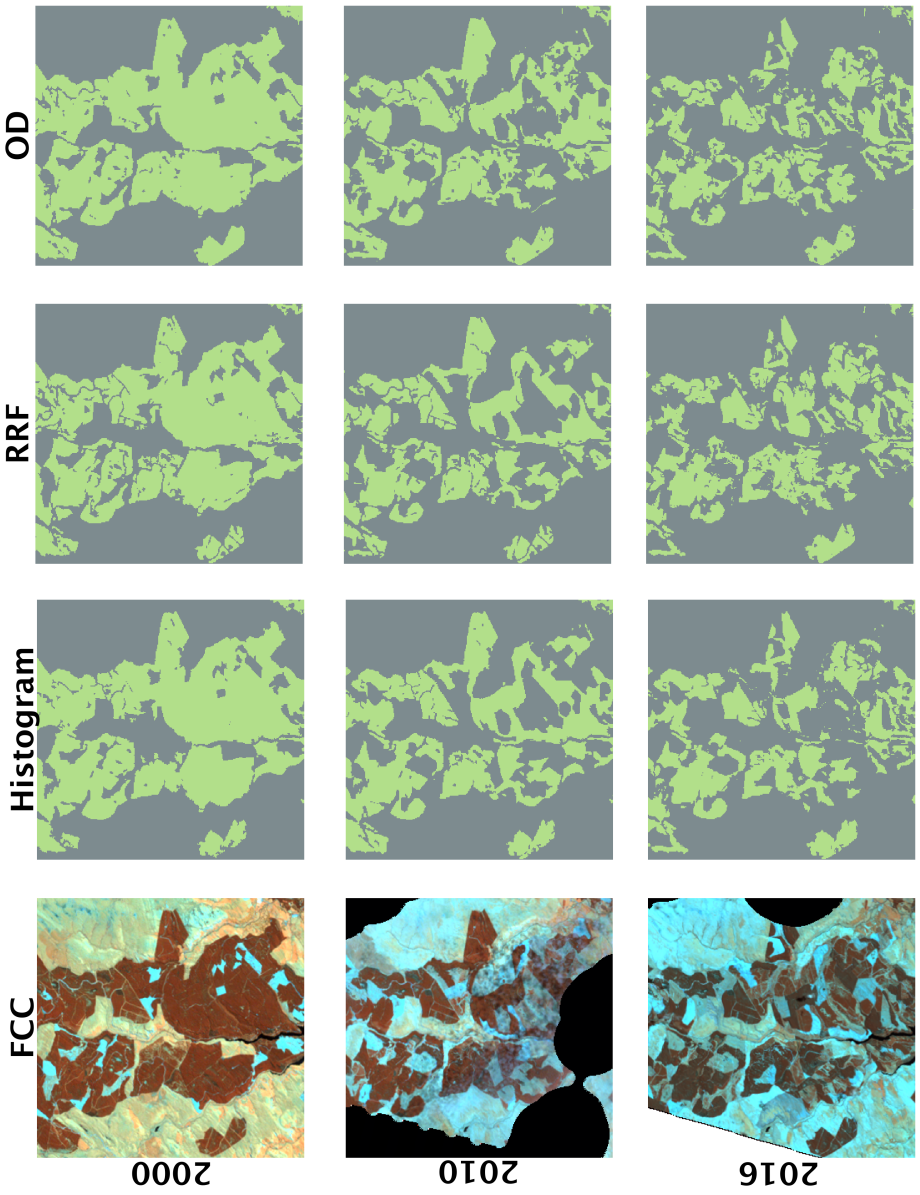

Figure 6.16: Example differences in the Histogram, repeated RF (RRF) and outlier change detection (OD) coniferous forest extent map products for a location in South Wales in August 2000, 2005 and 2015. The images are FCC where red = NIR, green = SWIR1 and Blue = SWIR2.

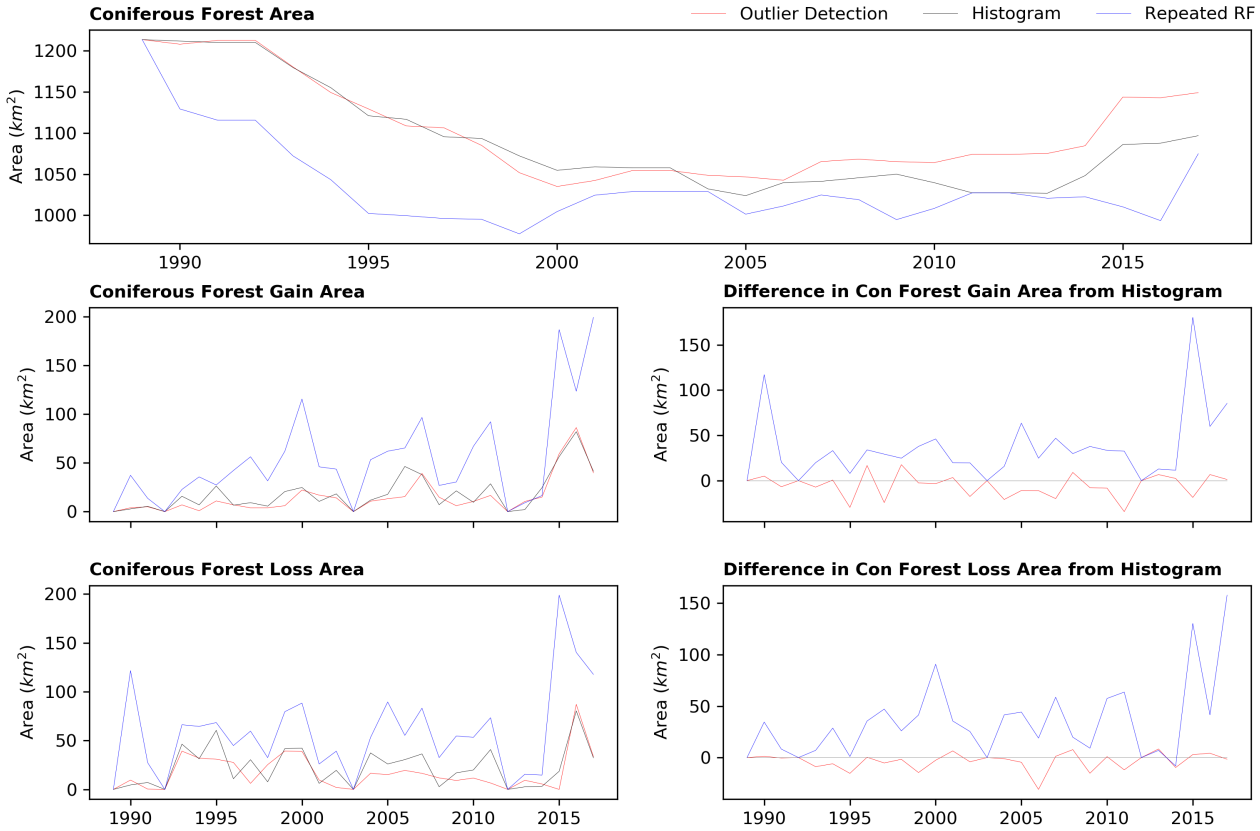

Figure 6.17: Different area metrics and changes in coniferous forest extent for each of the different change detection approaches. Red = Outlier change detection, grey = histogram and blue = repeater RF change detection derived statistics. Top = Total area change. Mid Left = Total coniferous forest gain area. Bottom Left = Total coniferous forest loss area. Mid Right = difference in total coniferous forest gain area from those recorded by the histogram change detection approach. Lower Right = difference in total coniferous forest loss area from those recorded by the histogram change detection approach.

This difference in approach led to large areas of forest loss being recorded by repeated RF classifier change detection in the first few years compared to the other techniques (Figure 6.17). After the year 2000, the changes in the total area become more similar. This is also reflected in a lower forest loss class accuracy in the repeated RF classifier change detection accuracy metrics (Table 6.6) and the higher quantity disagreement value (Table 6.7) . The locations which only repeated RF classifier change detection identified as change features were often areas of mixed coniferous forest where some of the spectral signatures differed slightly from the coniferous forest (Figures 6.14, 6.15 and 6.16). The features had not changed on the ground but recorded a lower probability of coniferous forest class ownership and subsequently were considered likely change features by repeated RF classifiers change detection approach. However, these features were not sufficiently different to be in the outlying 20% of data or outside of the parametric peak of a histogram. After the majority of these features were removed from the mapped coniferous forest area over the first few years of the time series, the changes in total coniferous forest area each year are reduced (until the increase in data with the launch of Sentinel 2).

This could represent a limitation of repeated RF change detection; in classes that are not well defined low-class ownership probabilities could lead to false positives of change. This limits applicability to accurately detect the type of change which are easily confused. For example, in a case where class ownership probabilities are around 50/50 between two classes, it becomes impossible to determine change or land cover from the spectral data alone and the approach can no longer be applied. The features may not have changed in spectral signature but they could plausibly belong to either class according to the classifier. Additionally, the repeated RF

classifiers change detection approach can only be applied to images where there is sufficient training data available to repeatedly sample for the classifier.

However, it also illustrates that repeated RF classifier change detection is potentially able to identify small-scale changes, unlike the histogram or outlier change detection approach. Large scale changes have a specific date of change (e.g. fire event changing forest cover to bare ground) unlike gradual changes,(e.g. a remixing of coniferous forest into the mixed coniferous and deciduous forest). Therefore, the point at which reclassification of small-scale changes occurs is unknown. This change is labelled when it becomes spectrally distinct from the land cover. Further research is needed to determine when the change point is and if this type of change can be measured accurately, as these types of objects could change class due to the types of training data in each image or differences in the spectral responses of objects in one image. Additionally, over classification of change features, commission error or false positives are easier to characterise in an accuracy assessment. Omission error in the other approaches may be larger than the accuracy figures would suggest.

The histogram approach slightly under-identifies change features, as it fails to identify changes in land cover where the spectral response remains within the 'normal' peak. The outlier change detection approach also slightly under-identifies change features due to the 20% threshold. Both are unable to identify change when areas remain vegetated but are no longer coniferous forest (e.g. changes in forest make up to mixed coniferous or degradation). Repeated RF classifier change detection approach can detect these types of changes whereas the other approaches require a greater magnitude of change.

The outlier change detection approach identified change accurately but requires

knowledge of the approximate percentage of change. The outlier change detection algorithm adds to the assumption that change is a small part of the whole by assuming it is always less than a given percentage. While the assumption was true to reality in this example, in highly dynamic locations or when the time between image capture dates varies, it is possible that the change percentage could also vary. An average of 96.4% of the data selected as likely change features in each image was classified as change features. This suggests that the threshold has a large effect on the map classification product (Figure 6.18). However, thresholds between 10 and 40% did not have a significant effect on the overall accuracy figure in the sensitivity analysis. Therefore, it is possible that applying a threshold according to the most dynamic change may be adequate. Further research is needed to determine the effect of threshold selection on different land covers and change dynamics.

There are two assumptions in all of the approaches; (i) change is small and (ii) change features are spectrally different from the previous land cover. These assumptions were again true to reality in this example. A key strength of the map-to-image approach is that EO datasets are not directly compared. Therefore different data sources can be used to increase the temporal resolution, this example includes two sources of optical satellite imagery. Potentially these approaches could also be applied to radar data, as could the histogram approach. Both approaches could likely be applied to large-scale areas with similar cloud cover and illumination and boreal coniferous forest (e.g. Scandinavia; Beland et al. 2017, Brandt et al. 2013, Swedish Wood 2019).

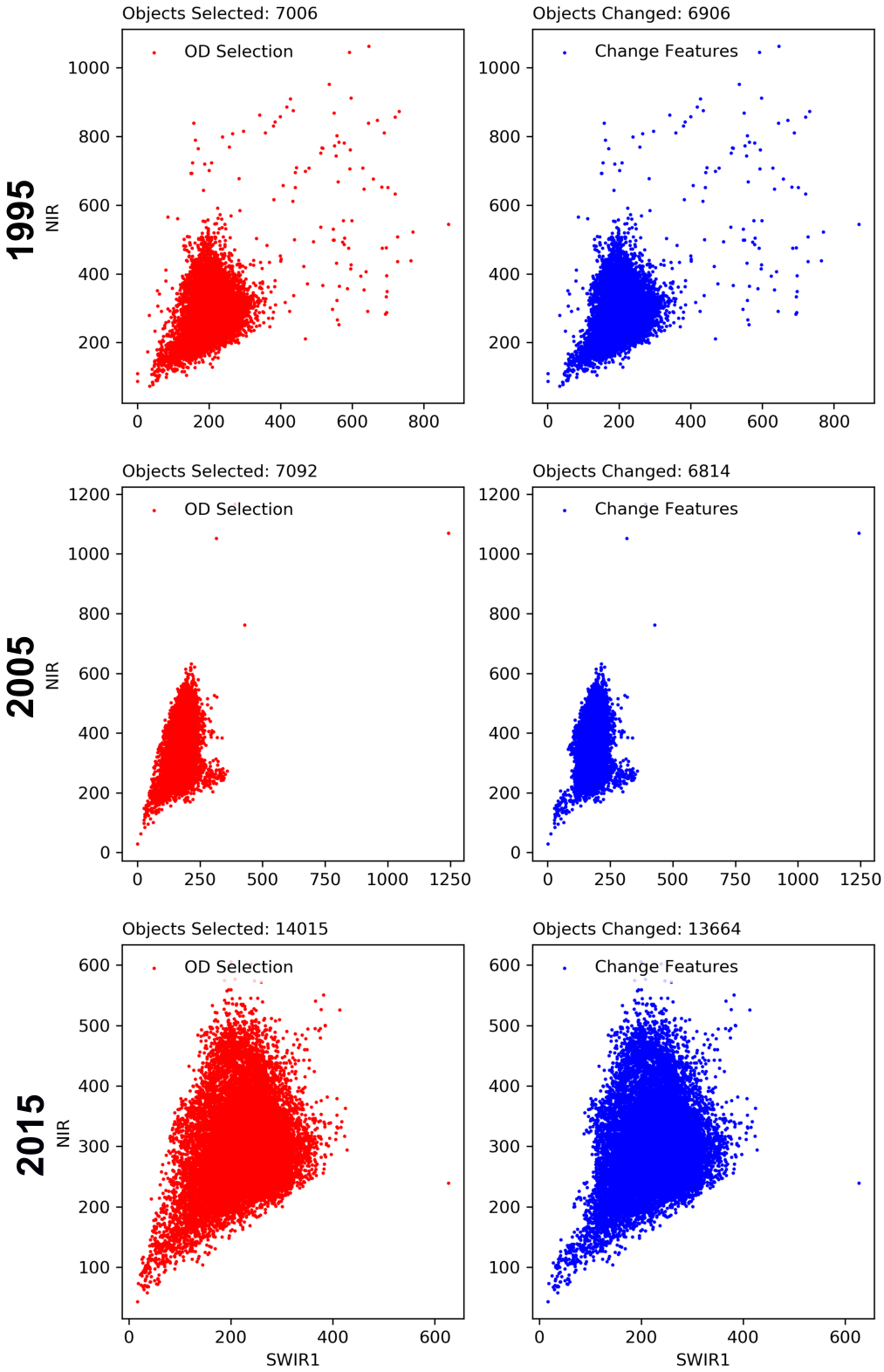

Figure 6.18: NIR and SWIR1 feature space plots of the objects selected as possible change features and those classified as change features. Outlier change detection is in more dimensions than illustrated here. Data and the number of objects selected in images from 1995, 2005 and 2015 is shown.

6.5 Conclusions

In conclusion, this chapter has presented two further statistical approaches for identifying likely change features which produce similar accuracies to the original histogram statistic. As there is no significant difference in the accuracy of each approach, change detection approach choice should be based on the limitations and caveats of each approach (Table 6.8). The histogram approach was the most accurate, computationally efficient, and required the least parametrisation, therefore it should be used in situations where the parametric assumption is met and large-scale changes have taken place. However, when it is uncertain that the parametric assumption can be met an alternative statistic should be employed. As the outlier change detection approach assumes a constant approximate percentage of change in the mapped class, in situations where the percentage change is not highly dynamic and can be estimated outlier detection should be used. As the most computationally expensive approach, but making the least assumptions of class distribution or the nature of change if these assumptions can not be met then repeated RF classifiers should be used instead.

Table 6.8: Comparison of computational and parameter requirements of the three approaches for change detection explored in this and the previous chapter; histogram change detection, outlier change detection, and repeated RF classifiers change detection. The limitations of each approach are presented in the final column. These requirements and limitations must be considered before an approach is selected.

Change Detection Approach	Computational Requirements	Parameter Tuning	Limitations and Assumptions
Histogram	Low	None	Assumes a parametric distribution in class values. High magnitude land cover change only
Outlier	Low	High	Assumes change area is less than a threshold. Not applicable to highly dynamic areas
Repeated RF Classifiers	High	None	Assumes spectrally distinct change

Chapter 7

Change Detection Approaches tested on Full Land Cover Map

7.1 Introduction

Statistics on land use are required by governments, policymakers, and other analysts (Kerr & Ostrovsky 2003, Gillanders et al. 2008, Van Lier et al. 2011). The land is a unique environmental resource that delineates the space in which economic activities and environmental processes take place and within which environmental resources and economic assets are located. Changes in this land cover could have economic impacts or help measure the effects of management policies. In Wales changes in land cover may occur as a result of forestry management policies, agricultural practices, or conservation incentives (Lucas et al. 2011).

The approaches developed in the previous chapter could potentially

automatically detect multiple types of land cover change at each time step on a full land cover classification. To test this land cover change between 1990 and 2006 (79 images) were analysed using the outlier change detection and repeated RF classifier change detection approaches. The period between 1990 and 2006 was selected for analysis as classification information (Updated Phase 1 Map; accuracy >80%; Lucas et al. 2011) already existed with a nominal date of 2006, significantly reducing the processing needed to generate a base classification.

Additionally, this period represents historic change with a lower data volume, a situation where the developed approaches are well suited, as it is expected that dense time series approaches such as Zhu & Woodcock (2012) would be applied to make use of all the available data when mapping current change. However, the approaches are untested when applied to multiple classes in a full land cover map. The time series was stepped through in reverse chronological order as this does not break the assumptions of the method that change is small and spectrally distinct.

The histogram change detection approach was not used as the parametric distribution assumption could not be met by all classes, in particular, the urban land cover classes. The outlier and repeated RF change detection approaches assumptions that change is a small area and should be spectrally distinct are likely to be met in this case. The effects of the approach limitations on product accuracy will be tested.

7.2 Methods

7.2.1 Generation of 2007 Base Classification

The Updated Phase 1 Habitat Survey for Wales (Lucas et al. 2011; nominal date 2006), a national map of semi-natural habitats, was used to produce a base land cover classification for the change detection process. The original Phase 1 map was based on two sets of field surveys; the upland survey completed in 1989 and the lowland survey completed in 1997, conducted using field data and aerial photography. The updated Phase 1 map was generated using this field data and RS data (Lucas et al. 2011) The classification system and rule values were developed using expert knowledge of vegetation distribution, characteristics of the plant and vegetation communities, spectral information from the EO data, topographical data, and land cover context (adjacency and enclosure with other land covers; Lucas et al. 2011). This rule-based classifier was applied to Wales to 16 separate biogeographical areas and mosaicked to form a national classification product. For most of the high-level Phase 1 habitats the accuracy was over 70% with the homogeneous habitats such as forestry and improved grassland over 85% (Lucas et al. 2011).

It is important that the base map produced is an accurate representation of the land cover class as erroneous statistics from an inaccurate classification will propagate through the change detection. Both approaches assume that the land covers are spectrally distinct. Therefore, spectrally similar Phase 1 habitat classes were aggregated into broader classes to ensure reliable change detection (Figure 7.1). A total of 17 potential classes were identified from the Phase 1

codes; Broadleaved, Mixed Forest, Coniferous, Bracken, Heath, Bare Ground, Scrub, Fen, Herb/Fern, Mire, Swamp, Semi-Improved Grassland, Flush, Urban, Water, Agricultural and Intertidal.

To ensure sufficient area of each class was available for change detection with lower resolution Landsat and Sentinel 2 data, the class regions were rasterised to 30m per pixel resolution. Classes that were highly clustered in one location only or had an area $>135km^2$ were aggregated. The Fen, Herb/Fern, Mire, and Swamp classes formed the Unimproved Grassland class, Bracken and Upland Vegetation formed the Bracken class and Mixed Forest and Broadleaved formed the Broadleaved class (Figure 7.1).

The developed approaches all assume that change objects and the classification classes are spectrally distinct, therefore class Spectral Separability was tested. Representative regions of the classes on the 2^{nd} row of Figure 7.1 were used to produce spectral separability plots and metrics (e.g. Table 7.2). The euclidean and Jeffries Matusita Distance (JM) distance of samples from each class were used to indicate the separability and likelihood of a classifier being able to accurately label the classes.

Final Classification Classes																
Broadleaf		**Coniferous**	**Less Productive Vegetation**			**Bare Ground**	**Grassland**					**Urban**	**Water**	**Agricultural**	**Intertidal**
Classes before aggregation based on spectral seprability															
			Bracken	Heath	Scrub		Unimproved Grassland				Semi-Improved Grassland	Flush				
Classes before aggregation based on clustering and area																
Mixed Forest	Broadleaf						Fen	Herb/ Fern	Mire	Swamp						
Orignal Phase 1 Codes																
A1.3.1 A1.3.2	A1.1.1 A1.1.2	A1.2.2	C1.1	D1.1 D1.2 D1.3 D2 D3 H6.6 H8.5	A2.1 J.1.4 H.6.7	A4.1 A4.2 A4.3 I* J4 H8.1	E3.1 E3.1.1 E3.2	C3.1 C3.2	E1.6.2 E1.6.3 E1.7 E1.8 E4 E3.2.1 E3.3.1	F1 F2.2	C2 B1.2 B2.2 B3.2	E2.1 E2.2	J3.4 J3.5 J3.6 J3.7	G1	B4 J1.1	H1.1 H1.2 H1.3 H2.6 H3.1 H3.2 H4

Figure 7.1: Phase 1 codes and classes aggregated based on spectral separability. Classes were initially grouped based on Clustering and then on spectral separability testing. The bold lines illustrate which codes are in each class in the final classification. The reduction of classes due to area and separability is shown at each step.

JM distance was selected as it is popular in remote sensing to determine the spectral separability of classes in n-dimensional space (Kavzoglu & Mather 2000, Padma & Sanjeevi 2014). It is used due to a tendency to over-emphasise low separability values, making less separable classes more obvious to the user (Kavzoglu & Mather 2000, Padma & Sanjeevi 2014). However, JM distance assumes the class data has a parametric distribution, which can not be guaranteed for all classes in this instance. Although, JM distance may be applicable to data with a loosely normal distribution (Padma & Sanjeevi 2014) the euclidean distance between class samples was also calculated, as euclidean distance does not assume distribution. The n-dimensional space of both approaches allows for sample distance in all five bands (Blue, Green, Red, NIR, SWIR1, SWIR2) to be accounted for in the same calculation.

Spectral data from 10 Landsat 5 and Landsat 7 images were sampled (image dates: 01-08-1990, 06-06-1993, 01-09-1993, 28-06-1995, 14-06-1996, 14-05-2000, 11-09-2002, 07-08-2004, 23-06-2005, 28-07-2006). Ten manually selected representative samples were selected for each class in each of these images, a total of 100 samples per class and 1300 samples across all classes and images were used in the calculation. For each image, the spectral data of the 10 sample points were used to calculate euclidean and JM distances between the classes. The distance values from each of the ten images were averaged to produce the values in Table 7.2 and 7.1.

Classes with a euclidean distance of <100 or a JM distance of <1000 were aggregated (Table 7.2, 7.1 and Figure 7.1; Congalton 2008). The Unimproved Grassland, Semi-Improved Grassland, and Flush classes became the Grassland class and Bracken, Scrub and Heath areas were joined to form the Less

Productive Vegetation class. An exception was made for Urban and Bare Ground as Urban growth is a statistic useful to land managers and removing the Urban class may limit the usefulness of the final map and change products.

This class selection should ensure the remaining classes are sufficiently spectrally distinct to meet the method assumption that change features exhibit a significant change in spectral signature. This limits the methods change detection, as it can not identify any changes which occur within each class. The approach can not be used to detect small-scale changes in habitat within a single land cover classification as they are not spectrally distinct, for example, changes between bracken and scrub are not detected. However, they could be detected in binary maps of the class of interest and a secondary 'other' class. There is a balance between meeting the assumptions of the approach and making the number of classes useful for land managers, the justifications for removing some types of changes between classes are given in Table 7.3

Table 7.1: Class Jeffries Matusita Distance Values.
* U Grassland = Unimproved Grassland, SI Grassland = Semi-Improved Grassland

	Broadleaf	Coniferous	Scrub	Bare Ground	U Grassland*	SI Grassland*	Bracken	Heath	Urban	Water	Flush
Broadleaf	0	1241	1122	1392	1266	1204	1202	1313	1397	1414	1250
Coniferous	1241	0	1329	1404	1393	1397	1403	1375	1412	1414	1406
Scrub	1122	1329	0	1378	1139	814	897	1143	1395	1414	1125
Bare Ground	1392	1404	1378	0	1321	1386	1407	1301	1090	1407	1357
U Grassland*	1266	1393	1139	1321	0	973	1233	972	1382	1412	836
SI Grassland*	1204	1397	814	1386	973	0	1304	1117	1402	1414	998
Bracken	1202	1403	897	1407	1233	1304	0	931	1411	1414	1253
Heath	1313	1375	1143	1301	972	1117	931	0	1387	1414	968
Urban	1397	1412	1395	1090	1382	1402	1411	1387	0	1414	1385
Water	1414	1414	1414	1407	1412	1414	1414	1414	1414	0	1414
Flush	1250	1406	1125	1357	836	998	1253	968	1985	1414	0

Expert rules were included to reduce the chances of error. The land cover classes and changes in Table 7.3 were removed from analysis due to a high likelihood of confusion, breaking method assumptions, or were deemed highly unlikely to be true change.

The change detection relies on the accuracy of the original map regions. The

Table 7.2: Class Euclidean Distance Values.
* U Grassland = Unimproved Grassland, SI Grassland = Semi-Improved Grassland

	Broadleaf	Conifer	Scrub	Bare Ground	U Grassland*	SI Grassland*	Bracken	Heath	Urban	Water	Flush
Broadleaf	0	145	106	218	108	116	189	112	191	373	106
Coniferous	145	0	204	221	225	254	332	146	174	239	217
Scrub	106	204	0	227	69	55	140	116	213	426	75
Bare Ground	218	221	227	0	179	235	354	127	50	310	167
U Grassland*	108	225	69	179	0	57	178	95	179	422	14
SI Grassland*	116	254	55	235	57	0	121	143	232	467	69
Bracken	189	332	140	354	178	121	0	55	346	562	189
Heath	112	146	116	127	95	143	55	0	108	330	85
Urban	191	174	213	50	179	232	346	108	0	273	165
Water	373	239	426	310	422	467	562	330	273	0	411
Flush	106	217	75	167	14	69	189	85	165	411	0

Table 7.3: Reasons for some classes or land cover changes being removed from analysis. From and to changes are given progressing forward in time.

Change Features	Reason
Agriculture	Breaks assumption that any change in spectral response is only due to land cover change.
Intertidal	Breaks assumption that any change in spectral response is only due to land cover change.
Urban to Bare Ground	Euclidean distance between classes suggests a high likelihood of confusion and false positives of change.
Bare Ground to Urban	Euclidean distance between classes suggests a high likelihood of confusion and false positives of change.
Urban to Conifer Forest	Highly unlikely that urban area would be removed and replaced with an established forest in the time span between image image acquisitions.
Urban to Broadleaved Forest	Highly unlikely that urban area would be removed and replaced with an established forest in the time span between image acquisitions.
Water to/from Conifer Forest	Highly unlikely for a water body to be removed and replaced with a established forest in the time span between image acquisitions.
Water to/from Broadleaved Forest	Highly unlikely for a water body to be removed and replaced with a established forest in the time span between image acquisitions.

Updated Phase 1 Map is >85% accurate, however, class area accuracy was improved by using change detection to identify the potential error. Erroneous objects typically have a different spectral signature to the rest of the class area, therefore they behave as change features. Applying the outlier change detection approach to the Updated Phase 1 Map and image data from 2007 identified some errors and increased the accuracy of the base classification. Additionally, it allowed for the identification of any change areas between the 2003 - 2006 Updated Phase 1 image acquisition dates and the base classification date, ensuring the accuracy and completeness of any change regions from this period.

A composite of 3 Landsat TM images from early (April-May) 2007 was used to provide a baseline for the change detection, 92% of the composites terrestrial area was from images acquired on April 5th, 2007. Using data from Spring is not ideal, but was unavoidable due to cloud cover. Error could be introduced by vegetation that exhibits seasonal variations in reflectance (e.g. broadleaved trees). These land cover types may change spectral signature between the image acquisition dates (e.g. broadleaved trees in leaf and without leaves). This may be a source of error in the 8% of the image area from different acquisition date. Representative training data were identified using the mean probability metrics of 100 RF classifiers (Chapter 5). The half of data most certain to belong to each class was sampled for training data. This was balanced at 4000 samples in each class and fed into an extremely randomised trees classifier optimised using a grid search of the number of estimators and the max features to consider when looking to split the classes. The optimal parameters of 250 trees and 8 max features were used to produce the final 2007 Base Classification.

Table 7.4: 2007 Base Classification Accuracy Metrics.

Metric	Accuracy
Overall Accuracy	95.6%
Kappa	0.951
Overall Agreement	0.948
Quantity Disagreement	0.0329
Allocation Disagreement	0.019
Z Score	277.86

Table 7.5: 2007 Base Classification Accuracy Assessment Confusion Matrix percentages. Would expect each class to have 10% of points due to class number and stratified sampling.

	Broadleaved	Less Productive Veg	Coniferous	Grassland	Bare Ground	Water	Urban	Intertidal	Agriculture	Users (%)
Broadleaved	10	0	0	2	0	0	0	0	0	90
Less Productive Veg	0	10	0		1	0	0	0	0	93
Coniferous	0	0	11	0	0	0	0	0	0	98
Grassland	0	1	0	10	0	0	0	0	0	94
Bare Ground	0	1	0	0	9	0	1	0	0	80
Water	0	0	0	0	0	11	0	0	0	99
Urban	0	0	0	0	0	0	11	0	0	94
Intertidal	0	0	0	0	0	0	0	11	0	99
Agriculture	0	0	0	0	1	0	0	0	11	96
Producers (%)	99	82	99	84	84	100	90	100	100	94

The 2007 Base Classification accuracy was tested using available Landsat 5TM and Landsat 7 imagery from 2005-2007 and Google Earth Pro. A total of 4500 points, 500 from each of the nine classes were randomly sampled for the accuracy assessment. The overall accuracy was 95.6% with error mostly associated with quantity (Table 7.4). All classes exhibited producer and users accuracies of >= 85%. Error was associated with confusion between the Broadleaved and Grassland classes, commission errors of Bare Ground in Urban areas, and Less Productive Vegetation in Bare Ground areas (Table 7.5).

7.2.2 Change Detection

The repeated RF classifiers and outlier change detection approaches were applied to multiple classes (Figure 7.2). Likely change features were identified from each

land cover independently in turn. The likely change features identified in each class were then reclassified using an extremely random trees classifier optimised with a grid search. The training data for this classifier was sampled using the histogram of the range of values in the stable regions and balanced at 20% of the total stable objects from the smallest class area. To reduce misclassification due to noise only persistent features present in two consecutive images were classified as change features (Figure 7.2).

7.2.2.1 Repeated Random Forests change detection analysis and parameters

The processing and parameters used in the previous chapter were adapted to identify changes in the seven classes analysed. To generate the class ownership probabilities, training data was balanced at 20% of the total number of objects from the smallest class. If a class region was <1000 objects, or <200 training objects, the volume of data was deemed insufficient for change detection, this occurred to the Water class in 12 images.

Fifty different sets of training data were extracted and used to train 50 optimised extremely randomised trees classifiers. The number of estimators and the max features parameters were determined separately using a grid search for each classification. The number of classifiers used to produce the mean class ownership probability was determined using a sensitivity analysis. The effect of the number of classifiers on the variation in the mean probabilities of each class was tested on five randomly selected images (20-08-1991, 06-06-1993, 27-04-1997, 02-05-2005, 21-09-2006; Figure 7.3). For all image classes, the reduction in variation after 50 classifiers have been trained represents an insignificant

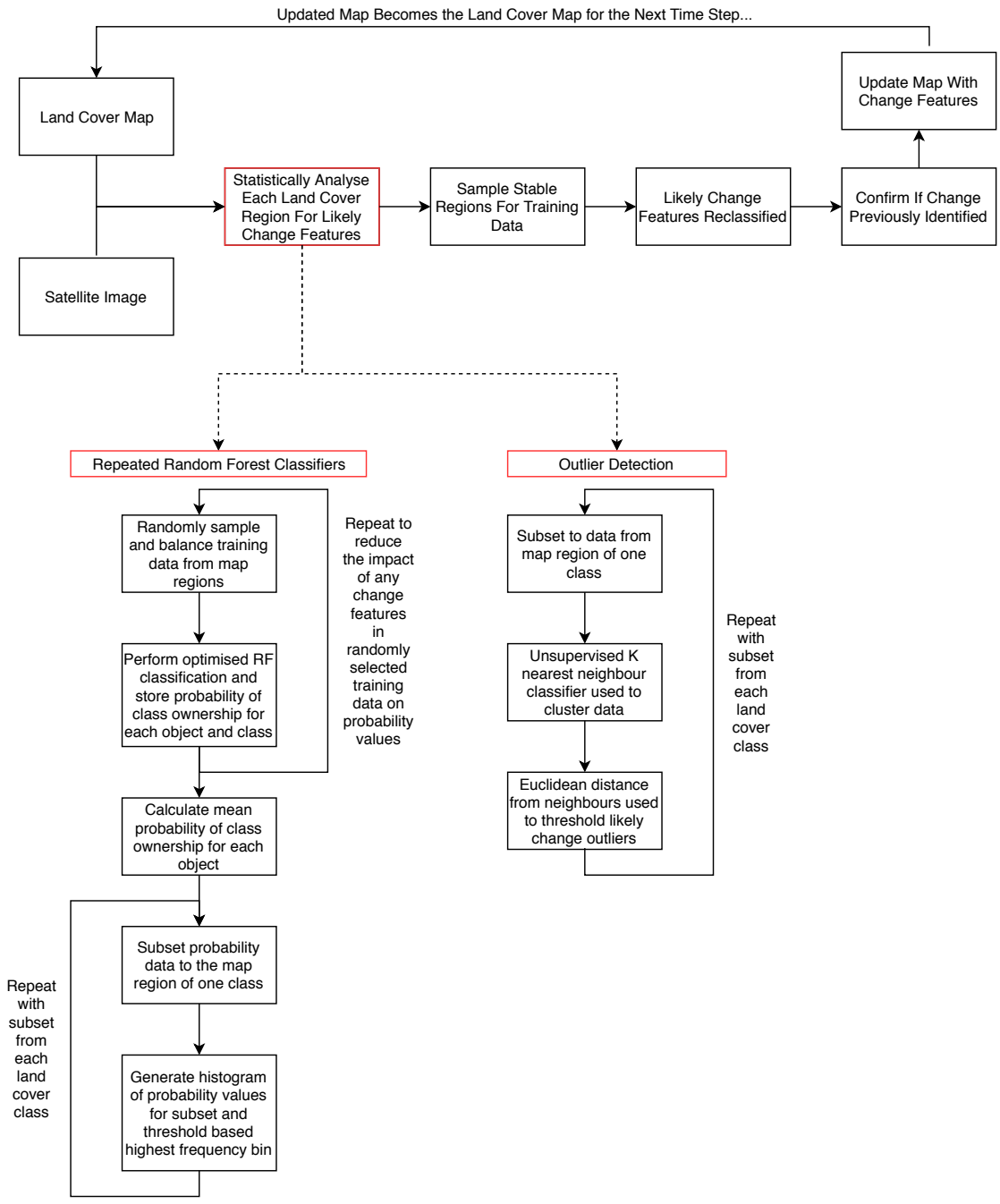

Figure 7.2: Processing chain adapted to run across multiple land covers. The red box indicates the step where the different analysis techniques were implemented. The left column illustrates the repeated RF classifier approach and the right the outlier change detection approach.

improvement. Therefore, the probabilities of 50 RF classifiers were used to calculate the mean probability of class ownership for each potential change object.

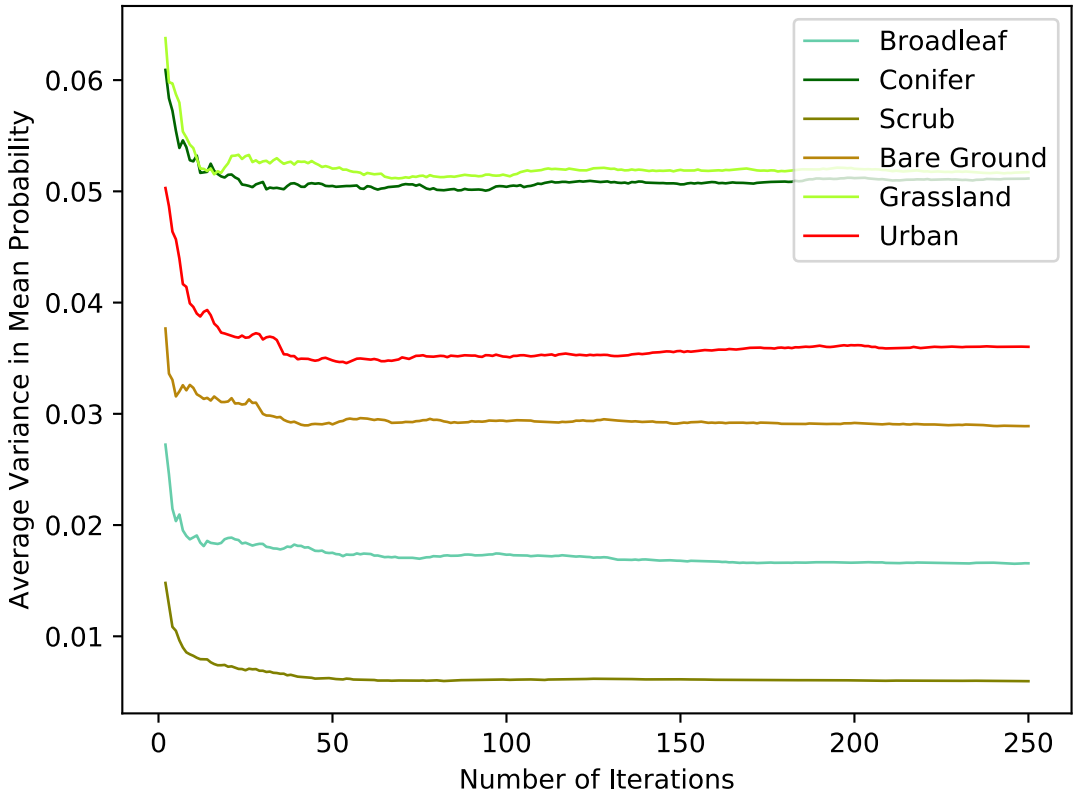

Figure 7.3: Selection of number of repeats to train for repeated RF classifiers. The X axis illustrates the average variation in mean probability of each object with each number of iterations of extremely randomised trees classifiers trained. Variation data shown is from Landsat 5 image dated 21-09-2006. At around 50 iterations of the classifier the variability does not reduce further.

The process of thresholding the mean probability values to identify likely change objects is the same as in the previous chapter. The highest frequency probability value was used to threshold change features. This process was repeated on subsets of mean probability of class ownership data for each change class (Figure 7.2).

7.2.2.2 Outlier Change Detection Analysis and Parameters

The processing and parameters in the previous chapter were adapted for several land cover classes. Ramaswamy et al. (2000)'s PyOD module was used on the data from each class region to identify outliers. The KNN and distance metric parameters were unchanged from the previous chapter as the outlier identification problem is the same. To prevent potential overfitting of a threshold to a specific image or class, the 20% threshold identified in the previous chapter was applied to all land covers. Coniferous forest is one of the most dynamic land covers in Wales and it is highly unlikely that another of the analysed land covers would exhibit a greater percentage of true change. Additionally, the sensitivity analysis in the previous chapter indicates that changes in the outlier threshold of <30% does not have a significant impact on change detection accuracy.

7.2.3 Accuracy Assessment

The accuracy assessment was performed on 20% of all output classifications (16 images). To ensure that the accuracy was measured across the range of the study period, 1 in every 5 images was selected randomly. Due to the complexities of designing a sampling strategy for 25 possible land cover changes (which do not occur in every image) and the stable areas of the seven classes a two-stage accuracy assessment was undertaken (Congalton 2008).

The accuracy of the classification products was analysed using a traditional accuracy assessment. In total 28,000 points were sampled across the 16 images, 1,750 per image and 250 points per class. As the change features are likely to

occupy a small section of the whole map area, it may be possible to produce accurate classifications even if the majority of the change features identified were incorrectly classified (Congalton 2008). Therefore, assuming that any omission is likely to be near identified change features, 75% (188 points) of the points sampled in each of the seven change classes (Broadleaved, Coniferous, Scrub, Bare Ground, Grassland, Urban, and Water) were selected from within the change objects and in a 400m buffer around them. The remaining 25% (62 points) were sampled from the whole class area. Although this sampling is biased towards potential areas of omission, change is typically such a small area of the whole, it is still likely omission error will be in the accuracy statistics.

To analyse the accuracy of the change detection and reclassification a further 5,600 points were sampled from the 16 images. In each image, 350 points were randomly selected stratified between the 'loss' area of each of the seven change classes. The sample for each class was limited to 50 points due to the small areas of these features. The change detection accuracy was obtained by collapsing this into a binary 'change/no change matrix' and assessing the percentage of true and false change features (Congalton 2008).

As in the previous chapters, high resolution or field sampled reference data to test accuracy point samples ground truth or 'real' class was not available for the study period. This is a challenge of verifying the accuracy for map products of 15+ years ago. As in the previous chapters, accuracy was measured against Google Earth imagery and the time series dataset. This is not ideal and can make verifying the ground truth class of some points difficult. Where the points class was very uncertain it was removed from the analysis and replaced with a newly sampled point. However, this form of reference data are not desirable and

further study should recalculate accuracy with a higher quality reference dataset if one is available. These limitations make the true accuracy figures impossible to characterise but the results provided by the assessment will be indicative, particularly of large-scale changes which are easily recognisable in the image data.

7.3 Results

Over the period 1990-2007, 79 classifications of Welsh land cover were generated using repeated RF classification and outlier detection. The outlier change detection approach performed better than the repeated RF classification approach (Table 7.6, Figure 7.4 and Figure 7.5). In the accuracy of the maps produced using the repeated RF classification approach there is a very slight trend ($r = 0.54$) of decreasing overall accuracy and agreement away from the base classification. In comparison there isn't a trend in the accuracies produced using outlier change detection, this suggests that likely change features were better identified using the outlier change detection approach. Of the objects identified as change features by the repeated RF classification approach 44% were false positives, identified as change when no change had occurred on the ground, compared to 20% of outlier change detection objects (Table 7.7 and Table 7.8).

The accuracy of the reclassification of likely change features indicates some class confusion for both approaches. The outlier change detection approach was slightly more accurate than the repeated RF classifiers change detection, reclassifying 70% of true change objects correctly compared to 65% in the repeated RF classifier

Table 7.6: Differences in key accuracy statistics between the Outlier and Random Forest approaches for detecting change features.

Accuracy Metric	Outlier	RRF
Overall Accuracy (%)	89	83
Kappa	0.85	0.81
Mean Agreement	0.85	0.77
Mean Allocation Disagreement	0.08	0.06
Mean Quantity Disagreement	0.07	0.15
Z Score	18.26	34.5
Z Score P Value	$< .00001$	$< .00001$
Average Change Reclassification Accuracy (%)	70	67
False Positives (%)	10.9	30.8

Table 7.7: Repeated RF classifiers change detection change/no change error matrix.

	Change	No Change
Change	27.96 %	0.03 %
No Change	22.04 %	49.07 %

Table 7.8: Outlier change detection change/no change error matrix.

	Change	No Change
Change	44.5%	9.87 %
No Change	5.5 %	40.13 %

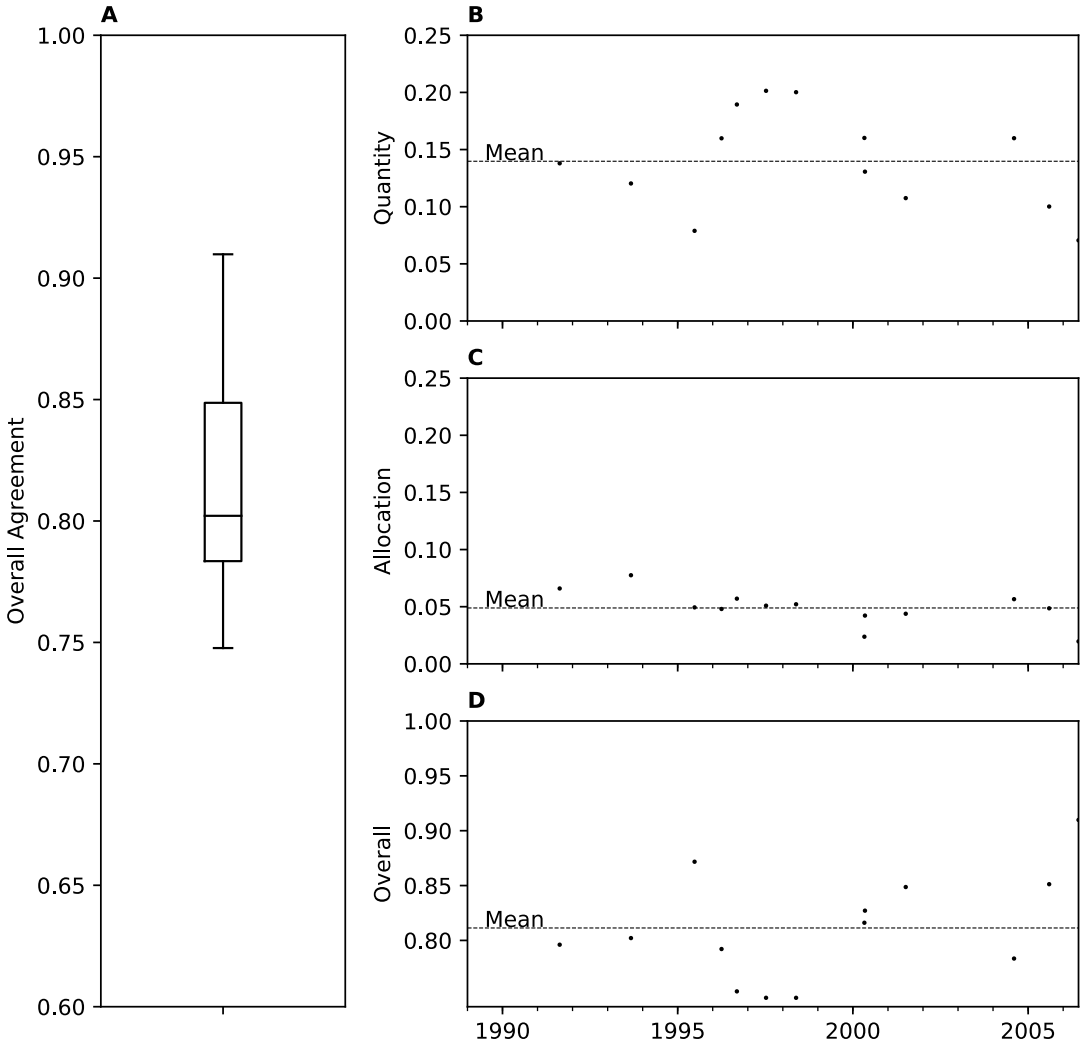

Figure 7.4: Accuracy statistics from repeated random forests classifiers on full land cover classification. A= box plot of overall agreement, B = Quantity disagreement (desirable to be near 0), C = Allocation disagreement (desirable to be near 0) and D = overall agreement (desirable to be near 1).

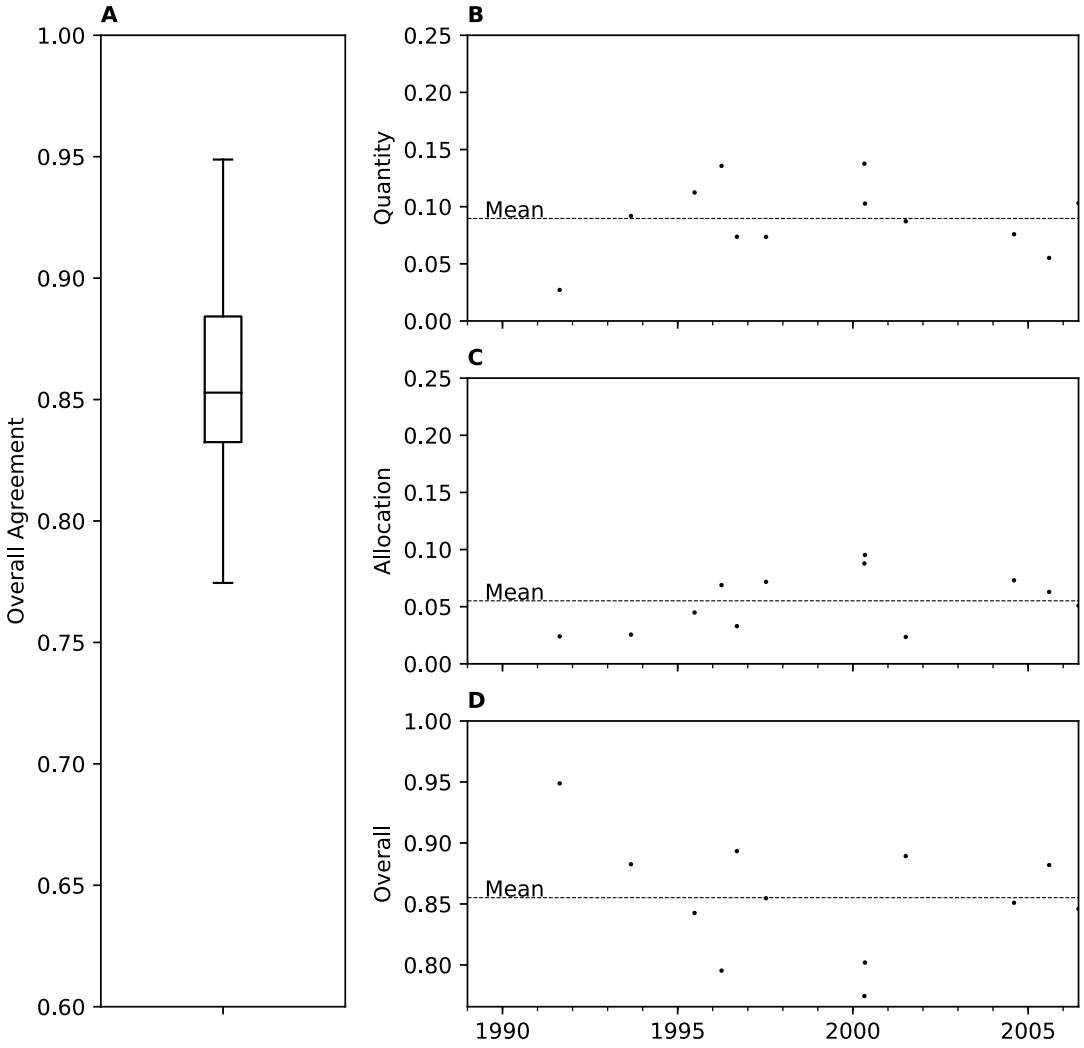

Figure 7.5: Accuracy statistics from Outlier based change detection on full land cover classification. A= box plot of overall agreement, B = Quantity disagreement (desirable to be near 0), C = Allocation disagreement (desirable to be near 0) and D = overall agreement (desirable to be near 1).

maps (Table 7.9 and Table 7.10). The overall confusion matrix for the mapped areas also suggest some confusion between vegetation classes in the maps produced by both approaches (Table 7.11 and Table 7.12).

Table 7.9: Confusion matrix for Outlier Detection change detection classification accuracy. As the number of points sampled in each of the classes is not stratified a percentage would be misleading, therefore the total number of points sampled as having changed to each class is shown. Users and producers accuracy are given as percentages.

	Broadleaved	Less Productive Veg	Coniferous	Grassland	Bare Ground	Urban	Water	Users (%)
Broadleaved	1498	120	230	0	0	0	0	81
Less Productivity Veg	240	456	22	34	44	27	0	55
Coniferous	130	32	1783	0	22	0	0	91
Grassland	298	12	55	29	9	13	0	6
Bare Ground	23	0	21	4	376	0	0	44
Urban	0	0	0	0	0	120	0	100
Water	0	0	0	0	0	0	2	100
Producers (%)	68	74	84	43	83	75	100	70

Table 7.10: Repeated RF classifier change detection classification of change regions confusion matrix. As the number of points sampled in each of the classes is not stratified a percentage would be misleading, therefore the total number of points sampled as having changed to each class is shown. Users and producers accuracy are given as percentages.

	Broadleaved	Coniferous	Less Productive Veg	Bare Ground	Grassland	Urban	Water	Users (%)
Broadleaved	1389	182	224	56	202	0	0	67
Coniferous	182	954	0	518	56	112	0	52
Less Productive Veg	51	0	521	0	0	0	0	90
Bare Ground	28	14	0	331	0	0	0	88
Grassland	67	98	73	42	328	14	0	52
Urban	14	0	0	0	0	123	0	89
Water	0	12	0	4	0	2	3	14
Producers (%)	80	75	63	34	55	49	100	65

The number of false positives of change produced using the repeater RF classification change detection approach has led to large areas of change at each time step. Most land cover in Wales is stable, however, in total an area of 5,075km^2, nearly a quarter of the study area was recorded to have changed land cover during the 16 year study period. The change areas produced by the outlier change detection approach were smaller at each time step and in total, a more reasonable 1933km^2 area was recorded to change land cover class at some point

Table 7.11: Confusion matrix for Repeated RF land cover classification accuracy assessment percentages. Would expect each class to have 14% of points due to class number and stratified sampling.

	Broadleaved	Less Productive Veg and Heath	Coniferous	Grassland	Bare Ground	Urban	Water	Users (%)
Broadleaved	12	1	0	2	0	0	0	85
Less Productive Veg	0	12	0	2	0	0	0	86
Coniferous	0	0	14	0	0	0	0	98
Grassland	0	1	0	14	0	0	0	96
Bare Ground	0	1	0	0	13	0	0	94
Urban	0	0	0	0	0	14	0	98
Water	0	0	0	0	0	0	14	100
Producers (%)	99	88	99	77	99	99	100	93

Table 7.12: Confusion matrix for Outlier Detection change detection classification accuracy percentages. Would expect each class to have 14% of points due to class number and stratified sampling.

	Broadleaved	Less Productive Veg	Coniferous	Grassland	Bare Ground	Urban	Water	Users (%)
Broadleaved	13	0	0	1	0	0	0	94
Less Productive Veg	0	13	0	1	1	0	0	88
Coniferous	0	0	14	0	0	0	0	98
Grassland	0	0	0	14	0	0	0	98
Bare Ground	0	2	0	0	12	0	0	85
Urban	0	0	0	0	1	14	0	96
Water	0	0	10	0	0	0	14	99
Producers (%)	99	85	98	89	89	99	100	94

during the 16 year study period. Once the objects have changed classes, whether true change or a false positive, they mostly remain stable within the new land cover class in both approaches. For repeated RF classifiers, of the total change area, 86% of pixels changed only once, and for the outlier change detection approach 84% of pixels changed land cover once. In the maps produced by the repeated RF classifier approach, a further 12% changed class twice during the 16 year study period. The remaining 2% changed up to six times. The outlier change detection approach maps were similar, with 12% changed classes twice and the remaining 4% changed class up to nine times. Therefore, for both approaches, only a small proportion of the change features changed to an unreasonable number of classes. The majority of these features were mixed pixel 'slivers' on the edges of land cover as in previous chapters.

The incorrect classification of changes by repeated RF classifiers change detection

lead to errors of quantity in the classifications, the percentage of the total map area taken up each class is too great or too small. Figure 7.6 and Figure 7.7 gives an illustrative example of land cover change throughout the time series. The largest trend is a movement from Broadleaved to the Less Productive Veg and Grassland classes. However, in the change classification confusion matrix and the overall matrix (Tables 7.10 and 7.11) there were errors of commission and omission associated with the Broadleaved, Grassland and Less Productive Veg classes. This combined with the low change detection accuracy and the large change areas in classes that should are managed and should be stable, suggests this is due to confusion in the change detection rather than a trend. Areas of Urban, Coniferous and Water remain stable during the 16 year study period (Table 7.13), water in particular was accurately classified (Tables 7.10 and 7.11).

By contrast, the outlier change detection approach had evenly distributed classification error between quantity and allocation throughout the data series. Suggesting that any error in the change detection was consistent and not increasing with each time step. The greatest source of error in the reclassification accuracy assessment was in the Grassland class which exhibited an even spread of errors of omission and commission with the Broadleaved and Less Productive Veg classes. The Urban area decreases by an average of $5km^2$ per year, this is unlikely to have occurred and is probably due to mixed pixel Urban and vegetation pixels being identified as an outlier and subsequently classified as vegetation.

Table 7.13: Annual area and change for Repeated Random Forest change detection. No imagery was available for 1993 and 2003.

Class (Km^2)	1990	1991	1993	1994	1995	1996	1997	1998	1999	2000	2001	2002	2004	2005	2006	2007 Base	Mean
Broadleaved	**3586**	**3549**	**3510**	**3368**	**2955**	**2950**	**2797**	**2774**	**2664**	**2436**	**2390**	**2312**	**2316**	**2175**	**2171**	**2172**	**2797**
	-37	*-39*	*-142*	*-413*	*-4*	*-153*	*-23*	*-110*	*-228*	*-46*	*-78*	*+3*	*-141*	*-3*	*+1*		*-94*
Coniferous	**1148**	**1138**	**1133**	**1154**	**1126**	**1105**	**1121**	**1116**	**1119**	**1226**	**1231**	**1225**	**1237**	**1301**	**1281**	**1281**	**1177**
	-10	*-4*	*+20*	*-27*	*-22*	*+16*	*-4*	*+2*	*+108*	*+5*	*-6*	*+12*	*+64*	*-19*	*-1*		*+9*
Less Productive Veg	**3291**	**3421**	**3514**	**3651**	**4584**	**4632**	**4720**	**4653**	**4735**	**4746**	**4695**	**4731**	**4582**	**4367**	**4333**	**4333**	**4310**
	+130	*+93*	*+137*	*+933*	*+48*	*+88*	*-66*	*+81*	*+11*	*-51*	*+36*	*-149*	*-215*	*-34*	-		*+69*
Bare Ground	**2079**	**2014**	**1987**	**1942**	**1521**	**1511**	**1534**	**1589**	**1576**	**1321**	**1274**	**1258**	**1280**	**1222**	**1224**	**1225**	**1556**
	-65	*-26*	*-45*	*-422*	*-9*	*+23*	*+55*	*-13*	*-255*	*-47*	*-17*	*+22*	*-58*	*+2*	*+301*		*-37*
Grassland	**699**	**682**	**658**	**684**	**616**	**602**	**626**	**659**	**694**	**1043**	**1179**	**1240**	**1356**	**1696**	**1740**	**1740**	**945**
	-17	*-24*	*+27*	*-68*	*-15*	*+24*	*+34*	*+35*	*+348*	*+136*	*+62*	*+116*	*+340*	*+44*	-		*+69*
Urban	**617**	**616**	**617**	**620**	**617**	**619**	**622**	**627**	**632**	**648**	**650**	**654**	**649**	**660**	**669**	**669**	**634**
	-1	*+1*	*+3*	*-3*	*+2*	*+3*	*+5*	*+5*	*+16*	*+2*	*+4*	*-5*	*+10*	*+10*	-		*-17*
Water	**3189**	**3189**	**3189**	**3189**	**3189**	**3189**	**3189**	**3189**	**3189**	**3189**	**3189**	**3189**	**3189**	**3189**	**3189**	**3189**	**3189**
	-	-	-	-	-	-	-	-	-	-	-	-	-	-	-	-	-

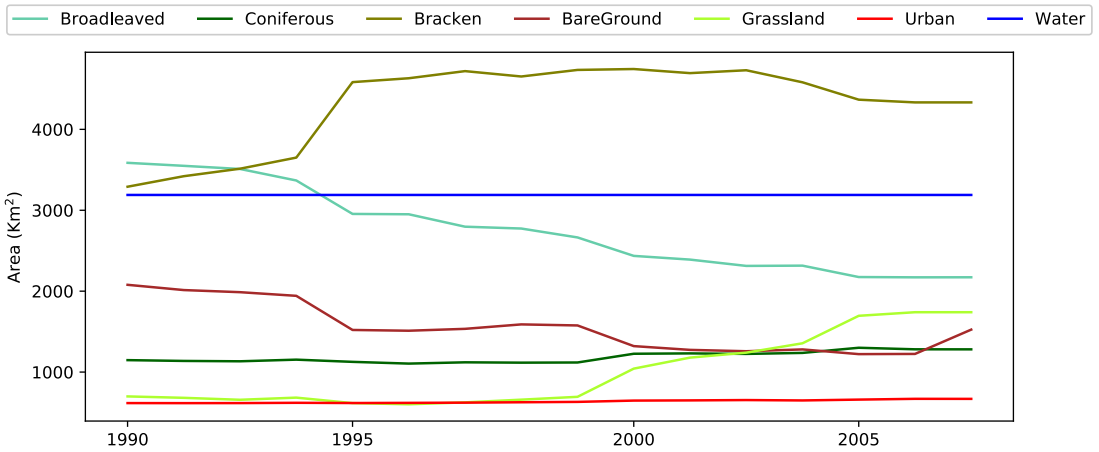

Figure 7.6: Total area produced using Repeated Random Forest Classifiers of each of the seven change classes in time.

Table 7.14: Annual areas and change for Outlier Change Detection. All areas are in km2, no imagery was available for 1993 and 2003.

	1990	1991	1993	1994	1995	1996	1997	1998	1999	2000	2001	2002	2003	2004	2006	2007 Base	Mean
Broadleaved	**1724**	**1753**	**1761**	**1813**	**1878**	**1906**	**1951**	**1979**	**2007**	**2087**	**2105**	**2122**	**2145**	**2167**	**2172**	**2172**	**1957**
	+28	*+8*	*+51*	*+65*	*+27*	*+45*	*+28*	*+28*	*+80*	*+18*	*+17*	*+23*	*+21*	*+5*	-		*+28*
Conifer	**1561**	**1535**	**1526**	**1488**	**1431**	**1414**	**1391**	**1376**	**1363**	**1333**	**1326**	**1317**	**1300**	**1284**	**1281**	**1281**	**1404**
Area (km2)	*-26*	*-10*	*-38*	*-57*	*-17*	*-23*	*-15*	*-12*	*-30*	*-7*	*-9*	*-17*	*-16*	*-3*	-		*-18*
Less Productive Veg	**3547**	**3580**	**3595**	**3663**	**3800**	**3840**	**3926**	**3975**	**4013**	**4148**	**4170**	**4195**	**4254**	**4323**	**4333**	**4333**	**3933**
	+34	*+15*	*+68*	*+138*	*+39*	*+87*	*+49*	*+38*	*+135*	*+22*	*+24*	*+59*	*+69*	*+10*	-		*+49*
Bare Ground	**1979**	**1969**	**1960**	**1914**	**1870**	**1840**	**1759**	**1685**	**1642**	**1441**	**1400**	**1369**	**1302**	**1238**	**1225**	**1225**	**1660**
	-10	*-8*	*-46*	*-44*	*-30*	*-81*	*-75*	*-42*	*-201*	*-41*	*-31*	*-67*	*-64*	*-14*	*+300*		*-28*
Grassland	**1862**	**1846**	**1845**	**1824**	**1739**	**1725**	**1710**	**1727**	**1721**	**1743**	**1750**	**1749**	**1750**	**1739**	**1740**	**1740**	**1770**
	-16	*-1*	*-22*	*-85*	*-14*	*-15*	*17*	*-6*	*+22*	*7*	*-1*	*1*	*-11*	*+1*	-		*-8*
Urban	**747**	**736**	**731**	**717**	**700**	**695**	**682**	**678**	**673**	**667**	**668**	**668**	**668**	**669**	**669**	**669**	**694**
	-11	*-4*	*-14*	*-17*	*-6*	*-13*	*-4*	*-5*	*-5*	*+0*	*+0*	*+0*	*+1*	*+1*	-		*-5*
Water	**3189**	**3189**	**3189**	**3189**	**3189**	**3189**	**3189**	**3189**	**3189**	**3189**	**3189**	**3189**	**3189**	**3189**	**3189**	**3189**	**3189**
	-	-	-	-	-	-	-	-	-	-	-	-	-	-	-		

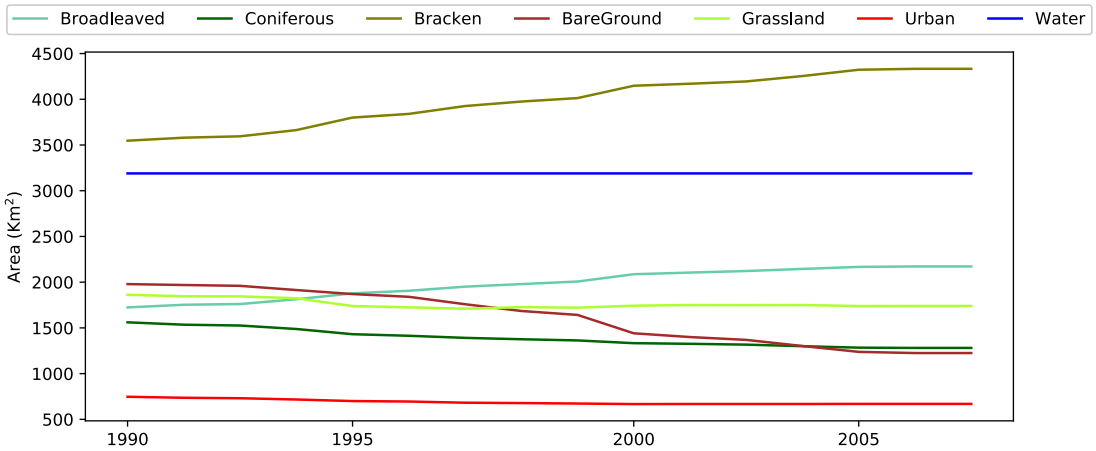

Figure 7.7: Total area produced using Outlier Detection of each of the seven change classes in time.

There were also some errors of commission between the Less Productive Vegetation and Bare Ground classes. However, as the error reduces further away from the base classification the large change area is due to correcting error in the base classification (Figure 7.8). Classification errors, like change objects, will exhibit a different spectral signature to the rest of the class objects. Identification and change of these objects lead to classification error being reduced with each time step.

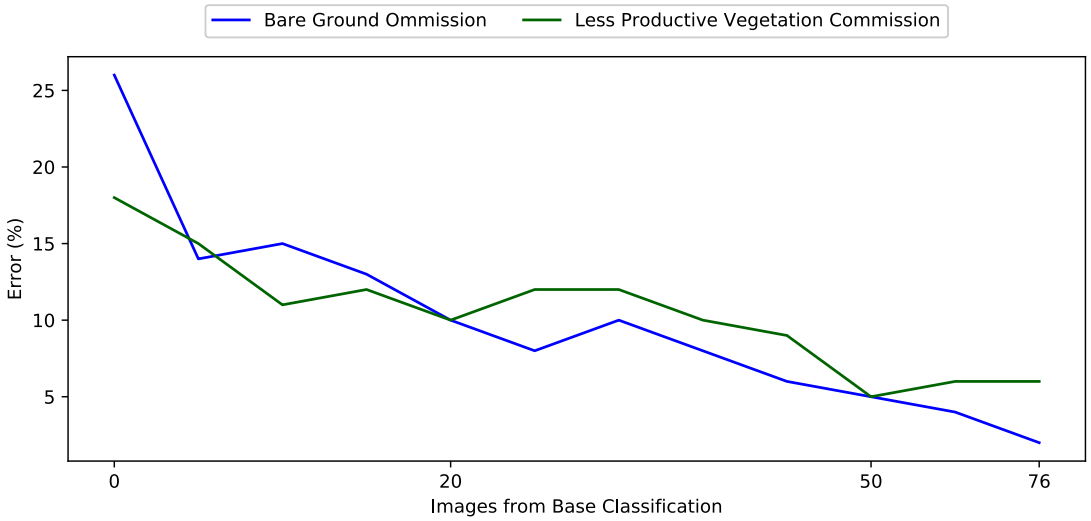

Figure 7.8: Changes in Omission and Commission (Producers and Users) accuracy with time steps away from the Base Classification

7.4 Discussion

7.4.1 Repeated Random Forest Classifiers Sources of Error

Repeated RF performed significantly worse than detecting outliers. Repeated RF classifiers exhibited a lower change detection and reclassification accuracy and much larger areas changed land cover than OD (Table 7.6). The threshold to identify likely change objects was not accurate in this case.

The likely change features were identified as objects with a mean probability of class ownership greater than the highest frequency mean probability value from the RF classifiers. The assumption being that the majority of the data are unchanged land cover and therefore should exhibit a similar mean probability of class ownership. This assumption held when studying change between well-defined and very spectrally distinct classes in the previous chapter. However, in the full land cover classification, there were several vegetation classes with more similar spectral signatures than the binary classes in Chapter 5. This resulted in reduced mean probabilities of class ownership.

In this case, the histograms produced for the vegetation classes (Low Prod Veg, Grassland, Broadleaved) and the Bare Ground class often had a small or no peak in the frequency of probability values (Figure 7.9). This led to variable and very large or small percentages of objects being identified as likely change features. For example, in one of the early images in the data series (LS5TM acquired 21-09-2006) around 50% of the objects from the Broadleaved, Bare Ground and Lower

Productivity Veg classes were identified as possible change features. Whereas from the Grassland Class only 12% of objects, with class ownership probabilities just larger than 0, were selected.

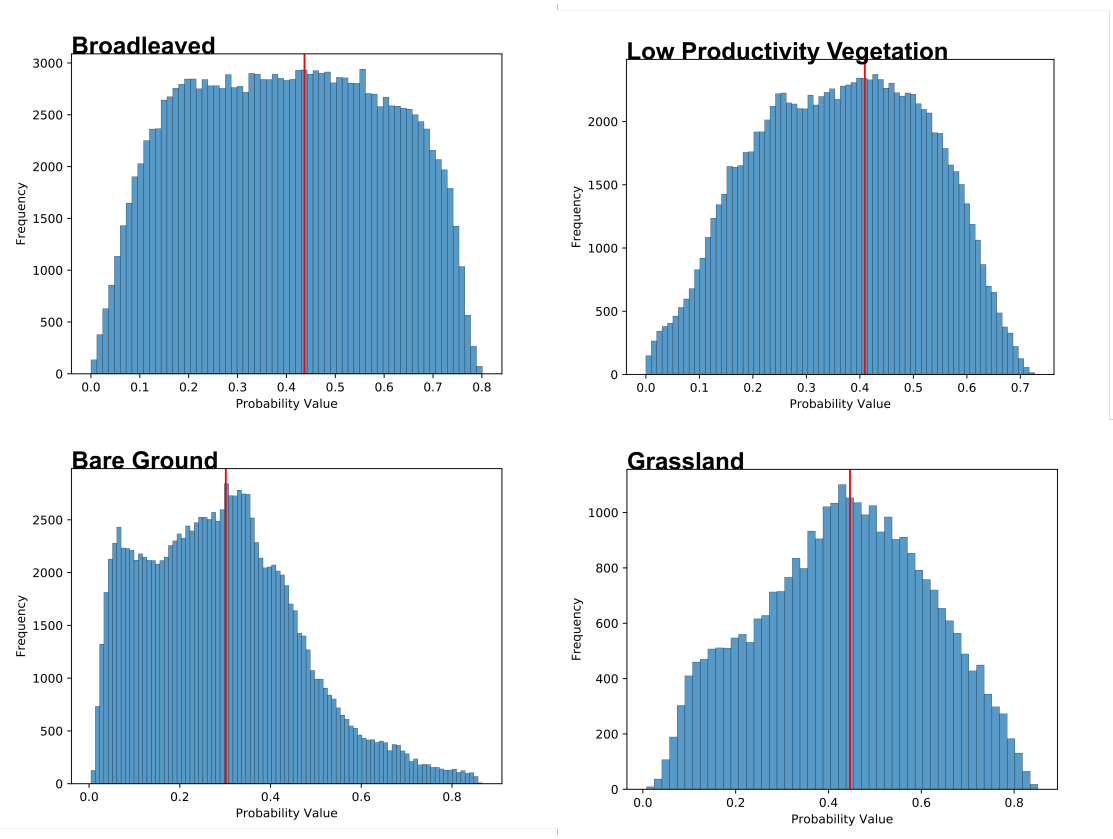

Figure 7.9: Illustration of histograms of mean probability values produced from Repeated RF for the Broadleaved (30-05-1997), Bare Ground (17-05-1998), Grassland (1996-08-17)and Low Productivity Vegetation (09-09-1996) Classes. The red line is the threshold mean probability value.

When a large percentage of potential change features is identified, most of it represents unchanged class data and the training data for the class is not representative. In the previous chapter, the outlier change detection threshold sensitivity analysis indicated that <60% of the original mapped area as training data for each class led to a decrease in accuracy. In this case, False Positives

were caused due to some features appearing closer to the training of another class than its own. For example, in Figure 7.10, 92% of the Grassland area was used to train the final classifier compared to just 39% of the Low Prod Veg. The majority of the likely change objects from the Low Prod Veg class are not change features, but they may now appear closer to the Grassland training than the restricted Low Prod Veg training data. Thereby causing a large area to change class at this time step.

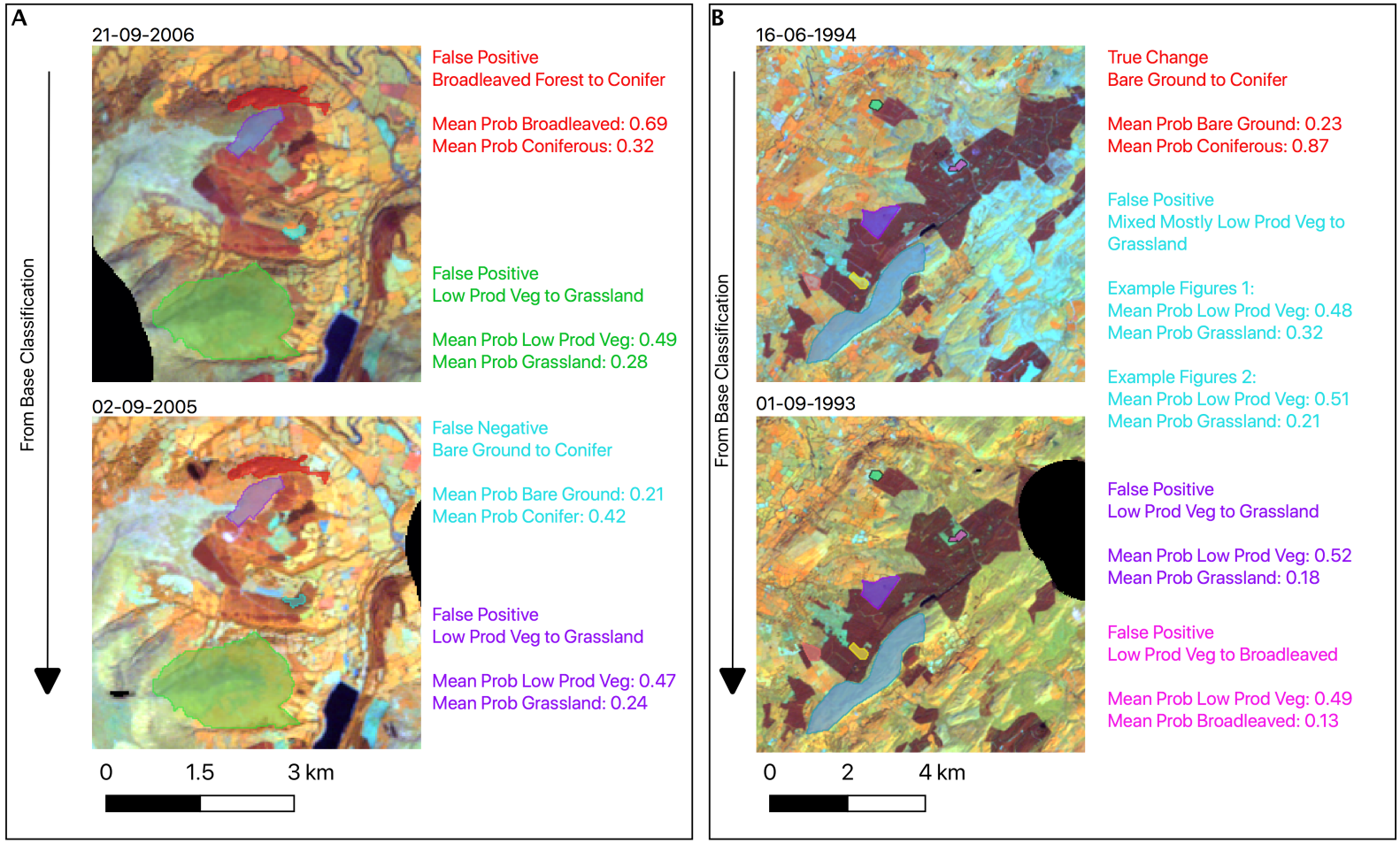

Figure 7.10: Illustration of errors caused by poor likely change threshold and variable percentages of the original map regions available for training the final extra trees classifier. The percentage of objects available for the classifier in each case is given. The imagery is false colour, blue = SWIR2, green = SWIR1 and red = NIR. A illustrates the errors in two images which are close to the Base Classification acquired in 2006 and 2005 and B two images much further from the Base Classification acquired in 1994 and 1993. The colour of the text describing the type of change is the same as the colour of the features on the images. For example, the purple low productive veg to grassland change is the purple shape in the false colour image.

However, the variation in threshold also causes this data to remain in the incorrect class (Figure 7.11). The false positives form part of the training data repeatedly sampled at the next time step and the map-to-image approach assumption that any change or error in the class area is small no longer holds. This creates a new distribution of mean probability values, in which the incorrect area may have a greater mean class ownership probability than the most common value, especially given the shape of some histograms. Therefore, error often remains committed to its new class. This type of error is exhibited in the Grassland, Bare Ground, Broadleaved, and Low Prod Veg classes and causes the overall error and quantity disagreement to increase with each time step away from the 2007 base classification.

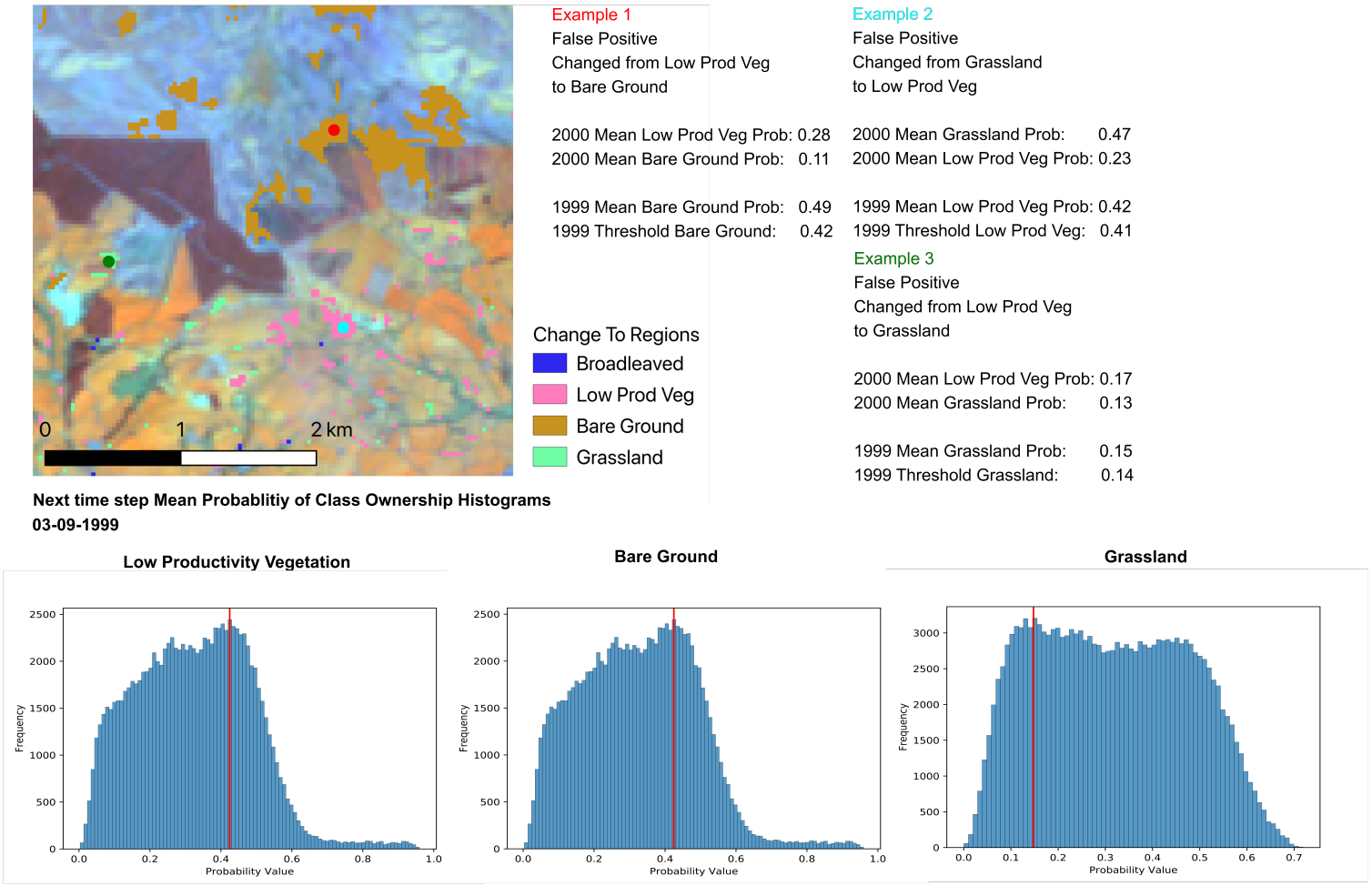

Figure 7.11: The effect of large variance in the percentage of each class area for training on a Landsat 7 image acquired 30-04-2000. A FCC (Red, NIR, and SWIR1) and areas which changed to each class. Data from 3 example changes where variance meant the false positive was not considered a possible change object at the next time step. Their location is indicated by the three coloured circles on the FCC.

The inclusion of the hard threshold when using outlier change detection to indicate potential change features stopped this from occurring. The threshold limits potential change features to 20% of the whole land cover area. Therefore, a set amount of data are removed from the potential training data and class variability is maintained. In situations where classes are spectrally similar the threshold can help limit any error. For example, the accuracy assessment from both approaches indicates confusion between the Grassland, Broadleaved forest and Low Productivity Veg Classes. However, the change areas are $\tilde{2}00km^2$ bigger when using repeated RF classifiers. The difference in quantity disagreement between the two approaches (Table 7.6) illustrates that these changes are in error. In this situation, the hard threshold maintains accuracy by limiting potential change using expert knowledge. However, it is important to note that setting the hard threshold requires expert knowledge or sensitivity analysis of the most dynamic class. If the threshold is set too low, false negatives of change would impact accuracy in both potential change features and through error in the training data.

Identifying change features using outlier change detection was significantly more accurate and faster to process. Although there was not a significant difference in overall classification accuracy, due to the effect of stable features, the change detection and change areas indicate that outlier change detection is a more accurate approach. Therefore, further discussion of error sources and the usefulness of the approach for policymakers will focus on the outlier change detection approach only.

7.4.2 Outlier Detection Approach Limitations and Assumptions

The two assumptions of the approach; (i) that change is small and (ii) that change features are spectrally distinct from the previous land cover, were true to reality for most classes in this example. The approach also assumes the base classification is mostly accurate. If error is added into the base classification at each time step this can propagate through the products. If enough error is introduced that the class statistics are no longer representative of the class features omission and commission of change features occurs. This error typically occurred in vegetation land covers where changes between them are more likely to be on a 'continuum' of change, for example, change from grassland to tree cover will be gradual and not have a sudden large-scale change event.

This occurred in some areas of coniferous forest which were felled and classified as grassland or bare ground in the 2007 base classification. The change from bare ground to grassland is typically gradual and was not always picked up by the outlier change detection approach. This error propagated through the classifications and in time led to the grassland class areas exhibiting more 'bare ground' characteristics. This also led to a reduction in changes to coniferous forest class as the grassland class exhibits some similar spectral characteristics. By the furthest point from the original base classification in the time series there can be enough objects of this type to cause the Conifer spectral signal to no longer appear as an outlier in the Bare Ground or grassland class, leading to errors of omission Figure 7.12). This omission is rare and occurs mostly when the change detection area is small due to cloud cover across most of the image and

the remaining areas happen to contain larger areas of propagated error. This type of error is typically corrected at the next time step where the error is a smaller feature in the dataset.

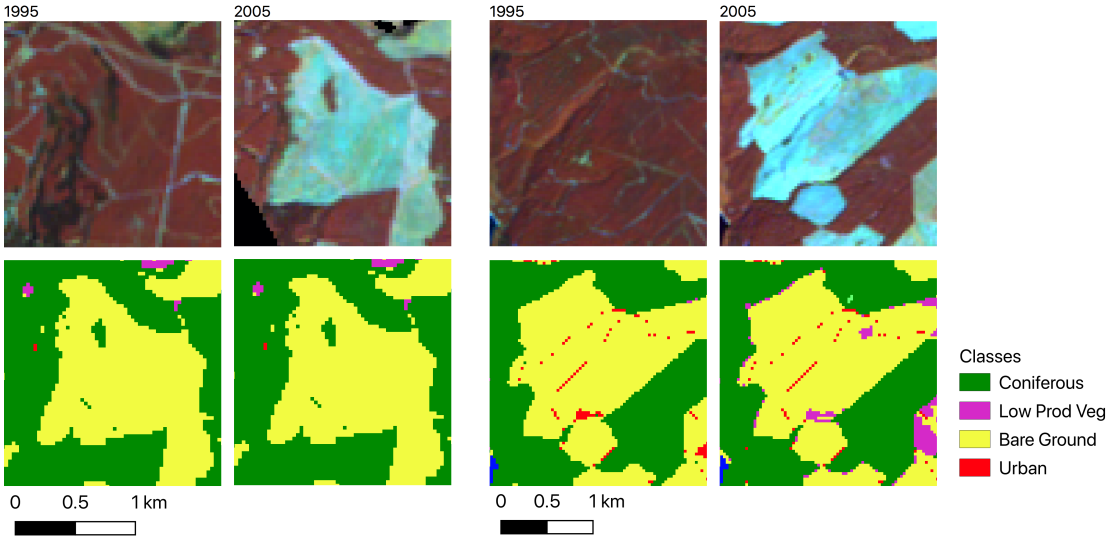

Figure 7.12: FCC of two example locations where Bare Ground did not change to Coniferous forest at the correct time step. This was caused by errors introduced to the base classification which had propagated through time and compounded by a small change identification area caused by high cloud cover in the images. This led to unrepresentative training data for classification of likely change features and these change features being omitted from the final classification. These examples were rare in the whole dataset. The colour bands are blue = SWIR2, green = SWIR1 and red = NIR.

Detection of these types of changes was also limited by similar classes. Despite a JM score of over 1000 Bare Ground and Urban classes had a Euclidean distance of only 50. Therefore, due to the high likelihood of false positives changes between these classes were not allowed. However, classification confusion between classes with similar spectral signatures is a common problem in multispectral data. This confusion led to reduced change feature classification accuracies in vegetation classes. This type of confusion appears as small features in a larger

contiguous area classified as a different vegetation class (Figure 7.13). Including other ancillary datasets or information about neighbouring objects classes could help combat this but would limit the applicability of the approach to times where the secondary data are available.

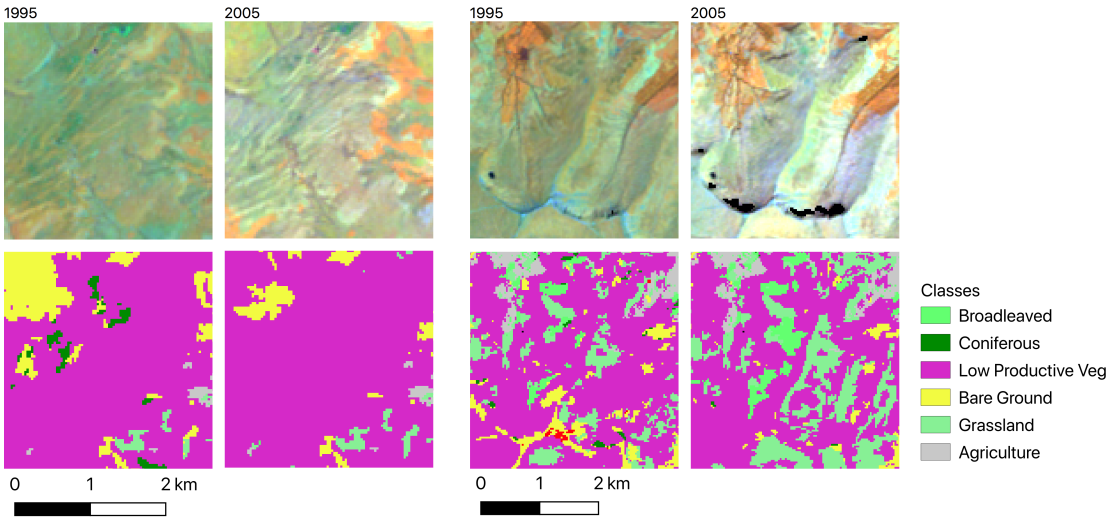

Figure 7.13: FCC and classification of two example locations where Low Productivity Veg, Broadleaved, Coniferous and Grassland classification was confused due to error in likely change features detection and spectral similarity in the final classification. The bands are blue =SWIR2, green = SWIR1 and red = NIR.

The assumptions were not broken by stepping through the time series in the reverse chronological order, allowing for the base classification to be generated at a point in time where there was higher resolution and quality data available for training data. Therefore, the base classification generation is not limited by available data and imagery at the start of the study period.

7.4.3 Usefulness of Map Product for Land Managers and Policy Makers

Numerous characteristics make a useful map product, as such not all use cases are considered here only broad indicators of usefulness to land managers. At the broadest level, it needs to be accurate, and the sources and subsequent manifestation of any error need to be known. The temporal and spatial resolution should be appropriate and the class information needs to be at an adequate level. Additionally, the data should be accessible and ideally queryable, especially in the time series. This approach produces land cover data at the highest temporal resolution possible in a fragmented archive. The class information is limited by the spectral separability of the class information, this means that only broad-scale changes in land cover can be characterised, habitat level changes which would be within each class can not be identified. The data could be manipulated to make it queryable in a time stack or data cube structure, so the history of a pixel or object could be easily viewable by land managers.

The 30m per pixel spatial resolution of the map products limits the use to national or regional studies. The temporal resolution is much higher than other datasets in this period. However, as most of the classifications exhibit only very small differences, it may be more appropriate to use maps of the majority class from a three-year period around a date (i.e. map for 1993 contains majority classes from classifications from 1992, 1993, and 1994). This would increase data accessibility and limit data redundancy, especially as in its current form the data are not qureyable or the history of land cover change of an object easily accessible. The

higher resolution data could also be used for any projects which require sub-annual data resolution (e.g. seasonal variation).

The outlier change detection approach produces an overall change detection accuracy of 89.1% and can be considered accurate. Additionally, the sources of change detection and classification omission, and commission error are known. Before use, the causes of such errors and class confusion should be considered. It may be that the map products are not reliable in monitoring all features and should not be considered for some studies. Caution should also be employed when extracting land cover trend information at a high temporal resolution. Reducing the temporal resolution reduces the effects of the errors and provides more accurate trend information which could be useful to monitor the planting of Broadleaved trees due to government initiatives.

The more data within the map information of a product the more studies it may apply to. If the class number was reduced to 4 (vegetated, forested, non-vegetated, and water) the accuracy would be increased but the usefulness of the map would be reduced. The number of classes mapped here is low compared to other land cover maps generated manually from composites of image data, like the Updated Phase 1 map. This product does not include separate classes for different types of semi-natural vegetation, limiting the usefulness in measuring changes for example tracking growth or loss specifically related to Bracken or Heath management. Changes in semi-natural environments are important for Government agencies in Wales and limit the usefulness of the product.

However, in products like the Updated Phase 1 map a series of complex rules were developed and applied to imagery, if the same number of classes were included in the change detection process it is unlikely that they would have been

classified accurately. The outlier change detection approach had difficulty classifying some classes with larger separability than these, suggesting any change detection of this number of classes in one product would be inaccurate. The classes could be included with a rule base that only allowed change from or to classes of sufficient spectral separability. However, the errors of omission in identifying gradual changes suggest that, if included the accuracies of these semi-natural vegetation classes would be compromised. It would likely be more useful to produce binary products studying changes in these specific classes.

The approach appears to work best when examining large-scale land cover changes in binary classification. All approaches were most accurate when identifying high magnitude changes in 'loss' areas from a single class. This would suggest that the approach works best and should be used when monitoring for features like felling or flooding. It is difficult to label and find a single 'change date' for more gradual changes, such as scrub to tree and as such pixel history information monitoring changes in productivity for example may be more appropriate.

7.5 Conclusions

The dominant land cover changes across Wales between 1990 and 2006 were found to be changes between Grassland, Forest, and Bare Ground and in the types of forest. The threshold for identifying likely change features using repeated RF was not accurate when used on multiple land covers and led to very large areas being falsely recorded as change. The outlier change detection approach was accurate in identifying and reclassifying change features. However, there are errors of omission associated with detecting gradual changes and some

errors of commission due to spectral separability and class confusion of the multi-spectral data. Errors of commission were predominantly associated with the Grassland and Low Productivity Vegetation Classes. The error in the Low Productivity Veg and Bare Ground Classes was reduced with distance from the base classification, suggesting error was removed with likely change features from the classes.

The map products provide a series of land cover classifications at a higher resolution than other land cover data during this period allowing for historic land cover change trends to be generated. The errors in the product and the number of classes that can be analysed limit applicability in some cases. Separability and accuracy of the series of land cover classifications suggests that binary maps may perform better in these circumstances. The land cover classifications contain data that is useful to land managers and policymakers but caution must be employed when studying types of change with known error.

Chapter 8

Discussion

Previous approaches have combined ancillary mapped land cover data with more recently acquired image data for change detection (Thomson et al. 2007, Cole et al. 2018). The histogram, outlier, and repeated RF classifier change detection approaches presented here build on the map-to-image change detection work of Thomas et al. 2018. The approaches have been shown to accurately identify binary change/no change data, in the same way as PCC and PV approaches. It has also been used, in the same manner as, PCC approaches, to produce a full land cover map and matrix of change data with passable accuracy. The approaches are automated and can be applied to a time series of image data, with reduced operator hours to PCC approaches, and can be applied to different sensors. Although the study area is smaller than some of PCC and PV examples in Chapter 2, the approaches are scalable to a larger area, if a suitable base classification can be located or generated.

The approaches presented here have been shown to be highly applicable where

change features and land cover dynamics need to be identified at a sub-annual frequency (at each image time step), but where the data are of an insufficient density to meaningfully model likely change processes on each pixel or object. The approach is also computationally efficient and robust to the effects of noise and different sensors. The general approach has also been shown to perform well when the image density is increased, it may be more suitable than dense time series approaches when studying change in large study areas (e.g. national or continental scale).

The underlying assumptions that change is small and spectrally distinct were true to reality in the majority of cases here. However, the different approaches used to identify likely change features also have unique limitations or assumptions, which must be considered before being used. Using the skew and kurtosis of the histogram works on the assumption that the underlying histogram is parametric. Using a percentage threshold-based outlier change detection approach assumes that all of the change features are included within this percentage. This is similar to several PV approaches (Malila 1980, Hoffmann 1975, Nackaerts et al. 2005, Wilkinson et al. 2008, Singh & Talwar 2014). It is important to consider that the percentage of outliers, which includes all change features, is not the same as the percentage of change from the whole. Breaking either of these parameters or assumptions is a severe limitation on potential accuracy. Repeated RF classifiers do not introduce assumptions but recorded false positives of change where objects were mixed signals or changed large amounts of the area changed class depending on the training data size.

8.1 Limitations and Assumptions

The underlying assumptions of the method; (i) change is small and (ii) change features are spectrally distinct from the previous land cover, were true to reality in the vast majority of the cases here. They are also likely to hold if detecting change features in similar locations, land, and cloud cover situations. The accuracy was also unaffected by the use of multiple satellite sensors and the chronological order the imagery was analysed.

The assumption that land covers are spectrally distinct limits the type of change features that can be analysed. Each statistical method for identifying likely change features is limited to spectrally distinct classes. The effect of this limitation is increased when analysing a full land cover map. Several classes were removed from the full land cover map change analysis because they had a high likelihood of confusion. For example, Semi-Improved and Unimproved Grassland were combined to form a Grassland class, because a meaningful classification of the two classes was unlikely. In these situations, it is impossible to determine true change features from spectral data alone and the approach can not be applied. An approach that stores pixel histories may be better able to identify these change features as they look for a difference from the previous instead and the previous may be the same just very similar to multiple land covers (Tuxen et al. 2008, Huang et al. 2009, Bontemps et al. 2008).

All of the change detection approaches presented have limited applicability when detecting change which is easily confused. This is also a limitation for PCC analysis (Bergen et al. 2005, Kozak et al. 2007, Silva et al. 2008, Fan 2008, Hester et al.

2010, Renó et al. 2011, Baumann et al. 2012, Souza-Filho et al. 2015, Liu & Yang 2015, Cardille & Fortin 2016). When working with classified data the overall accuracy is limited by any incorrect class labels, therefore the classification needs to be accurate (Congalton 2008, Lillesand et al. 2015). If the probability of class ownership for a given object is even across multiple classes then the classifier cannot determine class from the spectral data alone and the approach can not be applied. This confusion can also be caused by mixed pixels, these objects display the characteristics of multiple land covers (Congalton 2008, Lillesand et al. 2015). As such they caused confusion for each of the statistical approaches and were classified differently several times.

Additionally, unlike PCC there is not an operator carefully defining each set of training for each map (Bergen et al. 2005, Kozak et al. 2007, Silva et al. 2008, Fan 2008, Congalton 2008, Hester et al. 2010, Renó et al. 2011, Baumann et al. 2012, Souza-Filho et al. 2015, Liu & Yang 2015, Lillesand et al. 2015, Cardille & Fortin 2016) Therefore, it is even more important the classes are well defined and separable. Defining classes is a balance between the usefulness of the map and change detection and the likelihood of false positives due to confused classes. For example, despite having low euclidean distance both Bare Ground and Urban classes were included in the 2007 base classification because urban growth is a desirable metric. Here the confusion was handled by not allowing change between the two classes. Although this introduces some potential for errors of omission the false positives of change could be much greater if the change was allowed.

Using classified data and combining different data sources means that EO datasets are not directly compared. This allows different data sources to be used with minimal atmospheric correction. In the examples presented here, 4 different

optical satellite sensors are used. Potentially, all of the change detection approaches presented here could also be applied to radar data increasing the data volume further and reducing the effect of cloud cover (Guo et al. 2017, Lv et al. 2018). All EO approaches exhibit a 'lag' between when change occurs on the ground and when it is captured in satellite imagery. When data availability is limited, due to cloud cover or image acquisition issues, the differences can be a year or more. When a period of high data availability occurs large areas are updated this results in 'spikes' of a very large amount of change occurring in one year or image (Bontemps et al. 2008, Wang et al. 2009, Verbesselt et al. 2010, Zhu & Woodcock 2014, Olofsson et al. 2014, DeVries et al. 2015, Dutrieux et al. 2015, Zhu et al. 2016, Hamunyela et al. 2016).

8.2 Potential Developments and Future Research

There are several further uses and theories, which could be extrapolated or incorporated into the overall approach to increasing accuracy, output usefulness, and applicability in other situations.

Temporal correlation approaches like Bayesian logic could also be introduced (Bruzzone et al. 2004, Castellana et al. 2004, Liu & Zhou 2004, Benedek et al. 2015, Cardille & Fortin 2016, Wu et al. 2017, Ayele et al. 2018) to increase accuracy. When using Bayesian logic changes which are deemed more likely to occur are given extra weight in classification by using prior probabilities and classifier output to determine classification likelihood. This could increase

accuracy when determining change between spectrally similar but unlikely changes, for example between Coniferous forest and Water. However, how the prior probability should be calculated and the probability data should be incorporated into the map-to-image approach requires further study.

Other statistical approaches or adaptations of the approaches presented here could increase the applicability or accuracy of the map-to-image approach in some situations. For example, Network X, a python library, could be used to map and produce metrics from n-dimensional clusters (Hagberg et al. 2008). Statistics from this approach could be used to find different types of outliers with a hard threshold. Fuzzy Rough Nearest Neighbour may perform better with a more well-defined 'Other' class or with the incorporation of an unsupervised classification of the 'Other' class as was used in the repeated RF study (Congalton 2008, Lillesand et al. 2015). Further research is needed to explore the applicability of these other approaches.

All changes here were to the statistical analysis section of the approach, outside of this the processing was unaltered, potential change features were identified and classified using an RF classifier. However, this may not be the most accurate way of defining change features for all objects. Repeated RF classifier change detection loses all the information from the previous classifiers and can produce a training dataset that is too homogeneous and is unrepresentative of the whole class. Classifying all objects by the highest mean probability class or using the differences between these values to threshold and classify change features may produce more accurate results because it does not rely on the identification of an accurate yet representative training dataset. It instead relies on RF's' natural' ability to suppress outliers in training and an iterative sampling technique.

Currently, data are only gathered at each time step, but more information could be extracted by studying how each pixel changes land cover through time (Bontemps et al. 2008, Wang et al. 2009, Verbesselt et al. 2010, Zhu & Woodcock 2014, Olofsson et al. 2014, DeVries et al. 2015, Dutrieux et al. 2015, Zhu et al. 2016, Hamunyela et al. 2016). This information could be used to decrease the effect of mixed pixels. For example, an object which changes between two or three classes an unusually high number of time is likely the result of confusion. In this case, change accuracy could be increased by forcibly classifying the object into one class at all time steps.

This type of pixel history data could also increase the usefulness and applicability of the output for study and management practices. Currently, a large number of slightly different classifications are produced. These can be analysed to produce annual or sub-annual area change statistics but studying the change process of a particular object is more complex. If the pixel history could be stored and accessed for a stack of classifications, as it is for a stack of imagery in dense time series approaches (Bontemps et al. 2008, Eklundh et al. 2009, Bontemps et al. 2012, Huang & Friedl 2014, DeVries et al. 2015, Dutrieux et al. 2015, Schroeder et al. 2017), this data could be more accessible. Storing the data in this type of structure would also make the different update times of each region of the image easier to access. One classification of the study area may have last been updated at several different points, potentially becoming highly varied.

Accuracy could be further increased by separating classification error and true change features. Errors in the classification are often identified as likely change features in later imagery. A reduction in classification error was recorded between the Bare Ground and Less Productive Vegetation classes in the previous chapter.

If a method of separating the true change features from the classification error was developed these errors could be removed from the original classification. The error regions could be assigned their true land cover class in previous classifications, resulting in the classification product becoming more accurate over time.

The change detection approaches can accurately and automatically produce large volumes of labelled spectral data, which could be used to train a deep learning classifier. For example, Convolutional Neural Networks (CNN) have been used to great effect in image recognition and classification research (e.g. pattern recognition Krizhevsky & Hinton 2012, Jia et al. 2014, Simonyan & Zisserman 2015, Szegedy et al. 2015, object and face recognition Girshick et al. 2014, Taigman et al. 2014 and driver-less cars Huval et al. 2015). CNNs have been trained to classify objects in very high-resolution EO data with success (e.g. Hu et al. 2015, Längkvist et al. 2016, Sevo & Avramovic 2016, Liang et al. 2016, Zhang et al. 2016, Cheng et al. 2017, Zhao et al. 2017, Othman et al. 2017, Nogueira et al. 2017). A CNN classifier trained on the Welsh forest and other regions from the classifications generated could be used to classify forests in new imagery.

Chapter 9

Conclusions

Monitoring and collecting data about land cover change is vitally important to understand and manage the impacts of environmental and anthropogenic activities (Kerr & Ostrovsky 2003, Gillanders et al. 2008, Van Lier et al. 2011). Any land cover change can only be quantified by comparing data collected at different times (Singh 1989*a*, *Change detection techniques* 2009). Automating this process increases data volume and land cover monitoring potential. EO satellites provide cost-effective data at a meaningful scale and high temporal resolution. However, there is no universal approach for detecting land cover change, due to the variety of data sources, types, and change detection applications.

The study assessed the applicability of the 'map-to-image' change detection technique as a component of a monitoring system for Wales. The study determined that the approach, developed and applied to mangroves by Thomas et al. 2018, was able to accurately detect coniferous forest cover change, utilising and generating a time-series of accurate multi-class land cover classification maps

and change detection statistics. The 'parametric distribution map-to-image change detection' or histogram change detection approach was successfully applied to a fragmented archive of satellite imagery as part of an automated change detection system. This approach produced an overall accuracy of 93.6% and change and coniferous forest cover figures similar to the NFI.

However, the applicability of this approach is limited by the assumption that the land cover classes have a normal distribution. Three new ways of identifying likely change features were developed, outlier change detection, repeated RF classifiers change detection, and fuzzy-rough logic change detection. The outlier and repeated RF classifier change detection approaches were successfully used to characterise coniferous forest cover change. The approaches produced similar overall accuracies to the original histogram change detection approach of 91.6%, and 89.4% respectfully.

The overall aim of developing these new approaches was to generate a time series of accurate multi-class land cover classification maps and change detection statistics for Wales, UK. The outlier and repeated RF classifier change detection approaches were applied to a full land cover map of 9 classes (change analysed in 7) with partial success. Map products with passable accuracy were generated using the outlier change detection approach. However, the change detection accuracy and class definition requirements of the approaches for the final classification product limit the applicability and usefulness for land managers. Therefore, although the approach can be used to generate a 'living map', the types and drivers of change must be considered along with the final use case. The 'map-to-image' approach should be used when a computationally efficient, robust algorithm is needed to analyse a time series of data where the time period between capture dates varies

greatly or data volume is low. Requiring only a base map, the lower number of operator hours than PV or PCC approaches make it suitable to detect change features in a large number of images.

The study also aimed to identify situations where the approach was appropriate to use, and limitations. The approaches all performed best when detecting large-scale changes in a homogeneous class. As there were no significant differences in the overall accuracy of these approaches when applied to such a binary change problem, in situations where the parametric assumption is met the parametric histogram approach should be used as it requires a reduced compute time and no parameters. However, if the parametric assumption cannot be met a different statistical approach for identifying land cover change objects should be employed. In situations where the percentage change is not highly dynamic and can be estimated outlier change detection should be used, as it requires a vastly reduced compute time compared to repeated RF classifiers. Before being applied to analyse other types of change the causes of error and class confusion should first be considered. The results from the full land cover map indicate that a certain level of class distinctness and changes that do not occur gradually, produce the highest accuracy figures. Further research is needed to determine the types of change most suitable, it may be that binary classification products of these types of changes would perform better.

Further research is needed to improve the accuracies of these approaches, introduce storing of pixel histories and identity error in the classification separately to change features.

Bibliography

Abbes, A. B., Bounouh, O., Farah, I. R. & Jong, R. D. (2018), 'Comparative study of three satellite image time- series decomposition methods for vegetation change detection', *European Journal of Remote Sensing* **51**(1), 607–615.

Agjee, H., Mutanga, O., Peerbhay, K. & Ismail, R. (2018), 'The Impact of Simulated Spectral Noise on Random Forest and Oblique Random Forest Classification Performance', *Journal of Spectroscopy* **2018**, 8316918.

Aguirre-gutiérrez, J., Seijmonsbergen, A. C. & Duivenvoorden, J. F. (2012), 'Optimizing land cover classi fi cation accuracy for change detection , a combined pixel-based and object-based approach in a mountainous area in Mexico', *Applied Geography* **34**, 29–37.

Aide, T. M., Clark, M. L., Grau, H. R., López-Carr, D., Levy, M. A., Redo, D., Bonilla-Moheno, M., Riner, G., Andrade-Núñez, M. J. & Muñiz, M. (2013), 'Deforestation and Reforestation of Latin America and the Caribbean (2001-2010)', *Biotropica* **45**(2), 262–271.

Al-doski, J., B. Mansor, S. & Zulhaidi Mohd Shafri, H. (2013), 'Change Detection Process and Techniques', *Civil and Environmental Research* **3**(10), 37–46.

Allen, T. & Kupfer, J. (2000), 'Application of spherical statistics to change

vector analysis of landsat data: southern appalachian spruce-fir forests.', *Remote Sensing of Environment* **74**(3), 482–493.

An, W., Zongshan, L., Shuai, W., Xing, W., Yihe, L., Guohua, L. & Bojie, F. (2017), 'Exploring the effects of the "Grain for Green" program on the differences in soil water in the semi-arid Loess Plateau of China', *Ecological Engineering* **107**, 144–151.

Apollonio, C., Balacco, G., Novelli, A. & Tarantino, E. (2016), 'Land use change impact on flooding areas: The case study of cervaro basin (italy)', *Sustainibility* **8**(10), 996.

Arthur, D. & Vassilvitskii, S. (2007), K-means++: The advantages of careful seeding, *in* 'Proceedings of the Eighteenth Annual ACM-SIAM Symposium on Discrete Algorithms', SODA '07, Society for Industrial and Applied Mathematics, USA, p. 1027–1035.

Atkinson, P. & Tatnall, A. R. L. (1997), 'Introduction neural networks in remote sensing', *International Journal of Remote Sensing* **18**(4), 699–709.

Ayele, G. T., Tebeje, A. K., Demissie, S. S., Belete, M. A., Jemberrie, M. A., Teshome, W. M., Mengistu, D. T. & Teshale, E. Z. (2018), 'Time series land cover mapping and change detection analysis using geographic information system and remote sensing, Northern Ethiopia', *Air, Soil and Water Research* **11**.

Azzali, S. & Menenti, M. (2000), 'Mapping vegetation-soil-climate complexes in southern Africa using temporal Fourier analysis of NOAA-AVHRR NDVI data', *International Journal of Remote Sensing* **1161**.

Babst, F., Esper, J. & Parlow, E. (2010), 'Landsat TM/ETM+ and tree-ring based assessment of spatiotemporal patterns of the autumnal moth (Epirrita autumnata) in northernmost Fennoscandia', *Remote Sensing of Environment* **114**(3), 637–646.

Bagan, H. & Yamagata, Y. (2014), 'Land-cover change analysis in 50 global cities by using a combination of Landsat data and analysis of grid cells', *Environmental Research Letters* **9**(6), 2000–2010.

Bai, L., Lin, H., Sun, H., Mo, D. & Yan, E. (2012), 'Spectral Unmixing Approach in Remotely Sensed Forest Cover Estimation: A Study of Subtropical Forest in Southeast China', *Physics Procedia* **25**, 1055–1062.

Bansal, R., Gaur, N. & Singh, S. N. (2016), Outlier detection: Applications and techniques in data mining, *in* '2016 6th International Conference - Cloud System and Big Data Engineering (Confluence)', pp. 373–377.

Baumann, M., Ozdogan, M., Kuemmerle, T., Wendland, K. J., Esipova, E. & Radeloff, V. C. (2012), 'Using the Landsat record to detect forest-cover changes during and after the collapse of the Soviet Union in the temperate zone of European Russia', *Remote Sensing of Environment* **124**, 174–184.

Beland, K., Sténs, A., Sandström, C., Johansson, J., Lidskog, R., Ranius, T. & Roberge, J. (2017), 'Forest Policy and Economics The Swedish forestry model : More of everything ?', *Foretry Policy and Economics* **77**, 44–55.

Benedek, C., Shadaydeh, M., Kato, Z., Szirányi, T. & Zerubia, J. (2015), 'Multilayer Markov Random Field models for change detection in optical remote sensing images', *ISPRS Journal of Photogrammetry and Remote Sensing* **107**.

Benfield, S., Guzman, H. & Mair, J. (2005), 'Temporal mangrove dynamics in relation to coastal development in Pacific Panama', *Journal of Environmental Management* **76**(3), 263–276.

Bergen, K. M., Brown, D. G., Rutherford, J. F. & Gustafson, E. J. (2005), 'Change detection with heterogeneous data using ecoregional stratification, statistical summaries and a land allocation algorithm', *Remote Sensing of Environment* **97**(4), 434–446.

Blackstock, T., Burrows, C., Howe, E., Stevens, D. & Stevens, J. (2007), 'Habitat inventory at a regional scale: A comparison of estimates of terrestrial Broad Habitat cover from stratified sample field survey and full census field survey for Wales, UK', *Journal of Environmental Management* **85**(1), 224–231.

Boldt, M., Thiele, A. & Schulz, K. (2012), 'Object-based urban change detection analyzing high resolution optical satellite images', *Proceedings—SPIE the International Society for Optical Engineering: Earth Resources and Environmental Remote Sensing/GIS Applications III* **8538**, 1–9.

Bontemps, S., Bogaert, P., Titeux, N. & Defourny, P. (2008), 'An object-based change detection method accounting for temporal dependences in time series with medium to coarse spatial resolution', *Remote Sensing of Environment* **112**(6), 3181–3191.

Bontemps, S., Langner, A. & Defourny, P. (2012), 'Monitoring forest changes in Borneo on a yearly basis by an object-based change detection algorithm using SPOT-VEGETATION time series', *International Journal of Remote Sensing* **33**(15), 4673–4699.

Borak, J., Lambin, E. & Strahler, A. (2000), 'The use of temporal metrics for land

cover change detection at coarse spatial scales', *International Journal of Remote Sensing* **21**(6-7), 1415–1432.

Boser, B. E., Vapnik, V. N. & Guyon, I. M. (1992), 'Training Algorithm Margin for Optimal Classifiers', *Perception* **5**, 144–152.

Bourgeau-Chavez, L. L., Kasischke, E. S., Brunzell, S., Mudd, J. P. & Tukman, M. (2002), 'Mapping fire scars in global boreal forests using imaging radar data', *International Journal of Remote Sensing* **23**(20), 4211–4234.

Bovolo, F., Marchesi, S. & Bruzzone, L. (2012), 'A framework for automatic and unsupervised detection of multiple changes in Multitemporal Images', *IEEE Transactions on Geoscience and Remote Sensing* **50**(6), 2196–2212.

Brandt, J. P., Flannigan, M. D., Maynard, D. G., Thompson, I. D. & Volney, W. J. A. (2013), 'An introduction to canada's boreal zone: ecosystem processes, health, sustainability, and environmental issues', *Environmental Reviews* **226**, 207–226.

Breiman, L. (2001), 'Random Forests', *Machine Learning* **45**(1), 5–32.

Brocca, L., Melone, F., Moramarco, T., Wagner, W., Naeimi, V., Bartalis, Z. & Hasenauer, S. (2010), 'Improving runoff prediction through the assimilation of the ASCAT soil moisture product', *Hydrology and Earth System Sciences* **14**(10), 1881–1893.

Bruzzone, L., Cossu, R. & Vernazza, G. (2004), 'Detection of land-cover transitions by combining multidate classifiers', *Pattern Recognition Letters* **25**(13), 1491–1500.

Bruzzone, L. & Serpico, S. B. (1997), 'Detection of changes in remotely-sensed

images by the selective use of multi-spectral information', *International Journal of Remote Sensing* **18**(18), 3883–3888.

Bunting, P., Clewley, D., Lucas, R. M. & Gillingham, S. (2014), 'The Remote Sensing and GIS Software Library (RSGISLib)', *Computers and Geosciences* **62**, 216–226.

Bunting, P. & Gillingham, S. (2013), 'The KEA image file format', *Computers and Geosciences* **57**, 54–58.

Bunting, P., Rosenqvist, A., Lucas, R. M., Rebelo, L. M., Hilarides, L., Thomas, N., Hardy, A., Itoh, T., Shimada, M. & Finlayson, C. M. (2018), 'The global mangrove watch - A new 2010 global baseline of mangrove extent', *Remote Sensing* **10**(10).

Cai, S. & Liu, D. (2015), 'Detecting Change Dates from Dense Satellite Time Series Using a Sub-Annual Change Detection Algorithm', *Remote Sensing* **7**, 8705–8727.

Cardille, J. A. & Foley, J. A. (2003), 'Agricultural land-use change in Brazilian Amazônia between 1980 and 1995: Evidence from integrated satellite and census data', *Remote Sensing of Environment* **87**(4), 551–562.

Cardille, J. A. & Fortin, J. A. (2016), 'Bayesian updating of land-cover estimates in a data-rich environment', *Remote Sensing of Environment* **186**, 234–249.

Castellana, L., Addabbo, A. D. & Pasquariello, G. (2007), 'A composed supervised / unsupervised approach to improve change detection from remote sensing', *Pattern Recognition Letters* **28**, 405–413.

Castellana, L., Tarantino, C., Blonda, P. & Pasquariello, G. (2004), Bayesian

approach to land cover change detection using a priori scene description, *in* 'IGARSS 2004. 2004 IEEE International Geoscience and Remote Sensing Symposium', Vol. 2, pp. 1406–1409.

Centre for Ecology and Hydrology (1995), 'UK Land Cover Map 1990'.
URL: *https://www.ceh.ac.uk/services/land-cover-map-1990*

Chadfield, V. & Pautasso, M. (2012), 'Phytophthora ramorum in England and Wales: Which environmental variables predict county disease incidence?', *Forest Pathology* **42**(2), 150–159.

Chang, H., Jiang, X., Sun, Y. & Wang, J. (2001), 'Color image segmentation: Advances and prospects.', *Pattern Recognition* **34**, 2259–2281.

Change detection techniques (2009), *International Journal of Remote Sensing* **25**(October), 2365 – 2401.

Chauhan, P. & Shukla, M. (2015), A Review on Outlier Detection Techniques on Data Stream by Using Different Approaches of K-Means Algorithm, *in* '2015 International Conferecne on Advances in Computer Engineering and Applications (ICACEA)', pp. 580–585.

Chen, G., Hay, G., Carvalho, L. & Wulder, M. (2012), 'Object-based change detection', *International Journal of Remote Sensing* **23**(14), 4434–457.

Chen, J., Chen, X., Cui, X. & Chen, J. (2011), 'Change vector analysis in posterior probability space: A new method for land cover change detection', *IEEE Geoscience and Remote Sensing Letters* **8**(2), 317–321.

Chen, J., Gong, P., He, C., Pu, R., Shi, P., Peng, G., Chunyang, H., Pu, R. & Peijun, S. (2003), 'Land-Use / Land-Cover Change Detection

Using Improved Change-Vector Analysis', *Photogrammetric Engineering Remote Sensing* **69**(4), 369–379.

Chen, Q. & Chen, Y. (2016), 'Multi-Feature Object-Based Change Detection Using Self-Adaptive Weight Change Vector Analysis', *Remote Sensing* **549**(8).

Cheng, G., Han, J. & Lu, Z. (2017), 'Remote sensing image scene classification Benchmark and state of the art', *Proceedings of the IEEE* **105**(10), 1865–1883.

Chunyang, H., Yuanyuan, Z., Jie, T., Peijun, S. & Qingxu, H. (2013), 'Improving change vector analysis by cross-correlogram spectral matching for accurate detection of land-cover conversion', *International Journal of Remote Sensing* **34**(4), 1127–1145.

Clewley, D., Bunting, P., Shepherd, J., Gillingham, S., Flood, N., Dymond, J., Lucas, R., Armston, J. & Moghaddam, M. (2014), 'A python-based open source system for Geographic Object-Based Image Analysis (GEOBIA) utilizing raster attribute tables', *Remote Sensing* **6**(7), 6111–6135.

Cock, M. D., Cornelis, C. & Kerre, E. (2004), Fuzzy Rough Sets : Beyond the Obvious, *in* 'IEEE International Conference on Fuzzy Systems'.

Cohen, B., Maiersperger, K., Gower, S. & T., T. (2003), 'An Improved Strategy for Regression of Biophysical Variables and Landsat ETM+ Data', *Remote Sensing of Environment* **84**, 561.

Cole, B., Smith, G. & Balzter, H. (2018), 'Acceleration and fragmentation of CORINE land cover changes in the United Kingdom from 2006–2012 detected by Copernicus IMAGE2012 satellite data', *International Journal of Applied Earth Observation and Geoinformation* **73**(February), 107–122.

Congalton, R. (2008), *Assessing the Accuracy of Remotely Sensed Data: Principles and Practices*, CRC Press.

Congalton, R. G. (1991), 'A review of assessing the accuracy of classifications of remotely sensed data', *Remote Sensing of Environment* **37**(1), 35–46.

Coppin, P., Jonckheere, I., Nackaerts, K., Muys, B. & Lambin, E. (2004), 'Digital change detection methods in ecosystem monitoring: a review', *International Journal of Remote Sensing* **25**(9), 1565–1596.

Coppin, P. R. & Bauer, M. E. (1996), 'Digital Change Detection in Forest Ecosystems with Remote Sensing Imagery', *Remote Sensing Reviews* **13**(3-4), 207–234.

Darmawan, Y. & Sofan, P. (2012), 'Comparison of The Vegetation Indices to Detect The Tropical Rain Forest Changes using Breaks for Additive Seasonal and Trend (BFAST) Model', *International Journal of Remote Sensing and Earth Sciences* (April 2014).

De Barros Ferraz, S. F., Vettorazzi, C. A., Theobald, D. M. & Ballester, M. V. R. (2005), 'Landscape dynamics of Amazonian deforestation between 1984 and 2002 in central Rondônia, Brazil: Assessment and future scenarios', *Forest Ecology and Management* **204**(1), 67–83.

De Cock, M. D., Cornelis, C. & Kerre, E. E. (2007), 'Fuzzy Rough Sets : The Forgotten Step', *IEEE Transactions on Fuzzy Systems* **15**(1), 121–130.

de Espindola, G. M., de Aguiar, A. P. D., Pebesma, E., Câmara, G. & Fonseca, L. (2012), 'Agricultural land use dynamics in the Brazilian Amazon based on remote sensing and census data', *Applied Geography* **32**(2), 240–252.

Deng, J. S., Wang, K., Deng, Y. H. & Qi, G. J. (2008), 'PCA-based land-use change detection and analysis using multitemporal and multisensor satellite data', *International Journal of Remote Sensing* **29**(16), 4823–4838.

Dennison, P. E., Nagler, P. L., Hultine, K. R., Glenn, E. P. & Ehleringer, J. R. (2009), 'Remote monitoring of tamarisk defoliation and evapotranspiration following saltcedar leaf beetle attack', *Remote Sensing of Environment* **113**(7), 1462–1472.

Desclée, B., Bogaert, P. & Defourny, P. (2006), 'Forest change detection by statistical object-based method', *Remote Sensing of Environment* **102**(1-2), 1–11.

DeVries, B., Verbesselt, J., Kooistra, L. & Herold, M. (2015), 'Robust monitoring of small-scale forest disturbances in a tropical montane forest using Landsat time series', *Remote Sensing of Environment* **161**, 107–121.

Dewan, A. M. & Yamaguchi, Y. (2009), 'Land use and land cover change in Greater Dhaka , Bangladesh : Using remote sensing to promote sustainable urbanization', *Applied Geography* **29**(3), 390–401.

Dey, V., Zhang, Y. & Zhong, M. (2010), 'A Review on Image Segmentation Techniques With a Remote Sensing Perspective', *ISPRS TC VII Symposium – 100 Years ISPRS* **XXXVIII**, 31–42.

Diebel, J., Norda, J. & Kretchmer, O. (2019), 'Average weather in wales'.
URL: *https://weatherspark.com/y/41923/Average-Weather-in-Wales-United-Kingdom-Year-Round*

Dore, A. J., Mousavi-Baygi, M., Smith, R. I., Hall, J., Fowler, D. & Choularton,

T. W. (2006), 'A model of annual orographic precipitation and acid deposition and its application to Snowdonia', *Atmospheric Environment* **40**(18), 3316–3326.

Drake, B. & Jones, G. (2017), 'Public value at risk from Phytophthora ramorum and Phytophthora kernoviae spread in England and Wales', *Journal of Environmental Management* **191**, 136–144.

Dronova, I., Gong, P., Wang, L. & Zhong, L. (2015), 'Mapping dynamic cover types in a large seasonally flooded wetland using extended principal component analysis and object-based classification', *Remote Sensing of Environment* **158**, 193–206.

Du, Y., Teillet, P. M. & Cihlar, J. (2002), 'Radiometric normalization of multitemporal high-resolution satellite images with quality control for land cover change detection', *Remote Sensing of Environment* **82**(1), 123–134.

Dubois, D. & Prade, H. (1990), 'Rough fuzzy sets and fuzzy rough sets', *International Journal of General Systems* **17**, 191–209.

Dubovyk, O. (2017), 'The role of Remote Sensing in land degradation assessments: opportunities and challenges', *European Journal of Remote Sensing* **50**(1), 601–613.

Dutrieux, L. P., Verbesselt, J., Kooistra, L. & Herold, M. (2015), 'Monitoring forest cover loss using multiple data streams, a case study of a tropical dry forest in Bolivia', *ISPRS Journal of Photogrammetry and Remote Sensing* **107**, 112–125.

Duveiller, G., Caporaso, L., Abad-Viñas, R., Perugini, L., Grassi, G., Arneth, A. & Cescatti, A. (2020), 'Local biophysical effects of land use and land cover change:

towards an assessment tool for policy makers', *Land Use Policy* **91**(November 2019), 104382.

Duveiller, G., Defourny, P., Desclée, B. & Mayaux, P. (2008), 'Deforestation in Central Africa: Estimates at regional, national and landscape levels by advanced processing of systematically-distributed Landsat extracts', *Remote Sensing of Environment* **112**(5), 1969–1981.

Dymond, J. R., Shepherd, J. D., Newsome, P. F., Gapare, N., Burgess, D. W. & Watt, P. (2012), 'Remote sensing of land-use change for Kyoto Protocol reporting: The New Zealand case', *Environmental Science and Policy* **16**(2008), 1–8.

Eastman, J. R., Sangermano, F., Ghimire, B., Zhu, H., Chen, H., Neeti, N., Cai, Y., Machado, E. A. & Crema, S. C. (2009), 'Seasonal trend analysis of image time series', *International Journal of Remote Sensing* **30**(10), 2721–2726.

Eckert, S., Hüsler, F., Liniger, H. & Hodel, E. (2015), 'Trend analysis of MODIS NDVI time series for detecting land degradation and regeneration in Mongolia', *Journal of Arid Environments* **113**, 16–28.

Eklundh, L., Johansson, T. & Solberg, S. (2009), 'Mapping insect defoliation in Scots pine with MODIS time-series data', *Remote Sensing of Environment* **113**(7), 1566–1573.

Epting, J., Verbyla, D. & Sorbel, B. (2005), 'Evaluation of remotely sensed indices for assessing burn severity in interior Alaska using Landsat TM and ETM+', *Remote Sensing of Environment* **96**(3-4), 328–339.

Fan, F. (2008), 'Digital Change Detection by Post-Classification Comparison of

RS Data in Land Use of Guangzhou', *Journal of Computational Information Systems* **2**, 1–6.

Felzenszwalb, P. F. & Huttenlocher, D. P. (2004), 'Efficient Graph-Based Image Segmentation', *International Journal of Computer Vision* **59**(2), 167–181.

Feng, X., Li, J., Cheng, W., Fu, B., Wang, Y., Lü, Y. & Shao, M. (2017), 'Evaluation of AMSR-E retrieval by detecting soil moisture decrease following massive dryland re-vegetation in the Loess Plateau, China', *Remote Sensing of Environment* **196**, 253–264.

Fensham, R. J. & Fairfax, R. J. (2003), 'A land management history for central Queensland, Australia as determined from land-holder questionnaire and aerial photography', *Journal of Environmental Management* **68**(4), 409–420.

Fernandes, M. R., Aguiar, F. C., Ferreira, M. T. & Pereira, J. M. C. (2012), 'Spectral separability of riparian forests from small and medium-sized rivers across a latitudinal gradient using multispectral imagery', *International Journal of Remote Sensing* **34**(7), 2375–2401.

Fix, E. & Hodges, J. L. (1989), 'Discriminatory analysis. nonparametric discrimination: Consistency properties', *International Statistical Review* **57**(3), 238–247.

Foody, G. M. (2002), 'Status of land cover classification accuracy assessment', *Remote Sensing of Environment* **80**(1), 185–201.

Foody, G. M. (2009), Correcting estimates of land cover change and change detection accuracy for error in ground reference data, *in* 'International Geoscience and Remote Sensing Symposium (IGARSS)', Vol. 4, pp. 153–156.

Forest Research (2021), 'About the NFI'.

URL: *https://www.forestresearch.gov.uk/tools-and-resources/national-forest-inventory/about-the-nfi/*

Forestry Commission (2002), *National Inventory of Woodland and Trees*.

Forestry Commission (2015), 'Forestry Statistics 2015 - Woodland Areas and Planting'.
https://www.forestry.gov.uk/website/forstats2015.nsf/lucontents/0f1ad3c3d237a3df80257a7f00331506.

Forestry Commission (2017*a*), 'Forestry Statistics 2017'.
https://www.forestry.gov.uk/website/forstats2017.nsf/LUContentsTop?openview{&}RestrictToCategory=1.

Forestry Commission (2017*b*), 'National Forest Inventory 2017'.

URL: *http://data-forestry.opendata.arcgis.com/search?tags=Wales*

Freedman, D. & Diaconis, P. (1981), 'On the histogram as a densitiy estimator: L2 theory', *Probab. Theory Relat.* **57**, 453–476.

Frohn, R. C. & Hao, Y. (2006), 'Landscape metric performance in analyzing two decades of deforestation in the Amazon Basin of Rondonia, Brazil', *Remote Sensing of Environment* **100**(2), 237–251.

Fu, K. & Mui, J. (1981), 'A Survey on Image Segmentation Techniques', *Pattern Recognition* **13**, 3–16.

Fuchs, R., Schulp, C. J. E., Hengeveld, G. M. & Peter, H. (2016), 'Assessing the influence of historic net and gross land changes on the carbon fluxes of Europe', *Global Change Biology* **22**, 2526–2539.

Fuller, R. M., Smith, G. M., Sanderson, J. M., Hill, R. A., Thomson, A. G., Cox, R., Brown, N. J., Clarke, R. T., Rothery, P. & Gerard, F. F. (2002), Land Cover Map 2000 Final Report, Technical report, Centre for Ecology and Hydrology.

Gavade, A. B. & Rajpurohit, V. S. (2019), 'Systematic analysis of satellite image-based land cover classification techniques: literature review and challenges', *International Journal of Computers and Applications* **0**(0), 1–10.

Geurts, P., Ernst, D. & Wehenkel, L. (2006), 'Extremely randomized trees', *Machine Learning* **63**(1), 3–42.

Ghamisi, P. (2011), 'A Novel Method for Segmentation of Remote Sensing Images based on Hybrid GAPSO', *International Journal of Computer Applications* **29**(2), 7–14.

Gillanders, S. N., Coops, N. C., Wulder, M. A., Gergel, S. E. & Nelson, T. (2008), 'Multitemporal remote sensing of landscape dynamics and pattern change: describing natural and anthropogenic trends', *Progress in Physical Geography* **32**(5), 499–524.

Girshick, R., Donahue, J., Darrell, T. & Malik, J. (2014), 'Rich feature hierarchies for accurate object detection and semantic segmentation', *Proceedings of the IEEE Computer Society Conference on Computer Vision and Pattern Recognition* pp. 580–587.

Gislason, P. O., Benediktsson, J. A. & Sveinsson, J. R. (2006), 'Random forests for land cover classification', *Pattern Recognition Letters* **27**(4), 294–300.

Griffiths, P., Kuemmerle, T., Kennedy, R. E., Abrudan, I. V., Knorn, J. & Hostert, P. (2012), 'Using annual time-series of Landsat images to assess the effects of

forest restitution in post-socialist Romania', *Remote Sensing of Environment* **118**, 199–214.

Grogan, K., Pflugmacher, D., Hostert, P. & Verbesselt, J. (2016), 'Mapping Clearances in Tropical Dry Forests Using Breakpoints, Trend, and Seasonal Components from MODIS Time Series: Does Forest Type Matter?', *Remote Sensing* **8**(8), 657.

Guo, M., Li, J., Sheng, C., Xu, J. & Wu, L. (2017), 'A review of wetland remote sensing', *Sensors* **17**(4), 1–36.

Hadi, Korhonen, L., Hovi, A., Rönnholm, P. & Rautiainen, M. (2016), 'The accuracy of large-area forest canopy cover estimation using Landsat in boreal region', *International Journal of Applied Earth Observations and Geoinformation* **53**, 118–127.

Hagberg, A. A., Schult, D. A. & Swart, P. J. (2008), 'Exploring network structure, dynamics, and function using NetworkX', *7th Python in Science Conference (SciPy 2008)* (SciPy), 11–15.

Hamunyela, E., Verbesselt, J., de Bruin, S. & Herold, M. (2016), 'Monitoring deforestation at sub-annual scales as extreme events in landsat data cubes', *Remote Sensing* **8**(8), 126–138.

Hansen, M. C., Egorov, A., Roy, D. P., Potapov, P., Ju, J., Turubanova, S., Kommareddy, I. & Loveland, T. R. (2011), 'Continuous fields of land cover for the conterminous United States using Landsat data: First results from the Web-Enabled Landsat Data (WELD) project', *Remote Sensing Letters* **2**(4), 279–288.

Hansen, M. C. & Loveland, T. R. (2012), 'A review of large area monitoring of land

cover change using Landsat data', *Remote Sensing of Environment* **122**, 66–74.

Hansen, M. C., Potapov, R., Moore, M., Hancher, S. A., Turubanova, A., Tyukavina, D., Thau, S. V., Stehman, S. J., Goetz, T. R., Loveland, A., Kommareddy, A., Egorov, L., Chini, Justice, C. O. & Townshend, J. R. G. (2013), 'High-Resolution Global Maps of 21st-Century Forest Cover Change', *Science* **342**(15 November), 850–53.

Hansen, M. C., Townshend, J. R., Marufu, L., Sohlberg, R. & DeFries, R. S. (2002), 'Development of a MODIS tree cover validation data set for Western Province, Zambia', *Remote Sensing of Environment* **83**(1-2), 320–335.

Hansen, M., Potapov, P., Margono, B., Stehman, S., Turubanova, S. & Tyukavina, a. (2014), 'Response to comment on "High-resolution global maps of 21st-century forest cover change".', *Science* **344**(6187), 981.

He, C., Wei, A., Shi, P., Zhang, Q. & Zhao, Y. (2011), 'Detecting land-use / land-cover change in rural – urban fringe areas using extended change-vector analysis', *International Journal of Applied Earth Observations and Geoinformation* **13**(4), 572–585.

Healey, S. P., Cohen, W. B., Zhiqiang, Y. & Krankina, O. N. (2005), 'Comparison of Tasseled Cap-based Landsat data structures for use in forest disturbance detection', *Remote Sensing of Environment* **97**(3), 301–310.

Healey, S. P., Yang, Z. Q., Cohen, W. B. & Pierce, D. J. (2006), 'Application of two regression-based methods to estimate the effects of partial harvest on forest structure using Landsat data', *Remote Sensing of Environment* **101**(1), 115–126.

Henits, L., Jürgens, C. & Mucsi, L. (2016), 'Seasonal multitemporal land-

cover classification and change detection analysis of Bochum, Germany, using multitemporal Landsat TM data', *International Journal of Remote Sensing* **1161**(August), 1–16.

Hermosilla, T., Wulder, M. A., White, J. C., Coops, N. C. & Hobart, G. W. (2015), 'Regional detection, characterization, and attribution of annual forest change from 1984 to 2012 using Landsat-derived time-series metrics', *Remote Sensing of Environment* **170**, 121–132.

Hermosilla, T., Wulder, M. A., White, J. C., Coops, N. C. & Hobart, G. W. (2018), 'Disturbance-Informed Annual Land Cover Classification Maps of Canada's Forested Ecosystems for a 29-Year Landsat Time Series', *Canadian Journal of Remote Sensing* **44**(1), 67–87.

Hester, D. B., Nelson, S. A. C., Cakir, H. I., Khorram, S. & Cheshire, H. (2010), 'High-resolution land cover change detection based on fuzzy uncertainty analysis and change reasoning', *International Journal of Remote Sensing* **31**(2), 455 – 475.

Hill, F., Browning, K. & Bader, M. (1981), 'Radar and raingauge observations of orographic rain over south Wales.', *Quarterly Journal of the Royal Meteorological Society* **107**(453), 643–670.

Hird, J. N., Castilla, G., McDermid, G. J. & Bueno, I. T. (2016), 'A simple transformation for visualizing non-seasonal landscape change from dense time series of satellite data', *IEEE Journal of Selected Topics in Applied Earth Observations and Remote Sensing* **9**(8), 3372–3383.

Hoffmann, B. (1975), *About Vectors*, Dover Publications Inc, New York.

Hollmann, R., Merchant, C. J., Saunders, R., Downy, C., Buchwitz, M., Cazenave, A., Chuvieco, E., Defourny, P., De Leeuw, G., Forsberg, R., Holzer-Popp, T., Paul, F., Sandven, S., Sathyendranath, S., Van Roozendael, M. & Wagner, W. (2013), 'The ESA climate change initiative: Satellite data records for essential climate variables', *Bulletin of the American Meteorological Society* **94**(10), 1541–1552.

Hongquan, X., Yanyan, Z. & Xia, L. (2011), Land Use/Cover Change Study of Lianyungang Coastal Zone Based on Remote Sensing, *in* 'Geoinformatics, 2011 19th International Conference', IEEE, pp. 1–5.

Houghton, R. A. (1994), 'The Worldwide Extent of Land-Use Change', *BioScience* **44**(5), 305–313.

Houze, R. A. (2012), 'Orographic effects on precipitating clouds', *Reviews of Geophysics* **50**(1), 1–47.

Hu, F., Xia, G. S., Hu, J. & Zhang, L. (2015), 'Transferring deep convolutional neural networks for the scene classification of high-resolution remote sensing imagery', *Remote Sensing* **7**(11), 14680–14707.

Huang, C., Davis, L. S. & Townshend, J. R. G. (2002), 'An assessment of support vector machines for land cover classification', *International Journal of Remote Sensing* **23**(4), 725–749.

Huang, J., Wan, Y. & Shen, S. (2009), 'An object-based approach for forest-cover change detection using multi-temporal high-resolution remote sensing data', *Proceedings - 2009 International Conference on Environmental Science and Information Application Technology, ESIAT 2009* **1**, 481–484.

Huang, J., Zhu, Q., Yang, L., Cheng, D. D. & Wu, Q. (2017), 'A novel outlier cluster detection algorithm without top-n parameter', *Knowledge-Based Systems* **121**, 32–40.

Huang, X. & Friedl, M. A. (2014), 'Distance metric-based forest cover change detection using MODIS time series', *International Journal of Applied Earth Observation and Geoinformation* **29**(1), 78–92.

Hussain, M., Chen, D., Cheng, A., Wei, H. & Stanley, D. (2013), 'Change detection from remotely sensed images: From pixel-based to object-based approaches', *ISPRS Journal of Photogrammetry and Remote Sensing* **80**, 91–106.

Huval, B., Wang, T., Tandon, S., Kiske, J., Song, W., Pazhayampallil, J., Andriluka, M., Rajpurkar, P., Migimatsu, T., Cheng-Yue, R., Mujica, F., Coates, A. & Ng, A. Y. (2015), 'An Empirical Evaluation of Deep Learning on Highway Driving', *Robotics* pp. 1–7.

Hyde, H. (1977), *Welsh Timber Trees: Native and Introduced*, 4th edn, Qualitex, Cardiff.

Ishtiaque, A., Myint, S. W. & Wang, C. (2016), 'Examining the ecosystem health and sustainability of the world's largest mangrove forest using multi-temporal MODIS products', *Science of the Total Environment* **569-570**, 1241–1254.

Jacquin, A., Sheeren, D. & Lacombe, J.-p. (2010), 'Vegetation cover degradation assessment in Madagascar savanna based on trend analysis of MODIS NDVI time series', *International Journal of Applied Earth Observation and Geoinformation* **125**, 3–10.

Japan Aerospace Exploration Agency (2019), 'Dataset Distribution Services'.

URL: *https://www.eorc.jaxa.jp/en/distribution/standard_dataset/*

Jensen, R. & Cornelis, C. (2011), 'Fuzzy-rough nearest neighbour classification and prediction', *Theoretical Computer Science* **412**(42), 5871–5884.
URL: *http://dx.doi.org/10.1016/j.tcs.2011.05.040*

Jensen, R. & Shen, Q. (2009), 'New Approaches to Fuzzy-Rough Feature Selection', *IEEE Transactions on Fuzzy Systems* **17**(4), 824–838.

Jia, Y., Shelhamer, E., Donahue, J., Karayev, S., Long, J., Girshick, R., Guadarrama, S. & Darrell, T. (2014), 'Caffe: Convolutional Architecture for Fast Feature Embedding', *Computer Vision and Pattern Recognition* .

Job, D. A. & Taylor, J. A. (1978), 'The Production, Utilization and Management of Upland Grazings on Plynlimon, Wales', *Journal of Biogeography* **5**(2), 173.

Johnson, T., Kwok, I. & Ng, R. (1998), 'Fast computation of 2-dimensional depth contours', *American Association for Artifical Intelligence* (604), 224–228.

Jolliffe, I. & Cadmia, J. (2016), 'Principal componenet analysis: A review and recent directions', *Philosophical Transactions of the Royal Society A: Mathematical, Physical and Engineering Sciences* **374**.

Jones, K., Lanthier, Y., van der Voet, P., van Valkengoed, E., Taylor, D. & Fernández-Prieto, D. (2009), 'Monitoring and assessment of wetlands using Earth Observation: The GlobWetland project', *Journal of Environmental Management* **90**(7), 2154–2169.

Jong, R. D., Bruin, S. D., Schaepman, M. & Dent, D. (2017), 'Quantitative mapping of global land degradation using Earth observations', *International Journal of Remote Sensing* **32**(21), 6823–6853.

Joyce, J. (2019), Bayes' Theorem, *in* E. N. Zalta, ed., 'The Stanford Encyclopedia of Philosophy', spring 2019 edn, Metaphysics Research Lab, Stanford University.

Ju, J. & Roy, D. P. (2008), 'The availability of cloud-free Landsat ETM+ data over the conterminous United States and globally', *Remote Sensing of Environment* **112**(3), 1196–1211.

Kamlun, K. U., Bürger Arndt, R. & Phua, M. H. (2016), 'Monitoring deforestation in Malaysia between 1985 and 2013: Insight from South-Western Sabah and its protected peat swamp area', *Land Use Policy* **57**, 418–430.

Karlson, M., Ostwald, M., Reese, H., Sanou, J., Tankoano, B. & Mattsson, E. (2015), 'Mapping tree canopy cover and aboveground biomass in Sudano-Sahelian woodlands using Landsat 8 and random forest', *Remote Sensing* **7**(8), 10017–10041.

Kauth, R. J. & Thomas, G. S. (1976), 'The tasselled cap - A graphic description of the spectral-temporal development of agricultural crops as seen by Landsat', *Proceedings of the Symposium on Machine Processing of Remotely Sensed Data, West Lafayette, Indiana, U.S.A, 29 June-1 July 1976* pp. 41–51.

Kavzoglu, T. & Mather, P. M. (2000), 'The Use of Feature Selection Techniques in the Context of Artificial Neural Networks', *Proceedings Annual Conference of the Remote Sensing Society* (September), 12–14.

Kennedy, R. E., Yang, Z. & Cohen, W. B. (2010), 'Remote Sensing of Environment Detecting trends in forest disturbance and recovery using yearly Landsat time series : 1 . LandTrendr — Temporal segmentation algorithms', *Remote Sensing of Environment* **114**(12), 2897–2910.

Kerr, J. T. & Ostrovsky, M. (2003), 'From space to species: Ecological applications for remote sensing', *Trends in Ecology and Evolution* **18**(6), 299–305.

Kesgin, B. & Nurlu, E. (2009), 'Land cover changes on the coastal zone of Candarli Bay, Turkey using remotely sensed data', *Environmental Monitoring and Assessment* **157**(1), 89–96.

Keskin, S. (2006), 'Comparison of several univariate normality tests regarding Type I error rate and power of the test in simulation based on small samples.', *Journal of Applied Science Research* **2**(5), 296–300.

Kim, S., Liu, Y. Y., Johnson, F. M., Parinussa, R. M. & Sharma, A. (2015), 'A global comparison of alternate AMSR2 soil moisture products: Why do they differ?', *Remote Sensing of Environment* **161**, 43–62.

Kintz, D. B., Young, K. R. & Crews-meyer, K. A. (2006), 'Implications of Land Use / Land Cover Change in the Buffer Zone of a National Park in the Tropical Andes', *Environmental Management* **38**(2), 238–252.

Kittler, J., Hater, M. & Duin, R. P. W. (1996), 'Combining classifiers', *Proceedings - International Conference on Pattern Recognition* **2**(3), 897–901.

Kong, Y.-l., Meng, Y., Li, W., Yue, A.-z. & Yuan, Y. (2015), 'Satellite Image Time Series Decomposition Based on EEMD', *Remote Sensing* **7**, 15583–15604.

Kozak, J., Estreguil, C. & Vogt, P. (2007), 'Forest cover and pattern changes in the Carpathians over the last decades', *European Journal of Forest Research* **126**(1), 77–90.

Krislock, N. & Wolkowicz, H. (2012), Euclidean Distance Matrices and

Applications, *in* 'Handbook on Semidefiniate, Conic and polynominal Optimization', Springer, Boston, MA, pp. 879–914.

Krizhevsky, A. & Hinton, G. E. (2012), 'ImageNet Classification with Deep Convolutional Neural Networks', *Neural Information Processing Systems* pp. 1–9.

Lambin, E. F. & Ehrlich, D. (1997), 'Land-cover changes in Sub-Saharan Africa (1982-1991): Application of a change index based on remotely sensed surface temperature and vegetation indices at a continental scale', *Remote Sensing of Environment* **61**(2), 181–200.

Land Monitoring Service (2021), 'CORINE Land Cover'.
URL: *https://land.copernicus.eu/pan-european/corine-land-cover*

Längkvist, M., Kiselev, A., Alirezaie, M. & Loutfi, A. (2016), 'Classification and segmentation of satellite orthoimagery using convolutional neural networks', *Remote Sensing* **8**(4).

Li, Q., Gong, L. & Beijing, J. Z. (2018), 'Earthquake-Induced Building Recognition Using Correlation Change Detection of Texture Features Based on SAR Data', *Geodetski List* **72**(2), 93–112.

Liang, Y., Monteiro, S. & Saber, E. (2016), Transfer Learning for High Resolution Aerial Image Classification, *in* 'IEEE Applied Imagery Pattern Recognition Workshop (AIPR)', IEEE.

Liberti, L. & Lavor, C. (2010), *Euclidean Distance Geometry: An Introduction*, Springer.

Lillesand, E., Kiefer, R. & Chapman, J. (2015), *Remote Sensing and Image Interpretation*, 7 edn, John Wiley & Sons.

Lindquist, E. J., Hansen, M. C., Roy, D. P. & Justice, C. O. (2008), 'The suitability of decadal image data sets for mapping tropical forest cover change in the Democratic Republic of Congo: Implications for the global land survey', *International Journal of Remote Sensing* **29**(24), 7269–7275.

Liu, D. & Cai, S. (2012), 'A Spatial-Temporal Modeling Approach to Reconstructing Land-Cover Change Trajectories from Multi-temporal Satellite Imagery', *Annals of the Association of American Geographers* **102**(6).

Liu, D., Song, K., Townshend, J. R. G. & Gong, P. (2008), 'Using local transition probability models in Markov random fields for forest change detection', *Remote Sensing of Environment* **112**(5), 2222–2231.

Liu, H. & Zhou, Q. (2004), 'Accuracy analysis of remote sensing change detection by rule-based rationality evaluation with post-classification comparison', *International Journal of Remote Sensing* **1161**(May), 1037–1050.

Liu, T. & Yang, X. (2015), 'Monitoring land changes in an urban area using satellite imagery , GIS and landscape metrics', *Applied Geography* **56**, 42–54.

Lo, C. P. & Shipman, R. L. (1990), 'A GIS approach to land-use change dynamics detection', *Photogrammetric Engineering & Remote Sensing* **56**(11), 1483–1491.

Lu, M., Pebesma, E., Sanchez, A. & Verbesselt, J. (2015), 'Spatio-temporal change detection from multidimensional arrays: Detecting deforestation from MODIS time series', *ISPRS Journal of Photogrammetry and Remote Sensing* **117**, 227–236.

Lucas, R. M., Clewley, D., Accad, A., Butler, D., Armston, J., Bowen, M., Bunting, P., Carreiras, J., Dwyer, J., Eyre, T., Kelly, A., McAlpine, C., Pollock, S. & Seabrook, L. (2014), 'Mapping forest growth and degradation stage in the Brigalow Belt Bioregion of Australia through integration of ALOS PALSAR and Landsat-derived foliage projective cover data', *Remote Sensing of Environment* **155**, 42–57.

Lucas, R., Medcalf, K., Brown, A., Bunting, P., Breyer, J., Clewley, D., Keyworth, S. & Blackmore, P. (2011), 'Updating the Phase 1 habitat map of Wales, UK, using satellite sensor data', *ISPRS Journal of Photogrammetry and Remote Sensing* **66**(1), 81–102.

Lück, W. & van Niekerk, A. (2016), 'Evaluation of a rule-based compositing technique for Landsat-5 TM and Landsat-7 ETM+ images', *International Journal of Applied Earth Observation and Geoinformation* **47**, 1–14.

Luo, H., Liu, C., Wu, C. & Guo, X. (2018), 'Urban change detection based on Dempster-Shafer theory for multitemporal very high-resolution imagery', *Remote Sensing* **10**(7), 20–22.

Lupo, F., Reginster, I. & Lambin, E. F. (2001), 'Monitoring land-cover changes in West Africa with SPOT Vegetation : Impact of natural disasters in', *International Journal of Remote Sensing* **22**(13), 2633–2639.

Lutz, D. A. & Washington-Allen, R. A. (2008), 'Remote Sensing of Boreal Forest Biophysical and Inventory Parameters: A Review', *Canadian Journal of Remote Sensing* **34**, S286–S313.

Lv, Z., Liu, T., Zhang, P., Benediktsson, J. A. & Chen, Y. (2018), 'Land cover

change detection based on adaptive contextual information using bi-temporal remote sensing images', *Remote Sensing* **10**(6).

Lv, Z., Zhang, X. & Benediktsson, J. A. (2017), 'Developing a general post-classification framework for land-cover mapping improvement using high-spatial-resolution remote sensing imagery', *Remote Sensing Letters* **8**(7), 607–616.

Mabaso, S., Bunting, P., Hardy, A., Brown, S. & Lucas, R. (2016), Remote Sensing Data for Mapping and Monitoring African Savanna Woodlands, PhD thesis.

Macleod, R. D. & Congalton, R. G. (1998), 'A quantitative comparison of change-detection algorithms for monitoring eelgrass from remotely sensed data', *Photogrammetric Engineering and Remote Sensing* **64**(3), 207–216.

Macqueen, J. (1967), Some methods for classification and analysis of multivariate observations, *in* 'In 5-th Berkeley Symposium on Mathematical Statistics and Probability', pp. 281–297.

Malila, W. A. (1980), 'Change vector analysis: An approach for detecting forest changes with Landsat', *LARS Symposia* pp. 326–335.

Mancino, G., Nolè, A., Ripullone, F. & Ferrara, A. (2014), 'Landsat TM imagery and NDVI differencing to detect vegetation change: Assessing natural forest expansion in Basilicata, southern Italy', *IForest* **7**(2), 75–84.

Mandhare, H. & Idate, S. (2017), Distance Based Outlier Detection and Density Based Outlier Detection Techniques, *in* 'International Conference on Intelligent Computing and Control Systems', pp. 931–935.

Mariwah, S., Nana, K. & Amenyo-xa, M. S. (2017), 'Urban land use / land cover

changes in the Tema metropolitan area (1990 – 2010)', *GeoJournal* **82**(2), 247–258.

Marquardt, K., Pain, A., Bartholdson, Ö. & Rengifo, L. R. (2019), 'Forest Dynamics in the Peruvian Amazon: Understanding Processes of Change', *Small-scale Forestry* **18**(1), 81–104.

Martínez, B. & Gilabert, M. A. (2009), 'Remote Sensing of Environment Vegetation dynamics from NDVI time series analysis using the wavelet transform', *Remote Sensing of Environment* **113**(9), 1823–1842.

Masek, J. G., Hayes, D. J., Joseph Hughes, M., Healey, S. P. & Turner, D. P. (2015), 'The role of remote sensing in process-scaling studies of managed forest ecosystems', *Forest Ecology and Management* **355**, 109–123.

Masek, J. G., Huang, C., Wolfe, R., Cohen, W., Hall, F., Kutler, J. & Nelson, P. (2008), 'North American forest disturbance mapped from a decadal Landsat record', *Remote Sensing of Environment* **112**(6), 2914–2926.

Mason, W., Kerr, G., Simpson, J. & Britain, G. (1999), 'What is continuous cover forestry?', *Forestry Commission Information Note* pp. 1–8.

Mayes, J. (2014), 'Regional weather and climates of the British Isles - Part 5: Wales', *Weather* **68**(9), 227–232.

McDermid, G., Linke, J., Pape, A., Laskin, D., McLane, A. & Franklin, S. (2008), 'Object-based approaches to change analysis and thematic map update: Challenges and limitations', *Canadian Journal of Remote Sensing* **34**(5), 462–466.

McLachlan, G. (1989), 'Mahalanobis distance', *Reason* (4), 20–26.

Mekasha, A., Gerard, B., Tesfaye, K., Nigatu, L. & Duncan, A. J. (2014), 'Inter-connection between land use / land cover change and herders '/ farmers ' livestock feed resource management strategies : a case study from three Ethiopian eco-environments', *Agriculture, Ecosystems and Environment* **188**, 150–162.

Mendes, M. & Pala, A. (2003), 'Type I Error Rate and Power of Three Normality Tests', *Pakistan Journal of Information and Technology* **2**(2), 135–139.

MET Office (2015), 'Wales: climate'.
https://www.metoffice.gov.uk/binaries/content/assets/metofficegovuk/pdf/weather/learn-about/uk-past-events/regional-climates/wales{_}-climate---met-office.pdf.

Met Office (2016), 'Wales: climate'.
URL: *https://www.metoffice.gov.uk/climate/uk/regional-climates/wl https://www.metoffice.gov.uk/climate/uk/regional-climates/wl#rainfall*

Metternicht, G., Zinck, J. A., Blanco, P. D. & del Valle, H. F. (2010), 'Remote Sensing of Land Degradation: Experiences from Latin America and the Caribbean', *Journal of Environmental Quality* **39**(1), 42–61.

Meyer, W. & Turner, B. (1992), 'Human population growth and land use/land cover change', *Annual Review of Ecology and Systematics* **21**(1), 39–61.

Miralles, D. G., Holmes, T. R., De Jeu, R. A., Gash, J. H., Meesters, A. G. & Dolman, A. J. (2011), 'Global land-surface evaporation estimated from satellite-based observations', *Hydrology and Earth System Sciences* **15**(2), 453–469.

Morton, D., Rowland, C., Wood, C., Meek, L., Marston, C., Smith, G.,

Wadsworth, R. & Simpson, I. (2011), Countryside Survey: Final Report for LCM2007 – the new UK Land Cover Map, Technical report, Centre for Ecology and Hydrology.

Myneni, R., Hall, F., Sellers, P. & Marshak, A. (1995), 'The Interpretation of Spectral Vegetation Indexes', *IEEE Transactions on Geoscience and Remote Sensing* **33**(2), 481–486.

Nackaerts, K., Vaesen, K., Muys, B. & Coppin, P. (2005), 'Comparative performance of a modified change vector analysis in forest change detection', *International Journal of Remote Sensing* pp. 839–852.

NASA (2019), 'Data Products'.
URL: *https://smap.jpl.nasa.gov/data/*

Natural Resources Wales (2017*a*), 'Phytophthora ramorum (larch tree disease)'.
URL: *https://naturalresources.wales/guidance-and-advice/environmental-topics/woodland-management/tree-health-and-biosecurity/phytophthora-ramorum/?lang=en*

Natural Resources Wales (2017*b*), 'Statutory Plant Health Notice'.
URL: *https://naturalresources.wales/media/680531/2-sphn-faq-english.pdf*

Niu, Z., Shi, S., Sun, J. & He, X. (2011), A Survey of Outlier Detection Methodologies and Their Applications, *in* 'Artifical Intellitgence and Computational Intelligence Pt. 1', pp. 380–387.

Njoku, E. & Entekhabi, D. (1996), 'Passive microwave remote sensing of soil moisture', *Journal of Hydrology* **184**, 101–129.

Nogueira, K., Penatti, O. A. & dos Santos, J. A. (2017), 'Towards better exploiting

convolutional neural networks for remote sensing scene classification', *Pattern Recognition* **61**, 539–556.

Nori, W., Sulieman, H. & Niemeyer, I. (2009), 'Detection of land cover changes in El Rawashda forest, Sudan : A systematic comparison', *Geoscience and Remote Sensing Symposium, 2009 IEEE International, IGARSS 2009* (March).

NRW (2021), 'NRW Woodland sub-compartment data'.
https://lle.gov.wales/catalogue/item/NRWWoodlandSubCompartmentData/?lang=en.

Olofsson, P., Foody, G. M., Herold, M., Stehman, S. V., Woodcock, C. E. & Wulder, M. A. (2014), 'Good practices for estimating area and assessing accuracy of land change', *Remote Sensing of Environment* **148**, 42–57.

Olsson, P. O., Lindström, J. & Eklundh, L. (2016), 'Near real-time monitoring of insect induced defoliation in subalpine birch forests with MODIS derived NDVI', *Remote Sensing of Environment* **181**, 42–53.

Osmar, A., Renato, C., Guimarães, F., Gillespie, A., Silva, N. & Gomes Roberto, A. (2011), 'A new approach to change vector analysis using distance and similarity measures', *Remote Sensing* **3**, 2473–2493.

Othman, E., Bazi, Y., Melgani, F., Alhichri, H., Alajlan, N. & Zuair, M. (2017), 'Domain Adaptation Network for Cross-Scene Classification', *IEEE Transactions on Geoscience and Remote Sensing* **55**(8), 4441–4456.

Padma, S. & Sanjeevi, S. (2014), 'Jeffries Matusita based mixed-measure for improved spectralmatching in hyperspectral image analysis', *International Journal of Applied Earth Observation and Geoinformation* **32**(1), 138–151.

Pal, N. & Pal, S. R. (1993), 'A review on image segmentation techniquespdf', *Pattern Recognition* **26**, 1277–1294.

Parry, M. L., Hossell, J. E., Jones, P. J., Rehman, T., Tranter, R. B., Marsh, J. S., Rosenzweig, C., Fischer, G., Carson, I. G. & Bunce, R. G. (1996), 'Integrating global and regional analyses of the effects of climate change: A case study of land use in england and wales', *Climatic Change* **32**(2), 185–198.

Pawlak, Z. (1982), 'Rough Sets', *International Journal of Computer and Information Sciences* **11**(5), 341–356.

Pedregosa, G., Varoquaux, G., Gramfort, A., Michel, V., Thirion, B., Grisel, O., Blondel, M., Prettenhofer, P., Weiss, R., Dubourg, V., Vanderplas, J., Passos, A., Cournapeau, D., Brucher, M., Perrot, M. & Duchesnay, E. (2011), 'Scikit-learn: Machine Learning in Python', *Journal of Machine Learning Research* **12**, 2825–2830.

Phiri, D. & Morgenroth, J. (2017), 'Developments in Landsat land cover classification methods: A review', *Remote Sensing* **9**(9).

Pontius, R. G. & Millones, M. (2011), 'Death to Kappa : birth of quantity disagreement and allocation disagreement for accuracy assessment', *International Journal of Remote Sensing* **1161**.

Potapov, P., Siddiqui, B. N., Iqbal, Z., Aziz, T., Zzaman, B., Islam, A., Pickens, A., Talero, Y., Tyukavina, A., Turubanova, S. & Hansen, M. C. (2017), 'Comprehensive monitoring of Bangladesh tree cover inside and outside of forests, 2000-2014', *Environmental Research Letters* **12**(10).

Potapov, P. V., Turubanova, S. A., Hansen, M. C., Adusei, B., Broich, M.,

Altstatt, A., Mane, L. & Justice, C. O. (2012), 'Quantifying forest cover loss in Democratic Republic of the Congo, 2000-2010, with Landsat ETM+ data', *Remote Sensing of Environment* **122**, 106–116.

Radke, R., Andra, S., Al-Kofahi, O. & Roysam, B. (2005), 'Image change detection algorithms: A systematic survey', *IEEE Transactions on Image Processing* **14**(3), 294–307.

Radzikowska, A. & Kerre, E. (2002), 'A comparative study of fuzzy rough sets', *Fuzzy Sets and Systems* **126**, 137–155.

Ramaswamy, S., Rastogi, R. & Shim, K. (2000), 'Efficient algorithms for mining outliers from large data sets', *SIGMOD Record (ACM Special Interest Group on Management of Data)* **29**(2), 427–438.

Razali, N. M. & Wah, Y. B. (2011), 'Power comparisons of Shapiro-Wilk, Kolmogorov-Smirnov, Lilliefors and Anderson-Darling tests', *Journal of Statistical Modeling and Analytics* **2**(1), 21–33.

Rene, S. & Barbara, K. (2008), 'Change vector analysis to categorise land cover change processes using the tasselled cap as biophysical indicator.', *Environmental Monitoring and Assessment* **145**, 227–265.

Renó, V. F., Novo, E. M. L. M., Suemitsu, C., Rennó, C. D. & Silva, T. S. F. (2011), 'Assessment of deforestation in the Lower Amazon floodplain using historical Landsat MSS/TM imagery', *Remote Sensing of Environment* **115**(12), 3446–3456.

Rodriguez-Galiano, V. F., Ghimire, B., Rogan, J., Chica-Olmo, M. & Rigol-Sanchez, J. P. (2012), 'An assessment of the effectiveness of a random forest

classifier for land-cover classification', *ISPRS Journal of Photogrammetry and Remote Sensing* **67**(1), 93–104.

Roe, G. H. (2005), 'Orographic precipitation', *Annual Review of Earth and Planetary Sciences* **33**, 645–671.

Rowland, C., Morton, R., Carrasco, L., McShane, G., O'Neil, A. & Wood, C. (2017), Land Cover Map 2015 (vector, GB), Technical report, NERC Environmental Information Data Centre.

RSPB, Bangor University, Cynidr Consulting & Welsh Government (2017), 'The future of upland farming in Wales'.
URL: *https://www.bangor.ac.uk/natural-sciences/adnodd/ConferenceBookletEnglish.pdf*

Salih, A. A. M., Ganawa, E.-t. & Alsadat, A. (2017), 'Spectral mixture analysis (SMA) and change vector analysis (CVA) methods for monitoring and mapping land degradation / desertification in arid and semiarid areas (Sudan), using Landsat imagery', *The Egyptian Journal of Remote Sensing and Space Sciences* **20**, S21–S29.

Sazib, N., Mladenova, I. & Bolten, J. (2018), 'Leveraging the google earth engine for drought assessment using global soil moisture data', *Remote Sensing* **10**(8).

Scaramuzza, P., Micijevic, E. & Chander, G. (2004), SLC Gap-Filled Products Phase One Methodology, Technical report, USGS-United States Geological Survey (2004) Reston (Virginia).

Schmidt, M., Lucas, R., Bunting, P., Verbesselt, J. & Armston, J. (2015), 'Multi-resolution time series imagery for forest disturbance and regrowth monitoring in Queensland, Australia', *Remote Sensing of Environment* **158**, 156–168.

Schroeder, T. A., Schleeweis, K. G., Moisen, G. G., Toney, C., Cohen, W. B., Freeman, E. A., Yang, Z. & Huang, C. (2017), 'Testing a Landsat-based approach for mapping disturbance causality in U.S. forests', *Remote Sensing of Environment* **195**, 230–243.

Schultz, M., Clevers, J. G. P. W., Carter, S., Verbesselt, J., Avitabile, V., Vu, H. & Herold, M. (2016), 'Performance of vegetation indices from Landsat time series in deforestation monitoring', *International Journal of Applied Earth Observation and Geoinformation* **52**(May 2012), 318–327.

Serra, P., Pons, X. & Saurí, D. (2003), 'Post-classification change detection with data from different sensors: some accuracy considerations', *International Journal of Remote Sensing* **24**(23), 4975–4976.

Sesnie, S. E., Finegan, B., Gessler, P. E., Thessler, S., Bendana, Z. R. & Smith, A. M. S. (2010), 'The multispectral separability of Costa Rican rainforest types with support vector machines and Random Forest decision trees', *International Journal of Remote Sensing* **31**(11), 2885–2909.

Sevo, I. & Avramovic, A. (2016), 'Convolutional neural network based automatic object detection on aerial images', *IEEE Geoscience and Remote Sensing Letters* **13**(5), 740–744.

Sexton, J. O., Noojipady, P., Anand, A., Song, X. P., McMahon, S., Huang, C., Feng, M., Channan, S. & Townshend, J. R. (2015), 'A model for the propagation of uncertainty from continuous estimates of tree cover to categorical forest cover and change', *Remote Sensing of Environment* **156**, 418–425.

Shalab, Ã. & Ryutaro, T. (2007), 'Remote sensing and GIS for mapping and

monitoring land cover and land-use changes in the Northwestern coastal zone of Egypt', *Applied Geography* **27**(1), 28–41.

Shapiro, A. S. S. & Wilk, M. B. (1965), 'An Analysis of Variance Test for Normality (Complete Samples)', *Biometrika Trust* **52**(3), 591–611.

Sharma, J., Mishra, V. & Khanna, R. (2013), 'Impact of Topography in Accuracy of Land Cover Spectral Change Vector Analysis Using SWiFS in Western Himalaya', *J. the Indian Soc. Remote Sensing* **41**(2), 223–235.

Shepherd, J., Bunting, P. & Dymond, J. (2019), 'Operational Large-Scale Segmentation of Imagery Based on Iterative Elimination', *Remote Sensing* **11**(6), 658.

Shepherd, J. D. & Dymond, J. R. (2003), 'Correcting satellite imagery for the variance of reflectance and illumination with topography', *International Journal of Remote Sensing* **24**(17), 3503–3514.

Shi, C. & Wang, L. (2014), 'Incorporating spatial information in spectral unmixing: A review', *Remote Sensing of Environment* **149**, 70–87.

Sibley, A., Cox, D. & Titley, H. (2015), 'Coastal flooding in england and wales from atlantic and north sea storms during the 2013/2014 winter', *Weather* **70**(2), 62–70.

Silva, M. P. D. S., Câmara, G., Escada, M. I. S. & Souza, R. C. M. D. (2008), 'Remote-sensing image mining: detecting agents of land-use change in tropical forest areas', *International Journal of Remote Sensing* **29**(16), 4803–4822.

Simonyan, K. & Zisserman, A. (2015), Very Deep Convolutional Networks For Large-Scale Image Recognition, *in* 'ICLR 2015', pp. 1–14.

Singh, A. (1989*a*), 'Digital change detection techniques using remotely-sensed data', *International Journal of Remote Sensing* **10**(6), 989–1003.

Singh, A. (1989*b*), 'Review Article: Digital change detection techniques using remotely-sensed data', *International Journal of Remote Sensing* **10**(6), 989–1003.

Singh, S., Srivastava, P., Gupta, M., Thakur, J. K. & Mukherjee, S. (2014), 'Appraisal of land use/land cover of mangrove forest ecosystem using support vector machine', *Environmental Earth Sciences* **71**(5), 2245–2255.

Singh, S. & Talwar, R. (2014), 'A comparative study on change vector analysis', *Sadhana* **39**, 1311–1331.

Sinha, P. & Kumar, L. (2013), 'Independent two-step thresholding of binary images in inter-annual land cover change/no-change identification', *ISPRS Journal of Photogrammetry and Remote Sensing* **81**, 31–43.

Smith, J., Van De Kop, P., Reategui, K., Lombardi, I., Sabogal, C. & Diaz, A. (1999), 'Dynamics of secondary forests in slash-and-burn farming: Interactions among land use types in the Peruvian Amazon', *Agriculture, Ecosystems and Environment* **76**(2-3), 85–98.

Sohl, T. L., Sleeter, B. M., Zhu, Z., Sayler, K. L., Bennett, S., Bouchard, M., Reker, R., Hawbaker, T., Wein, A., Liu, S., Kanengieter, R. & Acevedo, W. (2012), 'A land-use and land-cover modeling strategy to support a national assessment of carbon stocks and fluxes', *Applied Geography* **34**, 111–124.

Soille, P. (2008), 'Constrained connectivity for hierarchical image decomposition

and simplification', *IEEE Transactions on Pattern Analysis and Machine Intelligence* **30**(7), 1132–1145.

Somers, B., Asner, G. P., Tits, L. & Coppin, P. (2011), 'Endmember variability in Spectral Mixture Analysis: A review', *Remote Sensing of Environment* **115**(7), 1603–1616.

Son, N.-T., Chen, C.-F., Chang, N.-B., Chen, C.-R., Chang, L.-Y. & Thanh, B.-X. (2015), 'Mangrove Mapping and Change Detection in Ca Mau Peninsula, Vietnam, Using Landsat Data and Object-Based Image Analysis', *IEEE Journal of Selected Topics in Applied Earth Observations and Remote Sensing* **8**(2), 503–510.

Song, C., Woodcock, C. E., Seto, K. C., Lenney, M. P. & Macomber, S. A. (2001), 'Classification and change detection using Landsat TM data: When and how to correct atmospheric effects?', *Remote Sensing of Environment* **75**(2), 230–244.

Souza-Filho, P. W. M., Nascimento, W. R., Versiani De Mendonça, B. R., Silva, R. O., Guimarães, J. T. F., Dall'Agnol, R. & Siqueira, J. O. (2015), 'Changes in the land cover and land use of the Itacaiúnas River watershed, ARC of deforestation, Carajás, Southeastern Amazon', *International Archives of the Photogrammetry, Remote Sensing and Spatial Information Sciences - ISPRS Archives* **40**(7W3), 1491–1496.

Sterling, S. M., Ducharne, A. & Polcher, J. (2012), 'The impact of global land-cover change on the terrestrial water cycle', *Nature Climate Change* **3**(4), 385–390.

Sun, S., Chen, B., Chen, J., Che, M. & Zhang, H. (2016), 'Comparison of remotely-sensed and modeled soil moisture using CLM4.0 with in situ measurements in the central Tibetan Plateau area', *Cold Regions Science and Technology* **129**, 31–44.

Swain, P. (1976), *Land use classification and mapping by machine-assisted analysis of Landsat multispectral scanner data.*, Purdue University, West Lafayette, Indiana.

Swedish Wood (2019), 'The forest and sustainable forestry'.
URL: *https://www.swedishwood.com/about_wood/choosing-wood/wood-and-the-environment/the-forest-and-sustainable-forestry/*

Szegedy, C., Liu, W., Jia, Y., Sermanet, P., Reed, S., Anguelov, D., Erhan, D., Vanhoucke, V. & Rabinovich, A. (2015), Inception-v1: Going deeper with convolutions, *in* 'Proceedings of the IEEE Computer Society Conference on Computer Vision and Pattern Recognition', pp. 1–9.

Taigman, Y., Yang, M., Ranzato, M. & Wolf, L. (2014), DeepFace - Closing the Gap to Human-Level Performance in Face Verification, *in* 'IEEE Conference on Computer Vision and Pattern Recognition'.

Tang, X., Bullock, E. L., Olofsson, P., Estel, S. & Woodcock, C. E. (2019), 'Near real-time monitoring of tropical forest disturbance : New algorithms and assessment framework', *Remote Sensing of Environment* **224**, 202–218.

Tasdemir, K. (2011), Neural Network based Approximage Spectral Clustering, *in* '2011 IEEE International Geoscience and Remote Sensing Symposium', IEEE, Vancouver, Canada, pp. 2884–2887.

Taubenböck, H., Esch, T., Felbier, A., Wiesner, M., Roth, A. & Dech, S. (2012), 'Remote Sensing of Environment Monitoring urbanization in mega cities from space', *Remote Sensing of Environment* **117**, 162–176.

Tewkesbury, A. P., Comber, A. J., Tate, N. J., Lamb, A. & Fisher, P. F. (2015), 'A

critical synthesis of remotely sensed optical image change detection techniques', *Remote Sensing of Environment* **160**, 1–14.

Thomas, N., Bunting, P., Lucas, R., Hardy, A., Rosenqvist, A. & Fatoyinbo, T. (2018), 'Mapping mangrove extent and change: A globally applicable approach', *Remote Sensing* **10**(9), 1–20.

Thomas, N., Lucas, R., Bunting, P., Hardy, A., Rosenqvist, A. & Simard, M. (2017), 'Distribution and drivers of global mangrove forest change , 1996 – 2010', pp. 1–14.

Thomas, S. J., Deschamps, A., Landry, R. & Van der Sanden, J. J. (2007), 'Mapping insect defoliation using multi-temporal Landsat data', *In Conf on 'Our Common Borders-Safety, Security, and the Environment through Remote Sensing'* p. 10.

Thomson, A. G., Manchester, S. J., Swetnam, R. D., Smith, G. M., Wadsworth, R. A., Petit, S. & Gerard, F. F. (2007), 'The use of digital aerial photography and CORINE-derived methodology for monitoring recent and historic changes in land cover near UK Natura 2000 sites for the BIOPRESS project', *International Journal of Remote Sensing* **28**(23), 5397–5426.

Thonfeld, F., Feilhauer, H., Braun, M. & Menz, G. (2016), 'Robust Change Vector Analysis (RCVA) for multi-sensor very high resolution optical satellite data', *International Journal of Applied Earth Observation and Geoinformation* **50**, 131–140.

Tilton, J. C. (1998), 'Image segmentation by region growing and spectral clustering with a natural convergence criterion', *International Geoscience and Remote Sensing Symposium (IGARSS)* **4**, 1766–1768.

Tin Kam Ho (1998), 'The random subspace method for constructing decision forests', *IEEE Transactions on Pattern Analysis and Machine Intelligence* **20**(8), 832–844.

Tuxen, K. A., Schile, L. M., Kelly, M. & Siegel, S. W. (2008), 'Vegetation colonization in a restoring tidal marsh: A remote sensing approach', *Restoration Ecology* **16**(2), 313–323.

Ullah, W., Wang, G., Gao, Z., Hagan, D. F. T. & Lou, D. (2018), 'Comparisons of remote sensing and reanalysis soil moisture products over the Tibetan Plateau, China', *Cold Regions Science and Technology* **146**(July 2017), 110–121.

Urban, M., Berger, C., Mudau, T. E., Heckel, K., Truckenbrodt, J., Odipo, V. O., Smit, I. P. & Schmullius, C. (2018), 'Surface moisture and vegetation cover analysis for drought monitoring in the southern Kruger National Park using Sentinel-1, Sentinel-2, and Landsat-8', *Remote Sensing* **10**(9).

Van Lier, O. R., Luther, J. E., Leckie, D. G. & Bowers, W. W. (2011), 'Development of large-area land cover and forest change indicators using multi-sensor Landsat imagery: Application to the Humber River Basin, Canada', *International Journal of Applied Earth Observation and Geoinformation* **13**(5), 819–829.

van Oort, P. a. J. (2005), 'Improving land cover change estimates by accounting for classification errors', *International Journal of Remote Sensing* **26**(14), 3009–3024.

van Oort, P. A. J. (2007), 'Interpreting the change detection error matrix', *Remote Sensing of Environment* **108**(1), 1–8.

Varshney, A., Arora, M. & Ghosh, J. (2012), 'Median change vector analysis algorithm for land-use land-cover change detection from remote-sensing data', *Remote Sensing Letters* **3**(7), 605–615.

Verbesselt, J., Hyndman, R., Newnham, G. & Culvenor, D. (2010), 'Detecting trend and seasonal changes in satellite image time series', *Remote Sensing of Environment* **114**(1), 106–115.

Verbesselt, J., Hyndman, R., Zeileis, A. & Culvenor, D. (2013), 'Phenological change detection while accounting for abrupt and gradual trends in satellite image time series', *Remote Sensing of Environment* **114**(12), 2970–2980.
URL: *http://dx.doi.org/10.1016/j.rse.2010.08.003*

Verbesselt, J., Zeileis, A. & Herold, M. (2012), 'Near real-time disturbance detection using satellite image time series', *Remote Sensing of Environment* **123**, 98–108.

VUA-NASA (2019), 'VUA-NASA Land Parameter Retrieval Model'.
URL: *https://www.geo.vu.nl/ jeur/lprm/*

Wang, F. & Xu, Y. J. (2010), 'Comparison of remote sensing change detection techniques for assessing hurricane damage to forests', *Environmental Monitoring and Assessment* **162**(1-4), 311–326.

Wang, G., Yang, K., Yang, Y. & Zhang, S. (2017), 'Coupling natural and human processes to simulate changes in the water environment in the Dianchi Lake basin, China', *Geosystem Engineering* **20**(4), 207–215.

Wang, H., Bah, M. J. & Hammad, M. (2019), 'Progress in outlier detection techniques: A survey', *IEEE Access* **7**, 107964–108000.

Wang, L., Chen, J., Gong, P., Shimazaki, H. & Tamura, M. (2009), 'Land cover change detection with a cross-correlogram spectral matching algorithm', *International Journal of Remote Sensing* **30**(12), 3259–3273.

Warner, T. (2005), 'Hyper spherical direction cosine change vector analysis', *International Journal of Remote Sensing* **26**, 1201–1215.

Welsh Assembly Government (2009), *Woodlands for Wales*.

Welsh Government (2017), 'June 2017 Survey of Agriculture and Horticulture : Final Results for Wales'.

URL: *https://gweddill.gov.wales/statistics-and-research/survey-agricultural-horticulture/?lang=en*

Wilkinson, D., Parker, R. & Evans, D. (2008), 'Change detection techniques for use in a statewide forest inventory program', *Photogrammetric Engineering and Remote Sensing* **74**(7), 893–901.

Wissmar, R. C., Timm, R. K. & Logsdon, M. G. (2004), 'Effects of Changing Forest and Impervious Land Covers on Discharge Characteristics of Watersheds', *Environmental Management* **34**(1), 91–98.

Wright, A. (2017), 'Phytophthora ramorum Situation Report Summary', (MARCH), 1–5.

Wu, C., Du, B., Cui, X. & Zhang, L. (2017), 'A post-classification change detection method based on iterative slow feature analysis and Bayesian soft fusion', *Remote Sensing of Environment* **199**, 241–255.

Wu, Q., Liu, H., Wang, L. & Deng, C. (2016), 'Evaluation of AMSR2 soil moisture products over the contiguous United States using in situ data from the

International Soil Moisture Network', *International Journal of Applied Earth Observation and Geoinformation* **45**, 187–199.

Wulder, M. A., White, J. C., Alvarez, F., Han, T., Rogan, J. & Hawkes, B. (2009), 'Characterizing boreal forest wildfire with multi-temporal Landsat and LIDAR data', *Remote Sensing of Environment* **113**(7), 1540–1555.

Xiao, Q. & McPherson, E. G. (2005), 'Tree health mapping with multispectral remote sensing data at UC Davis, California', *Urban Ecosystems* **8**(3-4), 349–361.

Xin, Q., Olofsson, P., Zhu, Z., Tan, B. & Woodcock, C. E. (2013), 'Toward near real-time monitoring of forest disturbance by fusion of MODIS and Landsat data', *Remote Sensing of Environment* **135**, 234–247.

Xu, R., Lin, H., Lu, Y., Luo, Y., Ren, Y. & Comber, A. (2018), 'A Modified Change Vector Approach for Quantifying Land Cover Change', *Remote Sensing* **10**(1578).

Xu, X., Harwood, T. D., Pautasso, M. & Jeger, M. J. (2009), 'Spatio-temporal analysis of an invasive plant pathogen (Phytophthora ramorum) in England and Wales', *Ecography* **32**(3), 504–516.

Yang, Y., Erskine, P. D., Lechner, A. M., Mulligan, D., Zhang, S. & Wang, Z. (2018), 'Detecting the dynamics of vegetation disturbance and recovery in surface mining area via Landsat imagery and LandTrendr algorithm', *Journal of Cleaner Production* **178**, 353–362.

Yao, Y. Y. (1997), Combination of rough and fuzzy sets based on α - level sets, *in* 'Rough Sets and Data Mining: Analysis for Imprecise Data', pp. 301–321.

Ye, L., Fang, L., Shi, Z., Deng, L. & Tan, W. (2019), 'Spatio-temporal dynamics of soil moisture driven by 'Grain for Green' program on the Loess Plateau, China', *Agriculture, Ecosystems and Environment* **269**(August 2018), 204–214.

Yin, J., Yin, Z., Zhong, H., Xu, S., Hu, X. & Wang, J. (2011), 'Monitoring urban expansion and land use/land cover changes of Shanghai metropolitan area during the transitional economy (1979 – 2009) in China', *Environmental Monitoring and Assessment* pp. 609–621.

Yiran, G. A., Kusimi, J. M. & Kufogbe, S. K. (2012), 'A synthesis of remote sensing and local knowledge approaches in land degradation assessment in the Bawku East District, Ghana', *International Journal of Applied Earth Observation and Geoinformation* **14**(1), 204–213.

Yoon, G., Yun, Y. & Park, J. (2003), Change vector analysis: Detecting of areas associated with flood using Landsat TM, *in* IEEE, ed., 'IGARSS 2003: IEEE International Geoscience and AND Remote Sensing Symposium, Vols I - VII, Proceedings : Learnging from Earth's shapes and sizes', IEEE, 345 E 47TH ST, New York, NY, USA, Toilouse. France, pp. 3396–3388.

Yuan, F., Sawaya, K. E., Loeffelholz, B. C. & Bauer, M. E. (2005), 'Land cover classification and change analysis of the Twin Cities (Minnesota) metropolitan area by multitemporal Landsat remote sensing', *Remote Sensing of Environment* **98**(2-3), 317–328.

Zadeh, L. A. (1988), 'Fuzzy Logic', *Computer* **21**(4), 83–93.

Zeng, J., Li, Z., Chen, Q., Bi, H., Qiu, J. & Zou, P. (2015), 'Evaluation of remotely sensed and reanalysis soil moisture products over the Tibetan Plateau using in-situ observations', *Remote Sensing of Environment* **163**, 91–110.

Zhang, L., Zhang, L. & Du, B. (2016), 'Deep Learning for Remote Sensing Image Understanding', *IEEE Geoscience and Remote Sensing Magazine* pp. 22–40.

Zhao, B., Huang, B. & Zhong, Y. (2017), 'Transfer Learning with Fully Pretrained Deep Convolution Networks for Land-Use Classification', *IEEE Geoscience and Remote Sensing Letters* **14**(9), 1436–1440.

Zhao, F., Liu, H. & Jiao, L. (2011), 'Spectral clustering with fuzzy similarity measure', *Digital Signal Processing: A Review Journal* **21**(6), 701–709.

Zhao, S., Liu, S., Sohl, T. & Young, C. (2013), 'Land use and carbon dynamics in the southeastern United States from 1992 to 2050', *Environmental Research Letters* **8**(4), 1–9.

Zhao, S. Q., Liu, S., Li, Z. & Sohl, T. L. (2009), 'Ignoring detailed fast-changing dynamics of land use overestimates regional terrestrial carbon sequestration', *Biogeosciences* **6**(8), 1647–1654.

Zhao, S. Q., Liu, S., Li, Z. & Sohl, T. L. (2010), 'A spatial resolution threshold of land cover in estimating terrestrial carbon sequestration in four counties in Georgia and Alabama , USA', *Biogeosciences* **7**(1), 71–80.

Zhao, Y. & Hryniewicki, M. (2018), 'XGBOD: Improving Supervised Outlier Detection with Unsupervised Representation Learning.', *IEEE International Joint Conference on Neural Networks* .

Zhou, W., Troy, A. & Grove, M. (2008), 'Object-based Land Cover Classification and Change Analysis in the Baltimore Metropolitan Area Using Multitemporal High Resolution Remote Sensing Data', *Sensors* **8**(3), 1613–1636.

Zhu, X., Helmer, E. H., Gao, F., Liu, D., Chen, J. & Lefsky, M. A. (2016),

'A flexible spatiotemporal method for fusing satellite images with different resolutions', *Remote Sensing of Environment* **172**, 165–177.

Zhu, Z. & Woodcock, C. E. (2012), 'Object-based cloud and cloud shadow detection in Landsat imagery', *Remote Sensing of Environment* **118**, 83–94.

Zhu, Z. & Woodcock, C. E. (2014), 'Continuous change detection and classification of land cover using all available Landsat data', *Remote Sensing of Environment* **144**, 152–171.

Zhu, Z., Woodcock, C. E. & Olofsson, P. (2012), 'Continuous monitoring of forest disturbance using all available Landsat imagery', *Remote Sensing of Environment* **122**, 75–91.

Zhuang, H., Deng, K., Fan, H. & Yu, M. (2016), 'Strategies Combining Spectral Angle Mapper and Change Vector Analysis to Unsupervised Change Detection in Multispectral Images', *IEEE Geoscience and Remote Sensing Letters* **13**(5), 681–685.

Zimek, A. & Filzmoser, P. (2018), 'There and back again: Outlier detection between statistical reasoning and data mining algorithms', *Wiley Interdisciplinary Reviews - Data Mining and Knowledge Discovery* **8**(6).